University of Surrey
Department of Civil Engineering

EXPERIMENTAL AND THEORETICAL INVESTIGATIONS OF BOLTED JOINTS FOR PULTRUDED COMPOSITE MATERIALS

By

Sherif F.M. ABD-EL-NABY, BSc., MSc. (Cairo)

A Thesis Submitted for the Degree of Doctor of Philosophy
in the Faculty of Engineering of the
University of Surrey
1992

To My Family

PUBLICATIONS

The following list of papers are based on the work contained in this thesis.

1. ABD-EL-NABY,S.F.M., HOLLAWAY,L. and GUNN,M.
"Load Distribution in Two-Pinned Polymer Composite Joints"
Presented in Composite Structures 6, Ed. by I.H.Marshall, Elsevier Applied Science, p.553, 1991

2. ABD-EL-NABY,S.F.M., HOLLAWAY,L. and GUNN,M.
"The Tangential Stresses in an Infinite Orthotropic Plate with a Loaded Hole"
Accepted for publication in Composites Engineering

3. ABD-EL-NABY,S.F.M., HOLLAWAY,L. and GUNN,M.
"A Simple Material Model for Unidirectionally Aligned Fibre Reinforced Composites"
Submitted for publication in Composites Structures

4. ABD-EL-NABY,S.F.M. and HOLLAWAY,L.
"The Experimental Behaviour of bolted Joints in Pultruded Glass Polyester Material; Part 1: Single Bolt Joints"
Under Preparation

5. ABD-EL-NABY,S.F.M. and HOLLAWAY,L.
"The Experimental Behaviour of bolted Joints in Pultruded Glass Polyester Material; Part 2: Two Bolt Joints"
Under Preparation

ERRATA

Page	Position	Error	Correction
44	Last paragraph	reinforced unidirectionally	orthotropic
58	Second paragraph	isotropically reinforced	both
122	Second paragraph	very different	different
138	Second paragraph	5%	2.5%
236	Equation (5.3)	P/a	P/r
240	Equation (5.8)	P/wt	P/2wt
249	Figure(5.4)	P/wt	P/2wt
255	Second paragraph	shapes.	shapes is needed.

Fig(A.1) Overview of the Thesis

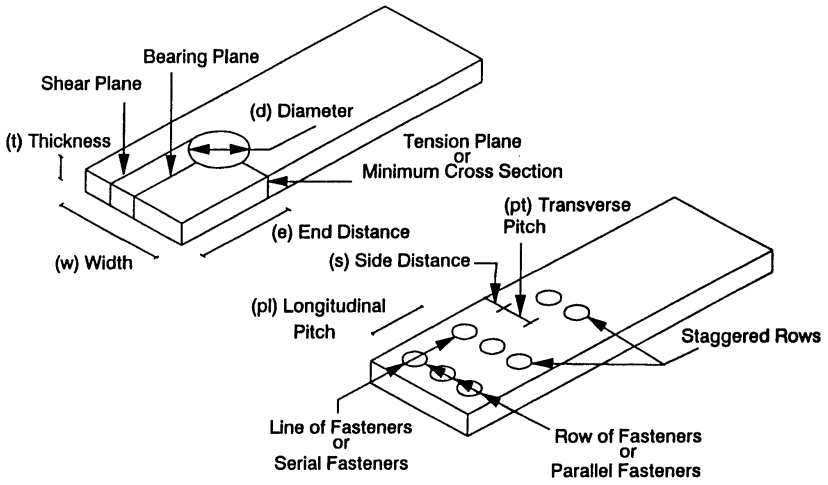

Fig(A.2) Joint Nomenclature

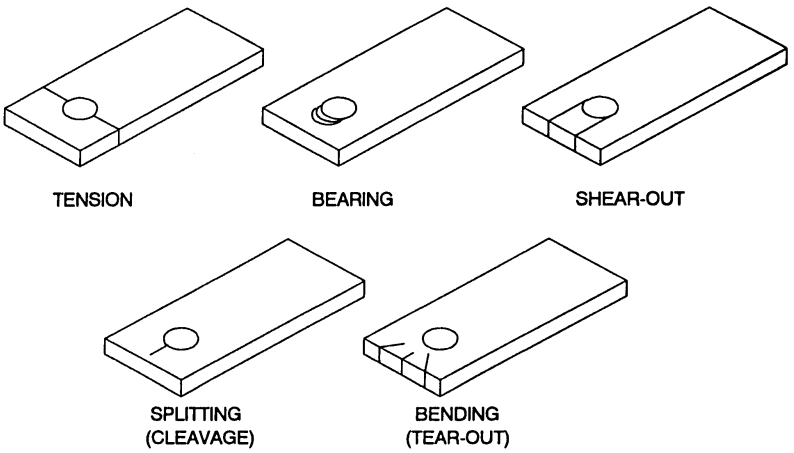

Fig(A.3) Failure Modes of Bolted Joints in Composite Materials

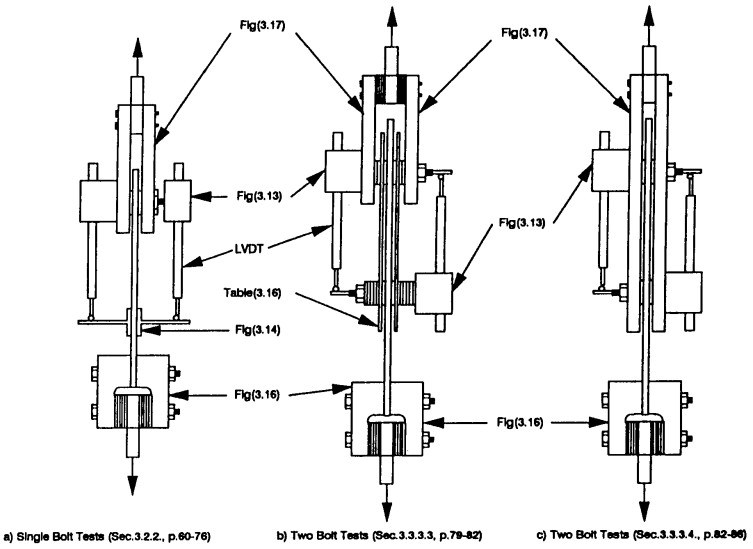

Fig(A.4) Details of the Experimental Set-up

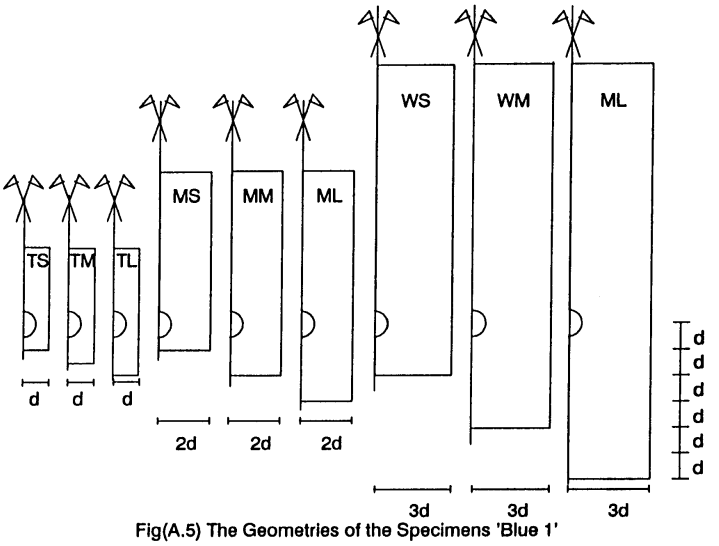

Fig(A.5) The Geometries of the Specimens 'Blue 1'

RESULTS

The main results of this work can be summarised in the following points:

1- The confinement area and material have a pronounced effect on the bearing strength of pultruded materials (sec. 3.3.2.3.).

2- The end distance responsible for the development of the maximum strength of a joint was found to be different from the end distance which results in bearing failure (sec. 3.3.2.4.). It was shown that the former end distance can be estimated using St Venant's length (sec. 5.4.1.).

3- The percentage of load taken by a bolt in a two-bolt serial joint changes with the applied load (sec. 3.3.3.).

4- Quasi-three dimensional problems of laminated materials, where no coupling between axial and shear behaviour exist, can be analyzed using general purpose finite element software (sec. 4.5.1.).

5- Improved results for in-plane quantities can be obtained using a laminated shell model which considers half the thickness of the laminate only while preventing the shell from out-of-plane movement (sec. 4.5.3.).

6- It is possible to use an averaging technique to obtain more reliable information at nodes lying at the interface of two materials using displacement based finite elements. For this purpose, only a part of the stresses and the strains will be averaged (sec. 4.5.5.2.).

7- The laminated plate theory can predict the in-plane behaviour of laminated materials fairly well (sec. 4.5.5.3.).

8- The analysis of a rough pin can be performed without iterations (sec. 4.6.3.).

9- The effect of the presence of a washer can be considered in two dimensional analyses (sec. 4.6.4.).

10- The non-linear mechanical behaviour of composite materials can be predicted based on the behaviour and the interaction of the constituents (sec. 4.7.1.).

11- The hoop stresses around a hole in an infinite orthotropic plate can be easily calculated using a closed form formula (sec. 4.8.).

TABLE OF CONTENTS

ACKNOWLEDGEMENTS

I would like to express my deep thanks and sincere gratitude to my supervisors, Professor Leonard Hollaway and Mr Michael Gunn for their guidance, encouragement and useful comments.

The funding of this research by Shell Research Ltd. is gratefully acknowledged. Special thanks go to Professor L. Hollaway and Dr Michael Collins for setting the financial framework for this project and to Dr Simon Frost for managing it.

I would like to express my gratitude to Professor Abd-El-Rahman Hindi and Professor Hassan Hosni of Helwan University (Egypt) as well as Dr Waleed Hindi for introducing me to Professor L. Hollaway.

My warm appreciation goes to Mr Anthony Thorne for his continuous and sincere help throughout the experimental and computational parts of this work.

I am greatly indebted to the technicians of the Civil Engineering workshop for their expertise and efficiency. Special thanks go to Mr Ian Rankin and Mr Tony Di-Franco for their admirable skills and invaluable help during the experimental investigations.

Sincere thanks go to all my friends and academic colleagues specially Mr Darren York, Mr Paul Fanning, Mr James Lee and Mr Kourosh Parsa for their helpful discussions and advice. Here, I would like to convey my special thanks to Dr Martin O'Neil and Dr Waleed Hindi for their invaluable advice on computational issues during the initial stages of this research and to Mr Kourosh Parsa and Mr Ashraf El-Hamalawi for their conscientious reading of parts of the manuscript of the thesis. Many thanks go to Dr Waleed Shatila and his family for their special role during the course of this research.

Finally I owe special debt of gratitude to my family for their patience, support and encouragement.

CHAPTER ONE

1.INTRODUCTION

1.1. COMPOSITE MATERIALS

According to Obraztsov (1982), a composite material is essentially a heterogeneous medium formed from two basic phases:

a) reinforcing elements providing the high strength and rigidity of the material and

b) an isotropic matrix providing the integrity of the material and the efficient action of the reinforcing phase.

The reinforcing elements may be granular or fibrous. Both types of composite have been used for a long time in construction. Concrete is a granular composite that has been widely used in the construction industry since Roman time. The use of fibre reinforced composite materials in structures dates back to ancient Egypt (Starr 1985). The ruins of houses from that epoch show that the bricks used were reinforced using chopped straws. This technology preserved the structural integrity of the bricks for thousands of years in spite of the fact that the bricks were not burnt to transform the clay into ceramic.

1.2. MODERN FIBRE REINFORCED COMPOSITE MATERIALS

Modern fibre reinforced composite materials use metals, ceramic or polymers as the matrix material and other metal, polymer, glass or carbon fibres as reinforcement. The high cost of most of these materials prevents their use in construction. Their basic field of application is the aeronautical and marine industries.

An exception to this is the composite made of polyester resin and glass fibres. The relatively low cost of this material has encouraged its use in the construction industry for shuttering and cladding. The material is also used for building folded plate roof systems. Small size domestic and industrial tanks are fields of the construction industry that are dominated by that material. In spite of all these applications, glass reinforced plastics have not been widely used as primary load bearing structural elements (Hollaway 1978). A major reason for this situation is the fact that the finished shapes of this material were not in the form of conventional

ABSTRACT

Fibre reinforced structural members are currently being produced using the pultrusion process. The mechanical properties of these members are fundamentally different from those of conventional metallic ones. Therefore, the approximate theories which are suitable for designing the latter elements have to be revised before they are applied to pultrusions.

An important aspect of the design of building frames is that of joints. The bolting technique is considered as the most suitable method for on-site jointing. Accordingly, experimental investigations are undertaken in order to establish the behaviour of bolted joints in pultrusions. Numerical and analytical methods are used to investigate the stresses in these joints.

Single and two-bolt joints were the subject of experimental investigations. It is shown that materials with high percentage of axial fibres do not develop bearing failure. However, provided the end distance is sufficient, the resulting shear failure will be ductile. The load distribution in joints with two bolts is measured and it is found that it varies with the load on the joint.

The theoretical investigations compare the use of the laminated plate theory with three dimensional analyses. Because the use of the laminated plate theory is found to be reasonably accurate, an improvement for the case of a symmetrical laminate is proposed where the laminated shell theory is used to model half the plate only. This technique is based on the assumption of a bi-linear variation of the stress through the thickness of the laminate.

The effect of the fastener is an important part of the behaviour of the joints. Three dimensional analyses are performed to assess its effect. To avoid the complications of performing three dimensional analyses, a two dimensional model for considering the effect of the washer on the joint is devised. In addition, a method which avoids iteration when considering the effect of friction is formulated. A finite element formulation for the non-linear and failure behaviour of uniaxial composite materials is developed to investigate the behaviour of the joints. Finally, a closed form analytical formula for calculating the tangential stress around a hole in an infinite orthotropic plate loaded on the hole is generated to simplify the design procedures.

construction elements, namely columns and beams. This difficulty has been overcome by introducing the pultrusion technique for manufacturing glass fibre reinforced polyester structural cross-sections.

1.3. THE PULTRUSION TECHNIQUE AND ITS PRODUCTS

In the pultrusion process, tightly packed continuous bundles of fibres, carrying other layers of fibres with the desired orientation and length, are soaked with catalyzed resin and then pulled through a heated die to form continuous prismatic members. The resulting structural elements have a high percentage of longitudinal fibres which means that the stiffness and strength in this direction is high (Hollaway 1989). Therefore, members made from this material can compete with the traditional steel sections because they also offer the following two major advantages:

a) The weight of these members is low. This is of great importance for structures which are to be erected in remote areas. Light weight can also be advantageous when the soil conditions are poor.
b) The corrosion resistance of these materials is high and can easily be improved by applying special resistant layers if needed.

The two properties given above are directly applicable to offshore oil rigs (Salama 1986). Therefore, the use of glass-fibre reinforced pultrusions in this field is favoured.

1.4. CONVENTIONAL MATERIALS VERSUS COMPOSITE MATERIALS

The replacement of the traditional steel sections by pultruded glass reinforced sections is not a straight-forward process because it is not possible to adopt directly the experience gained in the design and construction of steel structures to the new material. This is due to fundamental differences in the properties of the two materials. The most pronounced ones are:

a) Steel members are isotropic, while pultruded structural sections are highly orthotropic due to the presence of a high percentage of axial fibres.
b) Steel is homogeneous, while fibre reinforced polymers are heterogeneous on the microscopic and macroscopic levels. The heterogeneity on the microscopic

level is due to the differences between the matrix and the fibres. The heterogeneity on the macroscopic level is due to the laminated nature of the resulting members.

c) Steel is ductile while fibre reinforced polymers tend to be brittle. This is due to the dependence of the behaviour of the composite in the fibre direction on the linear behaviour of the fibre. In the direction perpendicular to the fibres, the presence of the fibres reduces the ductility of the matrix and causes failure to develop under low strains.

The above given differences necessitate reassessment of all design and construction practices of steel structures before they are adopted for structures made using glass reinforced pultruded members. Because most structural collapses originate at the joints, it is of great importance to establish rules and design practices for obtaining safe and economical structural joints for pultruded members.

1.5. STRUCTURAL JOINTS FOR COMPOSITE MATERIALS

A structural joint is a point in a structure at which loads are transmitted between two structural members. The load transmission can be affected using:

a) bolting,
b) bonding or
c) combined bolting and bonding.

It has to be noted that welding and fusion techniques are not considered because they only apply to thermoplastic materials which are still more expensive than thermosetting polymers and therefore their use in the construction industry is still not feasible.

The use of combined bolted and bonded joints can be achieved in the following two ways:

a) Bolts are added to a conventional bonded joint.
b) Special bolts are bonded to the surface of the member.

Hart-Smith (1985) has shown that adding bolts to a well designed bonded joint does not achieve any significant advantage. This is due to the high rigidity of bonded joints which prevents the load transfer through the bolts until the adhesive has failed. However, if the bonded joint is subjected to eccentricity, the addition of end bolts prevents the peeling action and therefore improves the strength. The second option seems more promising but it suffers from the relatively small bonding area and the moments that have to be transmitted through the adhesive.

Although it is well established that bonded joints can show higher efficiencies than bolted joints (Stockdale and Matthews 1976), the latter are preferred for on-site assembly; this is because:

a) the quality control procedures for such joints are less complicated than those for bonded joints;
b) there is no need for sophisticated surface preparation operations that are required for bonded joints;
c) damaged and wrongly assembled members are readily dismantled;
d) the removal of members to enable inspection of other parts of the structure is possible;
e) the joint is able to take the design load immediately after it is assembled;
f) the bolted joints present higher confidence under poor on-site working conditions and
g) the load is distributed uniformly over the thickness of the member.

These points outweigh the following disadvantages:

a) Lower efficiency compared to bonded joints due to the weakening of the members by holes.
b) Higher weight penalty due to the use of metal bolts. This, however, can be overcome by the use of composite bolts.
c) In the absence of skilled labour or suitable tools, the drilling operation may damage the material.
d) The cost of the joint increases rapidly with the size of the joint.

Therefore, the bolting technique will be adopted in this thesis for jointing structures erected using pultruded members.

1.6. FAILURE BEHAVIOUR OF COMPOSITE JOINTS

Although bolted joints made of composite materials show failure modes similar to the failure modes of steel joints, the following effects of the composite material properties have to be noted:

a) The tensile failure mode can occur at much lower loads due to the high stress concentrations resulting from the anisotropy of the material.

b) The bearing strength of composite materials depends heavily on the stacking sequence of the layers and on the presence of a washer. This is due to its low interlaminar tensile strength.

c) A shear failure mode can occur at relatively low loads in pultruded materials due to the high percentage of longitudinal fibres.

d) A mode of failure that is absent in the case of steel is the cleavage failure mode, which initiates by transverse tensile failure ahead of the bolt, followed by tensile failure on the minimum area cross section (Collings 1987).

e) The shearing of the steel bolts is very unlikely, however, small diameter bolts are liable to bend due to the lower stiffness of the composite compared to that of the bolts.

f) The pull-through of the fasteners is a further cause of failure of the joints. This mode of failure is usually associated with countersunk fasteners.

The differences summarized above indicate the need for an assessment of bolted joints in pultruded materials. Much work has been undertaken in the past concerning bolted joints in composite materials. This work, however, was for the aeronautical industry and did not use pultruded materials. Again, the adoption of the knowledge and experience obtained in that field has to be undertaken cautiously. This thesis therefore investigates the behaviour of joints in pultruded glass reinforced polyester material with the objective of using them in the construction industry.

1.7. STRUCTURE OF THE THESIS

The thesis consists six chapters. The first one is an introduction to the work and explains the need for it. Chapter two is a literature review for the research undertaken in the field of bolted joints in glass reinforced polymers. This review includes both experimental and theoretical investigations. Chapter three presents the experimental investigations undertaken in the present research. This includes material characterisation and tests on single and two fastener specimens. Chapter four describes the theoretical investigations performed during the course of the work. This includes

a) performing two and three dimensional finite element analyses,
b) formulation of a method for considering the effect of the washer in two dimensional analyses,
c) evolution of an approximate method for considering the friction effect,
d) development of a non-linear material model for composites and
e) generation of a closed form analytical formula for calculating the tangential stress around a hole in an infinite orthotropic plate loaded on the hole.

Chapter five discusses the results from the point of view of design. A new definition of the critical end distance is proposed and a method for determining its value based on the elastic properties of the material is presented. Finally, Chapter six summarises the conclusions of the present research program and makes recommendations for future work.

CHAPTER TWO

2.LITERATURE REVIEW OF PLANE STRUCTURAL JOINTS IN GLASS FIBRE REINFORCED POLYMERS

2.1. INTRODUCTION

Much research has been devoted to the mechanical jointing of fibre reinforced polymers. Many reviews have been prepared about this subject (Arnold (1989), Matthews (1987), Vinson and Sierakowski (1987), Poon (1986), Tsiang (1984), Godwin and Matthews (1980) and Murphy and Lenoe (1974)) but these reviews were general and considered different materials and types. This results in a difficulty in reconciling the various results. Snyder, Burns and Venkayya (1990) presented a review that concentrated on the software available for the design and analysis of composite bolted joints.

In the present review, the experimental results reported will be confined to glass fibre materials only unless the results are for another material but believed to be applicable to glass reinforced materials. The theoretical investigations, however, will be reported irrespective of the material properties used in the work. A description of the terms which are used throughout this thesis is given in Fig(2.1).

2.1.1. FAILURE MODES

Although some failure modes of fibre reinforced polymer joints are similar to those of metallic joints, the former joints experience modes which do not occur in metallic joints. These special modes are due to the anisotropic, inhomogeneous and brittle nature of the material.

When the width to diameter ratio of a joint is small, tensile failure is expected. For joints with small edge distance to diameter ratio, a shear failure will occur due to the shearing-out of the fastener. All the previous failure modes are also encountered in metal joints, however, the transition from one mode to the other in composite joints depends on the fibre/matrix system used. Quinn and Matthews (1977) showed that although the initial failure of pin-loaded specimens was due to bearing, their final failure involved tension, shear-out and mixed mode failures. They also reported that by stacking the layers in the order $(90/0/\pm 45)_s$, a final safe shear-out mode is achieved while the strength is kept high. Other stacking sequences of the same material either reduce the strength or fail catastrophically.

When the minimum requirements for the width and the edge distance are satisfied, bearing failure occurs. Kretsis and Matthews (1985) reported an out-of-plane buckling mode of glass epoxy joints for d/t greater than 3. They reported that the same effect was recorded previously by Kutsha and Hofer (1969) using Scotch ply material.

In addition to the stated modes, cleavage (splitting) and tear-out failure modes occur frequently (Fig(2.2)). The failure begins due to initial transverse cracking in the bearing area followed by cracking in the net area when the two sides of the joint act as cantilevers. This type of failure is associated with lay-ups which are basically made up of uniaxial layers (Collings 1977).

The pull-through of the fasteners is a further cause of failure of joints. This mode is usually associated with countersunk fasteners. Finally, because the fibre reinforced polymer plates do not support the fastener, bending failure of the fastener is frequently seen (Hart-Smith 1978).

2.1.2. DEFINITION OF THE FAILURE LOAD

The precise point at which fibre reinforced polymer joints are considered to have failed is not well defined. In order to get consistent information about the strength of joints, it is necessary to define their failure. Although Porter (1976) reviewed the methods used to define the failure of the joints, no general definition of the strength of the joint has been preferred. The absence of this definition has resulted in much confusion when using published results.

Matthews, Nixon and Want (1976) reported tension, bending tear-out and bearing failure modes for $\pm 45/0/\pm 45$ and $\pm 45/90/\pm 45$ glass polyester bolted and riveted specimens. They showed that the mode of failure was determined by the geometry of the specimens. Their results demonstrated that increasing the initial failure load did not always improve the final strength of the joints.

Quinn and Matthews (1977) used the first failure load as a measure of the strength of the joint. Pyner and Matthews (1979), on the other hand, considered the maximum load sustained on the specimen as the failure mode irrespective of the corresponding displacements. Other investigators defined the load corresponding to a specified amount of hole elongation as the failure load. Strauss (1960) reported that a hole elongation of 1.5 % is the elastic limit. Dastin (1969) proposed 0.4% elongation for glass fibre reinforced polymers as definition for the bearing strength. Johnson and Matthews (1979) showed that using the values of 0.4% for glass reinforced materials with polyester and epoxy matrices is equivalent to considering a factor of safety of 2 in association with the maximum load.

2.1.3. METHODS OF ASSESSMENT

Basically there exist three fundamental approaches to investigate the behaviour of mechanically fastened joints. These are the destructive, the non-destructive experimental approaches and the theoretical approach.

In the destructive experimental method, the specimens are loaded up to failure in order to determine the behaviour of the joint. This technique also gives detailed information about the damage and the development of failure under increasing load. These investigations measure the failure load only or they use strain gauging and displacement transducers to measure the deformations. The results obtained using this technique have been reviewed by Godwin and Matthews (1980).

Two non-destructive testing techniques have been applied in the investigation of the behaviour of joints. These techniques have mainly been used to verify the results obtained using theoretical analyses. The first is the Moire method which is based on the interference of light obtained using fine grids drawn on the surface of the specimens. The technique has been used to measure the in and out-of-plane deformations of the specimens. The second non-destructive experimental technique is the photoelasticity approach applied to glass/epoxy joints. The method is based on the phenomenon of bifringence of stressed materials. The technique is restricted to linear undamaged behaviour because at higher loading levels, the light is scattered due to cracks and the calibration coefficients change.

The theoretical method uses mathematical models to approach the problem. These models are usually obtained using certain simplifying assumptions. The resulting mathematical problem is finally solved either using analytical techniques which yield closed-form solutions or numerical methods which are straight forward to apply for a wide range of problems. The different methods of solution are reviewed by Matthews (1987).

The investigations undertaken using each of the above mentioned techniques will now be reviewed separately. This is done in order to expose the trends of development, the range of application and the potential of the different techniques.

2.2. DESTRUCTIVE EXPERIMENTAL INVESTIGATIONS

The major technique for investigating the behaviour of joints in composite materials has been the loading of coupons to failure. The advantage of this technique is that it gives the true behaviour of the coupon tested. However, the correspondence between the behaviour of these coupons and the behaviour of joints in real structures is still not clear. This technique

suffers from two major disadvantages. The first is its high cost and the second is its inability to provide information about the stress distribution in the coupon. The second problem can be partially solved by attaching strain gauges to the coupon. However, this method provides information about specific points only.

2.2.1. MATERIAL EFFECTS

The behaviour of joints in composite materials depends on the material from which it is made. The definition of a composite system involves the specification of the constituent materials, the form and the orientation of the fibres and the stacking sequence. Investigations which dealt with these points will be reviewed now.

2.2.1.1. FIBRE FORM AND ORIENTATION

The fibre form and orientation are important factors which influence the shape of the stress-strain curves of the material. Some fibre orientations show a form of softening resulting in the possibility of redistribution of stresses before failure. This is equivalent to the plastic behaviour of metals and results in the enhancement of the ultimate strength of the joint. In spite of the fact that the stacking sequence does not change the in-plane properties of the composite material, it does have a significant effect on its strength. This effect is more pronounced for laterally unsupported joints when they fail in bearing.

In addition to the fibre orientation, the form in which the fibres are inserted into the matrix also influences the material properties and its failure mechanism. This has direct effects on the strength and deformability of joints made from the corresponding material.

Matthews, Nixon and Want (1976) reported that for clamped specimens, the bearing strength of $\pm 45/0/\pm 45$ material is higher than that for $\pm 45/90/\pm 45$ lay-up. However, in order to obtain the full bearing strength, a larger non-dimensional end distance was needed for the former material.

Stockdale and Matthews (1976) considered 0/90/0/90/0/90/0 and 90/0/90/0/90/0/90 glass-epoxy specimens. They reported that the second lay-up gave higher strengths when the specimens were clamped, while for finger-tight conditions, the first lay-up was better.

Quinn and Matthews (1977) investigated the effect of the stacking sequence in pin-loaded glass reinforced GFRP laminates. They pointed out that placing 90° plies at or near the surface seemed to improve the pin bearing capacity. The strongest lay-up was about 30% stronger than the weakest one but the final failure was in a catastrophic tensile mode. They

explained this improvement of the strength by the compressive interlaminar stresses which would be expected in specimens with transverse outer layers.

Chandra and Kumar (1978) considered uniaxial, woven fabric, cross ply and $0/\pm 60$ glass-epoxy materials. The uniaxial material failed in pure shear-out while the other specimens failed in tension through the hole due to the small width of the specimens. Their results indicated that the cross ply configuration gave the highest efficiency. This seemed to be due to the reduced strength of the parent laminate rather than due to the increased strength of the joint.

Matthews, Godwin and Kilty (1982) investigated the strengths of joints made in chopped-strand mat material, woven roving materials and a 50/50 mixture of the two in GRP. They reported that for the same fibre volume fraction, chopped strand mat material resulted in a stronger joint than the one obtained for woven roving material. The failure of the joint in chopped strand mat was reported to occur due to tension through the hole failure irrespective of the width of the specimens. By increasing the width of woven roving material, however, it was possible to obtain fail-safe bearing failure.

Kretsis and Matthews (1985) considered the effect of stacking on the strength of the joint. Their results showed reduced strength for specimens which had bulks of laminae. They also investigated the effect of the percentage of $\pm 45°$ material on the behaviour of the joint. Their results showed that a laminate with 60% $\pm 45°$ layers resulted in the maximum strength for weight. However, it has to be noted that the objective function they used for obtaining this result did not consider the weight of the bolts.

Marshall, Arnold, Wood and Mousley (1989) considered the pin bearing strength in (0/90)s and (90/0)s glass reinforced polyester laminates. Their results showed that again, the strength of the material which had 90° outer layers failed at a higher strength. They were able to show distinct differences between the delaminated areas of the two types of material.

2.2.1.2. RESIN TYPE

Because the bearing failure of fibre reinforced materials is believed to be due to buckling of the fibres in the compressed area, the matrix material supporting the fibres has a pronounced effect on the behaviour of mechanically fastened joints.

Johnson and Matthews (1979) compared the behaviour of epoxy and polyester based specimens. They reported that the epoxy based specimens suffered a sudden increase in the deformation of the hole at around 60-70% of the first peak load. The polyester based specimens, on the other hand, showed a steady increase in the deformation.

Kretsis and Matthews (1985) compared the behaviour of joints for materials made using two different epoxy resins. They reported that the resulting joints possessed the same behaviour pattern except that one of them resulted in higher strength.

2.2.2. FASTENER PARAMETERS

The behaviour of a mechanical joint in a composite is a function of the interaction of the plates and the fasteners. Therefore, the fastener is the other important factor affecting the behaviour of the joint.

A variety of fasteners has been used to join fibre reinforced polymers. Rufulo (1961), Dastin (1969) and Cole, Bathe and Potter (1982) reviewed the different types of fasteners. These included bolts, rivets and screws.

The fasteners may be flush or protruding and blind or accessible from both sides. Rivets may be solid, tubular, semi-tubular, pop or even two-piece GRP rivets. Bolts may have special shapes of the head and the nut to eliminate pull-through failure. Screws may be self tapping or require previous drilling and tapping.

2.2.2.1. FASTENER TYPE

Matthews, Nixon and Want (1976) investigated the effect of using different types of rivets on the strength of GFRP joints. They reported that pop-rivets resulted in substantial damage to the laminate and that longer rivets increased the area of damage. However, the failure load of the longer pop-rivets was found to be higher than both the correct sized pop-rivets and the solid ones.

Fuchs and Greenwood (1977) reported the use of glass/epoxy bolts in the manufacture of a large turbo generator. These bolts were manufactured from unidirectional layers. The reported minimum fracture strength corresponded to that of steel bolts. However, the bolts were weak in torsion and therefore it was recommended that the bolts were compressed before tightening the nut. The bolts had flattened sides in order to detach the thread and prevent locking if the thread stripped. The nut used was also manufactured from glass/epoxy where the lamination was parallel to the threads. The shear strength reported for these bolts was about 180 MPa.

Tanis and Poullous (1978) proposed a glass fibre reinforced rivet. When thermoplastic resin was used, it was shaped as a solid rivet. When the resin was thermosetting, a two-piece

rivet was proposed. This rivet consisted of a pin which fitted in a sleeve and it used an adhesive to fix the two parts.

Found (1986) considered the use of surface bonded fasteners and encapsulated ones. His results showed that the bolts which were encapsulated in the laminate while it was being manufactured were stronger.

Malkan and Ko (1989) investigated the effect of the lay-up of the fibres on the shear behaviour of E-glass epoxy pins. They reported a shear strength of 182.62 MPa and failure strains ranging from 7.26 to 14.39%. The maximum strength was achieved by a fully braided fibre configuration and also a combination of outer braided fibre mesh covering a uniaxial core. This uniaxial core was about 80% of the total reinforcement. The second configuration resulted in a higher failure strain than the first one.

2.2.2.2. FASTENER CLAMPING

The presence of the bolt head and the washer or the nut as well as the tightening torque has a significant effect on the strength of mechanically fastened joints. This effect has been extensively investigated.

Stockdale and Matthews (1976) investigated the effect of clamping pressure on the bearing strength of GFRP. They reported a 40% increase in the bearing strength due to the finger-tight condition. For the maximum clamping load, the increase was 100% over pin-loaded joints. The clamping effect for lay-ups with 90° plies at the laminate surface was reported to be stronger. They showed that for clamped cases failure occurred by cracking at the hole and crushing at the washer edge. The failure load was found to be proportional to the ratio of the outer to the inner diameters of the washer when the clamping pressure was kept constant. By comparing the increase in strength due to clamping, to the friction force between the plate and the washer, they showed that the increase in strength was only partially due to the increase of friction forces.

Porter (1976) showed that by replacing one of the washers, which clamp the specimen, by a plate, the strength of the specimen increased. Accordingly, he concluded that the results obtained, using specimens clamped by two washers, were conservative.

Matthews, Nixon and Want (1976) investigated the effect of clamp-up on the riveted joints in GFRP. They found that the machine-clamped solid rivets gave higher failure loads than the hand-clamped rivets. Their results indicated the presence of an optimum clamping load. It was reported that the reduced strength associated with higher loads was not due to the higher damage. The maximum strength was achieved using a clamping force equal to 4000N.

Chandra and Kumar (1978) considered clamping torques ranging from 0 to 108 Nm. They found that the shear and tensile strength of their joints increased with clamping force. It has to be noted, however, that the specimens were so narrow that the whole width of the specimen was covered with the washer.

Matthews, Godwin and Kilty (1982) showed that replacing the washer by a GRP plate gave slightly higher failure loads. They explained this by the higher contact area between the inner and outer plates of the joint. They also reported that the bolt-loaded test specimens of small width failed at a slightly higher load than the equivalent small width test pieces with an unloaded hole. The clamp-up load for chopped strand mat and woven roving material was found to be decreasing with time; the reduction of the woven roving material was higher than for chopped strand material. However, they showed that in order to significantly affect the strength of the joint, a considerable drop in the bolt's tension was needed. They also showed that by tightening the bolts, the failure mode for a multi-bolt joint could change.

Ruben (1984) presented a curve showing the reduction of the bearing strength of chopped strand mat material with time. The same graph showed that the reduction in bearing strength was associated with reduced lateral pressure.

Maekawa, Kaji, Hamada and Nagamori (1985) investigated the effect of clamp up on the behaviour of joints in chopped strand mat material by varying the applied torque from 0 to 12.8 Nm. Their results showed that by increasing the bolt torque, the strength of the joint increased but the behaviour became more brittle. This was associated with higher tendency towards tension through the hole failure mode.

Kretsis and Matthews (1985) reported that the strength of GFRP increased with lateral pressure and that the effect depended on the washer size. They found that a lateral pressure of 12MPa will result in achieving 90% of the maximum possible strength of the joint.

Ruben (1987) reports that for thick laminates, the strength of joints using a pin in chopped strand mat material was greater than that for the clamped case. For thinner laminates, however, it was possible to increase the failure loads by clamping the specimens.

Arnold (1989) demonstrated that for chopped strand mat laminates the failure mode transition from tension to bearing changed with increasing the clamping load. For 'finger-tight' and pin configuration, the critical w/d was 6 while for a clamping force equal to 2 kN, the critical value for w/d was 12. It was also shown that only specimens with $w/d > 6$ demonstrate significant improvement in the strength moving from pinned to finger tight arrangements. The effect of the distribution of the clamp-up stress on the behaviour of the joint was also investigated. Plain, bevelled, recessed and plain washers supported by bevelled and recessed ones were considered. Although the ultimate load was found to be unaffected, significant

damage of the recessed washer was observed at 30% of the ultimate strength. The damage associated with the final failure of the latter case was high and resulted from a brooming type of failure under the washer.

2.2.2.3. HOLE TOLERANCE

In practice, some clearance between the hole and the fastener does exist. The reduction of this clearance is beneficial for the strength of the joint. The use of interference-fit bolts can also result in improvements in the load bearing capacity, provided that no excessive damage results during installing the fastener.

Stockdale and Matthews (1976) investigated the difference between the behaviour of joints using standard washers and washers with push fit holes. Their results showed that there is no difference between the strength obtained using both types of washers but the load-displacement behaviour was different at the initial loading stages.

Matthews, Godwin and Kilty (1982) reported that an oversize hole would reduce the strength of a joint. Their results also indicated that the effect was inversely proportional to the non-dimensional end distance.

2.2.2.4. FASTENER SIZE

Due to their low modulus of elasticity, glass reinforced polymers show low buckling strength. Therefore, the bearing strength of joints made from this material is not directly proportional to the diameter of the fastener. This is due to the development of local buckling failure when the ratio between the diameter and the thickness of the plate is increased.

Lehman and Hawley (1969) showed that the full bearing strength did not develop when the ratio between the diameter of the bolt and the thickness in 0/45° S-glass material exceeded two.

Matthews, Godwin and Kilty (1982) demonstrated that the bearing stress increased with falling d/t for finger tight bolts. For fully tight bolts, the bearing strength slightly increased with larger d/t. It is not clear, however, whether the bolt size or the thickness of the plate was varied. If the former was changed, then the increased strength of the fully tightened specimens might have been only due to the increased maximum allowed torque of bolts with larger diameters.

Matthews, Roshan and Phillips (1982) reported that for glass/epoxy, the bearing strength of finger tight joints using different diameters and plate thicknesses decreases with increasing d/t ratio.

Ruben (1984) presented curves for the dependence of the pin-bearing strength of chopped strand mat material on the thickness of the plate. These results showed that for a constant diameter, the strength increased with thickness which meant that the strength increased with reducing d/t.

Kretsis and Matthews (1985) showed that the strength of 'finger-tight' clamped specimens in glass/epoxy decreased with increasing the ratio of the diameter to the thickness of the plate. They used this phenomenon to explain the reduction of the critical non-dimensional end distance with increasing diameter.

2.2.2.5. FASTENER PATTERN

Strauss (1960) reported that joints fastened with multiple rows of fasteners displayed a higher strength than the joints with equivalent hole size and spacing, in which the fasteners were arranged in a single row. The strength per bolt, however, decreased with increasing number of bolts. His results also suggested that increasing the number of bolts per row resulted in a reduction of strength of the joint. These results could be explained by the small transverse pitch of the specimens resulting in increased stress concentration. The increased strength for the specimens in the multiple row specimens seemed to be due to stress shielding.

Porter (1976) investigated the correspondence between the strength of a single bolt joint and that of a joint employing four bolts in a row. He showed that provided the single bolt test results were obtained for specimens which were clamped in the same way as the multi-bolt specimen, the same strength per bolt could be achieved.

Pyner and Matthews (1979) showed that the single and multiple hole joints sustained the same maximum load per bolt, provided the holes were in a row normal to the loading direction. However, when the bolts were lying on a line which was parallel to the line of action of the force, the strength decreased with increasing number of rows. The strength was also reported to deteriorate with increasing the complexity of the joint. It has to be noted, however, that for the specimens employing rows of holes, the ratio between the width of the specimens to the number of bolts was not equal. This meant that their comments regarding the load distribution at failure were not valid specially that the failure was due to tension through the hole. They also showed that the load-deformation curves of multiple bolt specimens were

smooth while those for single bolt specimens were not. Their results for a staggered configuration were discouraging.

Godwin, Matthews and Kilty (1982) considered multi-bolt joints of GRP composites. The joints were designed such that stiffness matching was achieved. The specimens which contained two bolts arranged parallel to the loading direction had a non-dimensional pitch varying between 3 and 6. They reported that bolts in rows in woven roving material with equal fibres in both directions did not develop a failure load per bolt as high as bolts in joints employing one row due to the interaction between the rows. It was also shown that bolts in a line yielded a higher failure load at a reduced end distance when a full shear-out failure developed. A reduction of the strength per bolt occurred for bolts arranged in a row with small pitch. For chopped strand mat material, the strength per bolt of multiple-fastener joints was always lower than that for a single fastener joint. The failure of the chopped strand material was always in tension through the holes. No substantial improvement in strength using staggered rows of bolts was found, although an increase in energy absorption due to damage was evident. The strength of staggered bolts in woven roving material was found to be equal to that of a joint where the bolts had a spacing equal to half the pitch used in the staggered configuration irrespective of the back pitch. The effect of varying the side distance relative to the pitch of joints made using a row of fasteners was also considered. This effect was found important when the failure was due to tension through the holes. In some cases tensile failure developed between the fasteners and then the failure progressed in shear.

Ruben (1984) investigated the effect of using two pins in chopped mat materials. The failure load per pin for the specimens which had the pins in series was less than that for one bolt. Increasing the pitch of the joint improved the strength only marginally. The strength per pin, however, approached the strength for a single pin joint by increasing the width. The strength of specimens which had the pins in a row showed strengths which were higher than the strength of a single bolt joint when the pitch was large while the side distance and end distance were small.

Hamada, Maekawa, Kaji and Nagamori (1986) investigated the damage propagation in two-bolt joints for chopped strand mat material. They showed that the damage in the transverse direction at the inner bolt was significant. The failure of all specimens considered was in tension through that hole.

2.2.3. LOADING HISTORY

The properties of fibre reinforced materials are affected by their history. This is due to the development of damage and the viscous nature of the matrix. Therefore, the behaviour of joints made in this material is also affected by the loading conditions and the environmental effects.

2.2.3.1. LOADING CYCLES

Lehman and Hawley (1969) conducted fatigue tests on both single and double lap bolted joints in 0/45° S-glass fibre reinforced material. The maximum loads considered ranged from 60 to 80% of the static fatigue load at 900 rpm. This low speed was needed to prevent high temperature rise. They reported that the fatigue lives of double lap joints were longer than those of single lap joints.

Found (1986) considered the fatigue behaviour of bonded fasteners which were either bonded on the finished members or fixed during the lamination process. The results of this investigation showed that the bonded-in fasteners performed better. In addition, it was found that the shape of the edge of the bolt's head had a significant effect on the results.

Hamada, Maekawa, Harino and Kaji and Shina (1987) conducted low cycle and high cycle fatigue tests on chopped strand mat and woven roving glass polyester materials. They found that the deformations increased with time uniformly, until a sudden increase in the deformations developed. After that, the specimens were able to take more load, but they recommended this number of cycles to define the fatigue life of the joints.

Little and Mallick (1990) investigated the fatigue life of sheet moulding compound material subjected to tension cycles. Their work showed that chopped strand mat material failed away from the joint provided the bolt was highly torqued and that the ratio between the width and the diameter was less than four. This was in line with the findings of Mallick (1988) where it was shown that applying a lateral pressure had a beneficial effect on the fatigue life of specimens with open holes. When the width of the joint was increased, failure occurred at the joint. It was also found that the washer size and the thickness of the laminate had a strong influence on the fatigue life. A further recommendation was to apply of a clamping pressure that was high near the hole and reduced away from it.

2.2.3.2. LOADING DIRECTION

Because of the orthotropic nature of the material, it is expected that the loading direction will affect the behaviour of the joint. This aspect is of importance due to the uncertainty about the loading to which the joint will be subjected.

Dallas (1967) investigated the effect of applying the load parallel, perpendicular and at an angle of $\pm 45°$ to the longitudinal fibre direction in a 0/-45/0/$\pm$45/0/45/0 lay-up of S-glass epoxy laminate. The results showed that a small reduction in the strength occurred for riveted specimens.

Matthews and Hirst (1978) investigated experimentally the variation of the bearing strength with the direction of the load applied to joints in GFRP and GRP. They found that the shape of the load-deflection curve did not depend on the fibre direction. However, the variation of the strength of GFRP joints was similar to the change in axial stiffness. For GRP laminates, on the other hand, the ultimate strength varied in a similar manner as the shear stiffness, while the variation of the initial failure stress variation was like that of the normal stiffness.

2.2.3.3. LOADING TYPE

Oplinger (1978) investigated the experimental stress concentration due to the combined application of a bearing and a by-pass load. He reported that the effective stress concentration remained unaffected for by-pass loads equal to .75 of the total load or less.

The effect of bearing damage on the tensile strength was investigated by Godwin, Matthews and Kilty (1982). They tested specimens which were previously damaged by bearing and tensile loading. This was considered as a method of assessing the effect of by-pass loads on the bearing strength. They concluded that the damage due to bearing reduced the tensile strength of the material by about 12%. The damage due to subjecting the material to a tension force equal to the bearing load reduced the strength by about half that value.

Tsiang and Mandrell (1985) investigated the damage development due to different types of loading. The load for first cracking increased when the loading method changed from bolt tension loading to bolt compression and reached its highest value when the load was applied at the far ends. This indicated that the stress concentration in the last case was least.

Hamada, Maekawa, Kaji and Nagamori (1986) investigated the damage propagation in bolted joints for chopped strand mat material. They showed that the damage initiated in the bearing area; the damage in the net tension plane was low but for tensile failure modes, it increased suddenly.

2.2.3.4. ENVIRONMENTAL EFFECTS

Environmental effects have a strong influence on the material properties of fibre reinforced polymers. This is mainly due to the sensitivity of the polymers to heat and moisture. Because the joint properties depend to a certain degree on the properties of the material, it is necessary to investigate the influence of environmental factors on the behaviour of the joints.

Maekawa, Kaji, Hamada and Nagamori (1985) investigated the effect of temperature on the behaviour of chopped strand mat bolted material. They measured the strength under temperatures ranging from 20° to 120°C. The failure modes at 80° and 120°C were found to be always of the bearing type. It is important to note that the resulting strength was reduced dramatically.

Hamada, Maekawa, Horino and Kaji and Shina (1987) investigated the creep strength of mechanical joints in chopped strand mat and woven roving glass polyester material. They defined the creep life of the specimens as the time when the creep displacements increased suddenly. Their results showed that the failure of the long term specimens corresponded to the static failure mode. The creep displacement also corresponded to the static displacements. It was possible to predict the behaviour of hybrid materials which consisted of chopped strand mat and woven roving plies using the behaviour of each of the layers. They recommended the first significant damage time as the creep life. This time was shown to be generally earlier than the time of the final bearing failure.

2.2.4. DESIGN IMPROVEMENTS

The strength of joints in fibre reinforced materials can be improved using special designs. These improvements can be achieved by reinforcing the joint area or using revised fastener designs. In the following sections, the techniques applicable to glass reinforced materials will be reviewed. In some cases, the method discussed is not applied to glass fibre material but it is included because it can be applied to the present material.

2.2.4.1. LAMINATE DESIGN

Some fibre orientations improve the strength of the composite members but they result in joints which are not efficient. In these cases, the local reinforcement of the laminate is useful. The reinforcement can be achieved by encapsulating metal shims and metal inserts into the composite or by layer build-up at the bolt location.

Strauss (1960) obtained results which discouraged the use of local reinforcing layers at the points of high stress concentration. He found that the increase in the strength, compared with the required increase in the thickness, was small. The use of aluminium plates caused the specimen to fail at a lower load than the unreinforced specimens. This was explained by the great difference in the stiffness of the laminate and the reinforcing plate. It was also reported that the increase of the thickness would also increase the bending stresses in single lap joints.

Dallas (1967) showed that a 50% increase in the bearing strength of unreinforced bolt holes in S-glass/epoxy can be obtained by the introduction of glass fibre reinforcing layers or thin steel doublers. This meant that it is possible to achieve a unit efficiency. The efficiency of the joint is defined as the ratio between the strength of the joint to the strength of the parent material. His results showed that the improvement of strength due to adding steel shims was larger than the improvement due to adding local glass cloth reinforcement. The addition of a steel mesh at the end of the member resulted in reducing the strength of the joint.

Lehman and Hawley (1969) investigated the effect of reinforcing the holes in $0/\pm 45°$ material using either a composite or a steel shim reinforcement or a steel bushing. The joint efficiency was reduced by using steel bushings. The use of steel shims or the local thickening of the plate resulted in improved joint efficiency. Interestingly, they reported that a combination of bolted-bonded joint performed better than bolted or bonded joint. This, however, was caused by a change in the failure mechanism.

Sturgeon (1971) discussed the reinforcement of fibre reinforced composites using interleaved shims. He showed that in order to produce an economical design, the shims had to be wedged with their tip pointing into the plate.

Van Siclen (1974) considered the reinforcement of the joint using metallic interleaves, externally bonded metallic doublers and laminated cross-ply build-up. He showed that in some cases the failure occurred at the end of the reinforcing plates. His results demonstrated that the lightest design was that using extra layers at the area containing the hole. The next economical design was the one that used interleaved titanium plates. However, the calculations were based on the thickness only. This meant that the possible reduction in the needed end distance was not included.

Johnson (1978) used a wire mesh in carbon/glass hybrid composite to assist in carrying the load from the screws to the laminates. He reported that this type of reinforcement resulted in lowering the strength.

Oplinger (1978) proposed the use of slotted holes for multiple row specimens. This proposal was meant as a means of distributing the load more evenly. However, such an approach could result in problems under repeated loading.

Oken and Deppa (1978) investigated the use of an insert and a doubler on the fatigue strength. Their results showed that these designs did not present any improvement over unreinforced bolted joints.

Matthews, Roshan and Phillips (1982) investigated the effect of carbon fibre content on the bearing strength of joints in a hybrid carbon-glass reinforced polyester laminates. They found that a 1:1 hybrid had a strength close to all-glass material. The addition of smaller amounts of carbon fibres reduced the strength of the joint. The highest strength was achieved for all-carbon fibre material.

Nelson, Buinin and Hart-Smith (1983) investigated the effect of changing the design of the lap plates for joints in carbon-fibre reinforced laminates. They showed that the optimum strength of a joint that used four bolts was achieved by tapering the splice plates at their ends and reinforcing them near the middle section.

Knight (1989) investigated the effect of an unbonded inclusion on the failure load of a joint in a fibre reinforced laminate. He found that the tensile strength of the joint was not affected by this inclusion.

Nilsson (1989) reported an increase in the strength of graphite/epoxy bolted joints due to introducing a bonded metallic ring to the inner surface of the joint hole. This resulted in a 55% increase in the strength over the unreinforced case when using an aluminum ring and 30% when using a steel ring.

Herrera-Franco and Cloud (1992) considered relieving the strain in glass epoxy plates using bonded inserts. Their results showed that the use of aluminium inserts resulted in less stress concentration compared to an epoxy insert. The superiority of the aluminium insert prevailed even after its bond with the plate broke.

2.2.4.2. FASTENER DESIGN

It is possible to increase the efficiency of joints in glass fibre reinforced materials by updating the design of the fasteners. Investigations were conducted to replace metal fasteners by polymeric ones in order to decrease the weight and to overcome the corrosion problems. Other investigations were aimed at improving the performance of metallic fasteners.

Gangalez (1975) investigated the feasibility of producing GRP thermoplastic bolts. He found that the optimum fibre volume fraction that would satisfy the short and the long term structural requirements was 0.15.

Webb (1978) recommended the use of low shank-expansion rivets which require low tail-forming forces. He also proposed the use of metal backing plates or washers under the tail

of rivets. This was mainly meant as a precaution against the excessive damage of the laminate during fabrication.

Cole, Bathe and Potter (1982) reported many improvements in the bolt design to fit the requirements of jointing FRP, among them was the introduction of the big foot bolts.

Hao, Luhham and Sankar (1985) proposed the use of an interlocking moulded insert for jointing sheet moulding compound. The insert was hexagonal and had a hole for accommodating a bolt. In addition, one of each pair of inserts had a protruding ring that fitted into a recess in the other insert. This protruding part transmitted the load through an interlocking action. The strength of this system had the same strength as bolted systems but its stiffness was higher. The failure of this type of joints was due to debonding triggered by the eccentricity of the single lap joint. In a later investigation (Hao, Di Maria and Feldman 1987) the insert was manufactured from stainless steel and the effect of moisture on the strength was investigated. It was found that the difference between the dry and the wet strength of the insert joint was less than that for bolted joints.

Blosser (1989) proposed special fasteners for jointing orthotropic materials. The heads of the bolts were formed such that they could eliminate the stresses resulting due to the difference in the thermal coefficients of expansion of the plate material and the fastener material.

Carter (1989) suggested the use of surface-bonded fasteners to eliminate the problems associated with drilling and the subsequent stress concentration. A similar type of fastener was previously investigated by Found (1986).

2.3. NON-DESTRUCTIVE EXPERIMENTAL INVESTIGATIONS

Oplinger (1978) showed using Moire surface strain measurements on pin loaded fibre glass test pieces, that plastic deformations had a significant effect on stress distributions and failure.

Pradhakaran (1982) used photoelasticity to demonstrate the effect of reducing the end distance in glass-epoxy pin loaded plates. The material considered was quasi-isotropic and unidirectional. He showed that the maximum shear stress decreased when the end distance was increased and that the variation of stress for large end distances was limited. In addition, he pointed out the importance of choosing glass-fibre and resin materials which had the same refractive indices.

Rowlands, Rahman, Wilkinson and Chiang (1982) used Moire interferometry to investigate the stresses in unidirectional glass polyester material. Their experimental results for single and double hole joints were verified using finite element analyses.

Hyer and Liu (1983) investigated a joint employing two pins in series using photoelasticity. They showed that the load, which was shared between the pins, could be determined based upon the location of the isotropic point which was formed between the two holes. This investigation used normal bifringent isotropic material. The maximum tensile stress concentration factor on the inner bolt was found to be higher than that near the outer hole. The stress concentration of the outer hole was found to correspond to the stress concentration of the single bolt hole. The stress concentration, which was based on the nominal bearing stress, was shown to increase when the width to diameter ratio of the joint was increased.

Hyer and Liu (1984) considered quasi-isotropic materials and Hyer and Liu (1985) presented photoelastic results for orthotropic glass epoxy plates loaded by a pin. They demonstrated that the fringes in that material were less sharp than in usual bifringent material. The effect of anisotropy was demonstrated by comparing the results for quasi-isotropic, unidirectional and angle ply laminates. Results similar to Pradhakaran (1982) were reported, but in addition, they used equilibrium conditions to separate the stresses. Accordingly, they presented diagrams for the stresses on the critical planes.

Serabian and Oplinger (1987) demonstrated the need for considering the shear non-linearity of 0/90° S-glass epoxy laminates. This was undertaken by comparing the results obtained using Moire interferometry and those of a linear elastic finite element analysis on the curve where shear failure developed in experiments.

Zimmerman (1991) used the Moire technique to determine experimentally the stress concentration factors in some GFRP multi bolt joints. He showed that there was interaction between the stresses around the holes.

Serabian and Anastasi (1991) measured the out-of-plane deformations of pin loaded glass epoxy composite plates using Moire method. The results obtained were different from the results of linear finite element techniques. They considered this as an indication of non-linear through-thickness behaviour. This nonlinearity might have been due to interlaminar failure or non-linear material behaviour.

Herrera-Franco and Cloud (1992) used Moire interferometry to investigate the strain fields in glass epoxy joints. This investigation dealt with analyzing a joint which had an insert of a different material around the hole.

Pradhakaran and Naik (1986) developed a technique for measuring the contact angle between the plate and the bolt and Koshide (1986) and Tsai and Morton (1990) also conducted

Moire interferometry investigations. However, these studies will not be discussed further because they were performed for carbon fibre material.

2.4. THEORETICAL INVESTIGATIONS

The theoretical investigations of joints in composite materials has been undertaken using a diverse number of analysis techniques and models. In this review, the analysis techniques which have been applied to the problem of jointing composite materials will be reviewed as well as the models which have been proposed for the analysis.

2.4.1. METHODS OF STRESS ANALYSIS

The methods used for the stress analysis of joints in composite materials can be grouped under two headings; the first is the analytical technique and the second is the numerical technique. In addition, the analysis of joints includes solving a contact problem which has been solved using various techniques.

2.4.2.1. ANALYTICAL METHODS

This type of stress analysis technique is based on the classical theory of orthotropic elastic bodies advanced by Lekhnitski (1968). This method has only been used for the plane problem combined with the classical laminated plate theory for linear elastic materials.

Wazcazk and Cruse (1973) applied a superposition technique using the results of an infinitely large plate which was loaded by a pin together with the results of a notched plate which had a finite width and was subjected to tension to estimate the results for a finite plate loaded by a bolt. The solution for the notched plate was obtained using the boundary integral method and the pin was approximated using a radial cosine stress distribution.

Oplinger and Gandhi (1974) considered directly a plate of finite dimensions and imposed the boundary conditions using the least squares collocation method in association with the complex variable approach for plane elasticity. Their analysis considered a single pin and an array of pins in a finite rectangular plate and an isolated pin in an infinite plate.

De Jong (1977) used a sine series to represent the contact stress and solved the problem by determining the coefficients of the series using the boundary conditions along the hole. This solution was then superimposed on the solution of another infinite plate subjected to tension at

its far ends in order to get an approximate solution for the finite plate. In this investigation the contact angle was assumed to be a fixed value less than 180°.

Garbo and Ogonowski (1981) applied bearing and by-pass loading on the plate and used the cosine contact pressure distribution. The solution technique was similar to that of De Jong except that they only used the first term of the contact stress series.

Bohlmann, Renieri and Liebeskind (1981) developed a two dimensional compliance method to analyze an orthotropic repair patch. The influence coefficients were determined using the complex variable theory and the boundary collocation method.

To consider the friction between the plate and the pin, De Jong (1982) introduced a "release area" which made the problem mathematically more tractable by ensuring that the functions representing the radial and tangential stress varied smoothly between the slip and non-slip regions.

Mangalgiri (1984) applied an inverse technique to investigate the contact of a smooth rigid pin with an infinite orthotropic plate. The solution of this investigation was restrained to a sub class of orthotropic materials.

Zhang and Ueng (1984) presented an approximate solution for determining the stresses in an orthotropic plate loaded through a hole. The results were obtained using superposition of the solution of a pin loading a semi-infinite sheet on the solution of an infinite plate containing an unloaded hole. The result did not allow for the variation of the contact angle but it considered friction. The radial stress distributions obtained for the frictionless case showed good agreement with those of De Jong (1977), but the hoop stress predictions were quite poor. In a later paper (1985), they considered arbitrary loading directions.

Naidu, Dattaguru, Mangalgiri and Ramamurthy (1985) applied an analytical technique for finite size orthotropic plates loaded at the ends in the presence of a smooth rigid misfit pin. The conditions on the outer boundary were obtained by zeroing the boundary error functions. Their results were based on an inverse formulation.

Hyer and Klang (1985) considered the contact between an elastic pin and an infinite plate. The pin was modelled as a circular plate subjected to a body force equal to the average shear stress. An iterative method was used for finding the contact arc and non-slip area based on the "correctness of the radial and shear stress distributions".

Bohlmann, Renieri and Riley (1986) combined the boundary integral method with the collocation method to solve the problem of the loaded hole.

Wilson and Tsujimoto (1986) presented an approximate solution based on the action of the cosine distribution of the radial stresses on half a hole in an infinite plate. They approximated the stress conditions in a finite plate by adding the solution for an infinite plate

containing an unloaded hole and subjected to tension. They reported that the stresses predicted by this analysis for plates with widths ranging from 2 to 8 were reasonably accurate.

Mahajerin and Sikarskie (1986) compared the use of the boundary element method and the finite element method for the analysis of joints in composite materials. Their paper reports that the boundary element technique resulted in savings in computer resources.

Vable and Sikarskie (1988) used the boundary element method to find the stress distributions around loaded holes in finite-sized plates. Their work, which was based on Green's stress functions, presented explicit expressions of these functions using real variables. They used iterative methods to determine the contact and separation areas.

2.4.1.2. NUMERICAL METHODS

Numerical methods have been extensively used to analyze bolted joints in composite materials due to the ease of applying them. The accuracy of such an analysis must always be checked against analytical solutions or experimental results whenever they are available. The technique mainly used is the finite element method. The application of the laminated plate theory with finite elements has been generally undertaken using two dimensional displacement based elements. Most of these analyses were similar but some innovations were tried.

Baumann (1982) modelled the joint through the thickness but he assumed that it was a two dimensional problem. In that study the fasteners were modelled using beam elements.

Matthews, Wong and Chyrassafitis (1982) conducted a full three dimensional analysis but they limited the number of elements through the thickness to one. This was achieved using a special layered version of the 20 noded isoparamtric brick element.

Tsiang and Mandrell (1985) used a hybrid stress element in the analysis of a bolted joint to ensure the satisfaction of the stress free condition.

Wang and Han (1988) derived a special element to represent the fasteners in multi-fastener joints. This element was suitable for use in conjunction with a two dimensional formulation.

Barboni, Gaudenzi and Carlini (1990) developed an interesting finite element procedure where they reduced the geometry of the problem from three dimensions to two dimensions while retaining the possibility of having changes through the thickness. In that method, the degrees of freedom were taken as the contribution of each of the terms approximating the variation of the displacements through the thickness. This provided an unlimited degree of accuracy which was dependent on the number of terms considered.

Another method of numerical solution is the boundary element method. Since this method is considered as an extension of the analytical methods, it has been reviewed with the analytical investigations.

It seems that the finite difference method has not been used in the analysis of the problem under consideration. This might be due to the difficulty of specifying the boundary conditions along curved boundaries.

2.4.2. METHODS OF SOLVING THE CONTACT PROBLEM

Generally, the contact conditions between the plate and the pin can be satisfied by applying an iterative method. This iteration is usually done using special elements which can transmit compressive stresses only. Some of these elements can also consider friction. Wilkinson, Rowlands and Cook (1981) took friction into consideration and defined regions of slip in the contact area. The contact and slip areas were automatically determined using an incremental iterative technique. An interesting variation of the iterative technique was proposed by Murthy, Dattaguru, Narayana and Rao (1990) where they condensed the stiffness matrix of the joint such that only the degrees of freedom associated with the contact problem remained. This technique was equivalent to substructuring and could reduce the running cost dramatically.

The inverse technique can also be used if the material is orthotropic and the pin is not exactly fitting the hole. This is done by assuming a contact area and calculating the corresponding load (Rao 1978). The method has been applied in practice by solving two linear problems for the assumed contact area. The first is due to a radial displacement equal to the misfit of the pin and the second is due to the applied load. The two solutions are then combined such that the radial stress at the ends of the contact area are equal to zero. The technique has been used by Mangalgiri (1984) and Mangalgiri and Dattaguru (1986) to investigate the effect of misfit pins on infinite orthotropic plates. Naidu, Dattaguru, Mangalgiri and Ramamurthy (1985) used the same approach to investigate finite orthotropic plates. Mangalgiri, Dattaguru and Rao (1984) used an inverse formulation in association with the finite element method. In that investigation, they replaced the requirement of zero radial stress at the transition points by a condition of zero radial nodal force. Considering the definition of the radial nodal forces in the finite element method, it becomes clear that this method is only approximate.

A modified method for using the inverse technique has been proposed by Naik and Crews (1986). In this variant, the solutions which were combined to find the final solution were obtained under the effect of the misfit plus the effect of the load. The only difference between the two solutions was the level of the applied load. This method has been used by Ramamurthy

(1989a) where the effect of interference-fit pins was investigated. In that work, it was demonstrated that a compressive load on the lug can result in two contact areas. The positions of the contact areas were determined using a technique combining iterative and inverse methods. In a later paper Ramamurthy (1989b) considered the case of a clearance-fit pin. Naik and Crews (1991) considered the problem where a by-pass load was acting in the presence of a clearance-fit pin. In this investigation, the possibility of handling double contact conditions using the inverse technique was demonstrated.

2.4.3. THE MODELLING TECHNIQUES

The mechanical jointing of composite materials should be investigated as a three dimensional problem. However, due to its size, it has been generally solved as a plane problem which has resulted in different degrees of accuracy in modelling the fastener.

2.4.3.1. MODELLING THE FASTENER

The original problem of the contact between the bolt and the laminate is a non-linear contact problem between two elastic orthotropic inhomogeneous bodies in three dimensions. Due to the relatively high stiffness ratio between the plate and the fasteners, it is possible to model the latter as rigid. This implies that the fastener may be assumed as a rigid push-fit frictionless pin.

2.4.3.2. THE RIGID FRICTIONLESS ASSUMPTION

The correct application of the rigid frictionless boundary condition requires that the points along the contact surface move along the curved pin boundary. The points outside the contact area must be free from any stresses and their displacement must be directed away from the pin.

The size of the contact area was investigated by Oplinger and Gandhi (1974) who demonstrated that contact angle depended on the dimensions and the material properties of a finite size plates. Rowlands, Rahman, Wilkinson and Chiang (1982) showed the dependence of the contact area on the clearance between the plate and the pin. Mangalgiri (1984) investigated the effect of the loading level and the size of the pin relative to the hole diameter on the contact angle. He showed that for highly loaded infinite plates this angle did not depend on the degree of orthotropy of the material. Marshall, Arnold, Wood and Mousley (1989)

reported that the contact angle was variable through the laminate thickness. Ramamurthy (1989 a&b) and Naik and Crews (1991) showed that under certain conditions, it is possible to obtain multiple contact areas.

2.4.3.3. STRESS BOUNDARY CONDITIONS

The application of the rigid pin boundary conditions using analytical techniques is complicated. Therefore, Bickley proposed in 1928 the approximation of the contact stress using a cosine pressure distribution acting on the loaded half of a hole in an isotropic infinite plate. This method has been repeatedly adopted for other types of material and finite size plates. Therefore, many investigations were conducted to assess the accuracy of this method compared to more rigorous techniques.

The sensitivity of the stress field of a pin-loaded plate to changes in the contact pressure was investigated by Waszczak and Cruse (1971). In their investigation, they considered three different pressure distributions acting on the loaded half of the hole in a quasi-isotropic laminate; they concluded that no significant change in the stress field resulted.

Oplinger and Gandhi (1974) compared the stresses due to a radial cosine displacement with the stresses due to radial cosine pressure distribution in the contact area. They found that the cosine pressure distribution was adequate for end distance to diameter ratio values equal to or greater than two and with relatively small widths.

De Jong (1977) showed that for high degree of orthotropy, the difference between the actual and the cosine contact pressure was high and that the degree of change in the stress field depended on the degree of orthotropy.

Humphris (1978) agreed that the maximum stress beside the hole was insensitive to the pressure distribution. However, he reported that the stress pattern over the entire lug was significantly affected by the shape of the distribution.

Agrawal (1980) compared the cosine pressure distribution and the correct contact pressure and he concluded that they were similar. In addition, he investigated the effect of using different contact pressure distributions on the predicted joint strength using the average stress failure criterion. He found that the tensile and shear-out modes of failure seemed to be less sensitive than the bearing mode of failure. The bearing strength for a pressure distribution covering only a part of the hole was found to be significantly lower in value than the other two pressure distributions which covered half of the hole circumference. The same statement was given by Ramkumar (1981).

Wong and Matthews (1981) also investigated the differences between the cosine radial stress distribution and assigning constant axial displacements at the loaded part of the hole. They reported that the differences between the resulting stress fields were small.

Tsujimoto and Wilson (1986) investigated the displacements resulting from using a radial cosine stress distribution, radial cosine displacements and a completely fixed boundary condition. They found that only the radial cosine contact pressure distribution yielded appropriate deformations for the hole.

Chang (1986) also performed an analysis to evaluate the effect of the assumed pin load distribution on the calculated strength and the predicted failure mode using the characteristic curve failure hypothesis. He reported that the effect was small.

2.4.3.4. DISPLACEMENT BOUNDARY CONDITIONS

The representation of the rigid frictionless push-fit fastener is possible using displacement boundary conditions. The first variant of this technique is to prescribe the displacements of the points lying on the contact arc while preventing points lying on the far end of the plate from moving. Oplinger and Gandhi (1974) applied a cosine radial displacement. Wong and Mathews (1981) applied axial displacements. The second method allowed the movement of the contact points perpendicular to the joint axis and accordingly resulted in friction stresses.

The second variant of modelling the fastener using displacement boundary conditions is to prevent the pin from moving while acting on the far end by either a uniform pressure or a uniform displacement. Agrawal (1980), Ramkumar (1981), Soni (1981a), Chang, Scott and Springer (1982) and Conti (1986) restrained the radial displacement of the loaded part of the hole periphery.

Wilson and Pipes (1981) and York, Wilson and Pipes (1982) restrained the axial displacement of the loaded part of the hole. This violated the frictionless condition in the same way as applying axial displacements on the loaded part of the hole.

Here it has to be noted that the solutions obtained using the inverse technique also use displacement boundary conditions.

2.4.3.5. MODELLING FRICTION

The effect of friction was considered in some investigations. Oplinger and Gandhi (1974) considered friction by preventing the slip along the entire contact region. In a later study

(1975), they used Coulomb friction and considered slip and non-slip areas. They reported that including friction resulted in changing the predicted failure mode. The contact angle and the slip area were determined during the analysis by iteration.

Rowlands, Rahman, Wilkinson and Chiang (1982) investigated the effect of considering friction on the radial contact stress. It was found that it changed the distribution significantly but reasonable changes in the coefficient of friction seemed to have limited effect. They also reported that this effect disappeared at some distance below the pin.

De Jong (1982) also emphasised the effect of considering the friction between the plate and the pin on the stress distribution in an infinite plate. He reported that these changes can result in varying the failure mode. The stresses ahead of the bolt were reported to be reduced by friction. He also considered the effect of a load that did not act in the direction of the fibres. This showed that the maximum stresses changed with the principal fibre direction.

Zhang and Ueng (1984) derived an approximate closed-form formula for the stress in an infinite pin-loaded plate which assumed that the contact angle was 180° and that neglected the presence of a non-slip area. In a later paper, Zhang and Ueng (1985) extended their method of analysis to cope with arbitrary loading directions.

Tsujimoto and Wilson (1986) investigated the effect of including the friction stresses acting along the fastener-hole interface on the stress distribution around the hole in an elasto-plastic analysis. They showed that net tension failure was relatively insensitive to friction effects while bearing and shear-out failures were sensitive. However, when comparing the elasto-plastic results with the experimental results, the condition of no friction gave the best results.

Conti (1986) used the zero radial displacement technique for the contact area and considered the friction by applying a tangential force which was proportional to the radial stress and the cosine of the angle of inclination of the radius going through the point considered.

Eriksson (1986) considered friction and showed that it reduced the bearing and the tangential stress at 0° but it resulted in increasing the tangential stresses at 90°.

An interesting investigation was conducted by Smith, Ashby and Pascoe (1987), where they modelled the damage onset in composite laminates incorporating the effect of bolt clamp-up without using a three dimensional model. This was achieved by subtracting the contribution due to friction on the plate from the total load before it was applied on the hole.

Hyer, Klang and Cooper (1987) considered the effect of friction in a detailed analysis which took into consideration the effect of pin elasticity. Their results clearly showed the variation in the contact stresses under different friction cases.

Yogeswaren and Reddy (1988) considered the effect of friction and differentiated between the static and dynamic coefficient of friction. Their results which were obtained based

on an incremental-iterative technique, showed that the ratio of friction to radial stresses for loading conditions was a constant equal to the dynamic coefficient of friction. When the loading was reduced, the friction in a part of the contact area reversed direction and it took a value equal to the static coefficient of friction.

Liu and Li (1991) used the contact radial and shear stress distributions obtained by Zhang and Ueng (1984) to load finite element models of pin loaded finite plates.

Abd-El-Naby, Hollaway and Gunn (1991) showed that varying the coefficient of friction had a negligible effect on the load distribution of the joint load between the pins of a multiple-pin joint.

2.4.3.6. MODELLING PIN-FITTING

Oplinger and Gandhi (1974) considered various clearances between the fastener and the plate. Rowlands, Rahman, Wilkinson and Chiang (1982) also investigated the bolt clearance effects and concluded that it affected the stress distribution significantly.

Pradhan and Ray (1984) extended the method of assuming the stress distribution to account for the different angles of contact which were encountered in the cases of clearance-fit pins.

Mangalgiri (1984) investigated the stresses due to misfit fasteners in a large orthotropic plate. He clearly showed that except for the push-fit case the contact angles were a non-linear function of the load. However, the rate of change of this angle became slower when the load was increased. This investigation was later extended by Mangalgiri and Dattaguru (1986) to considered the case of a misfit pin under arbitrary oriented biaxial loading.

Hyer and Klang (1985) considered the effect of clearance-fit elastic pins on an infinitely large plate. They showed the variation of the contact area due to this effect.

Naik and Crews (1986) applied the inverse technique in conjunction with the finite element analysis to analyze the behaviour of clearance-fit bolts in a lug with finite dimensions.

Eriksson (1986) considered a clearance fit between a pin and a finite plate using finite elements. His results showed that by increasing the clearance, the contact area decreased. In addition he demonstrated that the contact area increased with increasing load.

Ramamurthy (1989a) considered the effect of an interference-fit pin on finite size plates using the inverse technique. In a later paper (1989b) he considered the case of a clearance-fit plate and showed how to use the inverse technique to handle the cases where multiple contact between the plate and the pin developed.

Naik and Crews (1991) considered the problem of a clearance-fit pin which was acting simultaneously with a by-pass load on a finite size plate. The solution was achieved using the inverse technique and special measures were taken to handle the conditions of double contact areas.

Murthy, Dattaguru, Narayana and Rao (1991) investigated the pin-clearance in anisotropic material. They showed that the contact stresses and the contact area were not symmetrical in general. The contact area reached a constant form when the load was sufficiently high.

2.4.3.7. MODELLING THE ELASTICITY OF THE PIN

The effect of the elasticity of the pin loading an orthotropic plate has usually been neglected due to the big difference in the rigidities but due to the possibility of using composite fasteners, this issue is of importance.

Crews, Hong and Raju (1981) used the finite element method to model the pin and the plate. The connection was modelled using short springs which only permitted the transfer of compressive forces. In that analysis the load was applied at the centre of the pin.

Mathews, Wong and Chyrassafitis (1982) used an arrangement of pin-jointed bars connected between the hole centre and the loaded side of the hole to represent a frictionless fastener. The stiffness of the bars was set sufficiently high to simulate a rigid pin.

Eriksson (1986) considered the elasticity of the pin using finite elements. He reported that changing the material properties of the pin from those of steel to those of titanium had almost no effect on the contact stresses.

Hyer, Klang and Cooper (1987) investigated the effect of pin elasticity, clearance and friction on the stresses in the plate. They considered slip, non-slip and contact areas. The effect of the elasticity of a steel or an aluminium pin was found negligible.

Serabian (1991) used the finite element method to solve the problem of contact with an elastic pin. Changes in the stress distribution with increasing load were reported for linear elastic materials as well as non-linear ones.

2.4.3.8. MODELLING THE CLAMP-UP

Matthews, Wong and Chyrassafitis (1982) modelled clamp-up by preventing the nodes lying between the laminate and the washer from movement in the direction normal to the plane of the plate. This investigation showed that considering clamp-up resulted in changes in the

predicted stresses. The major change being the reduction in the through-thickness tensile stresses.

Marshall, Arnold, Wood and Mousley (1989) considered the modelling of the clamp-up effect. The 'finger-tight' washer was modelled using the same method previously used by Matthews, Wong and Chyrassafitis (1982). A flexible washer was modelled by applying uniform pressure, while for a clamped washer they applied a uniform displacement. The interlaminar stresses were obtained and used to explain the development of the bearing failure at the end of the washer.

2.4.3.9. MODELLING MULTIPLE FASTENERS

The modelling of multiple fasteners which lie in series can be approached by considering the effect of by-pass loads. Oplinger and Gandhi (1974) investigated the effect of by-pass load on the stress distribution in a plate loaded by a pin. Their results showed that the bearing stress decreased ahead of the bolt due to the action of a by-pass load.

Crews and Naik (1986) used the inverse technique in association with the finite element method to obtain the stresses in a plate subjected to combined pin and by-pass loads. In a later paper (Naik and Crews 1991) they extended the method to deal with the combined effect of by-pass load and the clearance between the pin and the hole.

Oplinger and Gandhi (1974) modelled multiple parallel fasteners by preventing the lateral movement of the lines lying between the centres of the bolts. Wong and Matthews (1981) investigated a joint with two parallel pins using finite elements. They found that the maximum strain in the loading direction was greater in an equivalent single pin joint whereas, the opposite was true for the maximum transverse strain.

Rowlands, Rahman, Wilkinson and Chiang (1982) also considered two fasteners in their analysis. When the fasteners were in series, the load distribution between them was assumed. They reported that varying the back pitch in the range between 8 and 12 times the radius of the pin was insignificant as regards the distribution of the contact stress.

Bohlmann, Renieri and Riley (1986) presented a method which dealt with the analysis of composite repairs using multiple fasteners. This method employed analytical methods combined with the displacement method of structural analysis.

Chang, Scott and Springer (1984) considered the effect of by-pass loadings as well as analyzing two fasteners in series and in parallel. In the case of the fasteners loaded in series, they assumed that there was no relative movement between the centres of the pins.

Conti (1986) analyzed a joint containing three parallel bolts. He found that the central pin took 35% of the total load.

Wang and Han (1988) presented a method for determining the loads taken up by each fastener in a joint with multiple fasteners and nonuniform patterns. In that method, special elements were employed to represent the pins. However, these models were not able to consider the slipping and separation between the pin and the plate.

Yang and Ye (1990) proposed a technique for the determination of the load distribution between the bolts of a multi bolt joint. This method was general but it was based on some simplifying assumptions like the negligence of friction and that the contact stresses with the same bolt had the same distributions in all plates joined using this bolt. The method involved an iterative procedure. In 1991, Wan and Yang applied the same technique to a variety of pin arrangements.

Abd-El-Naby, Hollaway and Gunn (1991) investigated the effect of the lay-up of the laminate on the deformations of a plate loaded using two pins. This was shown to be the basis of the interaction between the two pins assuming linear elastic material behaviour.

2.4.4. DESIGN AND STRENGTH PREDICTION

The final aim of the analysis of the bolted joints is the determination of the strength of the joint. Different approaches to this problem have been pursued over the last 30 years but no generally accepted method has been developed. All the work in this field depended heavily on empiricism. The degree of success of the methods was judged based on its generality and the size of the data base needed for calibration.

The early work in the field depended completely on experimental results and therefore, its results were only applicable to one material. Such methods were developed by Kutscha and Hofer (1969) who have foreseen that the most effective method of design of joints for an isotropic materials was to employ semi-empirical methods of design. However, they indicated that a complete stress envelope in four dimensions was required to develop this semi-empirical procedure of design. Lehman and Hawley (1969) proposed two empirical equations to determine the bolted joint bearing and shear strength of $0/\pm 45°$ S-glass fibre material. Van Siclen (1974) added another empirical equation for the tensile strength of the bolted joints in carbon fibre reinforced material.

Hart-Smith (1978) presented a semi-empirical method based on corrected stress concentration factors. The stress concentration factors were those for isotropic materials. The use of these values was justified by the fact that they will be modified anyway using an

empirical factor to account for the development of damage. A similar approach was used by Ruben (1983) where the strength of the material was modified using empirical factors to take into account the stress distribution in the lug. Recently, Chamis (1990) proposed a simplified method for the design of single and multiple bolted joints. This method, however, did not consider the effects of stress concentration on the strength of the joint.

Later work relied on stresses obtained from full stress analyses. The stresses obtained were used in conjunction with a failure hypothesis and a failure criterion to predict the strength of the joint.

Waszczak and Cruse (1971) predicted the failure load based on the distortional energy criterion of Tsai. The circumferential elements of each ply around the hole were tested for failure. As soon as an element in any ply has satisfied the criterion, it was assumed that the lamina had failed and it was removed from the laminate. The load was then redistributed among the remaining laminae. The procedure was repeated until all laminae failed. This method resulted in conservative failure loads. The maximum stress and maximum strain criteria were also applied, but they only resulted in a slight increase in the failure load. The degree of error was reported to be proportional to the percentage of $\pm 45°$ laminates and the failure mode. The distortional energy contours for the main load bearing lamina under the failure load were plotted to determine the damage area which indicated the type of failure. This method was capable of distinguishing between all modes except the shear-out and the tear-out modes. For these cases it was necessary to consider the ratios of the lamina's principal stresses to its respective ultimate strengths in the regions of high distortional energy to differentiate between the two mentioned failure modes. The maximum stress and maximum strain criteria were also used to predict the failure mode, but it was found that the distortional energy method was the only reliable technique.

Oplinger and Gandhi (1975) used Hoffmann's modified distortional energy criterion for layer-by-layer failure detection. This criterion had the advantage of representing the difference of the values for the tensile and compressive strengths. They explained the large differences in the results for the shear failure mode by the disregard of the non-linear shear behaviour in the analysis. They predicted the failure mode by plotting the expected failure load for each lamina around the hole periphery. Comparison was then made with the corresponding ply strengths.

Eisenmann (1976) used fracture mechanics to predict the failure load and the failure location of bolted joints in composite materials. In his method, he determined the stress intensity factor at eight equidistant points along the hole boundary. This was done using the boundary integral method for isotropic materials. A correction to consider the effect of orthotropy was then applied. Failure at these points was detected when the stress intensity

factor was found to be greater than the experimentally determined fracture toughness. The excellent results reported in the paper might have been due to the correction factor applied.

Humphris (1978) improved the technique of Waszczak and Cruse (1971) by making a local change in the laminate stiffness when failure was detected. In that investigation, the failure criterion of Tsai-Hill was used to detect failure. A subsidiary failure criterion was also applied to check splitting normal to the fibres due to direct or shear stress. The failure load of the joint was taken as the load at which the stiffness matrix of the joint became singular. The difference between the calculated and the experimental failure loads was explained by the absence of the confinement effect and the material non-linearity. Using this technique he showed that the point of failure moved from the boundary of the hole into the lug.

Agrawal (1980) used the maximum strain theory to predict the unnotched laminate strength used in the prediction of the strength of the joints. The laminate allowable stress was taken to be the least allowable stress for each individual lamina. The average stress failure hypothesis was used to predict the failure load and the mode of failure. This hypothesis was based upon the principle that a laminate having a notch will fail when the average stress over a certain distance reached the value of the unnotched laminate strength. The direction of the line on which the averaging took place depended on the failure mode under consideration. When considering the tension failure the direction was normal to the load direction along the critical net area and the stresses considered were normal to this direction. For bearing failure detection, the direction of averaging was taken parallel to the load direction and the stresses were the stresses normal to this direction. For the shear failure mode, the direction of averaging was also parallel to the load direction but the stress considered was the shear stress and the line considered was originating from the side of the hole. He determined the failure mode as the one resulting in the least strength. It was reported that this method was incapable of predicting the correct failure mode when the material behaved non-linearly.

Wong and Matthews (1981) investigated the effect of the geometry on the stresses in orthotropic plates loaded using a pin. It was reported that the dependence of the stresses on the geometrical parameters was similar to the dependence of the strength on the geometry.

Tang (1981) proposed a tension failure factor to differentiate between bearing and tensile failure modes in a joint acted upon by a by-pass tensile forces in addition to the pin load.

Ramkumar (1981) used the average stress method to investigate joints in composites. He also described a technique for the analytical analysis of fatigue failure, but he concluded that it was a formidable task.

Garbo and Ognowski (1981) used the point stress hypothesis to predict the strength of bolted joints in composites. They detected failure using the Tsai-Hill criterion and assumed that the laminate fails when the first ply fails.

Soni (1981a) applied the Tsai-Wu criterion in association with the point stress hypothesis. In this investigation, no modification of the stiffness was considered after the detection of the failure in the plies. This was based on the fact that the plies which had failed before the last ply did, did not disintegrate but shared the load with the intact plies. Based on this idea he defined the ultimate strength as the failure strength of the strongest ply at the weakest point of the laminate. In the cases when there was more than one element having the same strength, the element with the minimum second largest ply strength was considered as the area of failure. The failure mode was predicted using the position of the point indicating the commencement of failure.

Wilson and Pipes (1981) investigated the shear-out strength of a pin-loaded composite laminate. They used the point stress hypothesis in association with the maximum stress criterion. For this purpose, they analyzed sixteen different joint geometries with e/d and w/d ranging from 2 to 6. A polynomial was then fitted to the results of the shear stress distribution along the shear critical plane. Thus, the coefficients of the polynomial were functions of e/d and w/d. By equating the shear stress at the critical distance to the unnotched shear strength of the laminate, the shear-out failure load was obtained. When the strength of the joint was higher than the unnotched shear strength, no shear-out failure occurred. This was satisfied for $w/d < 4$. If $w/d > 5.25$, shear-out failure always occurred irrespective of e/d. York, Wilson and Pipes (1982) used a similar technique to predict the bolted joint net tension strength.

Chang, Scott and Springer (1982) combined the Yamada and Sun failure criterion with a characteristic length technique. In their work they replaced the stress point criterion by a characteristic curve to determine the positions at which the failure criterion was evaluated. The criterion was checked for every ply and when one ply failed, the joint was assumed to have failed. They used the location of the point of failure on their characteristic curve to predict the failure mode. When this point was in the sector above the pin, bearing failure was assumed. When the failure point was beside the pin, tension failure was assumed. If the point was about at 45° to the joint axis, shear-out failure was assumed.

Chang, Scott and Springer (1984a) extended their method of analysis to deal with multiple pins. They reported that the accuracy of the predicted failure improved for smaller bolt diameters. Higher differences were reported for cross-ply materials due to the non-linearity of the shear stress-strain relationship. They also proposed a method for the design of these joints (Chang, Scott and Springer 1984b). In a later investigation (Chang, Scott and Springer 1984c)

they considered the non-linearity of the material using a relation proposed by Hahn and Tsai. A tangential formulation of the problem was used and the Yamada-Sun failure criterion was modified by incorporating Sandhu's strain energy failure criterion to consider the loading history. It was concluded that the laminates which had high tensile and compressive strengths compared to their shear strengths could be analysed using linear analyses.

Tsiang and Mandrell (1985) showed that the crack lengths measured experimentally were not related to the critical distance used in the prediction of strength. Accordingly, they concluded that the distance described above was only a curve fitting parameter.

Ueng and Zhang (1985) used their closed form solution with the characteristic curve of Chang, Scott and Springer (1982) to evaluate the ultimate load carrying capacity of mechanically fastened joints. In order to obtain the stresses on the critical curve, they assumed that the stresses decreased with the radial distance from the centre of the hole.

Conti (1986) used the Azzi-Tsai failure criterion. He assumed that the ply failure did not change the overall laminate stiffness and that the laminate failed when all the plies had suffered failure even if these failures occurred at different points in the laminae. This approach was similar to the method used by Soni (1981a).

Klang and De Jong (1984) showed that it is possible to improve the correspondence between the experimental bearing loads and those predicted using the nominal bearing stress by dividing the latter by the sine of half the contact angle.

Tsujimoto and Wilson (1986) conducted non-linear analyses on mechanically fastened joints using an elastic-plastic material model. They showed that the load interval between the damage onset and the ultimate failure was very small. Net tension failures were not accurately predicted using the elastic-plastic analyses when the finite element grids were coarse. However, the method predicted the two other failure types quite accurately. The failure mode was predicted by identifying the areas where plastic strains developed.

Wilson and Tsujimoto (1986) presented a comparison of several commonly employed failure criteria, coupled with a point stress failure hypothesis, used for bolted joint strength and failure mode prediction. They also conducted a sensitivity study for the effect of changes in the characteristic length on the failure strength and modes. By comparing the performance of the different methods, they concluded that they were sensitive to variations in the critical distance, and therefore, they could not be applied with confidence.

Chang and Chang (1987) proposed a progressive damage method, in which they also considered the geometrical non-linearity. This method was only used for tension and shear-out failures because it could not represent the through-the-thickness behaviour.

Serabian and Oplinger (1987) showed that the use of a non-linear shear stress condition for the stress analysis improved the strength predictions of the joints.

Arnold, Marshall and Wood (1990) presented a technique for determining the characteristic distance applicable to the model developed by Chang, Scott and Springer (1982). The model was calibrated for GRP and the resulting accuracy was high.

These failure analysis methods are usually applied using computer programs. Snyder, Burns and Venkayya (1990) compared the more widely available programs from the point of view of data preparation, capability and accuracy of failure prediction.

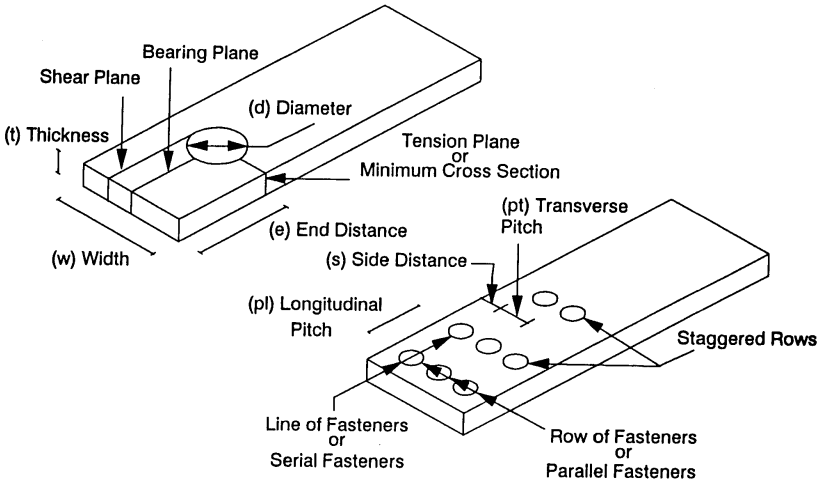

Fig(2.1) Joint Nomenclature

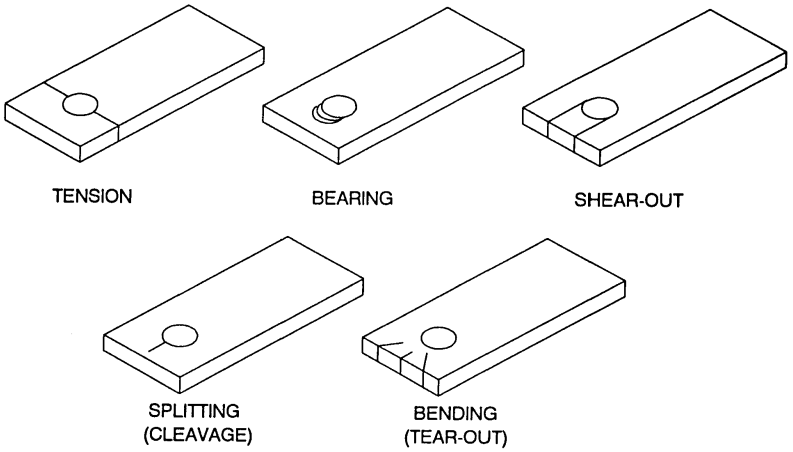

Fig(2.2) Failure Modes of Bolted Joints in Composite Materials

CHAPTER THREE

3.EXPERIMENTAL INVESTIGATIONS

3.1. INTRODUCTION

The experimental behaviour of joints in composite materials depends on the material composition as well as the geometry of the joint. Therefore, in order to understand the behaviour of joints, both aspects have to be investigated. In this chapter, the material behaviour of pultruded glass polyester materials will be characterised, then the characteristics of the behaviour of joints made from that material is studied experimentally.

3.2. MATERIAL ASPECTS OF PULTRUSIONS

3.2.1. INTRODUCTION

The investigation of systems manufactured from composite materials is complicated by the different and diverse possible combinations of the constituent materials. This is in contrast to conventional materials where reasonably accurate estimates of the material properties can be obtained from tabulated information.

Another complication in the analysis of composite materials is the large number of material constants needed for describing the mechanical behaviour. In plane problems of isotropic materials, it is well established (Bickley 1928) that the stress distribution does not depend on the elastic constants as long as the force resultant of the tractions on any boundary is zero. If the resultant of the tractions is a force, then the distribution depends on Poisson's ratio only. Stress distributions in plane composite materials depend on the material properties, but it is possible to establish effective material parameters that control the material behaviour. The analytical solutions of Lekhnitskii (1968) and Green and Taylor (1939) for an anisotropic plate confirm this fact and show that the number of these parameters is less than the independent material properties.

The absence of information about the bounds of the numerical values of the above mentioned parameters of orthotropy has prevented the generalisation of the information obtained about the behaviour of composite structures. Therefore, predictions of the behaviour were very

difficult and uncertain and the results of investigations were considered to be only applicable to the materials for which they were obtained.

Accordingly, the nature of composite materials in general will be discussed in the following sections and the material, which is used in the current work, will be presented; approximate formulae will be obtained for predicting its mechanical constants. Limits on the orthotropic parameters for general glass reinforced composite pultrusions will be established to provide a means for generalising the results of the present work.

3.2.2. DESCRIPTION OF GLASS FIBRE REINFORCED PULTRUSIONS

Glass fibre reinforced pultrusions are available in the form of thin walled cross sections (plates, angles, box sections, tubes, I, C and T sections) or solid rods of various cross sections (FIBREFORCE 1988). Generally, the thin walled cross sections are composed of laminae containing different fibre orientations and forms whilst the rods have only unidirectionally aligned reinforcement. Because of the small thickness of thin walled sections, the layered nature of the material can be considered using the laminated plate theory. This means that it is possible to obtain reasonably accurate estimates of the properties of the pultrusions from a knowledge of the properties of the laminae.

The lamination in pultrusions can result from adding glass fibre reinforcements in any of the following forms (FIBREFORCE 1988):

a) aligned long fibres in different directions in addition to the axial direction,
b) continuous filament mat,
c) chopped strand mat and
d) woven roving mats.

From a macroscopic point of view, the layers resulting from the use of the above mentioned reinforcements can be classified as either orthotropic or isotropic. The properties of composites reinforced using the isotropic forms can be predicted from the properties of the unidirectionally aligned ones. Hull (1981) gives the following expressions which were derived by Akasaka (1974) for the properties of in-plane random long fibres as:

$$\bar{E}=\left[\frac{E_L+E_T+2\nu_{LT}E_T}{1-\nu_{LT}\nu_{TL}}\right]*$$
$$\left[\frac{E_L+E_T-2\nu_{LT}E_T+4\,(1-\nu_{LT}\nu_{TL})\,G_{LT}}{3\,(E_L+E_T)+2\nu_{LT}E_T+4\,(1-\nu_{LT}\nu_{TL})\,G_{LT}}\right] \qquad (3.1)$$
$$\bar{G}=\frac{E_L+E_T-2\nu_{LT}E_T}{8\,(1-\nu_{LT}\nu_{TL})}+\frac{1}{2}G_{LT}$$
$$\bar{\nu}=\frac{\bar{E}}{2\bar{G}}-1$$

Where the subscripts L and T refer to the longitudinal and the transversal direction respectively, V_f is the volume fraction of the fibres and the properties with a bar are those of the randomly orientated materials.

This means that approximate properties of the pultrusion can be determined based on the properties of the unidirectionally aligned layer only. It has to be noted here, that this approximation implies that the packing of the fibres of different types in a laminate is similar to their packing in a rod reinforced using unidirectional fibres having the same fibre fraction. This is not strictly correct but is considered as an acceptable approximation.

3.2.3. MECHANICAL PROPERTIES OF AXIALLY REINFORCED POLYMERS

Glass fibres have a nearly circular cross section and therefore, composites reinforced with this type of fibre have been idealised as a block of matrix containing an array of cylinders Fig(3.1). This model is usually simplified further by assuming transverse isotropy. The latter assumption has been accepted for composites produced using manufacturing techniques where lateral pressure is applied (Whitney, Daniel and Pipes 1984). The pultrusion technique does not include pronounced pressures in the lateral direction and therefore, the assumption is more likely to be satisfied for the present material.

To describe the behaviour of a transversely isotropic material in three dimensions, five independent constants are needed. The first four describe the behaviour of the material in the planes parallel to the fibres and they are represented using the following engineering properties:

a) longitudinal elastic modulus E_L,
b) transverse elastic modulus E_T,
c) longitudinal shear modulus G_{LT},
d) major transverse Poisson's ratio ν_{LT}.

It has to noted that the given Poisson's ratio describes the deformation in the transverse direction due to a deformation in the fibre direction. The minor Poisson's ratio can be easily derived based on the reciprocality principle. The description of the behaviour in the transverse direction requires the determination of the following two engineering properties:

a) transverse elastic modulus E_T,
b) transverse Poisson's ratio ν_{TT}.

Based on the transverse isotropy assumption, the transverse shear modulus G_{TT} is a dependent property that can be calculated using the following formula:

$$G_{TT}=\frac{E_T}{2\,(1+\nu_{TT})} \qquad (3.2)$$

These material properties are indicated in Fig(3.1).

At this stage, it is important to remember that the bounds on Poisson's ratios are different from those for the isotropic case. These bounds are given by Theocaris and Philippidis (1992) for transverse isotropic materials as:

$$|\nu_{TT}|<1$$
$$|\nu_{LT}|<\left\{\frac{(1-\nu_{TT})\,E_L}{2E_T}\right\}^{\frac{1}{2}} \qquad (3.3)$$

3.2.3.1 FACTORS AFFECTING THE MATERIAL PROPERTIES

The material properties of the composite depend on the following:

a) the fibre properties,
b) the matrix properties,
c) the volume fraction of fibres,
d) the packing of the fibres and
e) the properties of the interface in the lamina.

Many formulae have been presented for the calculation of these material properties as a function of the properties of the constituents and their proportions. Most of the formulae were based on the idealised model mentioned above where the interface was assumed to be perfect. These expressions were of a sufficiently simple form and predicted the longitudinal elastic modulus and the major longitudinal and transverse Poisson's ratios accurately. The predictions of the transverse elastic modulus and the longitudinal shear modulus were not of the same quality because these two properties depended on the interface and the packing properties. More detailed models of the material which consider these factors resulted in complex expressions which were limited in application to a specified material. Halpin and Tsai (1967) simplified the elasticity solutions by introducing empirical coefficients which took care of the factors which were not included in the analysis. The resulting expressions were very simple and applicable to many material systems provided the correct factors were used. These factors were obtained using experimentally determined material properties. The expressions for the different material properties are given as:

$$E_L = (E_f - E_m)\, V_f + E_m$$

$$\nu_{LT} = (\nu_f - \nu_m)\, V_f + \nu_m$$

$$E_T = E_m \frac{1+\zeta_E \eta_E V_f}{1-\eta_E V_f} \qquad \text{where} \quad \eta_E = \frac{\frac{E_f}{E_m}-1}{\frac{E_f}{E_m}+\zeta_E} \tag{3.4}$$

$$G_{LT} = G_m \frac{1+\zeta_G \eta_G V_f}{1-\eta_G V_f} \qquad \text{where} \quad \eta_G = \frac{\frac{G_f}{G_m}-1}{\frac{G_f}{G_m}+\zeta_G}$$

$$\nu_{TT} = \nu_f V_f + \frac{\nu_m V_m \left(1+\nu_m - \nu_{LT}\frac{E_m}{E_L}\right)}{\left(1-\nu_m^2+\nu_m \nu_{LT}\frac{E_m}{E_L}\right)}$$

Where zeta is an empirical constant that takes care of the packing and interface properties. These expressions will be calibrated using results obtained by testing unidirectionally aligned materials. The strength of the present type of material will be discussed in a later chapter in conjunction with developing a progressive damage model.

The experimental values of the coefficient of friction for composite materials were found to be well approximated using the following equation (Tsukizoe and Ohmae (1986)):

$$\frac{1}{\mu} = V_f\left(\frac{1}{\mu_f} - \frac{1}{\mu_m}\right) + \frac{1}{\mu_m} \qquad (3.5)$$

The same reference also shows that no friction anisotropy is recognized. This means that the coefficient of friction of glass polyester against steel is the same irrespective of the orientation of the fibres with respect to the contact plane. This is in contradiction with the results of the investigation of Sung and Suh (1979) who reported a change in the coefficent of friction of of CFRP with variations in fibre orientation. Harrington and Sabbaghian (1991) related the latter effect to the surface condition of the material.

3.2.4. THE COMPOSITION OF THE USED COMPOSITE MATERIALS

The material used in the present work consisted of three different pultruded plates, a pultruded strip and a pultruded rod supplied by FIBREFORCE Ltd.. The pultrusions were manufactured from E glass fibres and a polyester resin. The material properties of the constituents as supplied by the manufacturer are given in Table(3.1).

MATERIAL	DENSITY (Mg/m3)	E (GPa)	Poisson'S RATIO	TENSILE STRENGTH (MPa)
POLYESTER	1.23	3.7	.35	53
E-GLASS	2.55	71.0	.25	2410

Table(3.1) Properties of components

The material density of the pultrusions was obtained according to CRAG (1988) Method 800. The specimens were weighed in air then their immersed weight was established to calculate the volume of the specimen. The resulting apparent densities are given in Table(3.2). In that table, the different materials are referred to according to their colour. This convention will be used throughout the thesis.

The lay-up, the weight fraction of the fibres and the fractions of the different types of fibres were determined according to CRAG (1988) Method 1000 section c). In this method, the specimens were weighed then burnt at 600°C to remove the resin. The remainder consisted of the fibres and the filler. The fibre volume fractions were determined using the following equation:

$$V_f=\frac{M_f\rho_c}{M_c\rho_f} \qquad V_r=\frac{M_r\rho_c}{M_c\rho_r} \qquad V_{fi}=\frac{M_{fi}\rho_c}{M_c\rho_{fi}} \tag{3.6}$$

$$V_v=1.-V_f-V_r-V_{fi}$$

MATERIAL	X-SECTION (mm)	DENSITY (Mg/mm3)
Brown	40x16	2.15
Grey 2	150x6	1.89
Yellow	40x3	1.94
Blue 2	150x4	1.80
Grey 1	150x3	1.79
Blue 1	120x4	1.61

Table (3.2) The size and density of the materials

The last of the expressions given in Eq(3.6) was not recommended by CRAG, but it was given by Hull (1981). The resulting fractions of fibre, resin and void volume and the weight percentage of the different types of fibre are given in Table(3.3). Comparing the results for the void volume fraction with the visual inspection of the material, the method predicted voids in the materials 'Grey 2' and 'Brown' which were thought to be solid. However, it correctly predicted a large void content for the material 'Blue 1' which showed visually detectable pores.

MATERIAL	Brown	Grey 2	Yellow	Blue 2	Grey 1	Blue 1
Vf	.707	.513	.534	.411	.375	.365
Vm	.277	.468	.458	.589	.541	.553
Vfil	.0	.001	.007	.0	.083	.006
Vv	.016	.018	.001	.0	.001	.076
% 0°	100	86.7	63.6	52.2	11.3	41.9
% csm	0.	13.1	35.4	47.8	32.0	57.4
% 45°	0.	0.	0.	0.	54.5	0.
% Filler	0.	0.2	1.	0.	2.1	0.7

Table(3.3) The fibre volume fraction and lay-up

All materials consisted of central axially aligned layers surrounded by two chopped strand mat layers with the exception of the 'Grey 1' which consisted of 11 central oval shaped strips of unidirectional fibres surrounded by two chopped strand mat layers which, in turn, were contained between two $\pm 45°$ plies on each side.

In order to determine the fibre volume fraction of the layers, the thickness of each layer was determined using a travelling microscope. Considering the constant area, the thickness of the layers was an indication of the volume of each ply. The volume fraction of the layers was calculated using the following equation:

$$V_{fi} = \frac{\%i * V_f}{\%V_i} \qquad (3.7)$$

Where '%Vi' is the percentage of the volume of the ply 'i' compared to the total volume. '%i' is the percentage of the fibres in the direction 'i' compared to all the fibres.

The measured volume fractions of the unidirectional and the chopped strand mat layers and the calculated fibre volume fractions of the two layers are given in Table(3.4). This table does not include the brown material because it is not laminated. The material 'Grey 1' is also not considered because its uniaxial layer was made up of strips for which the current approach is not applicable.

MATERIAL	Grey 2	Yellow	Blue 2	Blue 1
% uni % csm	73 27	59 41	29 71	25 75
Vf uni Vf csm	.609 .249	.576 .461	.660 .298	.612 .279

Table(3.4) The percentage volume and the fibre volume fraction of the uniaxial and csm layers

The values in Table(3.4) demonstrate that the fibre volume fraction in both layers is relatively constant. This supports the idea that the packing of fibres depends basically on the manufacturing technique. The volume fraction of the chopped strand mat layer in the material 'Yellow' varied from the other materials. This might be due to the smaller cross section which has resulted in higher packing.

3.2.5. EXPERIMENTAL DETERMINATION OF THE MECHANICAL PROPERTIES

In order to calibrate Eq(3.4), specimens prepared from the material 'Brown' were tested. The dimensions of the specimens used did not comply fully with standard specifications (ASTM D3039, ASTM D3518 and BS2782). The deviation from the standard tests was necessary because of the difference of the objective of testing in standard specifications from

the objective in this work. Most of the standard tests are designed for quality assurance and therefore the sizes of the specimens were not suitable for mounting strain gauges on. The results of the material testing performed showed that it is important to make sure that the material contained in the test specimen is representative of the material under consideration. In some cases this is in contrast to amendment 3351 of BS2782 Part3 which requires machining one face of the specimen only.

3.2.5.1. LONGITUDINAL MECHANICAL PROPERTIES

Three specimens with a nominal cross section of 3x25 mm and 335 mm length were manufactured. The samples were prepared from the material by cutting a central slice using a double saw. This saw was developed to overcome the complications due to the bending that occured when material was removed from one side of the specimen at a time; this deformation was the result of the release of residual stresses in the pultruded bars. While obtaining the specimens from these slices, no special care was taken to cut the specimens from the central area of the slice. Two of the specimens prepared had one edge which was originally on the surface of the pultruded bar. The specimens were also not provided with end tabs. Eight millimetre long strain gauges were mounted on the specimens in the axial and transversal directions on both sides.

The specimens were tested using an INSTRON 1185 machine and the data was sampled using an INTERCOLE SPECTRA-MS data logger connected to an HP200 computer. The program written for data logging is given in appendix(1). The rate of stretching was 0.5 mm/min and the specimens were held using conventional wedged jaws.

Two of the specimens failed prematurely due to their splitting in the longitudinal direction. These specimens were found to be the ones containing a part of the surface of the original bars. The splitting seemed to be caused by the variance of the internal stresses resulting from the manufacturing procedure and the surface treatment of the pultrusions. These two specimens sustained load after their initial splitting failure (Fig(3.2)).

The specimen which contained no surface treated parts failed at a higher stress but failure resulted in severe and sudden destruction of the specimen Fig(3.3). Many of the fibres were fractured and at the same time, others were pulled out. The fracture of the fibres mainly originated at the ends of the wedges of the jaws. A similar failure pattern was reported by Curtis and Moore (1983). This indicated the presence of stress concentration at that position. The failure of that specimen was instantaneous and the noise, indicating the commencement of failure, occurred at high loads which were very near the ultimate load.

In order to overcome the problems associated with the above mentioned specimens, three other specimens were prepared. These specimens were 230 mm long and had 2*25.4 mm nominal cross section. The specimens were provided with 50 mm end tabs made from glass fibre reinforced pultrusions. The pultrusions used for the tabs were prepared from the material 'Yellow' described above. These tabs were glued to the specimens using ARALDITE. The specimens were prepared this time using a single saw but to prevent them from bending, they were bolted to a rigid steel block. All specimens were cut from the central part of the pultruded member. Here, it has to be noted that the use of the double blade sawing technique resulted in higher precision, but it was more complicated and expensive.

The failure of these specimens was very similar to the specimens of the previous group which excluded the outer surface of the pultruded bars Fig(3.2). The presence of the end tabs did not have a pronounced effect on the stress concentration at the end of the gripping area, because much of the fibre breakage initiated at that position. However, none of the specimens of this group showed the splitting that occurred for the previous group.

The stress-strain curves for the specimens (Fig(3.2)) show a highly linear behaviour up to their final failure. The results obtained from the previous two sets of specimens are given in Table(3.5):

GROUP	NO	t(mm)	E (GPa)	v	STRENGTH (MPa)	NOTES
1	1	3.05	49.96	.27	507.3	
	2	2.95	48.36	.27	456.7	SPLIT & GLOSSY EDGE
	3	2.85	52.50	.28	376.0	SPLIT & GLOSSY EDGE
2	1	2.2	50.12	.26	505.3	
	2	2.5	50.08	.26	581.0	
	3	2.2	50.76	.26	588.5	

Table(3.5) The tensile test data

It can be seen from the table, that the results for the modulus of elasticity and Poisson's ratio were consistent while the strength of the specimens varied greatly. The results of the specimens that used end tabs were generally higher than the results obtained without them. The strength of the specimens which had one glossy edge showed lower strength than the specimens obtained from the middle of the pultrusions.

3.2.5.2. TRANSVERSE MECHANICAL PROPERTIES

The specimens used for the determination of the transversal material properties were also prepared from the brown pultruded bars. Due to the small width of the bars, the length of the specimens was restricted to 40 mm. The cross section of the specimens was 2*25 mm and each had four strain gauges, two on either side. One of the strain gauges was in the loading direction while the other was in the direction of the fibres. The small length to width ratio of the specimens was considered acceptable because the orthotropic nature of the material ensured that the clamping effects die out very rapidly.

The ends of the specimens were originally extended using two double lap joints to provide space for hanging and loading. The joints were made using ARALDITE and the overlap for the specimens was only 5 mm at each end. Unfortunately, the specimens cracked at the end of the overlap area possibly due to the shrinkage associated with the curing of the glue which resulted in concentrated stresses exceeding the small tensile strength of the material.

Another set of specimens was prepared where the double lap joint was replaced by a butt joint using SUPERGLUE and the end extensions were provided with holes for hanging the specimen and the loading weights. The specimens were suspended from a 100 N load cell using a string passing through a holes at one end of the specimen, while a weight hanger was provided at the other end. The use of the strings was decided to minimize the bending on the joints. Because of the brittleness of the joint, the loading level was kept under 100 N. Failure was at the joint as expected, but the results of two of the specimens showed high scatter and only one of the four specimens predicted the negative sign of the strain in the direction of the fibres. This was due to the very low loading level, which meant that even the stiffness of the wires connecting the strain gauges could affect the results. The obtained transversal elastic moduli were 15.2, 14.5, 20.88 and 27.5 GPa. Only the first two results were considered reliable. The only meaningful value for the transversal Poisson's ratio was found to be .047. The calculated value that satisfied the reciprocality conditions was .077.

Due to the scattered and unreliable results of the previous group of specimens, it was necessary to test the material again. An identical group of specimens was prepared, but this time it was directly attached to a JJ testing machine using its wedged grips. The data logging system described above was used for the retrieval of the data from the testing machine and storing it on the computer. Due to the small size of the specimens, the clamping area was only 5 mm wide at each end. Although the specimens were stretched at a rate of .5 mm/min, this rate resulted in a high rate of loading due to the short length of the specimens.

The resulting stress-strain curves were not smooth due to the low logging speed compared to the rate of loading. In order to obtain the material coefficients from this group, the results of the four specimens were combined and they were smoothed using the least square method. The resulting transversal elastic modulus was found to be 14.35 GPa and the corresponding Poisson's ratio was .087. This last value compares well with .077 which is the value that satisfies the reciprocality requirements. All specimens failed near the end of the clamped area. The average failure stress was found to be 20 MPa which was small compared with the values supplied by the manufacturer. This might be due to the high rate of loading. The elastic modulus of the present case was considered to be the correct value because it corresponded well with the one determined using the previous set of specimens.

In order to verify the correctness of Eq(3.4), it was necessary to determine the transverse elastic modulus of a unidirectionally reinforced material with a different fibre volume fraction. This was achieved by using specimens manufactured from the material designated 'Grey 2' by removing the external chopped strand mat layers. The resulting specimens were nominally 4 mm thick and 25 mm wide with a length of 150 mm and were clamped over a length of 30 mm on each side; strain gauges were positioned in the axial and the transverse directions on both faces.

The load-strain curves for these specimens were found to be perfectly straight up to failure. The results obtained from the tensile tests on the specimens are given in Table(3.6).

SPECIMEN	FAILURE STRESS MPa	ELASTIC MODULUS GPa	Poisson'S RATIO
1	5.2	10.6	.0724
2	11.9	10.6	.0734
3	10.1	10.6	.0727

Table(3.6) Results for the transverse tensile test

From that table, it can be seen that very good agreement between the results of the specimens for the elastic modulus and Poisson's ratio exist. On the other hand, however, the results for the strength show very high discrepancies. The reason for that is the sensitivity of the strength to any imperfections over the whole length of the specimens. It has been argued that a more appropriate test for determining the tensile strength of the specimens is a three point bending test (Adams, King and Blackketter 1990). The reason being that the specimens will always fail under the central load and therefore only imperfections at that point will affect the results.

Therefore, three point bending tests were performed on specimens which were identical to the above mentioned specimens. A part of the specimens were tested using a span equal to 100 mm while the rest had a span of 60 mm. The variation of span was undertaken in order to detect the effect of shear deformations on the results. The load deflection curves of all specimens were found to be perfectly straight upto failure. The failure planes of the second and third specimens tested using 100 mm span were not under the central load as expected and found for all other specimens. The calculated strength and elastic modulus, based on four specimens each, are given in Table(3.7). It has to be noted that the determination of the elastic modulus given in that table did not take into consideration the effect of the shear deformations.

SPAN(mm)	100		60	
SPECIMEN	σ(MPa)	E(GPa)	σ(MPa)	E(GPa)
1	43.26	9.7	34.86	9.6
2	43.93	9.9	32.57	8.7
3	44.90	9.8	38.32	9.6
4	37.51	10.6	47.58	9.3

Table(3.7)The results of the three point bending tests

The results in Table(3.7) show that the effect of varying the test span from 100 mm to 60 mm did not change the results. The reason for this is that the length to depth ratio of the specimens and the isotropic nature of the material in the plane of loading were sufficient to satisfy the slender beam conditions (i.e. not more than 10 (Gere and Timoshenko 1987)). A transverse Poisson's ratio equal to .4 (estimated based on equation 4) was used to investigate the effect of considering the shear deformations on the measured elastic constant. The change in the elastic modulus was estimated to be .5% for the long specimens and 1.5% for the short ones.

The transverse strength recorded using the present test was about four times the strength obtained using the direct tension specimens. A small difference existed between the results of the elastic modulus from the two tests. However, this difference can be due to experimental error in determining the thickness of the specimens.

3.2.5.3. THE SHEAR BEHAVIOUR

The measurement of the shear properties for uniaxial materials is difficult. Although many testing methods are available for measuring the shear rigidity of uniaxial materials (the

off-axis tensile test, the iosipescu shear test, the short beam test, the rail shear test, shear panel test, the plate twist test and the prism twisting test), it was decided that the most suitable test for the specimen sizes that could be obtained from the pultruded bars was the prism twisting test. In order to eliminate any fixing effects at the ends of the specimens, thin cylinders were used to transmit the torque. These were held by fixings with a hexagonal end suitable for attachment to the test machine. The testing machine had originally a spring type load cell. This was replaced by an electronic one which was connected to the data logging system described above. The specimens were loaded only lightly to determine the shear modulus of the undamaged material.

The shear moduli were calculated based on the assumption of transverse isotropy. This is acceptable, because the maximum deviation from isotropy in the transversal direction reported in the literature is less than 20% (Tsai & Daniel 1990). For the cross sections used in this work, it was found that neglecting such degree of orthotropy will result in errors less than 5%.

The size and the results of the tested specimens are given in Table(3.8):

No	X-SEC mm*mm	LENGTH mm	G GPa
1	2*25.5	96	6.68
2	3*25.4	183	7.34
3	2*41.2	135	9.00
4	2*34.4	135	7.30

Table(3.8) The shear test data

The measured shear moduli are also given in that table. It can be seen that the third specimen was stiffer than the previous ones. The edges of this specimen were the surface material of the bars. By removing a strip 3.4 mm wide from each side of that specimen, specimen number 4 was created. It is clear that the shear modulus of that specimen is comparable with the previous ones.

3.2.6. CALIBRATION OF MICROMECHANICS EQUATIONS

The results of the above mentioned tests were used to calibrate the micromechanics equations given in Eq(3.4). The equations use the constituent material properties given in Table(3.1). The resulting equations for glass polyester uniaxially reinforced pultrusions are:

$$E_L = 67.3V_f + 3.7$$
$$\nu_{LT} = .35 - .1V_f$$
$$E_T = \frac{3.7 + 2.02V_f}{1 - .9195V_f} \qquad (3.8)$$
$$G_{LT} = \frac{1.37 + 2.152V_f}{1 - .885V_f}$$
$$\nu_{TT} = \frac{.022 + .536V_f - .292V_f^2}{.0628 + V_f}$$

Fig(3.4) shows the relationship between E_T/E_L, ν_{LT}, G_{LT}/E_L, ν_{TT} and the fibre volume fraction V_f. These graphs demonstrate that for the practical values of V_f, the variation of these quantities is limited. This means that for preliminary investigations, it is acceptable to use an average value for these quantities. Based on Fig(3.4), ν_{TT} was fitted to a straight line equation. The resulting equation is:

$$\nu_{TT} = .518184 - .26432V_f \qquad (3.9)$$

Equations (3.8) were then used to calculate theoretically the properties of a chopped strand mat layer made of the same materials. The latter were approximated as randomly oriented long fibres and Eq(3.1) was used. Poisson's ratio for this case is also given in Fig(3.4). Again, within the practical limits of V_f, the variation of Poisson's ratio is small. The longitudinal moduli of elasticity for randomly oriented fibres and the longitudinally oriented fibres are given in Fig(3.5). The properties of the randomly oriented fibres were approximated as straight lines using regression analysis. The resulting expressions were:

$$\bar{E} = 2.975 + 31.233V_f$$
$$\bar{\nu} = .32 - .086V_f \qquad (3.10)$$

Using the data obtained by Tsukizoe and Ohmae (1986), the coefficient of sliding friction is given by:

$$\mu = \frac{1}{3.268 - .926V_f} \qquad (3.11)$$

3.2.7. THE PARAMETERS OF ORTHOTROPY OF COMPOSITE PLATES

As already mentioned in the introduction to this chapter, it was shown that the behaviour of an orthotropic plate depends basically on two real parameters k and n. When the force resultant on a closed surface of the plate is not equal to zero, Poisson's ratio becomes also an active factor. The parameters k and n are defined as follows (Lekhnitskii 1968):

$$k=\sqrt{\frac{E_L}{E_T}} \qquad n=\sqrt{2\,(k-\nu_{LT})+\frac{E_L}{G_{LT}}} \qquad (3.12)$$

The parameter k for isotropic materials is equal to 1 while the parameter n is equal to 2. Poisson's ratio of both materials is almost constant (Fig(3.4)) and therefore, the stress distribution in plates made of chopped strand mats or continuous filament mats with loaded holes is practically independent of the fibre volume fraction.

Eq(3.6) was used to plot the variation of n, k and ν_{LT} with V_f for a unidirectionally aligned material (Fig(3.6)). This graph shows that the variation of these quantities is less than 10% in the practical range of fibre volume fractions. The average values for these quantities are:

$$n=3.284 \qquad k=1.963 \qquad \nu_{LT}=.288 \qquad (3.13)$$

This suggests the insensitivity of the stress distributions which develop in a unidirectional layer to variations in the fibre volume fraction. It is interesting to note that both coefficients (which describe the degree of anisotropy) decrease with increasing fibre volume fraction. The reason for this decrease of orthotropy is the fact that the variation of G_{LT} and E_T is higher than the variation of E_L for the fibre volume fractions considered.

The parameters n, k and Poisson's ratio were also calculated for a layered material composed of uniaxially reinforced and chopped strand mat plies based on the laminated plate theory. Fig(3.7) shows that the variation of the major Poisson's ratio with the fraction of uniaxial plies is almost constant for different fibre volume fractions in the two layers.

Fig(3.8) shows three dimensional plots of n over the practical range of fibre volume fractions and lay-ups. In these plots, the results for the case when the chopped fibre volume

fraction is equal to .1 is repeated on all graphs for comparison. These results show that for low fibre volume fraction of the chopped strand layer, n varies non-linearly with the content of uniaxial layers. For higher chopped fibre volume fractions, this relationship becomes linear. Fig(3.9) demonstrates the same information for the parameter k. Although the behaviour of k seems similar to n, the increase in k for low chopped fibre fractions and high uniaxial fibre fractions does not become linear.

In both cases, the values of the parameters increase with increasing the fraction of uniaxial layers or decreasing the fibre volume fraction of the uniaxial layer. It can be seen that for low randomly orientated fibre volume fractions, the value of the parameter n is not lying between the values for the parent laminae. Therefore, contrary to the case of the wholly uniaxial material, the properties of a layered laminate, manufactured from randomly orientated and uniaxial fibres, depend upon the fibre volume fraction of both types of glass fibre reinforcements and are highly dependent upon the fraction of uniaxial layers in the plate.

Fig(3.10) shows that for angle ply material, the parameter n depends on the orientation of the layers and the fibre volume fraction, but when that angle is equal to about 23° and 68°, the factor n becomes independent of the fibre volume fraction. The variation of the parameter n with fibre volume fraction remains small for fibre orientation angles greater than 23°. Fig(3.11) presents the dependence of k on the orientation of the layers and the fibre volume fraction. When the angle of orientation is between 25° and 65°, the fibre volume fraction does not affect the factor k. Poisson's ratio, however, was found to be strongly dependent on the fibre volume fraction Fig(3.12). This means that for fibre orientation angles between about 20° and 70°, the stress distributions in angle ply material will be independent of the fibre volume fraction as long as the sum of tractions on the edges of the plate under investigation is equal to zero.

3.3. EXPERIMENTAL BEHAVIOUR OF MECHANICAL COMPOSITE JOINTS

3.3.1. GENERAL

The understanding of the behaviour of mechanical joints requires the gathering of experimental information about their performance. The complete characterisation of all materials, types and geometries of joints is not possible. Therefore, sample tests are performed which are used to infer the influence of the different parameters on the behaviour. Many topics related to the experimental behaviour of joints have been investigated (Chapter 2). However, none of the experimental results were for joints made in pultruded materials. In addition, some

of the general aspects of the behaviour of joints were not formally considered. Therefore, it was necessary to perform some experiments on selected joints to obtain information about the following topics:

a) The failure modes of joints made in pultrusions,
b) the effect of the confinement area and material on the behaviour,
c) the effect of varying the end distance in pultrusions with a high uniaxial fibre content,
d) the effect of applying the load at an angle to the fibre direction,
e) the effect of the stiffness of the plates to be jointed, on the load distribution in joints using two fasteners in series,
f) the effect of the failure mode on the load distribution at failure in joints employing two fasteners.

The tests performed in this work were grouped into two areas; the first involved tests on single bolt specimens while the second group dealt with the use of two fasteners in series for jointing.

3.3.2. TESTS ON SINGLE FASTENER SPECIMENS

3.3.2.1. THE EXPERIMENTAL SET-UP

The experiments were performed on two INSTRON machines. The first model was an INSTRON 1104 machine which used an CIL data logger and was controlled by an HP86B computer. The computer was used for real time display of the load-deformation behaviour and data storage. The second testing machine was an INSTRON 1185 which was connected to an INTERCOLE-SPECTRA data logger and an HP200 computer for data storage. The program written in HP-BASIC5 for data logging and storage is given in appendix(1). The first machine was used only in the investigation of the effect of the geometry on the failure mode of the joints.

The measurement of the movement of the fasteners was undertaken using Linear Voltage Displacement Transducers (LVDT). To facilitate holding an LVDT on each side of the specimen, the bolt illustrated in Fig(3.13) was manufactured. This bolt had a head that could accommodate an LVDT and, in addition, the other LVDT could be attached to the end of its shaft using a piece that was mounted after the nut was tightened. The diameter of that bolt was

3/8th of an inch. The movement of the bolt was measured relative to an arbitrary point on the plate chosen at 50 mm from the centre of the bolt. This method of determining the displacements was preferred because it eliminated any errors due to the slip of the specimens relative to the jaw.

A piece was fixed at the arbitrary reference point in order to support the plungers of the LVDT's. This piece was effectively made up of a bolt, a nut and a washer Fig(3.14). The bolt and the washer were formed from a solid cylinder of steel such that they had a stiff plate attached perpendicular to them. The plate mounted on the washer had a recess to allow for tightening the nut. The diameter of the washer was 15 mm and that of the bolt was 3 mm. This small diameter was chosen in order to reduce any disturbance to the stress state in the plate near the loading area. The relatively large diameter of the washer was necessary to ensure that the plates were supported properly.

The standard wedged clamps of the Instron machine were not suitable for fixing specimens which were wider than 25 mm. Therefore, special wedges for the grips were manufactured to hold samples; these are shown in Fig(3.15). It will be seen that the part outside the grip had a wide support for holding the wide specimens and in addition, they were also provided with two bolts near their edges to aid clamping the specimens. The use of these wedges was not entirely successful because the presence of the gripping area outside the jaws resulted in rotation of the wedges and therefore the specimens slipped.

A mark two design for the grips was manufactured and is shown in Fig(3.16). The grip basically consisted of a rigid T-shaped thick plate to which two blocks were bolted. These blocks had roughened surfaces to grip the composite plate. The grips had an additional central hole at the loading side of the specimens to provide extra pressure across the two blocks. This configuration was reliable but the bolts needed to be replaced frequently as their threads were rapidly damaged due to the repeated use.

Fig(3.17) shows the arrangement of holding the bolt and it consisted of two stiff steel plates (A) which were screwed through packing pieces to another central plate (B). This latter was shaped to give a tongue that could be attached to the testing machine. The thickness of the packing between the inner (B) and outer plates (A) was chosen such that the configuration could accommodate the specimen and the washers between the outer plates. The whole was assembled by placing the washers, plates and the bolt in position; the bolt was then lightly torqued using a torque wrench. The washers used were tight fitting with an outer diameter equal to 2.2 times the diameter of the bolt.

The loading was performed by monotonic stretching of the specimens at a rate of .5 mm/min. For the first set of specimens which investigated the effect of specimen geometry (see

section 3.3.2.2), the loading was stopped when a load reduction greater than 500 N was recorded. All subsequent specimens were loaded until the joint completely lost its load carrying capacity or excessive deformations were recorded.

3.3.2.2. THE EFFECT OF THE GEOMETRY OF THE SPECIMEN

3.3.2.2.1. OBJECTIVE

The objective of this test was the determination of the different failure modes that could develop in pultruded materials and their characteristics due to variation of the geometry.

3.3.2.2.2. THE SPECIMENS

Nine groups of specimens were prepared from the material designated 'Blue 1' which is described in sec 3.2.4.. Each of these groups consisted originally of three samples. However, in order to confirm the information obtained for some groups, it was necessary to add a fourth specimen. The group definition and geometry of these specimens is given in Table(3.9).

GROUP	WIDTH(mm)	END DISTANCE(mm)	e/d	w/d
TS	19.05	9.525	1	2
TM	19.05	14.29	1.5	2
TL	19.05	19.05	2	2
MS	38.10	9.525	1	4
MM	38.10	19.05	2	4
ML	38.10	28.58	3	4
WS	57.15	19.05	2	6
WM	57.15	38.10	4	6
WL	57.15	57.15	6	6

Table(3.9) The Geometry of the specimens BLUE1

3.3.2.2.3. THE FAILURE LOADS

The failure loads which are given in Table(3.10). The strengths in that table are defined as the first peak in the load deflection curves; these graphs are shown up to the peak values in Figs(3.18,3.19,3.20). The results for the specimens which failed in tension showed less variation than those failing in cleavage or bearing. This implies that the tensile strength of the specimens are independent of the voids. For the specimens which failed in bearing, the

variation was so high that it was not possible to draw meaningful conclusions about the effect of the geometry on the bearing strength.

GROUP	FAILURE LOAD (N)				AVERAGE (N)	MODE
	SPEC.1	SPEC.2	SPEC.3	SPEC.4		
TS	5030	5670	6330	-	5680	c
TM	8930	8760	9190	7860	8690	t
TL	9650	9330	9620	-	9530	t
MS	3850	3240	4160	4450	3930	c
MM	9590	9480	10310	-	9790	c
ML	15760	13810	14810	-	14790	cbt
WS	11490	10600	9350	-	10480	c
WM	13390	16050	12340	-	13930	b
WL	16440	17770	13590	12150	14990	b

Table(3.10) Failure Loads for Specimens Blue1

Where b, c and t indicates bearing, cleavage and tension failures respectively.

It is interesting to note that the cleavage-shear failure load of group MS is less than the load for the group TS, in spite of their equal end distance and the larger width of the specimens of group MS. This can be explained by the beam-like action of the end part of the specimen. The span of the imaginary beam was less in the case of the TS specimens and therefore the failure load was higher. The failure loads of the specimen groups MM and WS are of the same magnitude. Similar to the previous two groups, the latter ones have the same end distance but their width varies. This seems at first sight an argument against the explanation just given for groups TS and MS. However, it should be noted that the end distance for the latter groups of specimens was longer than for groups TS and MS. Accordingly, following the same line of argument, the beam now has become a deep beam ie. a large portion of the load will be transmitted by shear rather than by bending. Therefore, the failure load becomes relatively insensitive to the variation of the width. This is supported by the presence of cracks at 45° in addition to the crack due to cleavage in the specimens of group WS.

The similarity between the tension failure load values of group TL and those for cleavage failure of groups MM and WS suggests that the slightest increase in the width of specimen TL would change the failure mode to cleavage failure.

The failure loads of the groups show that the cleavage failure load increases with the increase in the end distance. Unlike shear failure, the cleavage failure load values depend also upon the width of the specimen.

From the above mentioned results, it can be seen that the failure loads have a big spread for each group and the specimens which had low stiffness showed low strength; one reason for this is the presence of air voids in the material which were clearly visible.

3.3.2.2.4. DESCRIPTION OF THE FAILURE MODES

No specimen failed originally in shear. All the specimens which were likely to fail by this mode failed first in cleavage and then some developed shear failure. This was due to the relatively small transverse strength of the material compared with its shear strength. However, after the initial transverse failure occurred, the remaining bearing capacity of the joint was due to the action of the end area as a cantilever. Due to the short span of these cantilevers, their strength was a function of the shear strength of the layers. Because the in-plane shear strength of chopped strand mat layer was high, the shearing of the central uniaxial layer could appear only after the interlaminar bond fails. In this case, the randomly orientated plies failed in tension on planes lying at 45° to the loading direction while the inside uniaxial layer was sheared parallel to the fibres.

The visual feature for bearing failure of the specimens was their swelling Fig(3.21). This occured on the bearing side of the plate but outside the washer area, however, a slight increase of the thickness was detected under the washer. The holes in these cases were elongated indicating severe damage. It is interesting to note that in some cases, the material under the washer had neat shear planes parallel to the loading direction and extending to the end of the washer. The formation of these shear failures was due to the suppression of the development of the bearing failure in that area.

The tensile failure was usually through the randomly orientated layers and a part of the longitudinal fibres adjacent to the hole Fig(3.22). In some specimens, the axial fibres at the outer parts remained intact and the randomly orientated plies were sheared from the central layer. This indicates the dependence of the failure development on the interlaminar shear capacity of the material.

The failure mode of the specimens of group ML shown in Fig(3.23) is of special interest because they failed relatively gradually as can be seen from the load deformation curves Fig(3.20). The failed specimens were completely destroyed because of the development of a combined tension through the hole, cleavage, interlaminar shear and bearing failure mode. The initiation of the failure in this case was in tension followed by interlaminar shearing and transverse tension failure.

3.3.2.2.5. THE MOVEMENT OF THE BOLT

The load applied by the bolt is plotted against its displacement relative to the reference point in Figs(3.18, 3.19, 3.20). These curves show that the cleavage and tension failures occur after relatively small bolt displacements while the bearing failure allows relatively large displacements before failure. This means that the bearing failure can be considered as ductile while the other two types of failure are brittle. Table(3.11) gives the slope of the load deflection curve for the different specimens; these are the secant value between the origin and the point at which the displacement is equal to .1 mm. This means that these are the initial values of the slope.

GROUP	STIFFNESS (N/mm)				AVERAGE (N/mm)
	SPEC.1	SPEC.2	SPEC.3	SPEC.4	
TS	17850	24600	23500	-	21980
TM	25200	25000	25700	23200	24780
TL	27400	25900	23000	-	25430
MS	-	17800	33300	29450	26850
MM	24170	19700	50300	-	31390
ML	39950	34500	35500	-	36650
WS	33800	32100	32350	-	32750
WM	38800	58800	28600	-	42070
WL	60600	49530	49950	23840	45980

Table(3.11) The Initial slope of the load-movement curves

By considering these results, it can be seen that an increase in the end distance for thin specimens causes an increase in the stiffness for the lower values of e/d only; for higher values of e/d, the stiffening becomes less. The average slope for each specimen group shows that increasing the end distance or the width of the specimen will result in higher stiffness.

3.3.2.3. EFFECT OF CONFINEMENT AREA ON THE BEHAVIOUR OF A JOINT

3.3.2.3.1. OBJECTIVE

The present tests were performed to determine the effect of the clamping area and material on the strength and the extensibility of a bolted connection.

3.3.2.3.2. THE SPECIMENS

Three specimen groups were considered where each of them was subjected to a different clamping condition. The material used for manufacturing the specimens was the material designated 'Grey 1' in section 3.2.4.. The geometry of all specimens was the same and was chosen to ensure the development of bearing failure. The width of the specimens was 70 mm while the end distance was chosen as 40 mm. All groups were subjected to the same small clamping torque.

The difference between the specimens of the three groups was the size of the clamping area and the material used for clamping. The first group used tight-fitting steel washers having an outer diameter equal to 2.2 times the inner diameter. The second group used steel plates which covered all the potential damage area. Smooth composite plates covering the same area were used to clamp the specimens of the final group.

3.3.2.3.3. RESULTS AND DISCUSSIONS

The numerical results for the specimens are given in Table(3.12). Here, it is necessary to mention that specimen G5 slipped and therefore it was reloaded. Specimen G8, on the other hand, failed in tension through the hole mode and therefore its results are to be interpreted cautiously.

GROUP	SPECIMEN	MAXIMUM LOAD (N)	DIAMETER OF FAILED HOLE (mm)	DISPLACEMENT AT FAILURE (mm)
1	G1	12639.7	15.4	9.01
	G2	14263.6	15.5	8.88
	G3	13583.1	15.6	9.61
2	G4	14776.0	12.0	4.58
	G5	12677.8	12.1	-
	G6	13096.4	13.1	5.00
	G7	15127.6	12.1	4.74
	G12	14099.5	12.9	4.92
3	G8	15098.6	12.4	2.95
	G9	14708.9	11.2	4.42
	G10	13039.0	12.2	4.05
	G11	15192.3	11.6	3.11

Table(3.12) Numerical results for the specimens

Comparing the failure loads of the first and the second group, a trend of increase in strength with an increase in confinement area can be established. When the failure loads of the second group are compared with those for the third, no definite difference can be observed.

Table(3.12) also shows that the final failure displacements of the first group were much higher than those of the other two. The movement of the bolt was reduced by replacing the washer with a steel plate and this movement was reduced further by replacing the steel plate by a composite plate. The same trend can be noticed for the major diameter of the deformed hole after failure.

3.3.2.3.4. DESCRIPTION OF THE FAILURE MECHANISM

The load-displacement curves for the specimens of the three groups are shown in Figs(3.24,3.25,3.26); these curves indicate fibre failure and redistribution of the load at various displacement values. The initial failure of the specimens, which were confined by using a washer, occurred at a load equal to about 10kN while the specimens of the other groups started to fail at lower loads. The opposite can be stated about the movement associated with the first failure. A possible explanation for this is the reducion in lateral pressure resulting from an increase in the confinement area. The variation of the results of the second and third groups is seen to be much higher than the first group. This is due to the dependence of the behaviour of these specimens on the friction between them and the loading plates.

The failure patterns of the specimens (Fig(3.27)) reveal that each group had a slightly different mode of failure. In general, the confinement using a washer resulted in a limited area of bearing failure, while the confinement using plates resulted in a much wider area of damage.

The load displacement curves of the first group were initially straight (Fig(3.24)), but after the initial failure occurred, the load supported by the specimens was reduced. After that, the specimens continued to sustain that load under increasing displacements. This was associated with swelling of the area ahead of the washers indicating bearing failure. The final failure of the specimens of this group was in cleavage resulting in another drop of the load supported by the specimens (Fig(3.27a)). This was followed by a uniform decrease of the load with increasing deformations.

A part of the material confined by the washers and loaded by the bolt was separated from the rest of the plate by two cracks which extended from the hole parallel to the axis of the specimen (Fig(3.27a)). Between these two cracks, the material was not damaged due to the presence of the washer which resulted in suppressing the bearing failure mechanism.

The load displacement curves of the specimens in the second group show non-linearity before the first failure occurred (Fig(3.25)); this indicated that the transition from the undamaged condition to the damaged one was gradual. When the ultimate load was reached, cleavage failure developed and the load dropped suddenly. The swelling of the bearing area for the specimens of this group was much less than the previous one, but the area of damage was large (Fig(3.27b)). Some of the failed specimens showed signs of tensile failure damage at the section of minimum area in addition to the cleavage failure.

The behaviour of the specimens in the third group was similar to that of the previous group (Fig(3.26)). The tensile failure mode, however, was more pronounced (Fig(3.27c)) and one of the specimens (G8) failed in tension through the hole without developing the cleavage failure. This was the result of the interlocking of the lug with the confining plates in the bearing area. The swelling of the bearing area of this group was larger than that for the previous one. This might be due to the reduced stiffness of the confining material.

The reduction of the load after the initial failure for the first group of specimens was due to the lack of confinement of the material outside the washers. This made the reduced strength of the unconfined areas control the load sustained by the joint. This explanation was supported by the fact that the provision of confinement for the whole specimen resulted in keeping the load level on the specimen at least equal to the initial failure load. The recorded increase of the load after the initial failure seemed to be due to the increased pressure between the loaded and the confining plates resulting in increased friction forces.

The higher nonlinearity of the load-displacement curves of the joints which were confined by plates was due to their gradual damage development. This effect resulted in spreading the damage area while keeping the degree of damage low. The opposite was true for the specimens confined by washers because the presence of confining pressure on only a part of the plate meant higher stiffness of the area under the washer. Therefore, the severe deformations and the damage was kept out of that area. This allowed the material under the washer to behave linearly until damage developed suddenly outside the washer.

The final cleavage failure of the three groups of specimens seems to have occurred when the damage area reached a certain distance from the end of the specimen. Therefore, the different ways in which damage of these groups of specimens spread can be used to explain the different extensibilities as follows. When the damage was localised but severe, the displacements became large before the critical end distance, discussed above, was reached. In the case of limited, but widely spread damage, the critical end distance was reached before developing large displacements.

The damage which developed before the occurrence of the cleavage failure also influenced the properties of the cleavage mode of failure. When the damage of the specimen was widely spread, tension failure cracks developed in the already weakened area due to the cantilever action of the sides of the failed plate. The encouragement of the tensile failure in the specimens which were confined using GRP plates must have been due to the higher friction and interlocking developed after the swelling of the loaded plate due to the initial bearing failure. This reduced the proportion of the load transferred through the bolt, thus increasing the load carrying capacity and reducing the load causing cleavage failure.

When the damage was localised in the area ahead of the washer, the side area was not weakened and the cleavage plane was responsible for developing the final failure.

3.3.2.4. THE CRITICAL END DISTANCE

3.3.2.4.1. OBJECTIVE

The objective of this set of tests is to determine experimentally the critical end distance for single bolt joints. This distance is defined as the end distance at which a joint of fixed width attains its maximum possible strength.

3.3.2.4.2. THE SPECIMENS

The specimens used in investigating the critical end distance were manufactured from the materials designated 'Yellow' and 'Grey 2' in section(2.4.3.). These materials were chosen because their high percentages of unidirectional layers required a long critical end distance. This allowed changing the end distance while remaining below the critical value. The specimens made from the material 'Yellow' had widths which varied between 20 and 38 mm and end distances varying between 10 to 70 mm while the specimens manufactured from the material 'Grey 2' had widths varying between 30 and 70 mm and end distances varying from 40 to 140 mm.

The movement of the bolt was usually measured relative to a point 50 mm from the centre of the bolt but in some specimens (EGNS, EGNM, EGNL, EGMS and EGMM), this distance was reduced to 30mm, in which case, the plates used to support the plungers of the linear voltage displacement transducer were replaced by the gripping blocks. This procedure was used when the material available was limited. The load displacement curves of these

specimens were not as reliable as the other specimens because the measured displacements included any possible slipping of the specimens.

3.3.2.4.3. DESCRIPTION OF THE FAILURE MECHANISM

The failure modes of the yellow specimens included tensile, shear, cleavage and bearing. Tensile failure occurred for specimens which had small width and large end distance. The failure of these specimens occurred by fracture of the outer chopped strand plies. This was followed by interlaminar failures of different types.

In some cases the interlaminar failure developed on one side of the hole only; this was associated with transverse tensile failure resulting in the formation of a hook-like support for the bolt. This meant that the part of the plane passing through the hole which was supporting the load was subjected to bending moment. Accordingly, the final failure occurred due to bending failure on that plane. The fibres which were lying near the bolt in the central layer were fractured while the fibres near the free surface failed in buckling. Some delamination between the three layers was also visible in that area.

In other cases, the delamination was complete over the whole end distance. This was associated with shear failure of the central layer resulting in a wedge that had the shape of a hat. The delamination for these cases was associated with crushing of the outer layers near the edge of the washer.

When the end distance was reduced, the delamination was less and failure approached ideal shear failure. The intermediate failures were a combination of shear and cleavage failures. The suppression of the interlaminar failure was the result of the confinement of the washer of the small end area.

When the width was increased, the specimens which had small end distances failed in the same shear modes as the narrow specimens (Fig(3.28a)). When the end distance was increased, bearing failure of the chopped strand mat layer developed in addition to the shearing failure that occurred in the central uniaxial layer Fig(3.28b&c). Increasing the end distance further resulted in localised bearing failures combined with delamination and shearing of the uniaxial layer Fig(3.28d). The specimens with very long end distances failed in bearing and some of them developed a prism of uniaxial material that extended out of the plate. In the latter case, swelling without visible damage over the long end distance was clearly seen.

For wide yellow specimens, the failure modes were similar to those of the previous group. Specimens with very short edge distance developed shear failure. Specimens with longer edge distances failed in the mode where the outer chopped strand mat layers were damaged

near the end of the washer only while a prism of uniaxial material was pushed out of the end of the plate; clearly, there was an interlaminar shear failure between the randomly orientated and unidirectional fibre laminae. The specimens with sufficiently long end distances developed bearing failure, where the material near the bolt was crushed resulting in swelling of that area while the end of the plate remained undamaged. The transition to the bearing failure involved a failure mode where a large part of the end area was delaminated.

For the grey specimens, failure always initiated at the hole on planes parallel to the fibres; the cracks on these planes went completely through the thickness of the specimens. The rate of failure thereafter depended on the end distance. For short end distances, the failure extended very rapidly while for longer end distances, the crack length increased slowly with increasing load until it was several diameters away from the bolt.

The final failure of these specimens involved interlaminar failure between the end part of a chopped strand layer and the central uniaxial layer (Fig(3.29)). The outer separated area was usually attached to a prism of uniaxial material which was formed by shearing the middle layer. The size of the delamination area was random. In some cases, the delamination area reached a size equal to half the width of the plate while in other cases, it occurred only near the shearing planes. It is important to note that in many cases the two parallel cracks stopped near the end distance and then tended to merge into a single central crack (Fig(3.30)). This crack was due to the change of the failure mechanism from shearing to bending and transverse tension in that area. Therefore, the final failure mode for this material was not a shear one.

The failure of the wide specimens which had very large end distances involved buckling of the central uniaxial layer Fig(3.31)). This occurred after the initial shear cracks had extended a relatively long distance. Under these conditions, the material between these two cracks acted as a strut which was loaded at one end by the bolt and supported at the other end by the edge of the plate. The final failure in this case was either due to the sudden failure of the end distance resulting in shearing and delamination as explained above, or the strut itself failed in a buckling shear mode while the edge remained intact (Fig(3.31)). Here it is important to remember that failure was affected by the presence of the steel plates supporting the bolt because they prevented the strut from undergoing large bending deformations.

The specimens with extremely large end distances developed a crack through the thickness which ran parallel to the loading direction from the bolt to the loaded side of the plate (Fig(3.29-3.31)); this crack developed at the final stages of failure. The reason for its development was the wedge action of the bolt as it placed a transverse load in the coupon which in turn caused a splitting action of the composite within the gauge length. In some cases, this crack resulted in completely splitting the plate into two parts (Fig(3.31c)).

In general, the difference between the two failure modes of the 'Grey 2' and 'Yellow' materials can be explained by considering the increased thickness of the chopped strand layer which allowed the plate to distribute the stresses more evenly and to overbridge the failure areas in the uniaxial material.

3.3.2.4.4. THE STRENGTH OF THE SPECIMENS

Table(3.13) and Table(3.14) give the failure loads for the specimens of the two materials. From the tables, it can be seen that increasing the end distance increases the strength of the joint until a critical end distance is reached. Any increase of the end distance over that value did not result in a corresponding increase in the strength of the joint. Here it is important to note that some of the results of the specimens were not correct because of problems encountered in the experimental procedure.

GROUP	w(mm)	e(mm)	1	2	3	4	AVERAGE*
EGNS	30	40	18143.	16707.	19846.		18232.
EGNM	30	50	21521.	19555.	18994.		20023.
EGNL	30	60	22740.	21432.	(19707.)		22086.
GGML	30	80	21479.	22921.	22029.		22143.
GGMLL	30	100	22370.	22035.	(17391.)	21366.	21924.
EGMS	45	50	23398.	20744.	19311.		21151.
EGMM	45	60	24361.	20019.	21891.		22090.
EGML	45	70	(18469.)	22582.	22409.	25204.	23398.
GGL	45	90	24370.	26594.	25508.		25491.
GGXL	45	130	23954.	25196.	25976.		25042.
TGM	70	60	22628.	25842.	23261.	22931.	23666.
TGL	70	80	24091.	26494.	26023.	24426.	25259.
EGWS	70	90	26710.	25629.	27630.		26656.
EGWL	70	100	27286.	28778.	26136.		27400.
EEGWM	70	120	28178.	27743.	28416.		28112.
EEGWL	70	140	29769.	28018.	27156.		28314.

* The average excludes the values given in brackets

Table(3.13) Failure loads (N) for the grey specimens

Fig(3.32) shows the variation of the failure load with the end distance for the two materials and for plates of different widths. This graph was used to determine the critical end distance of each of the cases considered.

The estimated critical end distances are given in Table(3.15). It can be seen from that table that the end distance increases with the width of the plate.

The above given graph shows that although the failure of the joints is not in tension through the hole, the strength is dependent on the width of the plate. It also indicates that only

the specimens made from the grey material have a gradual transition to the area where the failure load is independent of the end distance. The reason for this is the fact that all specimens of that group failed in shear-cleavage while the yellow specimens reached the independence of the strength of the end distance by failing in bearing. This can be considered as a cut off that prevents the cleavage-shear failure from developing.

GROUP	w(mm)	e(mm)	1	2	3	AVERAGE*
GTS	20	10	4753.	3383.	4343.	4160.
GTM	20	15	5263.	5996.	5477.	5579.
GTL	20	20	7359.	8375.	7441.	7725.
EYiS	20	30	11547.	10630.		11088.
EYiL	20	40	10903.	12125.	11090.	11372.
GMS	30	10	3782.	3490.	3599.	3623.
GMM	30	20	7862.	7643.	6384.	7296.
GML	30	30	10308.	10095.	10447.	10283.
EYiSW	30	40	13581.	12122.		12852.
EYiLW	30	60	11748.	13075.	13204.	12676.
GWS	38	10	4060.	4008.	3847.	3972.
GWM	38	20	7845.	7686.	(5262.)	7765.
GWL	38	30	11452.	10664.	10737.	10951.
GWXL	38	50	12129.	12044.	13095.	12422.
EYSXL	38	60	13859.	12728.		13294.
EYLXW	38	70	13983.	13682.	12935.	13533.

* The average excludes the values given in brackets

Table(3.14) The failure loads (N) of the yellow specimens

MATERIAL	WIDTH (mm)	CRITICAL END DISTANCE(mm)
GREY 2	30 45 70	60 90 120
YELLOW	20 30 38	30 40 60

Table(3.15) Critical end distance

3.3.2.4.5. THE MOVEMENT OF THE BOLT

The load displacement curves for some of the 'Yellow' specimens are displayed in Figs(3.33-3.41). The results of the different specimens of each group show a good correlation. It is interesting to note that all groups retained a load carrying capacity of at least 3000 N after failure. This was possibly due to the friction developed between the plate and the washers and

between the sheared wedge and the rest of the plate. A comparison between the patterns of failure of the specimens and the post failure load showed that the development of crushed material ahead of the washer resulted in increasing the load that was supported by the failed specimen. The displacement at which failure occured can be seen to be varying from .5 mm for narrow specimens with short end distances to 1 mm for wide specimens with long end distances. The reduction in load on the specimens was sudden for all except those which failed in bearing. The latter specimens were able to sustain the failure load for bolt movements ranging from .5 mm to 1 mm in addition to the displacement which occurred at failure initiation.

The load displacement curves for some of the specimens made from the material 'Grey 2' are given in Figs(3.42-3.48). These graphs show that the amount of displacement before the load deceases dramatically seems to be dependent on the end distance. The greater the end distance, the larger the displacement before the sudden decrease of the load. This shows that it is possible to obtain safe ductile shear failure (and not a bearing failure as usually quoted in the literature) by increasing the end distance. The same graphs indicate that the specimens were able to support about 6000 N after failure occurred. The reason for this might be the friction and interlocking associated with pushing the separated wedge in front of the bolt out of the plate. After excessive displacement of the bolt, the load droped again to about 3000 N.

3.3.2.5. THE EFFECT OF OFF-AXIS FIBRES

3.3.2.5.1. OBJECTIVE

The objective of this set of tests was to determine the strength and the behaviour of coupons which were mainly reinforced using unidirectionally aligned fibres which were not axial.

3.3.2.5.2. THE SPECIMENS

Three groups of specimens were prepared from the material designated 'Grey 2'. The width of all specimens was 70 mm while the end distance varied according to Table(3.16). The end distances were controlled by the size of the specimen that could be obtained from the pultruded plate. The three groups had fibre orientations varying from 0° to 90° at an interval of 30°.

SPECIMEN GROUP	TGL	TG3	TG6	TRN
FIBRE ORIENTATION	0°	30°	60°	90°
GAUGE LENGTH (mm)	50	45	30	50
END DISTANCE (mm)	80	80	60	50

Table(3.16) Geometry of Specimens

3.3.2.5.3. RESULTS AND DISCUSSIONS

The failure loads of the specimens are given in Table(3.17) and the load deformation curves of the specimens are given in Fig(3.49). The specimens whose fibres were not axial, failed in tension through the hole due to the limited tensile strength of the material Fig(3.50). The plane of failure in this case was always parallel to the fibres.

SPECIMEN NUMBER	GROUP			
	TGL	TG3	TG6	TRN
1	24091.4	18945.9	12040	9857.7
2	26493.6	19765.5	10678.9	9683.9
3	26023.2	17639.7	10482.5	8960.5
4	24426.0	-	-	-
AVERAGE	25258.6	18783.7	11067.1	9500.7

Table(3.17) The Strength of the Specimens (N)

Although failure initiated in all cases near the hole in the direction of the fibres, no consistent pattern for the development of failure was observed. In some specimens, the cracks extended towards the unloaded side of the plate while in others it extended towards the loaded side of the plate.

The post failure behaviour can be seen to be dependent upon the failure type because all specimens which failed in tension through the hole retained the same load after failure. The specimens which failed in shearing showed a much higher post failure load capacity.

The load deflection curves show two plateaus after the initial failure. The first described the stage where the specimens developed the cracks around the hole before they extended to the sides of the plates. The next plateau was reached at a lower load level when one of the cracks reached the edge of the specimen. The small load supported on the specimens in this

final stage was due to the bending stiffness of one side of the specimen. For the transverse specimen, this could not be seen because the test was stopped after the formation of the first crack.

A comparison of all load displacement curves for the different fibre orientations shows that by rotating the fibres from the axial direction to the transverse direction, the strength degrades and in addition, the joints become more brittle. It is interesting to note that the average failure displacement for the transverse specimens was larger than the failure strain of the specimens with the fibres directed at an angle equal to 60° to the axis of the specimen. This is due to the small gauge length used to measure the displacements for the latter group. The change in the strength of the specimens due to rotating the fibres from the axial direction, reduces with increasing angle. Therefore, small variation from the axial direction is expected to result in large reductions of strength, whilst for transverse specimens, the variation is small. It was noted that while the ratio of the axial to transverse strength of the material was about twenty, the corresponding ratio of the strength of the joints was only about 2.5.

3.3.3. TESTS INVOLVING TWO FASTENERS IN SERIES

The behaviour of specimens which were bolted using two fasteners lying in series was also investigated. The aims of these tests were to understand the behaviour of these joints in order to provide rules for the behaviour of more complicated cases.

3.3.3.1. DESCRIPTION OF THE SET-UP

The test equipment used for the present investigation was similar to the set-up used for the tests performed on single fastener specimens. The bolts had a facility for attaching an LVDT to their head (Fig(3.13)). In addition, the end of their shaft had a flat which served as a support for the plunger of the other LVDT. The bolts were installed such that their heads were on opposite sides of the plate and the LVDTs were positioned in opposite directions (Fig(3.51)).

When the effect of changing the relative stiffness of the plates forming the joint was investigated, it was decided to use two steel plates to transfer the load between the bolts. In this case, the bolt near the unloaded end of the plate was held in place using the same technique adopted for single fastener joints (Fig(3.51)). A different arrangement was used for the condition where it was assumed that the bolts were not moving relative to each other. In that case, a rigid steel plate which had two holes to accommodate the bolts was attached to the

testing machine (Fig(3.17)). The steel plates used for loading were separated from the composite plate using tight-fitting steel washers. This meant that no friction between the plates was considered. The composite plates were attached to the testing machine using the fixing techniques described previously and shown in Fig(3.16).

The bolt situated near the free ends of the composite plates will be referred to as the outer bolt while the other will be referred to as the inner bolt. The stretching rate was .5 mm/minute. The torque used to tighten up the bolts was the same as that used for the single bolt specimens.

All steel plates were provided with eight millimetre long electrical resistance strain gauges on each of their sides. The strain gauges were used to determine the load taken by the bolts. A calibration procedure for the steel plates was undertaken in order to establish the load-strain relationship. The steel plates which were not connected to the testing machine were calibrated by determining the strain corresponding to an applied load. For the rigid plates, the calibration was more difficult because applying a load on either hole affected the strain field of the whole plate. This topic will be discussed in more detail now.

3.3.3.2. THE LOAD MEASUREMENT

In order to determine the load transmitted by the steel plates to the inner bolt, it was necessary to calibrate the strain developed in the steel plates versus the load applied at the holes. For this purpose, the steel plates were loaded in the absence of the composite plates through each of the holes independently. The set-up was identical to the actual testing situation except that the composite plate was replaced by another steel plate which transmitted the load to one hole only. The load versus the average strain on the four strain gauges was recorded and it was confirmed that the resulting relationship was linear and reproducible. The following equations which predict the load using the measured strain were obtained from these graphs by regression analysis.

$$P_o = C_o + 186.3\epsilon_o$$
$$P_i = C_i - 898.6\epsilon_i \qquad (3.14)$$

where the load is measured in N and the strain in micro strain. The subscripts o and i are for the cases when the load was applied at the outer and inner hole of the steel plate respectively.

C_o and C_i are the intercepts which can be obtained using the strain reading at which the load is equal to zero. Here it should be emphasised that ϵ is the reading obtained from the data logger without relating it to zero initial strain. The reason for keeping the parameters C_o and C_i as variables, will be explained later in this section.

Finite element analyses of a plate loaded through two holes showed that it is acceptable to apply the superposition principle to determine the strain when both holes are loaded by a fraction of the total load. In this case it is possible to write:

$$\epsilon=\epsilon_o+\epsilon_i \qquad (3.15)$$

and from equilibrium it is known that:

$$P=P_o+P_i \qquad (3.16)$$

Substituting for the values of ϵ_o and ϵ_i

$$\epsilon=0.00537P_o-0.0011128P_i-C \qquad (3.17)$$

Eliminating P_i

$$\epsilon=0.00648P_o-0.0011128P-C \qquad (3.18)$$

Solving for P_o

$$P_o=0.1717P+150.431(\epsilon-C) \qquad (3.19)$$

Where C is a function of the parameters C_o and C_i. This parameter C controls the position at which the straight line in Eq(3.18) intercepts the load axis. It was found that the numerical values obtained experimentally for C_o and C_i to calculate C, resulted in a linear realtionship between the load and the strain, which did not yield zero load for zero strain. A reason for this situation was the slight inaccuracies in measuring the distance between the two holes during the drilling process which resulted in small prestressing forces. This constant was determined uniquely by enforcing the condition that the load on the outer hole of the steel plate had to be equal to zero when the total load applied by the testing machine was equal to zero. This value was different for each specimen and it was determined by knowing the strain reading corresponding to the zero load.

Therefore, by knowing the total load and its corresponding strain reading and the strain reading at zero load, the load taken by the outer bolt of the steel plate can be determined. It is important to note that this load corresponds to the load taken by the inner bolt of the composite plate.

This fully empirical approach was adopted in order to represent the conditions of the test as accurately as possible. An analytical method could not include all the effects which occur due to the interaction of the plates and the bolts.

3.3.3.3. EXPERIMENTAL BEHAVIOUR OF A PLATE LOADED BY TWO PINS

3.3.3.3.1. OBJECTIVE

The objective of this test was to establish firstly, the relationship between the relative movement of two bolts which were in series and, secondly, the distribution of the total load between them.

3.3.3.3.2. DESCRIPTION OF THE SPECIMEN

The specimens were prepared from the material designated 'Blue 1' and they were 57 mm wide. The end distance was 57 mm long and the back pitch was 95 mm long. Four groups were considered each consisting of three specimens of the same dimensions. The dimensions of the specimens were determined based on preliminary testing to ensure bearing failures for each of the holes.

3.3.3.3.3. DESCRIPTION OF THE SET-UP AND THE EQUIPMENT

The plate was loaded through two tightly fitting bolts. The load was distributed between the bolts using two steel plates which were mounted on both sides of the composite plate. The composite plate was separated from the steel plates by washers having a 22mm outer diameter. The test set-up is shown in Fig(3.51)).

The distribution of the load between the bolts was changed by altering the stiffness of the steel plates. It should be clear that the load transmitted by the two steel plates was equal to the load applied to the inner bolt. This load was experimentally measured by sticking two strain gauges onto the two faces of each of the steel plates. Before testing the composite plates, the load-strain relations for each pair of steel plates was determined. The result of that calibration was a linear equation relating the load taken by the plates to the average of the four measured strains. The cross section of the steel plates used with the different specimen groups is given in Table(3.18).

GROUP	DIMENSIONS OF STEEL PLATE
PA	2*40 mm
PC	2*120 mm
PE	2*40mm with two holes

Table(3.16) The dimensions of the steel plates

The steel plates were calibrated under the conditions which occurred in the tests where they were mounted on the bolts with washers separating them from the plates; the load was applied to the bolts through these plates. The relationship of the load versus the relative movement of the bolts was not linear. In some cases it showed an increase in the movement at a constant load of about 4kN. This was explained by the presence of a gap between the bolts and the holes in the steel plates. The movement of the bolts at constant load was due to their slip after friction had been overcome between the loaded plates and the push-fit washers.

Three problems occurred during that test. First the displacement associated with the failure of the specimen was relatively small, thus the slightest inaccuracy in measuring the displacements caused large errors. The second problem was the gripping of the specimens. Because the width of the specimen was relatively large, the conventional wedged grips were not able to be used and the method for single bolt joints was again employed. Because of the higher loads in the present experiment, slipping occurred repeatedly. The effect of slipping was a reduction of the applied load rather than an increase in the displacements. The reason was that the displacements were not measured from the cross head movement. A further problem was the determination of the ratio of the load on the inner bolt for low load levels. This was similar to the problem of measuring the displacements, because the results for small load levels were extremely sensitive to the accuracy of measuring the load.

3.3.3.3.3.1. RESULTS AND DISCUSSUIONS

The percentage load supported by the inner bolt for all specimens is displayed in Fig(3.52-3.54)). These figures show that at the initial loading levels, almost all the load was taken by the inner bolt. This was expected because originally, the composite plate was not strained and therefore, the load on the outer bolt had to be zero. Under increasing load, the specimens experienced a quick reduction of the load on the inner bolt. This occurred because the holes of the steel plates moved away from each other. This movement was resisted by the presence of the composite plate forcing the inner bolt to share the load with the outer one. It

should be noted that the percentage load supported by the inner bolt reduced until it became less than 50%.

Analytical solutions for the problem under consideration (Feodosyev 1977) predict that the inner bolt will always support a higher proportion of the total load. This and the closeness of the results for all groups in spite of the difference in the stiffnesses of the steel plates indicates that the set-up did not behave as expected. It is possible that the holes elongated due to the initial loading whilst calibrating them. Therefore, when performing similar tests, it is recommended to keep the thickness of the loading plates as large as possible. This avoids the development of local permanent deformations near the hole which may affect the effective stiffness of the steel plates.

After the total load on the plate reached a value of about 15kN, the percentage load on the inner bolt began to increase again. This could have been caused by a reduction of stiffness of the composite plate near the outer hole due to the initiation of damage in that area. This explanation is supported by the fact that the audible noise that signals the initiation of failure was heard at the point where the percentage of load on the inner bolt reached a minimum level.

All specimens loaded using two bolts showed signs of swelling outside the area confined by the washer (Fig(3.55)). This indicated the development of the bearing failure at the outer bolt which was due to the higher share of the load supported by that bolt. At the point where the share of load on the inner bolt began to increase, the load on the outer bolt was about 15 kN which was roughly the load at which the slope of the load displacement of the specimens in group PB began to reduce (Fig(3.56)). The specimens of group PB were loaded only through the outer bolt. This resulted in their failure in bearing at that hole (Fig(3.55)). The failure loads on the specimens were relatively variable because of the voids in the material. In all specimens, the swelling of the failure area was prevented by the presence of the washers. Therefore, outside the washers, the plate swelled until it came into contact with the steel plates which were supporting the bolt. These latter plates were rigid and prevented any further expansion.

All specimens which were loaded by two bolts failed in tension through the second hole although the specimens of group PB failed in bearing. The reason for this is that at the minimum cross section passing through the inner hole, the load was equal to the total load which was much higher than the bearing load. The tension through the hole failure resulted in the complete rupture of the chopped strand mat layers through the width of the specimen, while only a limited part of the uniaxial layer was fractured. The parts of the uniaxial layer which were not broken were sheared out of the laminate after the interlaminar bond had failed.

This explains the development of two post-failure stages. First the load sustained by the specimen suddenly dropped to about 8 kN, then, under further extension, it dropped to about 2 kN. It seems that the first drop was due the failure of the uniaxial layer near the hole, while the second drop was due to the failure of the chopped strand layer. The load sustained after that was due to the friction developed as the uniaxial layer was sheared out of the laminate.

The load is plotted against the relative movement of the two bolts in Fig(3.57-3.59). In general, all curves show a very stiff initial part followed by either a horizontal plateau at 4 kN or a line with reduced stiffness at 2 kN. It is possible that in the first case both bolts initially were not in contact with the steel plates and the load was transmitted initially by friction between the plate and the washers. When this friction force was overcome, the bolts moved under a constant force until they contacted the steel plate and the load resumed its increase. The length of the plateau was about .05 mm. The second case occured when the outer bolt was in contact with the steel plate while the inner bolt transmited the load by friction. The transition area in the last case was seen to be about .1 mm. Accordingly, it could be inferred that the misfit of the holes was about .1 mm which might be due to manufacturing tolerances and the repeated loading of the plates.

The relative displacement of the bolts is plotted in Fig(3.60) against the percentage load taken by the inner bolt. This figure shows that increasing the relative movement between the bolts results in reducing the percentage load on the inner bolt; the degree of reduction depends on the loading level. For low load, the change in the load distribution when varying the relative movement of the bolts is small while the opposite is true for higher loads.

The load distribution between the two bolts approached uniformity near the failure load. However, the condition where both bolts were supporting the same load was not reached because of the early tension failure of the composite plate. If ductile failure develops at both bolts, it is expected that they will take the same load.

3.3.3.4. THE LOAD DISTRIBUTION BETWEEN TWO BOLTS IN SERIES

3.3.3.4.1. OBJECTIVE

The objective of this test was to investigate the load distribution between two bolts in a composite plate, when different failure modes occured.

3.3.3.4.2. DESCRIPTION OF THE SPECIMENS

The specimens were prepared from three different pultruded lay-ups; Table(3.19) gives the dimensions and the material composition of these groups of specimens. These dimensions were chosen to ensure the development of all three basic failure modes. The specimens were loaded using the set-up described in sec. (3.3.3.3.3).

SPECIMEN	Vf	t(mm)	w(mm)	e(mm)	% UNI	MATERIAL
GTPW	.513	6	150	60	87	Grey2
GTP	.513	6	70	60	87	Grey2
P2B	.416	4	120	60	52	Blue2
PD	.368	4	57.15	57.15	42	Blue1

Table(3.19) The Dimensions and the Materials of the Specimens

3.3.3.4.3. RESULTS AND DISCUSSIONS

For all materials considered, the strength under the action of a single bolt was also determined to provide a comparison for the specimens loaded using two bolts. Table(3.20) gives details of the single bolt specimen dimensions and the measured strengths.

MATERIAL	w(mm)	e(mm)	MODE	FAILURE LOAD
Blue1	57.15	57.15	BEARING	14987.5N
Blue2	57.15	60.00	BEARING	16127.5N
Grey2	70.00	80.00	SHEAR	25258. N

Table (3.20) The Failure due to Single Bolt Loading

The ratio of the load on the inner bolt relative to the total load is plotted for group GTPW in Fig(3.61). From this figure, it can be seen that the load on the inner bolt was larger than half the total load for all loading levels. It is important to note that the first specimen of that group was preloaded to about 18.5 and 30 kN respectively. This resulted in the higher share of load supported by the inner bolt at the initial stages of loading. This happened due to the elongation of the holes of the composite plate. However, when this effect was overcome at higher loads, the behaviour of the specimen was comparable to the others. The failure of this group of specimens was in shearing where neat shear cracks ran along the tangents to the holes. The material lying between these cracks slipped relative to the rest of the plate and remained undamaged. It is interesting to note that specimen GTPW2 developed a crack behind the inner

bolt. This crack developed due to irregularity of the shearing planes which resulted in subjecting the plate to transverse tension.

The specimens of group GTP also failed in a shearing mode similar to the previous group. In this case, the failure initiated at the loaded side of the outer bolt. After that, shear cracks parallel to the shaft of the bolt proceeded to the free edge. The first and third specimen of that group failed by combined shear and interlaminar shear as shown in Fig(3.65). When the cracks approached the ends of the specimens, failure of the outer bolt occurred. The complete failure of the joint was rapid and this was followed quickly by the extention of the cracks from the inner to the outer bolt. Subsequently, the two bolts, and the material laying between them, slid out of the plate under a constant total load. The failure cracks of this case were different from those developed in the wider specimens of group GTPW. The shear cracks in the former specimen developed in the unidirectional layer but they did not continue through the chopped strand mat layers. This meant that interlaminar shear took place between the two types of layers Fig(3.65).

The proportion of load on the inner bolt of the specimens of this group was originally high as predicted using linear elastic material properties Fig(3.62). The share of the inner bolt reduced with increasing load until it reached a minimum value which was slightly less than the load on the outer bolt. After that, the part of load carried by the inner bolt increased to become greater than that of the outer one. The load distribution remained almost constant until near failure. When approaching failure, the proportion of load taken by the inner bolt began to reduce again indicating the weakening of the area around that bolt.

The specimens of group P2B failed in bearing at both bolts (Fig(3.66)). The greatest load sustained by the specimens was shared equally between the two bolts (Fig(3.63)). The bearing failure that developed at both bolts (Fig(3.66) resulted in substantial displacement of the bolts; this allowed the final failure to occur due to shear of the outer bolts. The material which was confined by the washers and ahead of the bolts was completely separated from the rest of the plate by two shear cracks and the material outside the washer was crushed into powder.

The final shear failure at the outer bolt was associated with interlaminar failure between the chopped strand layers and the central unidirectional one resulting in non-uniform patterns of failure in the chopped strand mat layers. It is interesting to note that in the second and third specimens, one of these cracks in the chopped strand layer was on the centre line indicating that it was formed due to splitting forces rather than shearing. The first specimen failed on the shearing planes, but there was evidence of cracks on the centre line.

Fig(3.64) shows the change in the ratio of the load taken by the inner bolt with the load applied on the specimens of group PD. It can be seen that at low load levels, the total load was taken by the inner bolt but subsequently, there was a sharp drop in this load until that bolt supports about 60% of the total load. This was followed by a further reduction, which was more gradual, and it continued until the plate failed. At failure, the load taken by the two bolts was almost equal.

The specimens of group PD (similar to groups PA, PC and PE considered above) failed in tension through the inner hole and occurred by fracturing the two outer chopped strand mat layers over the width of the specimen (Fig(3.55)); the central uniaxial layer was only fractured near the hole. The complete failure occurred when the chopped strand mat layer fractured after the interlaminar bond between the three layers failed.

SPECIMEN	LOAD FRACTION BEFORE FAILURE	LOAD FRACTION AT FAILURE	FAILURE LOAD N	MODE
GTP1 GTP2 GTP3	.55 .55 .55	.44 .48 .48	47167.7 45355.6 48448.0	SHR.
GTPW1 GTPW2 GTPW3	.62 .60 .57	.58 .58 .57	47044.9 45305.5 46034.5	SHR.
P2B1 P2B2 P2B3	.58 .62 N.A.	.50 .52 .53	32625.2 33430.2 34254.7	BER.
PD1 PD2 PD3	N.A. N.A. N.A.	.50 .50 .40	28438.3 30229.5 28422.2	TEN.

Table(3.21) Results for the different groups

The results given in Table(3.21) show the failure loads for the specimens of the different groups. By comparing these results with the results of the specimens which employed only one bolt, it becomes clear that the failure load per bolt of the specimens which failed in shear was less than the failure load of the single bolt specimens. The specimens which failed in bearing and tension, on the other hand, developed a failure load approximately equal to double the failure load of single bolt specimens. This can readily be explained when noting the fraction of load supported by each of the bolts at failure given in Table(3.21). This shows that the specimens which developed failure loads equal to double the strength of specimens employing single fasteners, distributed the load almost equally between the two bolts at failure. This means that it is possible to design joints employing multiple fasteners which have the same efficiency as

the specimens with single fasteners provided the load on each of the fasteners is the same. This can be achieved by ensuring that a ductile failure mode develops.

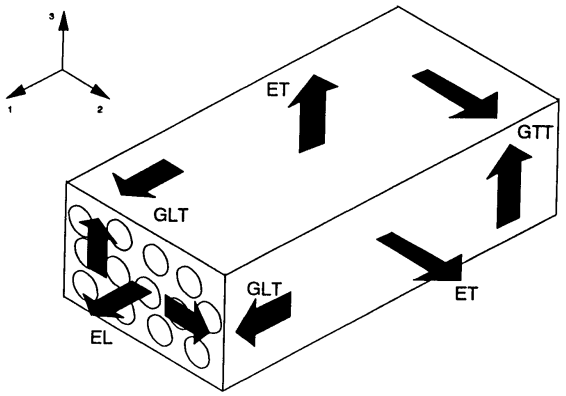

Fig(3.1) Definition of Material Properties for a Unidirectional Composite

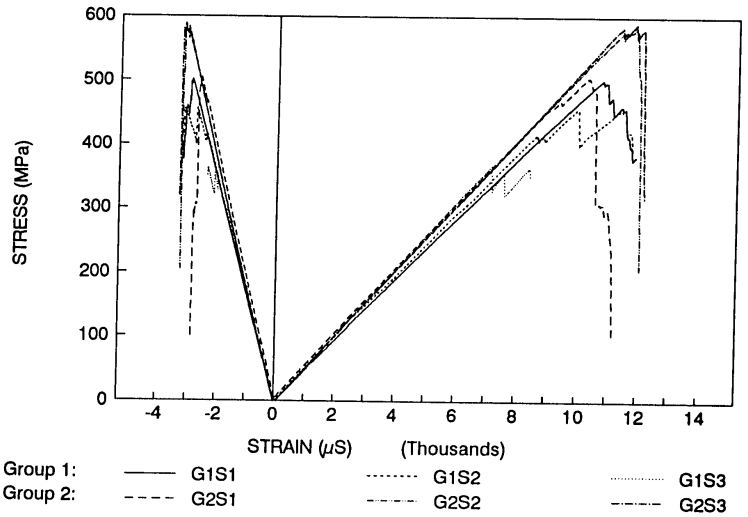

Fig(3.2) Experimental Stress-Strain Curves

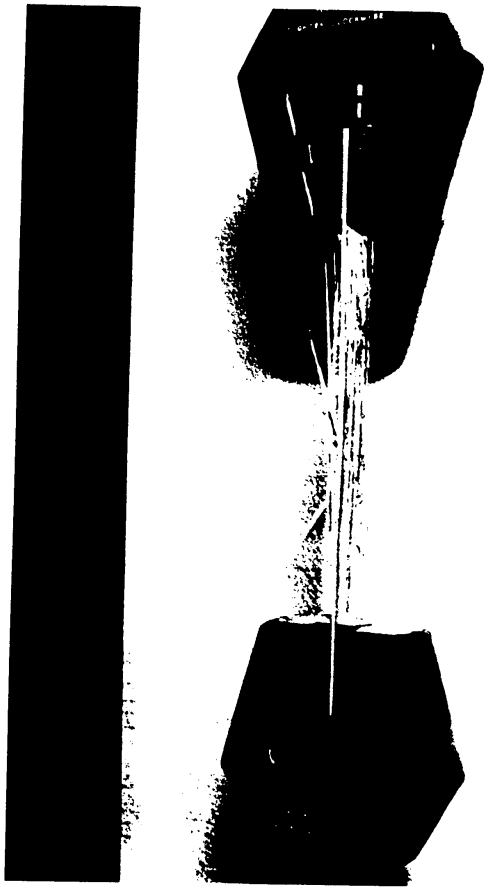

Fig(3.3) Failure in Uniaxial Tension

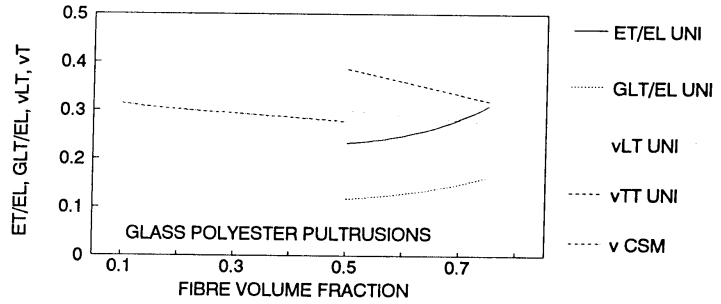

Fig(3.4) Effect of Vf on Material Properties

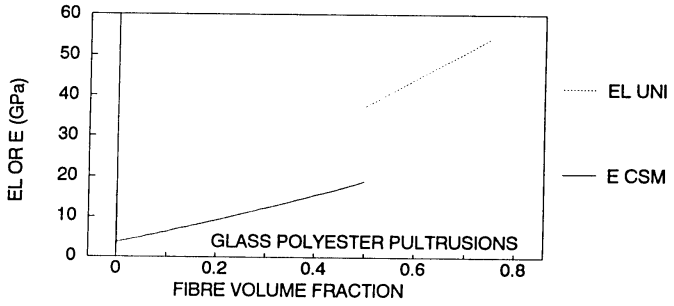

Fig(3.5) The Variation of EL & E with Vf

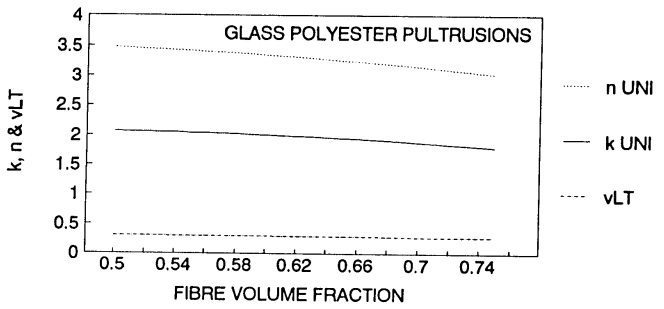

Fig(3.6) The Variation of k, n & vLT with Vf

Fig(3.7) Poisson's Ratio for a Composite Made-up of

Uniaxial and CSM Glass Polyester Layers

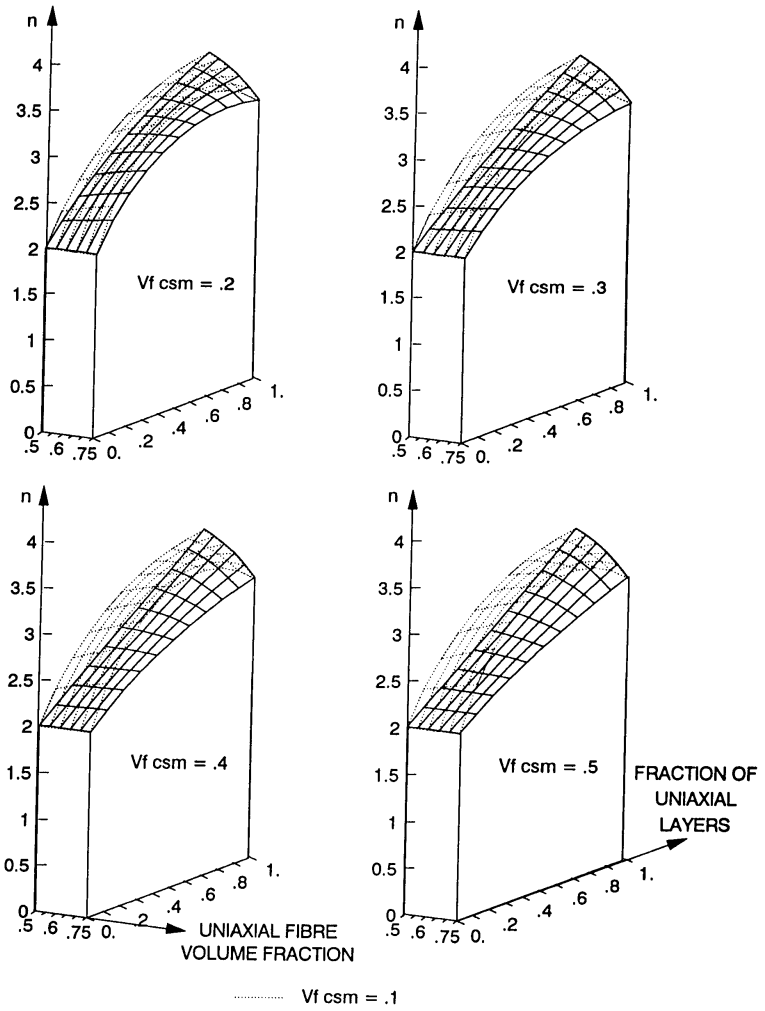

Fig(3.8) n for a Composite Composed of
Uniaxial and CSM Glass Polyester Layers

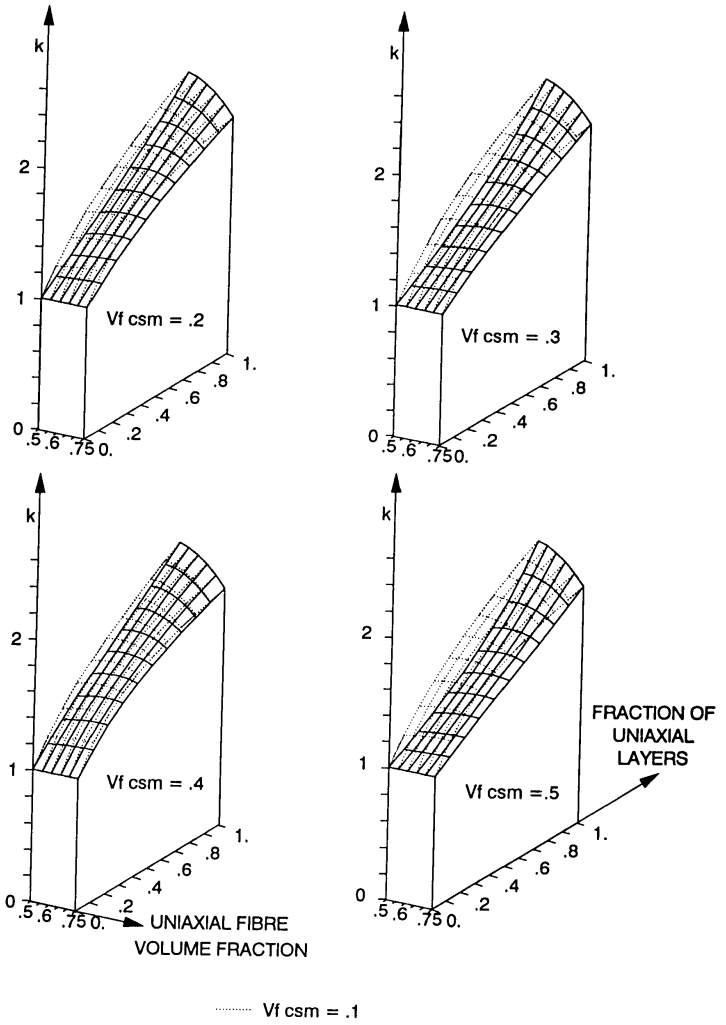

Fig(3.9) k for a Composite Composed of Uniaxial and CSM Glass Polyester Layers

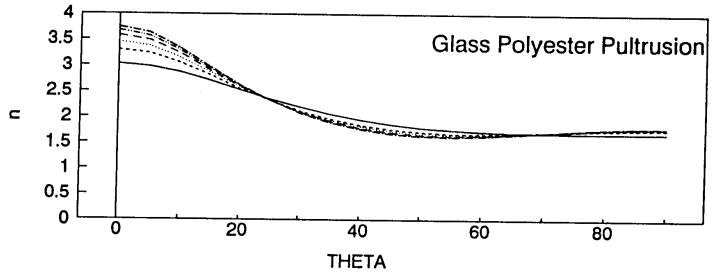

Fig(3.10) n Values for Angle Ply ±Theta Composite

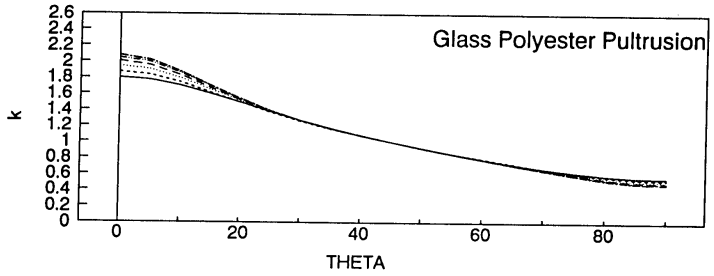

Fig(3.11) k Values for Angle Ply ±Theta Composite

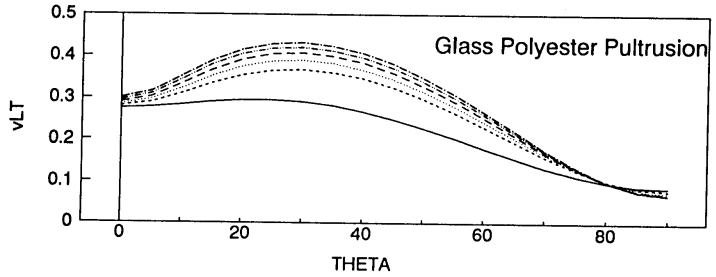

Fig(3.12) Poisson's Ratio for Angle Ply ±Theta Composite

Vf = .5 Vf = .55 Vf = .6
Vf = .65 Vf = .7 Vf = .75

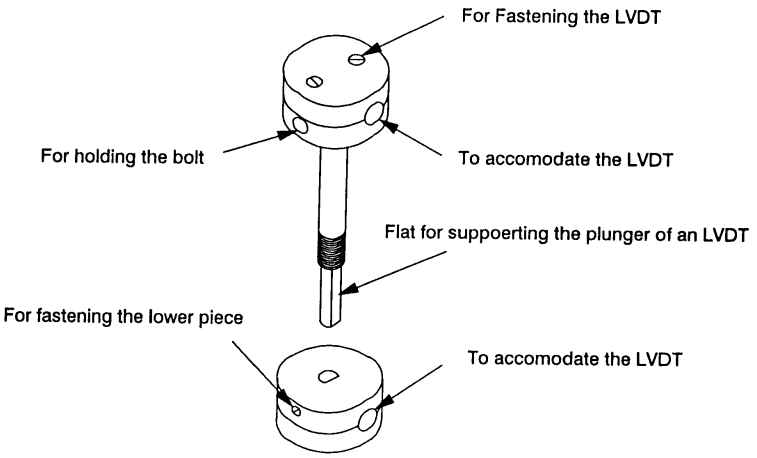

Fig(3.13) Bolt with Arrangement for holding LVDT

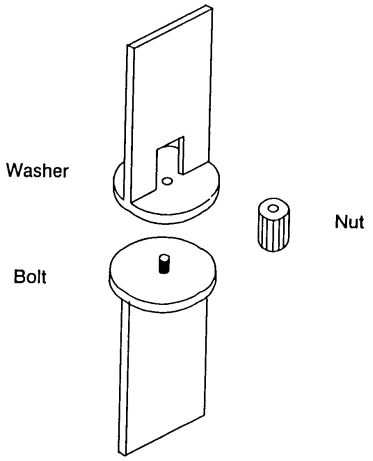

Fig(3.14) Arrangement for supporting the LVDT

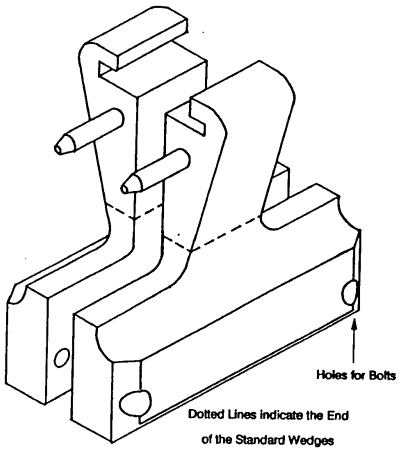

Fig(3.15) Modified Wedges for Holding Specimens

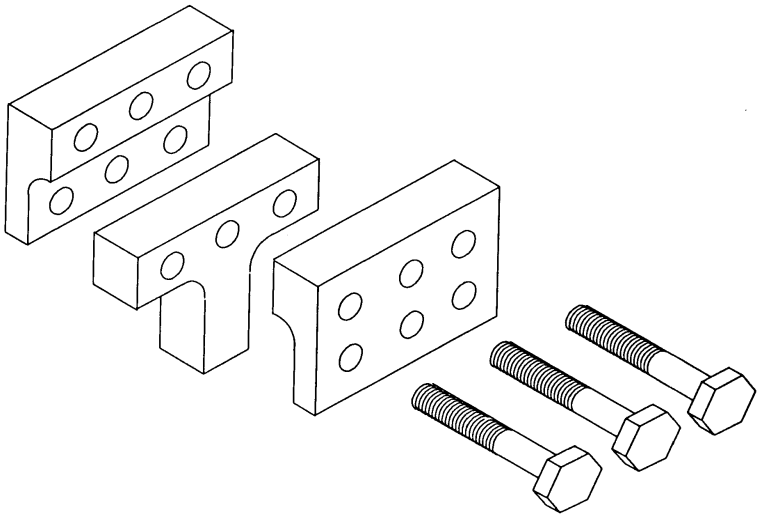

Fig(3.16) Alternative Gripping Arrangement

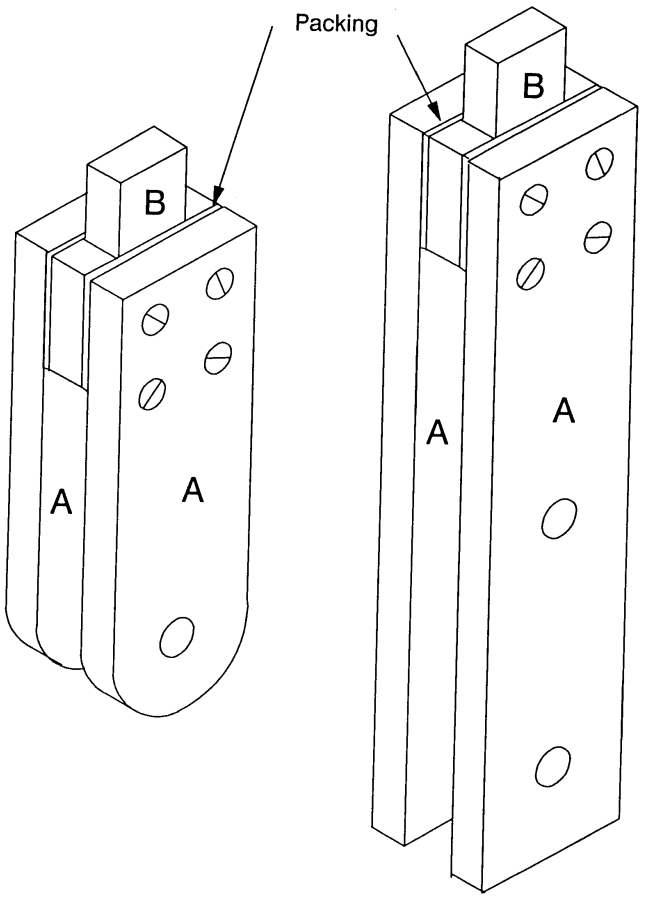

Fig(3.17) Arrangements for Holding the Bolts

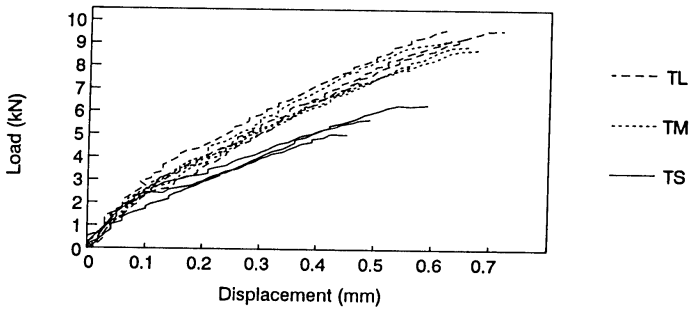

Fig(3.18) Load Displacement Curves for Narrow Specimens

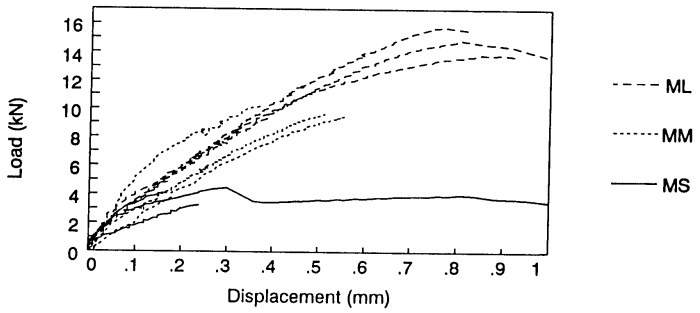

Fig(3.19) Load Dispalcement Curves for Medium Speciemens

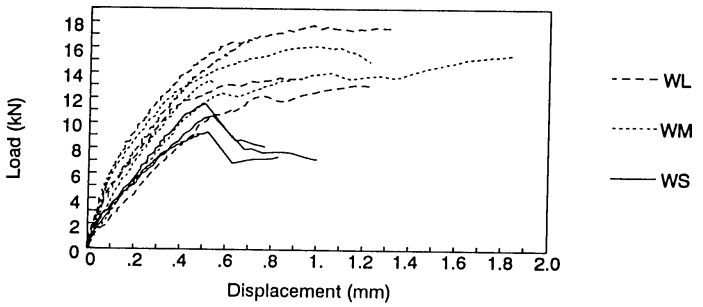

Fig(3.20) Load Displacement Curves for Wide Speciemns

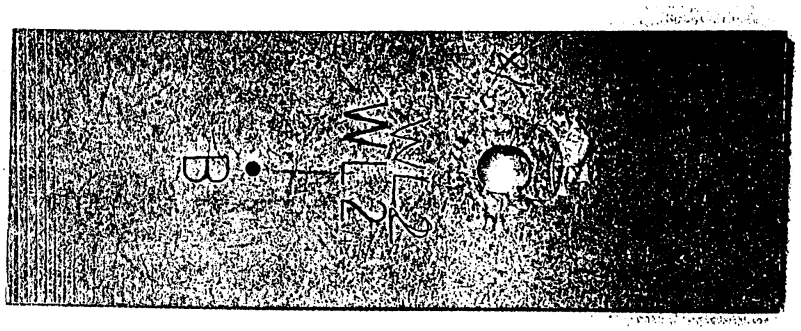

Fig(3.21) Typical Bearing Failure

Fig(3.22) Typical Tensile Failure

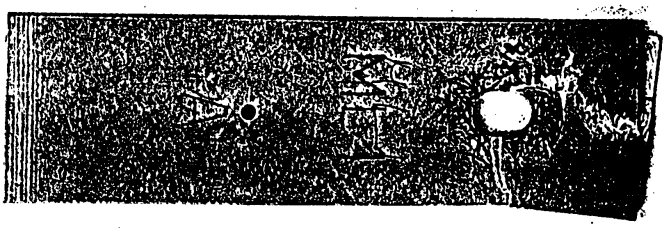

Fig(3.23) Typical Combined Failure

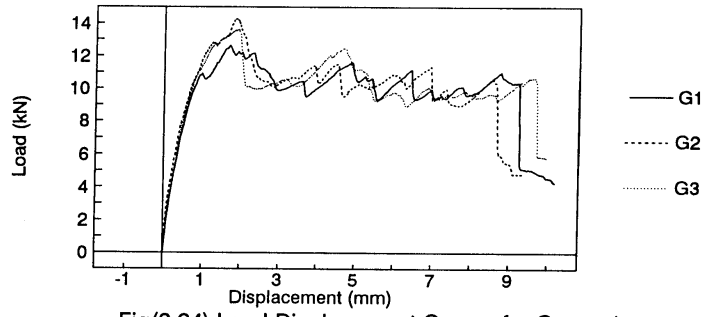

Fig(3.24) Load Displacement Curves for Group 1

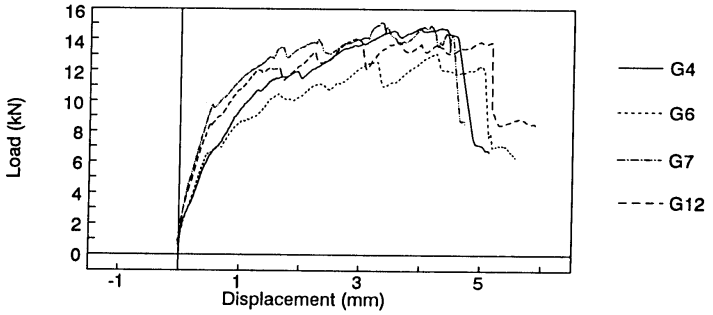

Fig(3.25) Load Displacement Curves for Group 2

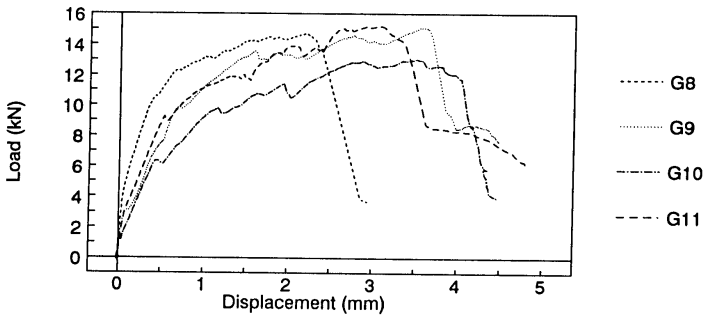

Fig(3.26) Load Displacement Curves for Group 3

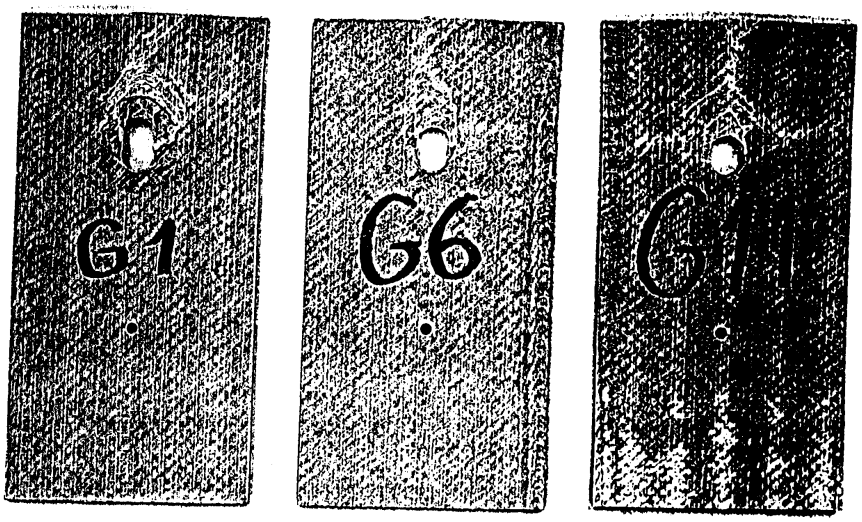

Fig(3.27) Effect of Confinement Area on Failure Pattern

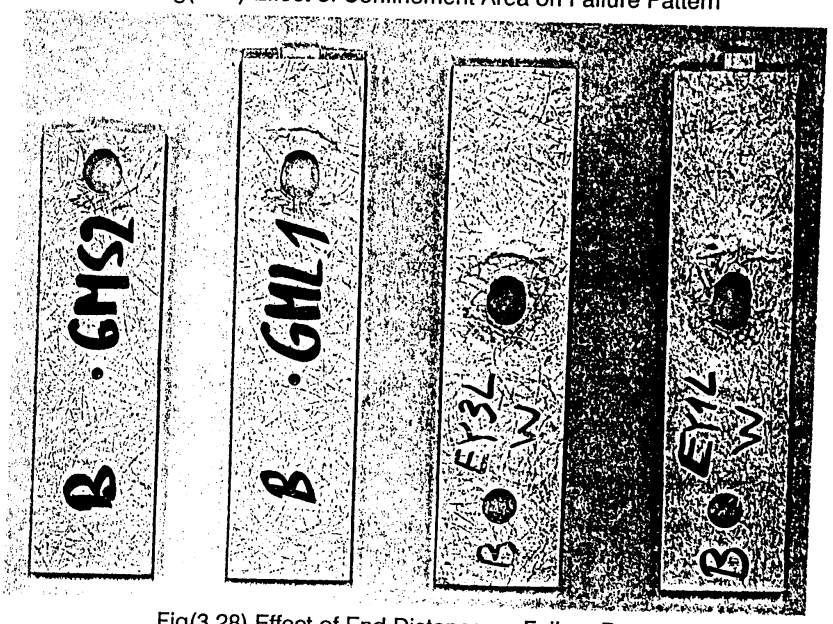

Fig(3.28) Effect of End Distance on Failure Pattern

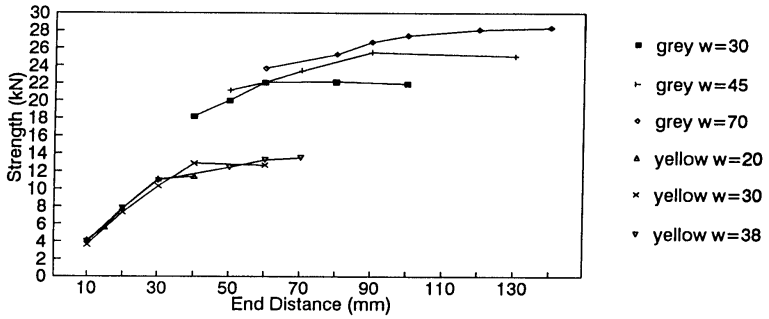

Fig(3.32) The Dependence of the Shear Strength on the Geometry

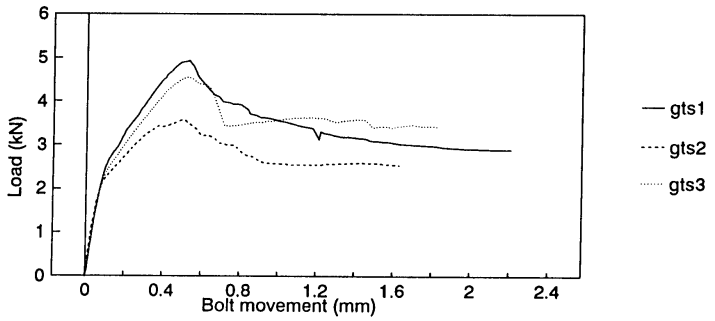

Fig(3.33) Load Displacement Curves for Group GTS

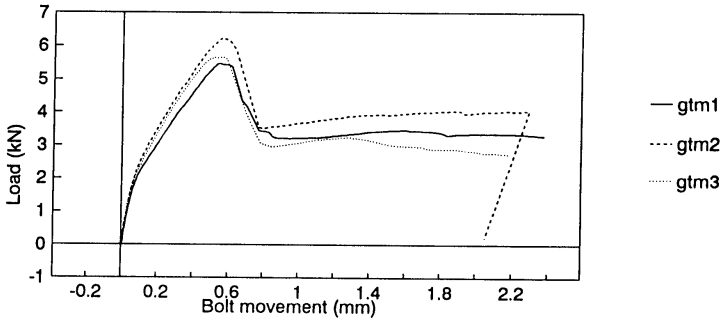

Fig(3.34) Load Displacement Curves for Group GTM

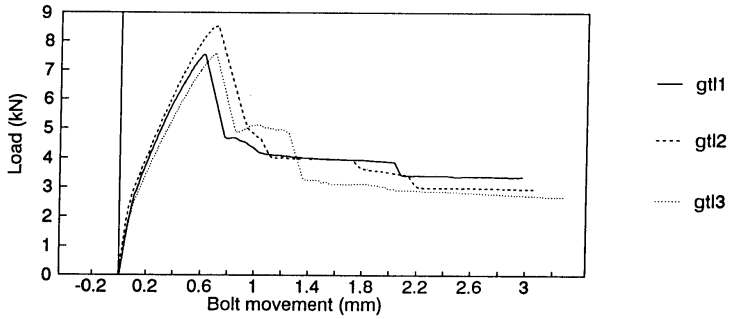

Fig(3.35) Load Displacement Curves for Group GTL

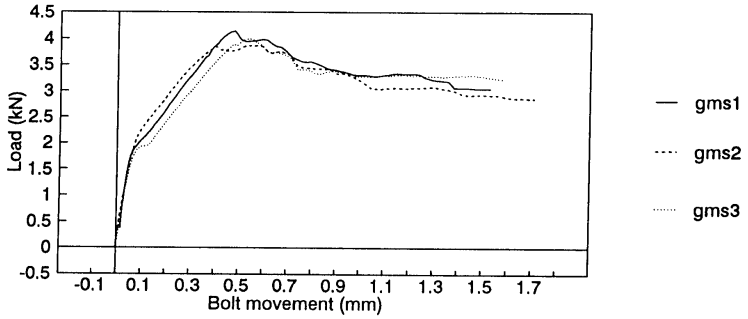

Fig(3.36) Load Displacement Curves for Group GMS

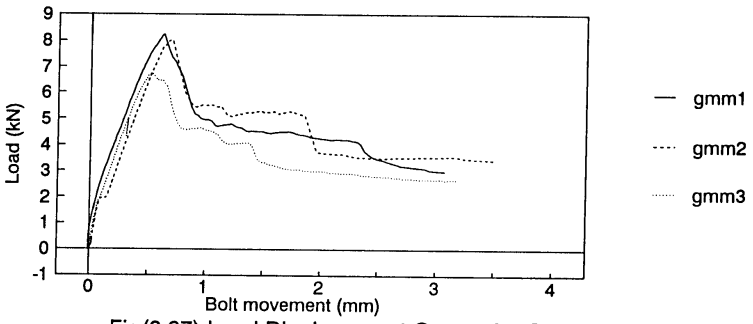

Fig(3.37) Load Displacement Curves for Group GMM

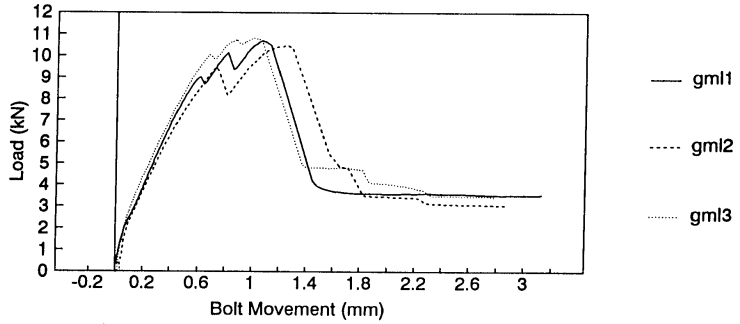

Fig(3.38) Load Displacement Curves for Group GML

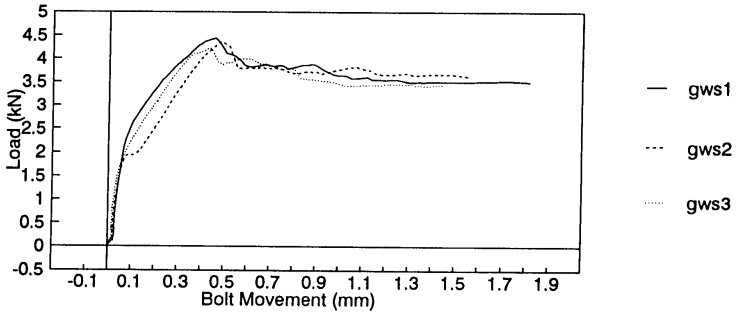

Fig(3.39) Load Displacement Curves for Group GWS

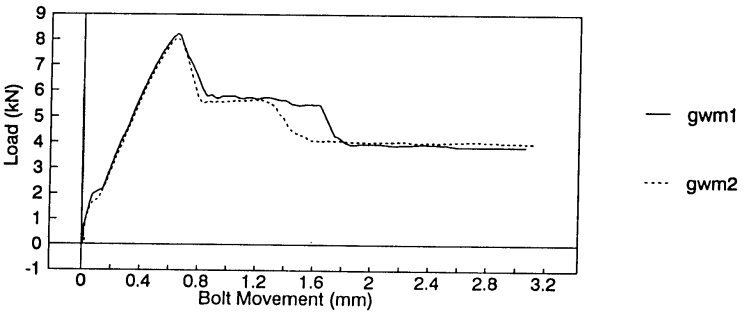

Fig(3.40) Load Displacement Curves for Group GWM

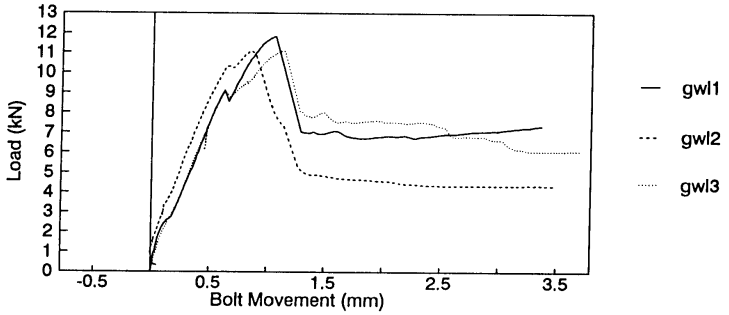

Fig(3.41) Load Displacement Curves for Group GWL

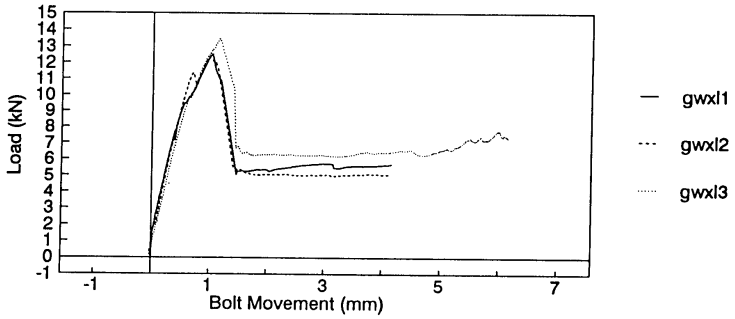

Fig(3.42) Load Displacement Curves for Group GWXL

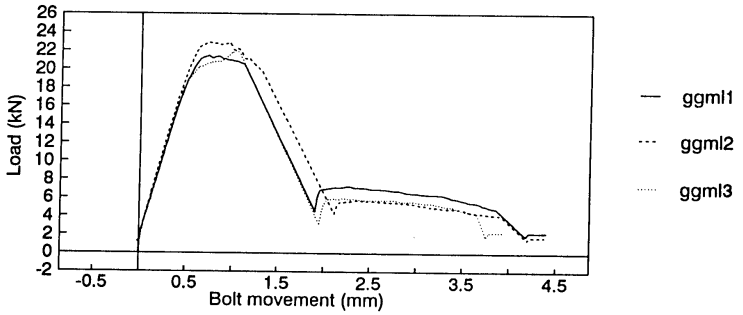

Fig(3.43) Load Displacement Curves for Group GGML

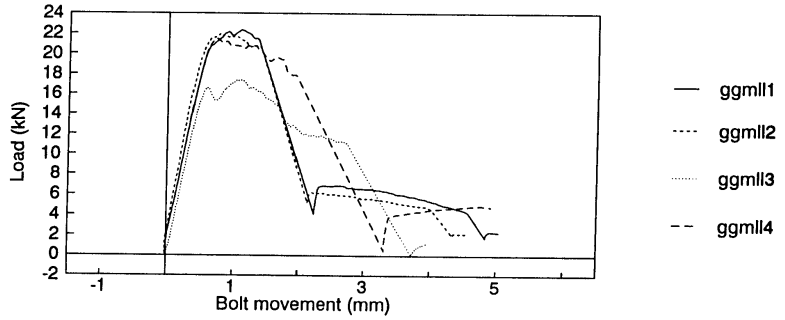

Fig(3.44) Load Displacement Curves for Group GGML

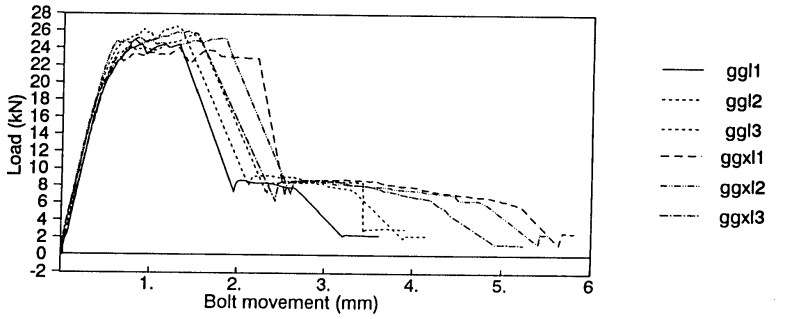

Fig(3.45) Load Displacement Curves for Group GGL and GGXL

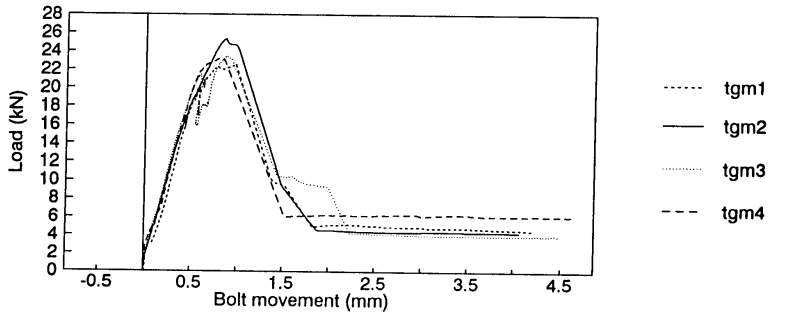

Fig(3.46) Load Displacement Curves for Group TGM

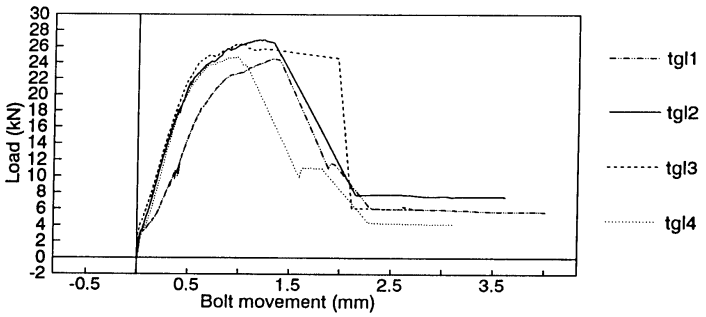

Fig(3.47) Load Displacement for Group TGL

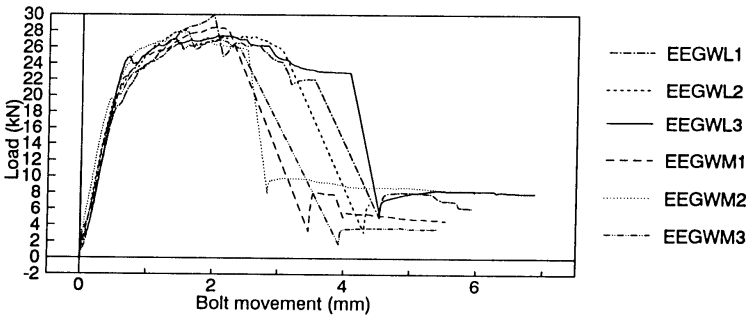

Fig(3.48) Load Displacement for Groups EEGWM and EEGWL

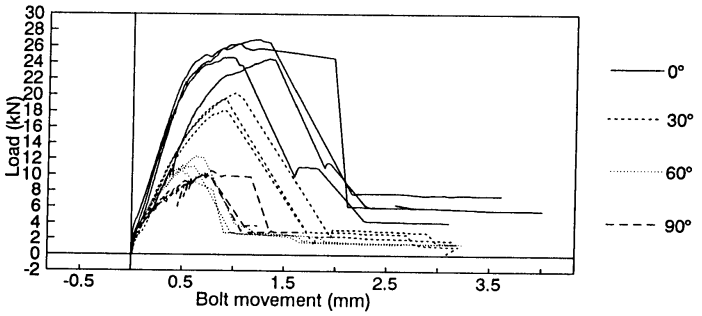

Fig(3.49) Load Displacement for Different Fibre Orientations

Fig(3.51) Set-up for Tests involving Two Bolts

Fig(3.50) Effect of Fibre Direction on Failure

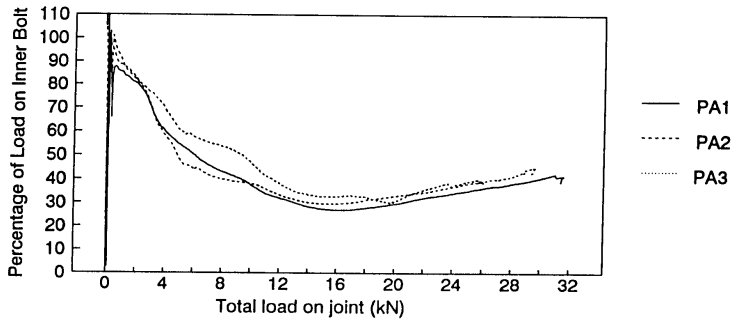

Fig(3.52) Load Distribution for Group PA

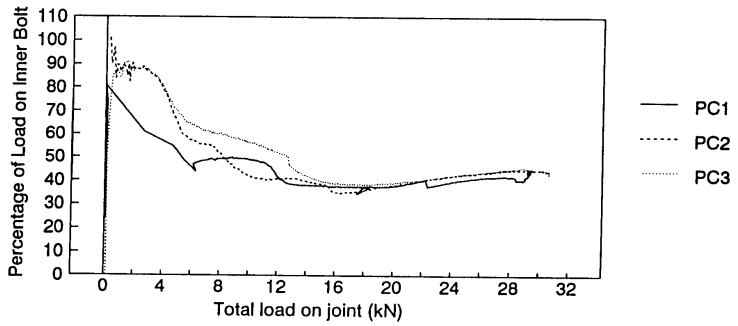

Fig(3.53) Load Distribution for Group PC

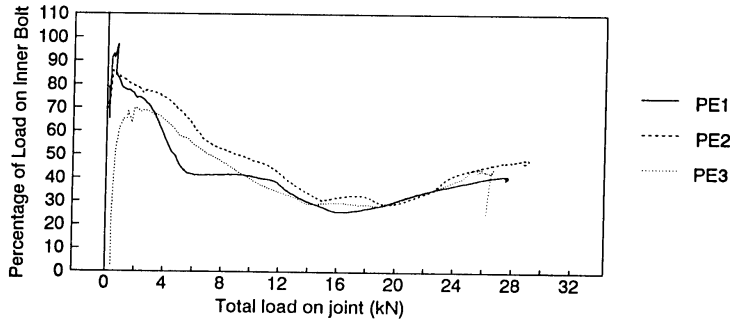

Fig(3.54) Load Distribution for Group PE

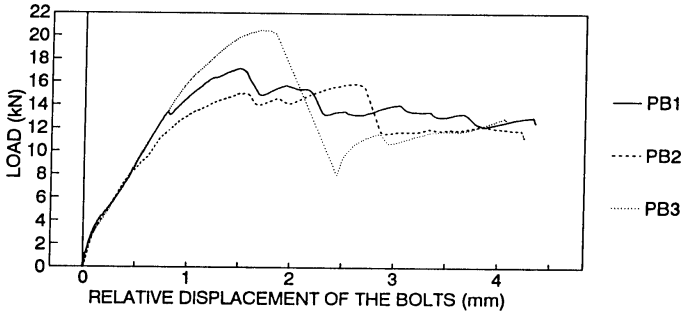

Fig(3.56) Load Displacement Curves for Group PB

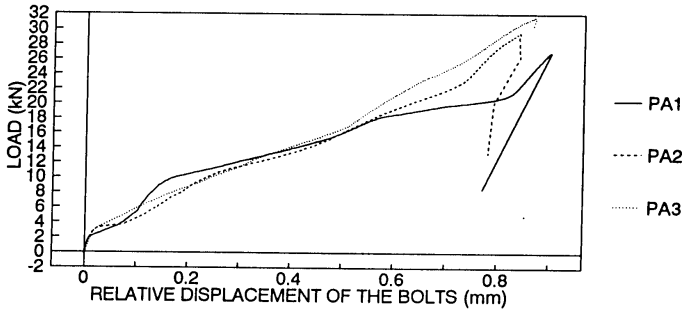

Fig(3.57) Load Displacement Curves for Group PA

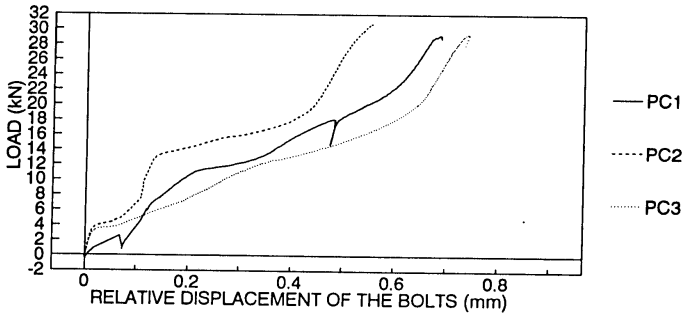

Fig(3.58) Load Displacement Curves for Group PC

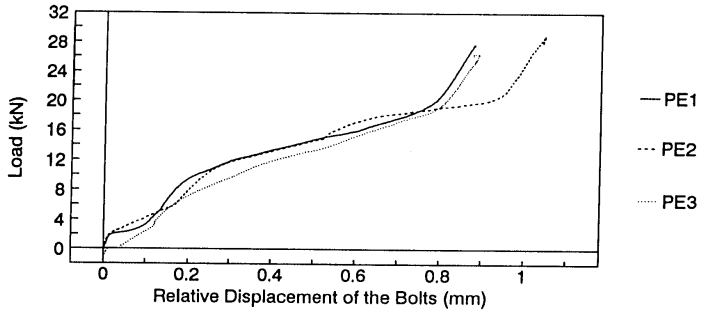

Fig(3.59) Load Displacement Curves for Group PE

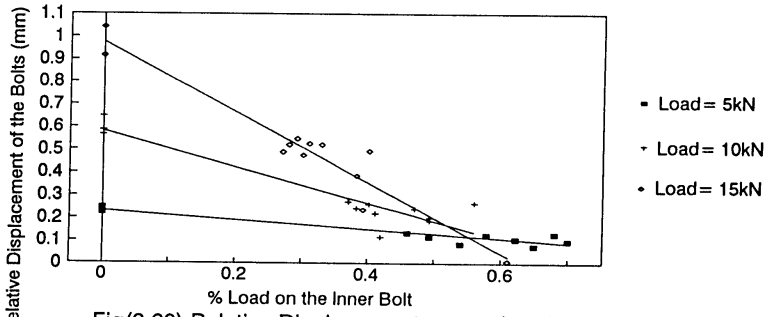

Fig(3.60) Relative Displacement versus Load Distribution

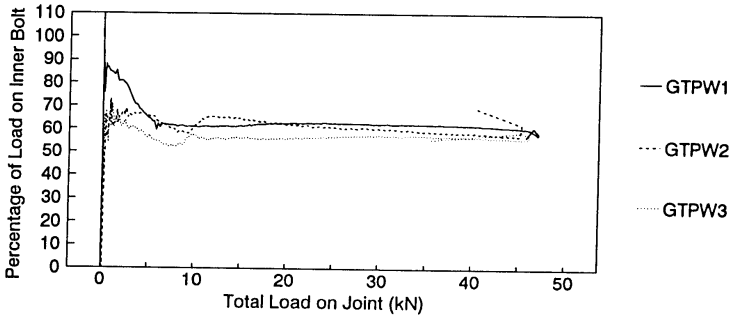

Fig(3.61) Load Distribution for Group GTPW

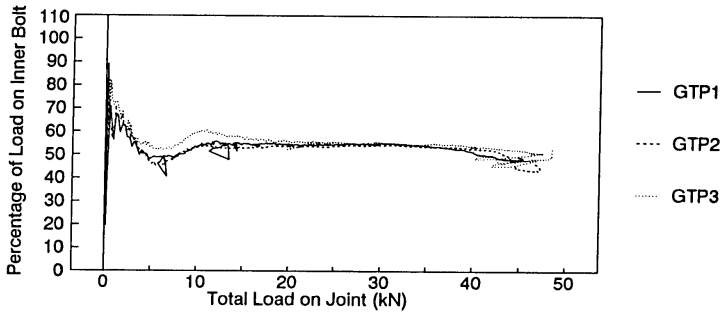

Fig(3.62) Load Distribution for Group GTP

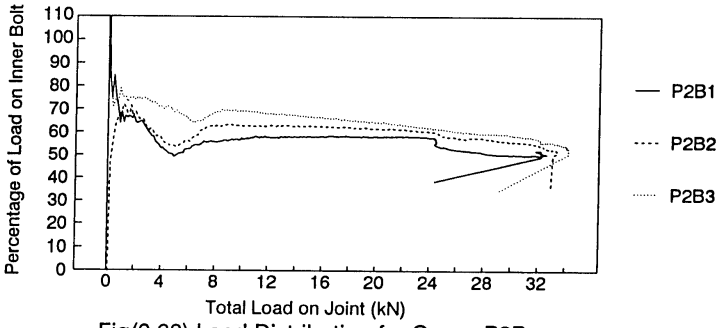

Fig(3.63) Load Distribution for Group P2B

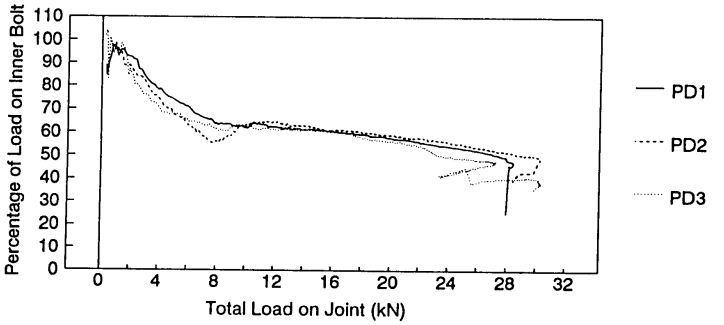

Fig(3.64) Load Distribution for Group PD

CHAPTER FOUR

4. THEORETICAL INVESTIGATIONS

4.1. INTRODUCTION

The stress analysis of joints is undertaken in order to verify the adequacy of their design from the point of view of strength and stiffness. To achieve that goal, two fundamentally different approaches can be adopted. The first approach requires the theoretical model to include as many features of the prototype as possible. This detailed model is created with the intention of using it (after it has been calibrated) as a replacement for the expensive and time consuming physical testing. The second approach, which is more popular among practical engineers, is the semi-empirical approach. In this case, the stress analysis is undertaken for a reasonably accurate model of the prototype, then the difference between the real behaviour and the predicted behaviour is catered for using empirical failure prediction procedures.

In most of the previous analyses of mechanical joints in composites, the second approach was pursued and accepted as the standard approach for investigating their behaviour theoretically. The results of the published work in that field show that in order for this approach to give reliable predictions, the empirical procedures need to be calibrated for different materials, lay-ups and geometries. This is believed to be a result of the great number of simplifications applied to the models used in stress analysis.

The successful analysis of joints depends on the correctness of the numerical model for which the analysis is performed. The formulation of a theoretical model of a structure requires a decision on the following considerations:

a) The geometrical model,
b) the material model and
c) the boundary and loading conditions.

The acceptable accuracy for the model is a compromise between the required quality of the results and the available computing facilities.

Stress analysis of joints can be performed using numerical or analytical techniques. The first category of analysis methods is easy to use and, provided sufficient computing power is available, it can consider sophisticated theoretical models. These methods, however, are not

efficient tools for performing parameter studies. The latter investigations are ideally performed using closed form analytical solutions.

Accordingly, in this chapter the finite element method is used for the investigation of the more detailed models of the joints while the complex variable approach of the plane theory of elasticity associated with the laminated plate theory is used to investigate the tangential stresses around a loaded hole in an infinite plate.

4.2. THE FEATURES OF THE PROTOTYPE

In order to judge the models of the joints, it is necessary to monitor the behaviour of the prototype and obtain information about the required aspects of the model. These features can be grouped under the following headings.

a) Geometrical features: The geometry of the joints involves rectangular and circular boundaries and the thickness of the plate is much smaller than its other dimensions.

b) Material features: The plate is made from composite material which is a layered elastic-plastic fracturing anisotropic material. The anisotropy of the material is usually restricted to orthotropy due to symmetry. The bolt and the washer, on the other hand, are made from an elastic-plastic material which is usually much stiffer than the composite material.

c) Loading and support features:

i) Kinematic features: The plate is restrained from radial movement relative to the bolt shaft in the area of contact. The same applies for the surface of the plate which lies below the washer. In this area, when the plate is in contact with the washer, its surface is restrained from out-of-plane movement.

ii) Kinetic features: In the areas of contact described above, friction forces develop which restrain the sliding of the plate relative to the bolt and the washer.

iii) Loading features: Because the load is introduced to the joint through the rest of the member, it is necessary to model that end as if it is continuous.

In addition to these special features, it has to be noted that the stacking of most practical composite materials is symmetric and the loading is axial. This usually permits the reduction of the size of the model to a quarter of the size of the prototype.

4.3. THE SIMPLIFIED MODEL FOR JOINTS

The model commonly adopted for analyzing composite joints is a two dimensional one. In that model, the joint is modelled as an orthotropic plate with a hole. The elastic properties of the plate are obtained using the classical laminated plate theory. The large stiffness difference between the plate and the fastener is exploited by assuming that the fastener is rigid. In some investigations, the friction between the plate and the rigid fastener is neglected. No account is made for the presence of the washer and the material is assumed to behave linearly elastic. This model suffered from the following major inaccuracies.

a) The clamping and friction which develop due to the presence of the washer can not be modelled.
b) The variation of the stresses in the plies due to altering the stacking sequence can not be modelled.
c) The successive yielding and fracture of the material is not modelled and therefore, the ultimate deformations are underestimated.
d) The use of the laminated plate theory can result in erroneous stresses on the free edges of the plies.

These inadequacies of the stress analysis model were circumvented using the procedures employed for the strength predictions as follows.

a) The failure hypotheses applied involved stresses distant from the interface between the fastener and the plate. At these positions, the three-dimensional effects on the stresses are not significant (Chang, Scott and Springer 1984a).
b) The empirically obtained failure criteria were manipulated to compensate for the inadequacy of the stress analysis (Wilson and Tsujimoto 1986).
c) The effect of the presence of the washer can be included in the parameters for the strength of the material (Arnold 1989).

In the rest of this chapter, the accuracy of these simplifications will be discussed and methods of removing some of the short comings will be proposed.

4.4. THE FINITE ELEMENT METHOD

The displacement finite element method is at the present time the most widely used stress analysis method. The popularity of this technique is partly due to the development of general-purpose software that is based on the method. The wide scope of these packages is the result of the simplicity of the concept which the method is based on. The fundamental idea of the technique is the replacement of the continuum by a set of elements of finite size connected together through a number of nodes. Thus the behaviour of the continuum can be represented using the behaviour of the finite number of nodes which is controlled by the load-deformation characteristics of the elements. Although the behaviour of the single element is only an approximate estimate obtained using energy methods and in spite of the limited connectivity between the elements representing the continuum, the error in the predictions of the stresses can be arbitrarily decreased by reducing the size of the elements.

The fundamental concept described above enables the consideration of different types of continua, materials and stress analysis problems. The strength of the method is due to the simplicity of extending the classical techniques applicable to single degree of freedom problems to complicated real structures.

This part of the thesis will investigate different aspects of using the finite element method in the analysis of bolted joints. Unless otherwise indicated, the material chosen for the investigations is the material 'Blue 1' described in Chapter 2. The material of the plate consisted of a longitudinally oriented uniaxial glass polyester lamina surrounded by two outer chopped strand mat glass polyester layers where the uniaxial layer occupied one quarter of the plate's thickness. The material properties assumed for the analysis were calculated according to the results of Chapter 2. The resulting properties are given in Table(4.1).

	El	Et	vlt	Glt
CSM	17.2	17.2	.25	6.88
UNI	45.9	14.3	.23	5.00

Table(4.1) The material properties for 'Blue 1'

4.4.1. THE MESH OF A BOLTED JOINT

The choice of the mesh of the finite elements used in the analysis is an important factor which controls the quality of the solution. In bolted joint problems, the area to be discretised

is usually rectangular and contains one or more circular cuts for the holes. The basic unit of the mesh is a rectangle containing a hole. Fig(4.1) shows different meshing strategies which use quadrilateral elements only. In that figure, symmetry is used and accordingly only half the mesh is shown.

The mesh shown in Fig(4.1a) has the advantage of simple numbering because the connectivities are uniform throughout the area. The simple topology of that mesh also allows the automatic generation of the mesh with the least effort. The techniques in Fig(4.1b) and Fig(4.1c), on the other hand, are not as easy to generate as the mesh of Fig(4.1a) and they do not provide any special advantages concerning the geometry of the element. Therefore, only the technique given in Fig(4.1a) will be discussed further.

Fig(4.2) shows how the mesh strategy under consideration can be used to model a general rectangular area. The techniques in Fig(4.2a) and Fig(4.2b) have the advantage of simple numbering but in some cases they suffer from distorted elements and great variation in the size of neighbouring elements. The meshes given in Fig(4.2c) allow the analyst to control the relative sizes of the elements, but the systematic numbering of such a mesh needs further consideration. The mesh in Fig(4.2d) demonstrates that surrounding the hole by a hexagonal area which is meshed radially can improve the angles at the corners of the elements. The hexagonal area can also be replaced by a suitable curvilinear area (Oplinger 1978).

Based on the previous brief survey, the two meshes given in Fig(4.3) are proposed. The basic feature of these meshes is that the radially meshed area surrounding the hole is extended to an edge of the plate. This results in the topological uniformity of the mesh and accordingly, the numbering of these meshes can be easily performed automatically. The simplicity of generating and numbering these meshes automatically, does not impose any restriction on the relative sizes of the elements.

It is recommended to apply an adaptive strategy for updating the mesh according to preliminary runs, but this might prove expensive for design purpose. Accordingly, it is important to establish rules for dimensioning the meshes. This involves the determination of the number of elements and the sizes of the elements which can be determined based on the known performance properties of quadrilateral elements and the nature of the stress distribution for the present type of problem. The meshing technique adopted is fully described by specifying the number of elements in the radial and the tangential directions.

Ramamurthy (1989a) showed, using 4-noded elements, that sufficient accuracy can be achieved using an angle equal to 2.8° between the successive nodes. Serabian (1991), however, used 8-noded elements and showed that it is sufficient to have the nodes on the hole at 5° intervals.

To confirm the accuracy of using a mesh with this spacing, a plate loaded by a pin was analyzed. The plate chosen was square and its width was equal to double the diameter of the hole as shown in Fig(4.4). The two meshes were produced based on the same criteria, but with different number of elements on the hole boundary. The meshes were generated such that the aspect ratio of all elements was approximately equal to unity. Due to symmetry, only half the problem was modelled. Table(4.2) gives the statistics of both meshes.

	ELEMENTS AROUND THE WHOLE HOLE	ELEMENTS IN MODEL	NODES IN MODEL
COARSE	40	120	473
FINE	80	400	1502

Table(4.2) Statistics of the Meshes Considered

The contact with the rigid pin was simulated by equating the radial displacement in the contact area to zero. The loading was affected by prescribing a unit displacement at the end of the plate. The stresses reported were normalized using the nominal bearing stress.

Fig(4.5) compares the radial and hoop stresses obtained using the two meshes. The results were generated using ABAQUS and LUSAS to confirm their correctness. The element used was the 8-noded reduced integration isoparametric element. It can be seen that the results correspond fairly well except near the end of the contact area. The reason for this is the higher precision in determining the contact area using the dense mesh. The movement of the loaded edge was used to calculate the apparent stiffness of the plate as a whole. This served as an indicator for global performance. The stiffness of the coarse mesh was found to be only .6% more than the fine mesh. Taking into account that a three fold increase in the model size is accompanied by the 5 % localised difference in the stresses, the coarse mesh was considered sufficiently accurate.

It is possible to improve the results without increasing the size of the mesh. This can be achieved by refining the mesh near the transition point lying between the contact and separation zones. It is also recommended to increase the mesh density near the centre line of the joint. The reason for this is that this region contains the transition point separating the sticking and sliding areas if friction is considered.

4.4.2. COMPARISON OF AVAILABLE SOFTWARE

During the course of this study, three finite element packages were available for use. These systems were ABAQUS version 4.8, LUSAS version 8 and MSC/NASTRAN version

65. Before deciding on which system was more suited for the analysis of joints, the capabilities of these systems were compared. The basis for comparison was the accuracy of the results, the mesh generation capabilities, the material models and the output options.

The two important preprocessing facilities for generating nodes and elements were available in all three packages. The generation of nodes on a line with any predetermined ratios of the distances between the nodes was possible in LUSAS and NASTRAN. In ABAQUS, this facility was limited to the case where these ratios formed a geometric sequence. This did not allow the generation of nodes lying on the intersection of a line with a family of radial lines which have a constant angle between them. This situation arises when generating the nodes on the boundary of a rectangular area containing a hole. The generation of nodes lying on a circular arc was also possible in all three packages. In ABAQUS, in contrast to LUSAS and NASTRAN, the nodes were always equally spaced. This complicated the generation of meshes where the mesh was refined near chosen points.

The preprocessor of ABAQUS and LUSAS allowed a nested repetition of the generation operations but the preprocessor of MSC/NASTRAN/MSG did not provide such a facility. LUSAS allowed the change of the ratios of the distances between the nodes during this nesting while in ABAQUS this was not possible.

In general, the experience of using the three preprocessor showed that for the present type of problems, the geometrical preprocessing facilities of LUSAS provided generality and simplicity, while ABAQUS provided higher simplicity but posed some restrictions and MSC/NASTRAN provided generality but suffered from complexity.

The three packages were capable of handling anisotropic materials but in addition, ABAQUS and MSC/NASTRAN provided a facility to calculate internally the effective material properties according to the laminated plate theory. This facility has been added to later versions of LUSAS. It has to noted, that the 8-noded element in MSC/NASTRAN did not allow the material axes to be defined globally. This meant that only the 4-noded element of MSC/NASTRAN was available for this investigation.

ABAQUS calculated the stresses in the different layers on request. These stresses were in the layer's coordinate system. The in-plane force in the plate as a whole was also calculated. In LUSAS and ABAQUS these forces were calculated either at the nodes or at the integration points and they were given in the global coordinate system. If the stresses were calculated at the nodes, they were output either for each element separately or as an average at each node. MSC/NASTRAN calculated the stresses in the layers, but this was restricted to the element corners (max 4 points) and the centre of the element. The averaged stresses were only calculated for plots and could not be output to a file. The stresses were output in the local

element coordinates. This meant that unless the post processing facilities of MSC/XL were available, these results had to be post-processed by the user.

To compare the accuracy of the different systems, the stresses around the hole in the problem previously considered were determined using the different programs. The results of these analyses are given in Fig(4.6); it can be seen that the results are similar for 8-noded elements. The results of the 4-noded element obtained from LUSAS and MSC/NASTRAN were different. This might be because of the different approaches applied to improve the performance of the element. It can be seen that both elements did not succeed in predicting the stresses correctly. The solution using LUSAS predicted the tangential stresses accurately, but it underestimated the radial stresses. MSC/NASTRAN, on the other hand, predicted the radial stresses fairly well but the tangential stresses were underestimated.

Based on the above, the finite element package LUSAS is recommended for performing linear and standard non-linear analyses. ABAQUS and MSC/NASTRAN, on the other hand, provides the facility of including user written subroutines which perform special tasks. The use of ABAQUS for this task is recommended because of its relative simplicity.

4.4.3. THE CHOICE OF ELEMENT TYPE

In order to establish the most suitable type of element, the problem described above was used to assess the accuracy of the different elements. The comparisons focused on the stresses calculated around the hole.

The elements chosen for the analysis were the 4-noded, the 8-noded and the 9-noded isoparametric elements in association with full and reduced integration. When the 4-noded element was considered, each 8-noded element was replaced by four 4-noded elements using the same mesh. Fig(4.7) shows the resulting stresses obtained using the different elements. All the stresses are normalised by the nominal bearing stress which is equal to P/dt. The figure shows that the results obtained using different parabolic elements were practically identical. Although the model generated using the 4-noded elements has 533 nodes (12.7% more than the 8-noded mesh), it's results are worse than the results obtained using the two other elements.

Table(4.3) gives a summary of the normalized critical stresses and the apparent stiffness of the plate. It has to be noted that the erroneous shear that develops near the separation point is of relatively small value and does not show a definite dependence on the element or mesh type. Based on these results, the 8-noded element using reduced integration was chosen as the most suited element for analyzing the joint problem.

PROG.	NDS	INT	MSH	MAX SHR ERROR	MAX HOOP STRESS	MAX RADL STRESS	NTRL RADL STRESS	REL STIF
LUSAS	4		CRS	.49	10.86	4.29	2.714	100.61
LUSAS	8	2x2	CRS	.21	10.67	4.72	2.956	100.60
LUSAS	8	2x2	FIN	.29	10.80	4.76	2.965	100.00
LUSAS	8	3x3	CRS	.25	10.81	4.74	2.941	100.62
LUSAS	9	3x3	CRS	.27	10.99	4.74	2.926	100.61
ABAQUS	8	2x2	CRS	.20	10.68	4.79	2.962	100.67
ABAQUS	8	2x2	FIN	.32	10.81	4.77	2.986	100.10
NASTRAN	4		CRS	.40	10.73	4.44	2.879	99.17

Table(4.3) Comparison of the Stresses obtained using different packages

4.5. MODELLING THE GEOMETRY

The lamination of composite materials suggests the use of three-dimensional analysis. Because this requires large computing facilities, it is common to use the classical laminated plate theory to model laminated composite materials. This technique was found to give reasonable results except near the edges of the plate. This was due to the limited variation of the displacements which could occur over the small thickness of the material.

The classical laminated plate theory is based on the following assumptions.

a) Plane sections before deformation remain plane after deformation
b) Normals to the middle surface remain normal after deformation.
c) No direct stresses develop in the transverse direction.

These assumptions were originally made by Kirchhoff and successfully applied in the thin isotropic plate and shell theories. They imply that the out-of-plane shear rigidity is infinite. Their applicability becomes questionable for orthotropic laminated plates and shells because of the following.

1) The first assumption results in the development of parasitic edge stresses in each of the constituent plies of the composite laminate.
2) The transverse shear stiffness of composite materials is usually small compared to their normal stiffnesses.
3) The lamination increases the deviation of the deformations from linearity through the thickness.
4) The transverse stresses which are neglected in the analysis initiate interlaminar failure.

To assess the error resulting from applying the above mentioned assumptions, the problem shown in Fig(4.8) will be considered. The same problem has been used repeatedly to analyse the free edge effect by different researchers (Shah and Krishna Murthy 1991). It is chosen here because of its relatively small size, the extreme lay-up of the laminate and the extreme orthotropy of the plies. Here, it has to be noted that the material properties quoted in Table(4.4) are not truly representative of a fibre reinforced polymer because the isotropy condition in the plane normal to the fibre direction is not satisfied (Tsai and Daniel 1990). However, they are used here to enable the comparison with the results of the previous investigators.

Ex	20msi
Ey=Ez	2.1msi
vxy=vzx=vyz	.21
Gxy=Gzx=Gyz	.85msi

Table(4.4) Material properties of the 0° ply

The problem under consideration is a quasi three-dimensional problem which can be reduced to a plane problem because its solution does not vary with respect to the loading axis. This was the basis of many finite element procedures written for these special cases (Shah and Krishna Murthy 1991). Due to their specialized nature, these procedures are not readily available in general purpose finite element packages. Here, it will be shown that a certain class of quasi three-dimensional problems can be analyzed directly using any general purpose finite element package.

4.5.1. THE METHOD OF ANALYSIS

In a quasi-three dimensional problem, all planes normal to the loading direction experience similar deformations. This corresponds to a generalised plane strain condition. This property was indirectly exploited (Whitecomb and Raju 1983) to obtain a solution that could be added to the results obtained via the laminated plate theory to remove the edge stresses. However, it will be shown here that it is possible to apply the axial load and satisfy the free edge conditions simultaneously when no coupling between the axial strains and the shear strains of the plies exists.

The technique is developed by manipulating the three dimensional material compliance matrix so that the entities involving the axial direction are removed from the set of equations.

The material compliance matrix for an orthotropic material having its planes of symmetry parallel to the coordinate axes can be written in the following form:

$$\begin{bmatrix} \epsilon_x \\ \epsilon_y \\ \epsilon_z \\ \gamma_{yz} \\ \gamma_{xz} \\ \gamma_{xy} \end{bmatrix} = \begin{bmatrix} a_{11} & a_{12} & a_{13} & 0 & 0 & 0 \\ a_{12} & a_{22} & a_{23} & 0 & 0 & 0 \\ a_{13} & a_{23} & a_{33} & 0 & 0 & 0 \\ 0 & 0 & 0 & a_{44} & 0 & 0 \\ 0 & 0 & 0 & 0 & a_{55} & 0 \\ 0 & 0 & 0 & 0 & 0 & a_{66} \end{bmatrix} \begin{bmatrix} \sigma_x \\ \sigma_y \\ \sigma_z \\ \tau_{yz} \\ \tau_{xz} \\ \tau_{xy} \end{bmatrix} \tag{4.1}$$

Eliminating the effect of σ_x from all rows corresponding to the yz plane:

$$\begin{bmatrix} \epsilon_x \\ \epsilon_y - \frac{a_{12}}{a_{11}} * \epsilon_x \\ \epsilon_z - \frac{a_{13}}{a_{11}} * \epsilon_x \\ \gamma_{yz} \\ \gamma_{xz} \\ \gamma_{xy} \end{bmatrix} = \begin{bmatrix} a_{11} & a_{12} & a_{13} & 0 & 0 & 0 \\ 0 & \left[a_{22} - \frac{a_{12}}{a_{11}} * a_{12}\right] & \left[a_{23} - \frac{a_{12}}{a_{11}} * a_{13}\right] & 0 & 0 & 0 \\ 0 & \left[a_{23} - \frac{a_{13}}{a_{11}} * a_{12}\right] & \left[a_{33} - \frac{a_{13}}{a_{11}} * a_{13}\right] & 0 & 0 & 0 \\ 0 & 0 & 0 & a_{44} & 0 & 0 \\ 0 & 0 & 0 & 0 & a_{55} & 0 \\ 0 & 0 & 0 & 0 & 0 & a_{66} \end{bmatrix} \begin{bmatrix} \sigma_x \\ \sigma_y \\ \sigma_z \\ \tau_{yz} \\ \tau_{xz} \\ \tau_{xy} \end{bmatrix} \tag{4.2}$$

Now considering the lines corresponding to the yz plane only:

$$\begin{bmatrix} \epsilon_y - \frac{a_{12}}{a_{11}} * \epsilon_x \\ \epsilon_z - \frac{a_{13}}{a_{11}} * \epsilon_x \\ \gamma_{yz} \end{bmatrix} = \begin{bmatrix} \left[a_{22} - \frac{a_{12}}{a_{11}} * a_{12}\right] & \left[a_{23} - \frac{a_{12}}{a_{11}} * a_{13}\right] & 0 \\ \left[a_{23} - \frac{a_{13}}{a_{11}} * a_{12}\right] & \left[a_{33} - \frac{a_{13}}{a_{11}} * a_{13}\right] & 0 \\ 0 & 0 & a_{44} \end{bmatrix} \begin{bmatrix} \sigma_y \\ \sigma_z \\ \tau_{yz} \end{bmatrix} \tag{4.3}$$

It can be seen that the resulting equation uses the plane strain compliance matrix (Tsai 1987). The effect of the straining in the x-direction is now taken into consideration as an initial strain in the yz-plane. It should be clear that the constants by which the strain ϵ_x is multiplied correspond to Poisson's ratios which link the in-plane strain to the axial strain. Because the strain ϵ_x is known in advance, the problem can be completely modelled in the yz-plane only.

The general case, where the in-plane normal and shear stresses of the plies were coupled, was also considered, but the resulting reduced plane equations involved the shear strains in the transverse direction. These were not known before the analysis and therefore in such a case the present method was not applicable.

The problem shown in Fig(4.8) can now be solved using any general purpose finite element package. One way of achieving this is by applying the initial strains to a two dimensional model. The other way is based on an analogy between the present type of loading and temperature loading. The analogy is due to the fact that both types of loading effectively result in initial straining. Accordingly, the applied temperature difference corresponds to the axial strain while the thermal expansion coefficients correspond to the above mentioned Poisson's ratios.

To check the correctness of this method, the problem given in Fig(4.8) was solved twice; the first solution used the proposed analogy with the thermal loading and the second one used a three dimensional analysis. Both solutions were performed using rigid format solution procedures of the MSC-NASTRAN package. The mesh used in the analysis employed two 8-noded elements through the thickness. This choice was decided based on the already known deformed shape of the plate given by Shah and Krishna Murthy (1991) which could be approximated by two parabolas only.

	y/h	z/h	[1]	Present	
				3D	Q3D
v	20	0	-.739	-.743	-.753
v	20	1	-	-.862	-.869
v	20	2	-1.176	-1.167	-1.156
w	0	1	-.202	-.205	-.206
w	0	2	-.444	-.452	-.453
w	20	1	-.048	-.059	-.106
w	20	2	-.271	-.284	-.320

Table(4.5) Deformations obtained using different techniques

Table(4.5) compares the displacements obtained using the two techniques applied by the present author with the results given by Shah and Krishna Murty (1991) using their quasi three dimensional technique and a refined mesh. The results demonstrate the correctness of the present technique and the adequacy of the mesh. The slight differences are believed to be the result of the difference in the formulations of the two and three dimensional elements, the errors due to the conversion of the units of the material properties and the refinement of the mesh.

Table(4.6) compares the stresses obtained from three, and quasi-three dimensional analyses at the centre of the elements representing the 90° ply. Again very good correlation exists. Having established the correctness of the solution technique, it will be used to check the assumptions of the laminated plate theory.

y/h	σy/(Ex*εx)		σz/(Ex*εx)	
	3D	Q3D	3D	Q3D
1.25	-.0179	-.0179	-5.554e-8	-1.000e-8
3.75	-.0179	-.0179	-2.231e-8	-6.930e-8
6.25	-.0179	-.0179	-1.069e-6	-5.295e-7
8.75	-.0179	-.0179	-5.190e-6	-3.901e-6
11.125	-.0179	-.0179	-2.380e-5	-2.443e-5
13.375	-.0177	-.0178	-1.110e-4	-1.323e-4
15.5	-.0166	-.0171	-5.181e-4	-5.470e-4
17.25	-.0129	-.0150	-1.605e-3	-1.256e-3
18.5	-.0062	-.0111	-1.690e-3	-9.225e-4
19.25	-.0001	-.0078	1.773e-3	1.733e-3
19.75	-.0033	-.0043	8.925e-3	6.870e-3

Table(4.6) The Stresses obtained using 3-D and Quasi3-D Analyses

4.5.2. THE EFFECT OF THE PLANE SECTIONS ASSUMPTION

The plane section assumption of the classical laminated plate theory will be investigated in order to see its effect and whether it is acceptable. The assumption is applied to the quasi three-dimensional solution by enforcing displacement constraints on the horizontal movement of the nodes. No constraints are specified for the vertical movements.

The requirement that plane sections remain plane after deformation means that the displacement (in the y direction) of all the points having the same y coordinate are the same. Mathematically this is given as:

$$\delta_v(y_0,z)=constant(y_0) \qquad (4.4)$$

This corresponds to a membrane structure where only in-plane deformations are considered.

Fig(4.9) compares the correct v-deformation at y=20h with the deformation satisfying the requirement that plane sections remain plane after deformation. Gross errors in the deformation of the free edge can be seen. A maximum error of 31% occurs at z/h=2. The variation of the lateral stress σ_y at z=1.5h for that case is compared with the correct results in Fig(4.10). It can be seen that the application of the present assumption also results in the development of residual stresses on the outer free edge of the laminate.

A close examination of the above given results suggests that the large errors reported are due to:

1) the high difference in the properties of the laminae,
2) the small number of plies,
3) the small out of plane shear modulus.

For laminates with a larger number of plies having a cyclic order and having high shear rigidity, the error is expected to be much smaller. The error in the stresses is a local effect and therefore, if the structure is large relative to its boundaries, the present assumption is expected to be sufficiently accurate.

4.5.3. NON-CONVENTIONAL APPLICATION OF THE LAMINATION THEORY

In the previous section, the symmetry of the laminate resulted in keeping its cross-sections, after deformation, perpendicular to its middle plane resulting in large errors in the deformations. To improve the results, this effect will be artificially eliminated. In other words, the variation of the deformations over the thickness of a symmetrical laminate will be approximated using two linear parts. This is done by considering only half the laminate while enforcing the plane section assumption. To retain the characteristics of the original symmetrical laminate, it is necessary to restrain the movement of the middle plane of the laminate in the out of plane direction. Accordingly, the problem was re-analyzed using the following relationship between the displacement of the nodes at the same y position.

$$\delta_v(y_0,z)=\delta_v(y_0,0)+(\delta_v(y_0,h)-\delta_v(y_0,0))*(z/h) \qquad (4.5)$$

where h is half the thickness of the plate. The results of that solution are also given in Figs(4.9 & 4.10). It can be seen that the error in the displacement and the stress in the y-direction is now reduced.

In order to be able to apply this technique to the analysis of structures of general shapes, the method under consideration has to be available in general purpose finite element packages. Noting that the linear approximation described above can be represented by the average displacement and the slope of the straight line, the modelling of these degrees of freedom can be performed using thin shell elements. Thus, only half the laminate thickness is modelled using layered shell elements which are constrained against out of plane deformation.

The above proposed thin shell element model was applied and the results of that analysis were compared with the previous ones in Figs(4.9 & 4.10). It is clear that the two solutions give different results. The reason for that is the infinite out-of-plane shear rigidity typical for thin shell solutions. This means that better results can be obtained using thick shell elements. The infinite shear rigidity also results in replacement of the interlaminar stresses acting on the mid plane by a concentrated force at the edge of the plate. However, this is not a major drawback because it is possible (as argued by Pagano and Pipes 1973) to establish allowable design values based on such a force.

The advantage of the present model is that it reduces the free edge stresses and the error in estimating the in-plane deformations. The model also presents information about the interlaminar stresses in the form of the forces preventing the shell from out-of-plane deformation.

4.5.4. THE EFFECT OF THE SHEAR MODULUS

The effect of the shear rigidity on the deformations in the y-direction was investigated and the results of that investigation are shown in Table(4.7).

z/h	Shell Element	G12 (msi)					SEPARATE LAMINAE
		1e9	999.	.85	.1	1e-9	
0.	-.7010	-.7493	-.7484	-.753	-.6990	-.7171	-.4410
.5	-.7827	-.7733	-.7727	-.751	-.6899	-.3030	-.4410
1.	-.8644	-.8453	-.8460	-.869	-.9689	-.8097	-
1.5	-.9461	-.9546	-.9596	-1.08	-1.438	-5.454	-4.2
2.0	-1.028	-1.090	-1.096	-1.16	-1.501	-1.691	-4.2

Table(4.7) The effect of out-of-plane rigidity on edge deformation

It can be seen that increasing the shear modulus results in reducing the variation of the displacements through the thickness. The limiting case of a straight line was not achieved, but it is interesting to note that the shell solution given above can be considered as an approximation of the shear rigid solution. The other limiting case where the shear rigidity is zero was expected to be identical to a solution of separate laminae. The numerical results for that case (given in Table(4.7)) do not support this expectation. It can be seen, however, that the deformations measured at the centre of the plies in the two models are similar to the case of separate laminae. The reason for that is the assumption that the deformations of the separate plies are constant over the thickness of each ply. The averages of the deformations in each of

the plies was checked and it corresponded reasonably well with the case of two separate laminae.

	Ply	LPT	Separate Laminae	CORRECT	
				Centre	Edge
σx/(Ex*εx)	0° 90°	1.0038 .1046	1.0000 .1050	1.0039 .1046	1.0007 .1069
σy/(Ex*εx)	0° 90°	.0179 -.0179	0.0000 0.0000	.0179 -.0179	≈0.000 ≈0.000

Table(4.8) In-Plane Stresses for different out-of-plane shear rigidities

The stresses for three cases are given in Table(4.8). These cases are the two limiting ones of no relative movement, completely free relative movement and the correct solution. The stresses obtained using the laminated plate theory approximate the stresses in the internal part of the laminate fairly well while the separate laminae solution approximates the stresses at the edge.

It is interesting to note that the error in the higher stresses is insignificant. This suggests that the solution of the laminate can be obtained based on the solution that considers each ply separately. Soni (1981b) proposed a method based on approximating the stress resulting from a laminated plate analysis by using a law of mixtures that uses the stresses developed in each of the laminae when they were analyzed separately. The results of the application of that proposal were found to be practically identical to the solution given in Table(4.5) for the laminated plate theory. This approximation can prove extremely valuable when optimizing the lay-up of a laminate, however, the method was found to fail in some cases.

4.5.5. THREE DIMENSIONAL ANALYSIS OF COMPOSITE JOINTS

4.5.5.1. DESCRIPTION OF THE NUMERICAL MODELS

In order to assess the applicability of the laminated plate theory, a series of single bolt joints were analyzed using three-dimensional analysis and two dimensional laminated plate analysis. The technique proposed in the previous section was not included in this comparison because it is known beforehand that it will result in stresses intermediate between the two considered cases.

The joints considered were the 'Blue 1' specimens which have been tested experimentally and failed in different modes. This meant that their geometries covered all

useful variations in the stress fields of such joints. The geometries of the joints considered are given in Fig(4.11). The models for the two sets of analyses had equal meshes in the plane of the plate. The dimensions of the plates are also indicated in Fig(4.11). The fastener was modelled as a rigid frictionless pin by restraining the radial movement of the contact area. No attempt was made to model the fastener in a more sophisticated way because this would have made it difficult to compare the results of the three-dimensional with those of the two-dimensional ones. Loading was achieved by applying equal prescribed displacements to all nodes lying on the far end of the plate.

The three dimensional models were created using 20-noded elements. The models included only one quarter of the real joint. This was possible because of the symmetry of the geometry and the material. Half the central layer was modelled using a layer of elements while the outer chopped strand mat layer was modelled using three layers of elements. The calculation of the stresses in this case was done automatically using the finite element package. The resulting stresses were obtained using the stiffness matrix of each element. Consequently, it would be expected to have different values of stress for the same node.

In homogeneous materials, this is usually overcome by averaging the stresses calculated at a node resulting from the different elements. This is not directly possible for laminated materials because of the discontinuity of the normal stresses which are acting parallel to the plane of lamination and lying in different layers. The same applies to the shear stresses which are in planes perpendicular to the plane of lamination. Because of the simplicity of the averaging technique, an equivalent technique for laminated materials was developed.

4.5.5.2. AVERAGING THE STRESSES IN LAMINATED MATERIALS

For this purpose, suppose that the plane of lamination is parallel to the xy plane. In order to satisfy equilibrium, the stresses σ_z, τ_{zx} and τ_{yz} have to be continuous over the interface while σ_x, σ_y and τ_{xy} are not. Accordingly, it is possible to apply the averaging technique to the former quantities in a straightforward manner. In order to obtain smoothed and more accurate values for the latter quantities, the compatibility conditions are used. These conditions require that the axial and shear strains acting parallel to the plane of lamination (ϵ_x, ϵ_y and 'o'$_{xy}$) are continuous. Accordingly, it is possible to obtain an improved value for these strains by averaging them. This means that six averaged quantities have been arrived at. Using these quantities and the constitutive relations for each layer at a time it is possible to obtain averaged stresses at planes lying between two materials as follows. Let the stress-strain relationship of each of the layers be given in the following form:

$$\begin{bmatrix} \overline{\sigma_x} \\ \overline{\sigma_y} \\ \overline{\sigma_z} \\ \overline{\tau_{xy}} \\ \tau_{yz} \\ \tau_{zx} \end{bmatrix} = \begin{bmatrix} C_{11} & C_{12} & C_{13} & C_{16} & 0 & 0 \\ C_{21} & C_{22} & C_{23} & C_{26} & 0 & 0 \\ C_{31} & C_{32} & C_{33} & C_{36} & 0 & 0 \\ C_{61} & C_{62} & C_{63} & C_{66} & 0 & 0 \\ 0 & 0 & 0 & 0 & C_{44} & C_{45} \\ 0 & 0 & 0 & 0 & C_{54} & C_{55} \end{bmatrix} \begin{bmatrix} e_x \\ e_y \\ \overline{e_z} \\ \overline{\gamma_{xy}} \\ \overline{\gamma_{yz}} \\ \overline{\gamma_{zx}} \end{bmatrix} \quad (4.6)$$

In the above equation, the quantities with a bar vary from one layer to the other. The latter quantities can be obtained by rearranging and solving this determinate system of equations. This can be accomplished by solving the third row for ϵ_z and then substituting this quantity in rows 1, 2 and 4 to obtain the quantities σ_x, σ_y and τ_{xy}. This technique is general because it only uses the local information at the point considered. This means that it can be used for non-homogeneous materials in general irrespective of the shape of the interface. It has to be noted, however, that in the case of curved surfaces, the global stresses have to be rotated such that they are acting parallel and perpendicular to the interface.

4.5.5.3. COMPARISON OF THE TWO TECHNIQUES

The results obtained from the analyses performed were the stresses on the boundary of the hole, the bearing plane and the minimum cross section plane. All the stresses given are normalized using the nominal bearing stress which is defined as (the force on the pin divided by the thickness of the ply and the diameter of the pin). The following graphs compare the stresses obtained using the three-dimensional analyses and the two-dimensional ones. In order to include the effect of varying the specimen's geometry, the graphs of all cases are given. Therefore, when discussing a general trend, reference will be given to a group of graphs which show the point considered.

The stress in the axial direction on the minimum cross section for all nine specimens is given in Figs(4.12 to 4.20). It is clearly shown that the two dimensional results are good approximations of the three-dimensional ones. The reason for this is that the assumptions for the laminated plate theory on that plane are acceptable. This means that this cross section is basically subjected to strains which are nearly uniform over the thickness of the plate as can be seen from the very small difference between stresses obtained for the outer and inner layers of each ply. It is interesting that the stresses for specimens MS and WS become negative near

the straight edge (Fig(4.15) and Fig(4.18)). This is due to the extremely short end distance compared to the width of the specimen which results in increasing the stress concentration near the hole. Accordingly, in order to maintain equilibrium on that plane, negative stresses develop.

The in-plane stresses on the bearing plane are given in Figs(4.21 to 4.29). The bearing plane extends from the end of the hole to the edge of the plate in the direction of loading. The stresses obtained using the three dimensional analysis vary over the thickness in an area which approximately extends a distance equal to one tenth of the diameter of the pin from each end (i.e. d/10 from a and b in Fig(4.21)). This is equivalent to the thickness of the central layer which is the area expected to be subjected to edge effects in laminated materials. Outside that area, the stresses are constant over the thickness.

The axial stresses (Figs(4.21 to 4.29)) showed errors at the free edge of the plate. These errors occurred for both types of analysis, but they were not expected in the three dimensional one. However, on reviewing the results of that analysis, the error was explained by the coarse mesh near that area. This meant that the analysis could not cope with the rapid changes in the interlaminar stresses at that position and therefore resulted in the reported error. This explanation is supported by the results obtained for the interlaminar stresses. It has to be noted that the error for the specimens with short end distance is larger than for the specimens with long end distance.

The quality of the solution using the laminated plate theory is good in the inner part of the specimen. At the outer surfaces, the error due to the use of this approximation is acceptable because it provides an average solution for each of the layers. The specimens which have a very short end distance develop higher edge errors than the ones with long end distance. Here it is important to note that the difference between the results obtained using the two techniques is less than the error associated with either solution.

The trend of the behaviour of the axial stress ahead of the pin is that the stress keeps decreasing until it becomes equal to zero at the edge of the plate as shown in Fig(4.23). In general, it can be seen that the results for the uniaxial layer obtained from the laminated plate theory slightly overestimates the stress while the stress in the chopped strand layer is underestimated. It can also be seen that the maximum stress in the layers increases with increasing the end distance. The width of the specimen has a small effect on the maximum bearing stress and there is evidence of its decrease with increasing the width while keeping the end distance the same.

The results for the transverse stresses (also shown in Figs(4.21 to 4.29)) on the bearing plane show that within .1d from the edges of the plate, noticeable variation in the stresses over the thickness of the plate exists. The results obtained using the laminated plate theory

underestimate the stresses in the uniaxial layer but they give an average value for the chopped strand layer. Again, when the edge distance of the plate was increased, the length over which the stresses were in agreement increased.

In general, the transverse stresses at the edge of the plate were larger than the stresses near the pin. When the edge distance increased, the stresses near the pin increased and those at the far end decreased. An explanation for the high stresses which develop near the edge of the plate is the beam-like behaviour of the edge area. When this distance increases, a deep beam effect occurs and the stresses become localised splitting stresses near the point of application of the load.

It has to be noted that the results of the three dimensional analysis show that the axial stresses on the bearing plane for the outer layers is less affected by varying the end distance compared to the stresses in the unidirectional layer. The stresses near the contact area are insensitive to the variation of the end distance. Conversely, the transverse stresses at the edge of the plate were very sensitive to changes in the end distance.

The in-plane stresses around the hole are given in Figs(4.30 to 4.38). The graphs for the radial contact stresses (Figs(4.30 to 4.38)) show that the two dimensional results give an adequate approximate value for the stresses obtained using three dimensional analysis. It can be seen that the stresses obtained using the laminated plate theory for the uniaxial layer are slightly higher than the ones obtained using the three dimensional analysis. It is also interesting to note that the separation area (between theta approximately equal to 90° to 180°) is subjected to radial stresses (Fig(4.30)). These stresses are developed in both analyses. The reason for the development of these stresses which have a relatively small magnitude in the three dimensional analysis is the inability of the finite element technique to handle the sudden change of slope of the stresses at the transition point between contact and separation. This is also the reason for the observed general trend of increased errors near that position. For the two-dimensional analysis, the error is due to the failure of the laminated plate theory in satisfying the stress free conditions on each layer separately. This error is of a similar magnitude as the error obtained in the three dimensional analysis.

The radial stresses in the uniaxial layer can be seen to increase from the mid-plane of the plate to the interface between the layers (Fig(4.30)). The stresses in that layer increase with increasing the end distance. Reducing the end distance results in reducing the stress in the chopped strand layer at theta equal to 0° while at about 60° (Fig(4.30)), the contact stress increases. The stresses at about 40° in the two layers are of same value for all geometries considered.

The results for the hoop stresses around the hole given in Figs(4.30 to 4.38) show that reasonable correspondence exists between the laminated plate solution and the three dimensional one. The maximum stresses always develop near the minimum cross section. It is interesting to note that the stresses near the loading axis do not vary much between the layers. In all cases, the stresses obtained in each of the layers did not show large variations. It can be seen that the reduction of the end distance results in increasing the maximum tangential stress for all geometries (e.g. Fig(4.30) to Fig(4.33)). In general, the results of the laminated plate theory underestimate the maximum stresses in the uniaxial layer by a small value while for the case of the stresses in the chopped strand layer, it predicts an average (Fig(4.30)).

The interlaminar stresses play an important role in the failure of composite materials. The experimentally obtained failure modes of the previous chapter demonstrated that final failure of some joints was controlled by the development of delamination between the layers. These stresses can only be obtained using a three-dimensional analysis.

Figs(4.39 to 4.47) show the interlaminar stresses on the bearing plane. It can be seen that the present analysis fails to satisfy the shear stress free conditions on the outer surface and on the mid plane. The interlaminar shear stress is a maximum on the interface between the two materials Fig(4.39). For small edge distances, the stress is distributed over the edge distance relatively uniformly Fig(4.39). When the edge distance is increased, the stresses become more localised near the bolt Fig(4.46). In Figs(4.39 and 4.43), it is important to note that the stresses near the free edge on the interface between the layers do not reduce to zero. It is believed that this is due to the coarse mesh used at this edge where the stress gradients are very steep.

The interlaminar shear stresses developed in the tangential direction around the hole are shown in Figs(4.48 to 4.56). These results show that the finite element analysis develop fictitious stresses on the outer surface and on the mid plane of the specimens. The magnitude of the error for the outer plane is small while for the plane of symmetry it is relatively large. It is possible that the latter error is due to the modelling of half the plate only which has prevented the application of the averaging technique of the stresses on that plane. To verify this statement, specimen WL was modelled taking into account its whole thickness. However, due to limitations on the computing facilities, the whole thickness was modelled using four elements. The results obtained using that analysis are shown, utilising dots, in Fig(4.56). It can be seen that the resulting stress on the interface is slightly smaller in magnitude relative to the previous solution but its general shape is the same. This is possibly due to the use of only one element to model the outer chopped strand layers. The form of the stress distribution on the mid plane changed substantially and the magnitude of the stresses reduced to a low value comparable to the erroneous interlaminar shear stress on the free surface, albeit still in error.

From the results of Fig(4.48 to 4.56) it can be seen that the interlaminar shear stresses around the hole became maximum at the interface. The shear on the interface shows three maxima. The first is at about 30° the second occurs at about 70° while the last is at 120°. The position at which the absolute maximum shear stress has occurred changes for different geometries. For narrow specimens, the maximum developed at about 120° (Fig(4.48, 4.49 and 4.50)) while wider specimens develops the maximum at about 30° as can be seen from Figs(4.51 and 4.56). The absolute maximum shear stress is seen to be decreasing with increasing end distance. The maximum shear stress also decreases with increasing the width of the plate.

The possibility of obtaining an indication of the interlaminar shear stress using the erroneous shear stresses that developed on the hole surface of the plies (when the laminated plate theory was used) was investigated. For this purpose, the stresses reported above were compared to the stresses obtained using the laminated plate theory. It was found that the erroneous stresses which developed when using the laminated plate theory were larger than the interlaminar shear stresses of the three dimensional analysis. The reason for this was that the interlaminar stresses were distributed over a larger area compared to the free surface on which the erroneous stresses were distributed; thus it is unsuitable.

The through-thickness stresses for the different cases are plotted around the hole in Figs(4.57 to 4.65). It can be seen that the maximum stress around the hole occurs near the minimum cross section. The stress in this area is tensile and can therefore result in delamination while the rest of the hole is subjected to compressive stress. For large widths, however, the central bearing area is subjected to increased interlaminar tensile stresses (Figs(4.63 to 4.65)). The stresses obtained on the free surface showed some error that increases near the position of minimum cross section (Fig(4.57)). In general, the magnitude of the through-thickness stresses decreased with increasing the size of the plate.

4.6. THE MODELLING OF THE FASTENER

The effect of the fastener on composite plates forming a joint is a fundamental aspect of the behaviour of the joint. The effect of the presence of the fastener can be summarized as follows.

a) The presence of the fastener restricts the in-plane movement of the part of the plate which is in contact with it. This effect can be associated with friction stresses between the shaft of the fastener and the plate.

b) The presence of the washer, head of the fastener or the nut restricts the out-of-plane movement of the plate. Again this can be associated with friction stresses on the contact area.

Due to the high stiffness difference between the fastener and the composite, it is possible to replace the fastener by its effect on the plate. This means that although the finite element model does not model the fastener, it caters for its presence in some form.

In general, most finite element analyses considered the first effect only. This was due to the general view that considering the effect of the washer requires the use of three-dimensional analyses. It is therefore of interest to investigate the latter effect and the possibility of modelling it in a form suitable for two dimensional analysis. In addition, the consideration of friction in the analysis of pin-loaded plates results in a large increase in the computing time of the solution. This is due to the iterative nature of the conventional analysis techniques. It is therefore of interest to develop a more economic technique for the analysis of this problem.

4.6.1 CONSIDERING THE FASTENER IN THREE-DIMENSIONAL ANALYSES

In order to determine the effect of the fastener on the composite plate, three-dimensional analyses of the problem given in Fig(4.66) were performed. The mesh considered for this analysis was slightly finer than the previously considered ones and it was kept circular in the area with which the washer came in contact. The following five conditions were considered in the analysis.

a) Smooth pin,
b) Rough pin,
c) Finger-tight smooth washer,
d) Finger-tight rough washer and
e) Clamped smooth washer.

The clamping force was taken equal to one quarter and half the in-plane load. All contact areas were modelled using the rigid surface facility of ABAQUS in association with interface elements. The washer was assumed to have a diameter equal to 2.2 the diameter of the fastener. When a clamping force was applied, all degrees of freedom representing the out-of-plane movement of the nodes supporting the interface elements were connected (using the 'EQUATION' facility of ABAQUS) to a single degree of freedom node to which the lateral

force was applied. For the finger-tight condition, the latter degree of freedom was restrained from movement.

The percentage of load taken by the washer was found to be equal to about 75% for the rough finger-tight condition. This part of the load was transmitted to the fastener by friction between the washer and the composite plate and was associated with a clamping force equal to 8.2% of the total in-plane force. The results obtained from these analyses for the in-plane stresses around the hole are shown in Fig(4.67). From that figure, it can be seen that the stresses on different planes in the same layer are similar. The clamping of the laminate did not change the in-plane stresses substantially but it has reduced the variation of the stresses over the layer's thickness. The roughness of the pin, on the other hand, is seen to have a strong influence on the in-plane stresses around the hole; the bearing stress reduces as well as the splitting stress ahead of the bolt. It has to be noted that the reduction of the transverse stresses is of great importance for the uniaxial layer due to its poor transverse strength.

Fig(4.68) shows the out-of-plane stresses at different levels of the bearing plane. From that figure it can be seen that under the washer, the stresses remain compressive over the whole thickness of the plate. For the pinned case, however, the compressive stresses acting on the inner plies of the plate change sign and they become tensile near the outer surface of the laminate. It is important to note that outside the clamped area, the finite element solution wrongly predicted tensile stresses on the free surface. This error is small of magnitude compared to the bearing stress. It is interesting to note that the friction between the shaft and the plate results in compressive out-of-plane stresses which develop near the bearing area.

Fig(4.69) gives the variation of the out-of-plane stresses around the hole. The stresses in the smooth pinned case are negligible except near the tension plane (theta equal to 90°). It can be seen that the rough pin results in stresses diminishing towards the outer surface and that compressive stresses develop near theta equal to 180°. A closer examination of the results explained these stresses by the development of a small contact area at this position. The contact area between the washer and the plate always includes this small part. The maximum tensile stresses can be seen to develop near the area of minimum cross section. This result is of importance because it explains the development of the delaminations which are associated with the tensile failures of this material which was reported in the previous chapter. The consideration of friction is seen to have increased the compressive stresses at 0° due to the greater confinement of the plate at that position.

The interlaminar shear stresses on different levels of the bearing plane are given in Fig(4.70); this figure shows that the maximum shear stresses develop on the interface between the two layers. The roughness of the washer is seen to be causing a reduction of the shear

stresses on the interface between the layers of different materials. This is due to the development of shear stresses on the two surfaces of the chopped strand mat layer which are acting in the same direction. Because the amount of load to be taken by the chopped strand mat layer is constant and can be approximately determined by the laminated plate theory, the sum of the interlaminar shears on the two surfaces of a layer has to be constant for any stacking sequence. Accordingly, the presence of the washer results in relieving the shear stress on the interface between the chopped strand layer and the uniaxial one. Therefore, it is expected that this 'relieving' action of the washer will only occur if the washer is in contact with the radially softer layer of the laminate. The increase in the compressive stresses on the washer results in a local increase of the shear stresses near the end of the washer. It is interesting to note that this effect is proportional to the amount of clamping and that for the rough case the effect is not pronounced. The same effect was previously reported by Arnold (1989) and was considered as an explanation of the development of the bearing failure outside the washer.

Again, it is important to note the erroneous shear stresses predicted by the finite element solution for the pinned cases on the outer surface of the plate. To avoid these errors, very fine finite element meshes with mesh refinement towards the edges of the plate are needed, however, to include such refined meshes in association with iterative analysis techniques was not feasible using the available computing resources.

4.6.2. MODELLING THE EFFECT OF A PIN

A number of techniques were considered for modelling the pin-loaded plate using two dimensional finite element analysis; these are summarised is Fig(4.71).

4.6.2.1. DISPLACEMENT BOUNDARY CONDITIONS

These conditions are applied either as fixed boundary conditions or by enforcing some linear relationships between the displacements of the nodes in contact with the plate.

The first technique is used successfully in models containing a single frictionless fastener. For this purpose, the radial components of the displacements of the nodes in contact with the plate are equated to the value of the misfit of the pin. The use of that technique for joints containing multiple fasteners implies that the plate under consideration is jointed to a rigid plate.

In order to consider the flexibility of both plates, it is necessary to describe the movement of the pins relative to each other. This can be achieved by adding fictitious nodes

to the model which are used to describe the positions of the pins. The displacements of the nodes lying on the contact area have to satisfy the requirement that the distance between them and the fictitious node representing the position of the centre of the pin remains constant. Accordingly:

$$[(x_h+u_h)-(x_p+u_p)]^2+[(y_h+v_h)-(y_p+v_p)]^2=R_p^2 \qquad (4.7)$$

Where the subscripts h and p refer to the hole and the pin respectively, x, y are the coordinates the nodes and u and v are the corresponding displacements. Rearranging and neglecting second order effects,

$$(u_h-u_p)(x_h-x_p)+(v_h-v_p)(y_h-y_p)=0 \qquad (4.8)$$

This is a linear equation between the displacements of the nodes lying in the contact area and the displacement of the pin. It has to be noted here that Eq(4.8) can be given in polar coordinates as:

$$(u_h-u_p)+(v_h-v_p)*\tan(\theta)=0 \qquad (4.9)$$

The above given condition can also be used for the case of a single pin when the finite element package does not contain a facility for rotating the degrees of freedom.

The misfit between the pin and the hole can also be included in this type of analysis. Naik and Crews (1991) developed an equation for a clearance-fit pin which is not allowed to move. When that equation is updated to account for movement of the pin, the following formula is arrived at

$$(u_h-u_p)*(R\cos(\theta)-c)+(v_h-v_p)*R\sin(\theta)=Rc*(\cos(\theta)-1) \qquad (4.10)$$

where c is the difference between the radius of the pin and the radius of the hole R.

The consideration of friction using a displacement boundary condition has been investigated. This was attempted by requiring that the reactions at the nodes lying in the contact area were inclined to the surface of the hole by an angle equal to $\tan^{-1}\mu$. In order to achieve this, the movement in that direction was restrained while the perpendicular direction was left free from constraints Fig(4.72). This technique was found to be reasonably accurate for coefficients of friction which were less than .1. For higher values, however, the use of that

technique resulted in the movement of the nodes which were in the contact area away from the pin. This was a direct consequence of allowing the nodes on the hole to move in a direction that had a radial component. Therefore, it was concluded that the consideration of friction using displacement boundary conditions is not possible.

It has to be noted that the techniques described above require prior knowledge of the contact area. Because this information is generally not available, these methods have to be applied iteratively, where the contact area is changed manually. Wise judgement of the analyst can greatly accelerate the convergence.

4.6.2.2. THE USE OF SPECIAL CONTACT ELEMENTS

In order to fully automate the solution of contact problems, a great number of special contact elements has been proposed. These elements were designed such that they were rigid if contact occurred and they lost their stiffness when separation was predicted. In addition, when contact was established, the effect of misfit and Coulomb's friction could be considered. These elements can be divided in two groups which are.

a) Contact elements which are designed for use between two elements or an element and a node representing a rigid body.
b) Spring elements which are designed for use between two nodes.

In general, the use of the first type of element results in improved accuracy. The reason is that spring elements do not provide for the interaction between the nodes of the elements modelling the structure. Fig(4.73) demonstrates that effect by giving spring elements equivalent to a linear and a parabolic contact element. The stiffnesses of these springs can be obtained from the stiffness matrices of the contact elements. The absence of that interaction reduces the accuracy of the results obtained specially when separation begins at points intermediate between the nodes.

The major disadvantage of using contact elements is the need for computer controlled iterations. It is difficult to establish an iteration and incrementation procedure that will efficiently solve different types of problems. A model containing 41 nodes around the hole boundary was analyzed using ABAQUS. It was found that the use of contact elements resulted in increasing the running time of the problem to about 40 times the time required for solving the problem using a prescribed contact area.

4.6.2.3. THE USE OF THE INVERSE TECHNIQUE

In order to reduce human intervention and at the same time avoid excessive iterations, the inverse technique has been proposed. This technique has been originally used to consider the effect of misfit of the fastener. In this method, the loading level that will fit an assumed contact area is sought instead of trying to find the contact area associated with a given load level. The advantage of reversing the logic of the procedure is due to the linearity of the problem of contact with a known contact area.

The solution is obtained by superposing two solutions for the assumed contact area under two loading conditions. The first solution is due to a unit load applied at the end of the plate while the nodes on the contact area are prevented from radial movement. The second solution is for the case when the contact area is subjected to radial displacement equal to the misfit of the pin. The load of the first solution is then adjusted such that it results in a stress at the transition point between the contact and separation area equal to the stress resulting from the second solution but with opposite sign. By adding the two solutions, the required solution, which causes the stress to become zero at the end of the contact area, is obtained. By choosing different contact areas, the behaviour of the plate under different load levels is found. Crews and Naik (1986) used a different implementation of the technique where the radial action of the misfit was applied to both linear solutions. The difference between the two solutions was the axial loading level. The solutions were then combined such that the sum of the stresses on the edges of the contact area were equal to zero. The latter implementation of the technique is more efficient because it uses the same stiffness matrix of the structure for both loading cases. This means that the stiffness matrix does not need to be recalculated or refactorised.

In some investigations using the finite element technique (Mangalgiri, Dattaguru and Rao 1984 and Ramamurthy 1989a&b), the requirement for the radial stress to be equal to zero was replaced by the condition that the nodal force is equal to zero. Fig(4.74) demonstrates that the latter approach is not equivalent to assuming that the stresses are equal to zero. For the case of linear elements, if the force at point B is equal to zero then the stress at point B as well as point C has to be equal to zero. For parabolic elements, if the force at point E is set equal to zero, then either the stresses at points F and G are equal to zero or the stress at point F is fixed at a value equal to half the stress at point G. These statements are direct results from the statically equivalent force systems shown in the upper part of Fig(4.74). Although this technique is not exact, it is acceptable because of the poor stress predictions of the finite element technique near the transition point. In addition, by refining the mesh, the discrepancy between the two techniques diminishes.

The inverse technique has been applied to the case of a plate subjected to a by-pass load. In this case the two fundamental solutions were due to the unit loads applied at both ends of the plate. Under certain conditions, this problem resulted in two contact areas and this was overcome by Naik and Crews (1991) by determining the ratio of the bearing to the by-pass load as a part of the solution rather than having it as a condition of the problem. The result of such an analysis is the relationship between the contact angle and the axial and by-pass load combinations.

The main advantage of the inverse technique is that it does not require iterations to determine the contact area but in its original form, it could not consider friction, multiple pins or general axial and bending loading.

The inefficiency of the contact elements is usually tolerated because of their straightforward nature that does not need the intervention of the analyst. However, when performing parameter studies, it is important to find a more efficient technique. The inverse technique is the most suited candidate for this purpose. Therefore, it will be investigated whether the field of application of the inverse technique can be extended to deal with problems where the pin is rough, multiple pins are considered and bending in addition to the axial force is present.

The latter two cases can be considered as straightforward extensions of the cases where the technique has been already applied. This is shown in Fig(4.75) and Fig(4.76) where the parameters to be varied are shown. In the case of a plate containing two holes in series (Fig(4.75)), the contact area is established by defining an angle of contact for each of the holes. In order to have zero contact stress at the ends of the contact area, two quantities need to be varied. These quantities will be chosen as the axial loads applied at each of the pins. Because the stress at each of the ends of the contact areas is a linear function of these two quantities, the mathematical forms involve three coefficients each. Accordingly, three loading cases are needed to determine the coefficients for each function. A total of six loading cases are used to establish the correspondence between the radial stresses at the ends of the contact areas and the applied loads on each of the pins. By equating these stresses to zero, two simultaneous equations for determining the loads on each of the two pins result. The solution of this set of linear equations gives the loads which correspond to the assumed contact areas.

The second case is the case where the bending and axial loads are applied to a coupon Fig(4.76). This case is different from the single pin case discussed previously because the contact area is not symmetrical with respect to the coupon's axis. This means that two quantities need to be varied in order to satisfy the conditions at the two ends of the contact area; the bending moment and the axial force applied on the coupon are chosen for this

purpose. As mentioned above, this means that six loading cases are needed to determine the relationship between the stresses at the two ends of the assumed contact area and the applied loads. Again, by equating the stresses at these positions to zero, the bending moment and the axial force corresponding to the assumed contact area are obtained. It has to be noted that the bending moment has to be associated with a shear force in order to maintain the equilibrium of the lug.

In general, in order to use the inverse technique to solve a problem with 'n/2' contact areas, 'n' loading variables have to be identified. In order to obtain the n relationships between the stress on the n ends of the contact areas and the n loading variables, n*(n+1) different loading cases are needed. The loading variables are then obtained by equating the stresses at the ends of the contact areas to zero and solving the resulting set of simultaneous equations. It should be clear that the consideration of a large number of ends of the contact areas will require the consideration of a number of loading conditions which increases quadratically. This means that the inverse technique is only efficient when the number of contact areas is small.

4.6.3. THE EFFECT OF PIN ROUGHNESS

A procedure similar to the inverse technique is proposed for considering the effect of the roughness of the shaft of the fastener. The method can also be considered as a reduced basis application. The technique is based on the idea that it is possible to obtain a sufficiently accurate approximation for a plate loaded by a rough pin by superposing a finite number of solutions for the plate with an assumed contact area whose nodes are restrained from radial movement and subjected to prescribed shear stresses. Accordingly, the solution considering the friction between the plate and the pin can be obtained as the sum of the solutions due to the following loading conditions (Fig(4.77)).

a) A unit load applied at the far end,
b) radial displacement of the contact area which is equal to the misfit of the pin and the hole and
c) a finite number of fundamental shear stress distributions.

The contribution of each solution is adjusted such that the radial contact stress at the end of the assumed contact area becomes equal to zero and Coulomb's friction law is satisfied on the contact area.

The fundamental shear stress distributions considered in loading case c) given above have to be chosen such that they can represent the expected shear stress profile sufficiently accurately. Here, it has to be noted that it is possible to use stress distributions which extend over the whole contact area or choose stress distributions such that they act on small sections of the area. The second choice corresponds to spline approximation of the shear stress. It was found that the use of the latter method resulted in better approximations. It has also to be noted that the use of a number of stress distributions which are equal to the number of nodes on the contact area of the hole boundary will result in exact solutions of the problem. This, however, is not recommended because it does not reduce the amount of computing required and at the same time results in solutions with stress concentrations which the finite element method can not solve accurately. The shear stress distributions must also ensure the development of continuous friction stresses over the contact area. This can be achieved by using stress distributions which have the same form as the shape functions of parabolic elements. In order for these shape functions to represent the shear stress distribution accurately, it is recommended to reduce the size of the area over which they act near the separation area and near the axis of the plate. This is equivalent to mesh refinement in the finite element method.

The calculation of the coefficients of the shear stress splines is undertaken by enforcing Coulomb's friction law which requires that

$$\mu\sigma=\tau \tag{4.11}$$

at all the points of the slip area. Where σ is the radial contact stress, τ is the shear stress and μ is the coefficient of friction. Here it is assumed that no sticking area exists. This assumption is justified because this area is usually confined between the node on the centre line and the next node on the contact area.

The spline approximation of the radial and shear contact stress can be given in the following form:

$$\begin{aligned}\sigma&=\sigma_m+a_0\sigma_0+\Sigma_{i=1}^{n}(a_i\sigma_i)\\ \tau&=\Sigma_{i=1}^{n}(a_i\tau_i)\end{aligned} \tag{4.12}$$

Where

σ_m is the radial stress due to the radial deformation,

σ_0 is the radial stress due to the applied unit load,

σ_i and τ_i are the radial and the shear contact stress due the 'i'th shear stress spline.
n is the total number of splines used to approximate the shear stress.
a_i are variable coefficients.

The variable coefficients can now be determined by enforcing Coulomb's law and the condition of zero radial stress at the transition point between the contact and separation areas. For this purpose, Eq(4.12) is substituted into Eq(4.11) and rearranged to obtain:

$$\mu\sigma_m+a_0\mu\sigma_0+\Sigma_{i=1}^{n}a_i(\mu\sigma_i-\tau_i)=0 \qquad (4.13)$$

Here, it is important to note that the above given set of equations will automatically contain the condition of zero radial stress at the transition point provided that all shear stress splines are equal to zero at that point.

The number of equations given above is equal to the number of nodes in the contact area excluding the ones lying on the sticking area. The number of unknowns, however, is chosen by the analyst and is generally less than the number of equations. This means that, in general, the above given system of linear equations has no exact solution. It is possible, however, to obtain an approximate solution by minimizing the norm of the left hand side vector. The latter can be chosen as the Euclidian norm and accordingly the well established least squares technique can be used.

This technique has been used to investigate the effect of friction on the behaviour of a large plate loaded by a pin. The end distance and the width of the plate were 10d. For the purpose of this example, μ was varied from 0.1 to .5 with increments of .2 and the radial misfit in this case was neglected. The resulting stresses for the different cases are shown in Fig(4.78). It is essential to note that the solutions in that figure were obtained using one computer run with four linear loading conditions. This has to be compared with non-linear solutions of unsymmetrical stiffness matrices which result when using the usual procedure for frictional contact. The results show that by considering friction, the radial contact stresses reduce and the tangential stresses in the contact area change sign to become negative.

4.6.4. THE EFFECT OF THE WASHER

The consideration of the effect of the washer on the behaviour of a plate loaded using a fastener has been traditionally undertaken using three dimensional analysis; the reason for this is the dependence of the behaviour on the out-of-plane deformations. The results of section

4.6.1, however, show that this argument is not well founded. These results demonstrated the local nature of the effect of the washer and their small effect on the in-plane behaviour. This can be explained by the possibility of approximating the out-of-plane deformation of thin plates using straight line approximations. Accordingly, this means that the deformation can be fully represented using the strain in that direction. Therefore, such an approximation provides the possibility of dealing with the problem at the material level. It has to be noted, however, that this approach neglects the shear deformations in that plane.

Consider the stress strain relationship of a transversely isotropic material. If the plane of isotropy is assumed to be the y-z plane, then the material stiffness matrix can be written as:

$$\begin{bmatrix}\sigma_x\\ \sigma_y\\ \sigma_z\\ \tau_{xy}\\ \tau_{zx}\\ \tau_{yz}\end{bmatrix} = V\begin{bmatrix}(1-\nu_{TT}^2)E_L & \nu_{LT}(1+\nu_{TT})E_T & \nu_{LT}(1+\nu_{TT})E_T & 0 & 0 & 0\\ \nu_{LT}(1+\nu_{TT})E_T & (1-\nu_{LT}\nu_{TL})E_T & (\nu_{TT}+\nu_{LT}\nu_{TL})E_T & 0 & 0 & 0\\ \nu_{LT}(1+\nu_{TT})E_T & (\nu_{TT}+\nu_{LT}\nu_{TL})E_T & (1-\nu_{LT}\nu_{TL})E_T & 0 & 0 & 0\\ 0 & 0 & 0 & \frac{G_{LT}}{V} & 0 & 0\\ 0 & 0 & 0 & 0 & \frac{G_{LT}}{V} & 0\\ 0 & 0 & 0 & 0 & 0 & \frac{G_{TT}}{V}\end{bmatrix}\begin{bmatrix}\epsilon_x\\ \epsilon_y\\ \epsilon_z\\ \gamma_{xy}\\ \gamma_{zx}\\ \gamma_{yz}\end{bmatrix} \quad (4.14)$$

$$where \quad V=\frac{1}{(1+\nu_{TT})(1-\nu_{TT}-2\nu_{LT}\nu_{TL})}$$

$$and \quad G_{TT}=\frac{E_T\,V(1-\nu_{TT}-2\nu_{LT}\nu_{TL})}{2}$$

When no contact occurs between the plate and the washer, σ_z is equal to zero. Therefore, the in-plane stresses can be calculated based on plane stress conditions. ϵ_z can be calculated from the third row of the above given equation to yield:

$$\epsilon_z=-\frac{\nu_{LT}(1+\nu_{TT})}{1-\nu_{LT}\nu_{TL}}\epsilon_x-\frac{\nu_{TT}+\nu_{LT}\nu_{TL}}{1-\nu_{LT}\nu_{TL}}\epsilon_y \quad (4.15)$$

The above given procedure for calculating the stress and strain can be applied until ϵ_z becomes numerically greater than the prescribed strain due to the presence of the washer ϵ_z^o. When this value is exceeded, the plate bears against the washer and the material is prevented from moving in the out-of-plane direction and therefore the strain is maintained at the limiting level ϵ_z^o. To calculate the stresses under these conditions, the superposition principle will be used. The first contribution to the stresses will be due to the in-plane strains under the assumption that the out-of-plane strain is equal to zero. This solution can be directly obtained using the plane strain material matrix. In addition, the effect of the out-of-plane straining ϵ_z^o is added under the assumption of zero strain in the two other directions. The second solution results in the following additional in-plane stresses:

$$\sigma_x = V\nu_{LT}(1+\nu_{TT})E_T\epsilon_z^o$$
$$\sigma_y = V(\nu_{TT}-\nu_{LT}\nu_{TL})E_T\epsilon_z^o \qquad (4.16)$$

An approximate value for ϵ_z^o can be obtained from the average value of stress acting on the washer σ_z^o by using the third row of Eq(4.14). This means that the present technique does not distinguish between the application of a stress or a displacement at the outer surface of the plate.

In addition to the confinement effect, the pressure of the washer results in reducing the load transmitted by contact between the shaft and the fastener. This effect can also be considered using two dimensional analysis as follows.

Due to the small thickness of the plate, it is possible to assume that the friction stress which is acting on the surface of the plate is distributed through the thickness of the plate. By doing so, the stress acting on the surface of the plate can now be considered as a body force that can be dealt with in a two dimensional analysis. The friction shear stress that develops is equal to $\sigma_z\mu$ where μ is the coefficient of friction. σ_z can be calculated using the plane strain assumption, but the additional effect of any clamping force has to be included. The shear stress can be converted into an equivalent body force by equating the forces resulting from both stress systems.

$$F_b = AtF_e$$

$$F_s = 2A\tau$$

$$\textit{therefore} \qquad \textbf{(4.17)}$$

$$F_e = 2\frac{\tau}{t} = 2\frac{\mu\sigma_z}{t}$$

where F_e is the equivalent body force, F_s is the resultant shear force on both sides of the plate, A is the area of contact, F_b is the resultant body force, τ is the frictional shear stress, 't' is the thickness of the plate and σ_z is the normal contact stress.

The force that tries to move the plate relative to the washer can be obtained from the equilibrium conditions of the theory of plane elasticity as

$$\frac{\partial\sigma_x}{\partial x} + \frac{\partial\tau_{xy}}{\partial y} + X = 0$$

$$\frac{\partial\tau_{xy}}{\partial x} + \frac{\partial\sigma_y}{\partial y} + Y = 0 \qquad \textbf{(4.18)}$$

$$F = \sqrt{X^2 + Y^2}$$

Where σ_x, σ_y and τ_{xy} are the stresses acting in the composite plate when it is prevented from movement relative to the washer. This condition can be modelled in two dimensional analysis by assigning the area of sticking material properties which are calculated using the laminated plate theory where the washer is considered as a layer of the plate (Table(4.9)).

CONDITION	$\epsilon z - \epsilon z^\circ < 0$	$\epsilon z - \epsilon z^\circ > 0$	
CONTACT	SEPARATION	CONTACT	
2-D MATRIX	PLANE STRESS	PLANE STRAIN	
		F>Fe	F<Fe
FRICTION	NONE	SLIPPING	STICKING
MATERIAL USED	PLATE	PLATE	PLATE & WASHER
ADDED FORCES	NONE	INITIAL STRAIN	INITIAL STRAIN & BODY FORCE

Table(4.9) The Washer Model

The force F is trying to move the plate relative to the washer while F_e is the force that is holding them together. If F is smaller than the equivalent friction force F_e, the plate remains stuck to the washer. If slipping occurs, then only the plate's material properties are used, and the equivalent friction force F_e is added in the direction of the initial body forces. The model

described above has been implemented as a user subroutine for the general purpose subroutine ABAQUS. The listing of the subroutine UMAT is given in Appendix(2). Unfortunately, in ABAQUS, the user does not have access to the stresses of all points simultaneously. Therefore, the gradient of the stresses required in Eq(4.18) was not available. Accordingly, the implementation considered the clamping effect only. A flow chart of the subroutine is given in Fig(4.79).

4.7. THE NON-LINEAR BEHAVIOUR OF COMPOSITE MATERIALS

Composite materials are non-homogenous anisotropic non-linear fracturing materials. They are non-homogenous on the microscopic level because each layer is an assembly of matrix and fibre and on the macroscopic level because usually they are made up of stacks of plies. If the plate is modelled in three dimensions, only the microscopic anisotropy needs to be considered because the plies can be considered discretely. The non-linearity, on the other hand, is due to the non-linear behaviour of the resin and the fracture of the plate.

The modelling of fibre reinforced materials involves two tasks. The first is the prediction of the stress-strain relationship and the second is to define criteria for failure. Both aspects result from the action and interaction of the constituent materials.

The models developed for analyzing these materials can be grouped under the following headings:

a) linear elastic models which ignore non-linearity,
b) non-linear elastic models,
c) elastic-plastic models.

Traditionally, it has been assumed that the constitutive materials are linear elastic up to failure and that the bond between the fibres and the matrix is perfect. This has enabled the development of simple micromechanics formulae for the material constants, but these formulae have been found to have insufficient accuracy for off-axis loading. This is essentially due to the non-linearity of the shear behaviour of the composite and due to the successive fracture of the plies.

Non-linear elastic models have been suggested to improve the accuracy of the previous group. They are adequate for the analysis of simple structures under monotonic loading. When dealing with more complicated structures and environmental effects, monotonic behaviour is

not assured throughout the structure and accordingly, their accuracy becomes questionable. Many of the models of this category considered the non-linearity of the shear behaviour only.

A more accurate way of modelling fibre reinforced materials is to consider the non-linearity of the material in the framework of deformation plasticity. This approach can be applied at one of the following three levels.

a) A micromechanical model that describes the behaviour of the material.
b) A macromechanical model that describes the behaviour of the laminae.
c) A macromechanical model that describes the behaviour of the laminate.

The micromechanical approach will be pursued here due to its generality. This approach has been extensively used for the characterisation of the material behaviour of fibre reinforced composites, but only a few investigators proposed models which are suitable for analyzing structures of general shape. The few models which were applicable to structures of general shape were based on two different methodologies; the first method explicitly employs a representative volume of the material where the fibres and the matrix are modeled explicitly to determine the average stress and strain behaviour. Aboudi (1984) used this approach to derive closed form compliance matrix of a composite material. The representative model he used was rectangular and the fibres were also assumed to be rectangular. The matrix was assumed to be elastic-plastic while the fibres were assumed to be linear elastic. The model was later used for investigating different aspects of the non-linear and visco-elastic behaviour of composites (Aboudi 1990). Wu, Shephard, Dvorak and Bahei-El-Din (1990) also presented a method that used a control volume that was triangular with a circular sector at a corner. This geometry represented a hexagonal distribution of the fibres. A closed form solution of that configuration was not available and therefore, they used the finite element method. This meant that in order to establish the behaviour of a macro finite element model of a structure, it was necessary to analyse a micro finite element model of the material at each point of the structure. This clearly resulted in excessive computation time.

The second type of micromechanical models is based on assumptions about the stress and strain fields in the composite. These relationships are then used to combine the constitutive relations of the phases to calculate the constitutive relationships of the composite. Dvorak and Bahei-el-Din (1982) assumed that the fibres had a vanishingly small diameter and accordingly they assumed that the transverse stresses in the fibres and the matrix were equal. Ha, Wang and Chang (1991) used this technique in an accurate way where they applied the stress partitioning idea explicitly. Sun and Chen (1991) also presented a simple method to describe the non-linear

behaviour of fibrous composites. In that model, they assumed that the material was composed of the fibre and the matrix and they obtained the two dimensional behaviour of the resulting composite by assuming that the stress field was uniform in certain regions of the cross section while in other regions the strain was assumed constant.

The second approach considered above is clearly not as accurate as the first one, however, it is readily available for use with numerical techniques for the analysis of structures of complex form. Accordingly, this approach will be used for developing a general three dimensional model for the non-linear analysis of fibre reinforced composite materials.

4.7.1. A MODEL FOR THE DEFORMATIONAL BEHAVIOUR OF A COMPOSITE

Fibre reinforced polymeric plies are composite materials whose behaviour can be defined by the behaviour of representative volume elements which are large compared to typical phase region dimensions (Hashin 1983). For a composite, this relationship can be arrived at using the relationship between the averaged stress and the averaged strain in the constituents. If the averaging is undertaken over the volume, the following relationships are obtained:

$$d\sigma_c = V_m * d\sigma_m + V_f * d\sigma_f$$
$$de_c = V_m * de_m + V_f * de_f \qquad (4.19)$$

where σ_c is the average stress in the composite
σ_m is the average stress in the matrix
σ_f is the average stress in the fibre
ϵ_c is the average strain in the composite
ϵ_m is the average strain in the matrix
ϵ_f is the average strain in the fibre.

Glass fibres are known to behave linearly, while polymeric matrices show a non-linear behaviour. Therefore, it is possible to write the material constitutive relationships of the constituents as follows:

$$de_m = [S_m^e] * d\sigma_m + de_m^p$$
$$de_f = [S_f^e] * d\sigma_f \qquad (4.20)$$

where $[S_m^e]$ is the elastic compliance matrix for the matrix material
$[S_f^e]$ is the elastic compliance matrix for the fibre material and
$d\epsilon_m^p$ is the incremental plastic strain of the resin.

For a unidirectional composite with fibres in the x direction, the following conditions are used to approximate the interaction between the fibre and the matrix.

$$\epsilon_m^x = \epsilon_f^x$$
$$\sigma_m^i = \eta^i * \sigma_f^i \qquad i=y,z \qquad (4.21)$$
$$\tau_m^{ij} = \eta^{ij} * \tau_f^{ij} \qquad i,j=x,y,z$$

Where the superscripts x, y and z stand for the fibre direction and two transverse directions respectively, eta^i is a normal stress partitioning factor for direction i and eta^{ij} is a shear stress partitioning factor for the plane ij. The first of conditions (4.21) is generally accepted for long fibres while the other conditions can be considered as empirical approximations of the real behaviour.

The partitioning factors in the latter conditions are used to approximate the fact that for transverse and shear loading, the stress is transmitted partially by the continuous matrix layers and partially by the layers which contain the fibres. The factors depend on the packing and the geometry of the fibres in the composite as well as the properties of the interface and therefore, have to be determined from experimental measurements.

The above given conditions can be written using Eq(4.20) in matrix form as:

$$\begin{bmatrix} \frac{1}{E_m} & -\frac{\nu_m}{E_m} & -\frac{\nu_m}{E_m} & 0 & 0 & 0 \\ 0 & 1 & 0 & 0 & 0 & 0 \\ 0 & 0 & 1 & 0 & 0 & 0 \\ 0 & 0 & 0 & 1 & 0 & 0 \\ 0 & 0 & 0 & 0 & 1 & 0 \\ 0 & 0 & 0 & 0 & 0 & 1 \end{bmatrix} * d\sigma_m + \begin{bmatrix} 1 & 0 & 0 & 0 & 0 & 0 \\ 0 & 0 & 0 & 0 & 0 & 0 \\ 0 & 0 & 0 & 0 & 0 & 0 \\ 0 & 0 & 0 & 0 & 0 & 0 \\ 0 & 0 & 0 & 0 & 0 & 0 \\ 0 & 0 & 0 & 0 & 0 & 0 \end{bmatrix} * d\epsilon_m^p =$$

$$\begin{bmatrix} \frac{1}{E_f^x} & -\frac{\nu_f}{E_f^x} & -\frac{\nu_f}{E_f^y} & 0 & 0 & 0 \\ 0 & \eta^y & 0 & 0 & 0 & 0 \\ 0 & 0 & \eta^z & 0 & 0 & 0 \\ 0 & 0 & 0 & \eta^{yz} & 0 & 0 \\ 0 & 0 & 0 & 0 & \eta^{zx} & 0 \\ 0 & 0 & 0 & 0 & 0 & \eta^{xy} \end{bmatrix} * d\sigma_f \qquad \textbf{(4.22)}$$

Solving for $d\sigma_m$

$$d\sigma_m = [\alpha] d\sigma_f - [\beta] d\epsilon_m^p$$

where

$$[\beta] = \begin{bmatrix} E_m & 0 & 0 & 0 & 0 & 0 \\ 0 & 0 & 0 & 0 & 0 & 0 \\ 0 & 0 & 0 & 0 & 0 & 0 \\ 0 & 0 & 0 & 0 & 0 & 0 \\ 0 & 0 & 0 & 0 & 0 & 0 \\ 0 & 0 & 0 & 0 & 0 & 0 \end{bmatrix} \qquad \textbf{(4.23)}$$

Ha, Wang and Chang (1991) obtained a similar result for the two dimensional case. Here it has to be noted that the material properties used are those of a block of material. The difference between the behaviour of a block of material and the material in the composite will be assumed to be included in the experimentally determined partitioning factors. These factors are included in the matrix [α] which is assumed to be independent of the stress level. This assumption is not correct due to the stress relaxation in the matrix resulting from the local

yielding of the resin and the change in the interface conditions. However, it is used here because it is less severe than all the assumptions considered in previously considered models. The matrix $[\alpha]$ will be given later as function of the material matrices of the constituents and the composite.

Rewriting Eq(4.19) and taking into account the constitutive behaviour of Eq(4.20)

$$\begin{aligned} de_c &= V_m * ([S_m^e]\, d\sigma_m + de_m^p) + V_f\, [S_f^e]\, d\sigma_f \\ d\sigma_c &= V_m\, d\sigma_m + V_f\, d\sigma_f \end{aligned} \qquad (4.24)$$

Eliminating $d\sigma_m$ using Eq(4.23)

$$\begin{aligned} de_c &= (V_m\, [S_m^e]\, [\alpha] + V_f\, [S_f^e])\, d\sigma_f + V_m\, ([I] - [S_m^e]\, [\beta])\, de_m^p \\ d\sigma_c &= (V_m\, [\alpha] + V_f\, [I])\, d\sigma_f - V_m\, [\beta]\, de_m^p \\ &\textit{thus} \\ d\sigma_f &= (V_m [\alpha] + V_f\, [I])^{-1} (d\sigma_c + V_m\, [\beta]\, de_m^p) \end{aligned} \qquad (4.25)$$

Eliminating $d\sigma_f$ from Eq(4.25)

$$\begin{aligned} de_c &= (V_m\, [S_m^e]\, [\alpha] + V_f\, [S_f^e])(V_m\, [\alpha] + V_f\, [I])^{-1} d\sigma_c + \\ &\{(V_m\, [S_m^e]\, [\alpha] + V_f\, [S_f^e])(V_m\, [\alpha] + V_f\, [I])^{-1}\, [\beta] + [I] - [S_m^e]\, [\beta]\}\, V_m de_m^p \\ &\textit{thus} \\ de_c &= [S^e{}_c]\, d\sigma_c + [\gamma]\, de_m^p \\ [S^e{}_c] &= (V_m [S_m^e]\, [\alpha] + V_f [S_f^e])(V_m [\alpha] + V_f [I])^{-1} \\ [\gamma] &= \{([S^e{}_c] - [S_m^e])\, [\beta] + [I]\}\, V_m \end{aligned} \qquad (4.26)$$

Here it has to be noted that S_c^e can be obtained directly using the conventional methods of linear micromechanics given in Chapter 3.

The expression of S_c^e in Eq(4.26) can be used to find the inverse of $[\alpha]$ as a function of the elastic material matrices as follows:

$$[S^e_c] = (V_m[S_m]\ [\alpha]+V_f\ [S_f])(V_m\ [\alpha]+V_f\ [I])^{-1}$$

thus

$$[\alpha]^{-1}=\frac{V_m}{V_f}\ ([S_f]-[S^e_c])^{-1}([S^e_c]-[S_m]) \qquad (4.27)$$

or

$$[\alpha]^{-1}=\frac{V_m}{V_f}\ ([D^e_c]\ [S_f]-[I])^{-1}\ ([I]-[D^e_c]\ [S_m])$$

Noting that $[D^e_c] = [S^e_c]^{-1}$, it is possible to write Eq(4.26) in the following form which is suitable for solution using the initial stress method.

$$d\sigma_c=[D^e_c]de-[D^e_c]\ [\gamma]\ de^p_m$$

where (4.28)

$$[D^e_c]\ [\gamma] = V_m\{([I]-[D^e_c][S_m])\ [\beta]+[D^e_c]\}$$

The plastic increment $d_m{}^p$ is the plastic strain increment developed in the matrix. It will be assumed that the resin behaves isotropically and that it is isotropically strain hardening. This assumption does not have a global effect on the model and accordingly, it can be replaced by any other elastic-plastic model. When yielding plastically, the plastic strain is assumed to be satisfying the associative flow rule according to the yield condition $F(\sigma,k)=0$ where k is the hardening parameter. When yielding occurs the following condition applies.

$$F(\sigma_m)=k(\kappa) \qquad (4.29)$$

Using the normality rule (Owen and Hinton 1980)

$$de^p_m=d\lambda\frac{\partial F}{\partial\sigma_m}$$

thus (4.30)

$$de_m=[D_m{}^{-1}]d\sigma_m+d\lambda\frac{\partial F}{\partial\sigma_m}$$

When differentiating the condition that the stresses remain on the yield surface (Eq(4.29)), the following condition is arrived at.

$$\left(\frac{\partial F}{\partial \sigma_m}\right)^T d\sigma_m - A d\lambda = 0 = a^T d\sigma_m - A d\lambda$$

$$a = \frac{\partial F}{\partial \sigma_m} \qquad (4.31)$$

$$A = -\frac{\partial F}{\partial \kappa} d\kappa \frac{1}{d\lambda}$$

By pre-multiplying Eq(4.30) by $a^T[D_m]$ and using Eq(4.31) to substitute for the term $a^T d\sigma_m$

$$a^T[D_m]de_m = a^T d\sigma_m + d\lambda a^T[D_m]a$$

$$a^T[D_m]de_m = A d\lambda + a^T[D_m]a\ d\lambda \qquad (4.32)$$

$$d\lambda = \frac{a^T[D_m]de_m}{A + a^T[D_m]a}$$

Therefore, from Eq(4.30)

$$d\epsilon_m^p = \frac{a^T D_m^e de_m}{[A + a^T D_m^e a]} a \qquad (4.33)$$

The quantity 'A' representing the hardening of the material can be obtained from the tensile uniaxial stress-strain curve. Assuming that the matrix is linearly strain hardening and resulting in a post yielding modulus equal to 'E_{Tang}', 'A' can be calculated from the following relationship (Owen and Hinton 1980).

$$A = \frac{E_{Tang}}{1 - \frac{E_{Tang}}{E_m}} \qquad (4.34)$$

Accordingly, it is possible to relate $d\epsilon_m$ to its plastic component as follows:

$$d\epsilon_m^p = \frac{(a\ a^T[D_m])}{(A + a^T[D_m]a)} de_m = [\delta] de_m$$

therfore

$$d\sigma_m = [D_m]\ ([I] - [\delta])\ de_m \qquad (4.35)$$

but

$$d\sigma_m = [D_m^{ep}] de_m$$

therefore

$$[\delta] = ([I] - [S_m][D_m^{ep}])$$

Which is the conventional form for the stress strain relationship for an isotropic material which is deforming plastically and isotropically hardening.

It has to be noted that when calculating the stresses for the case when the material has just yielded, it is necessary to scale the stresses such that they do not come out of the yield surface. In the same way, the reduction of the material stiffness matrix resulting from plasticity has to be implemented only partially because a part of the step is linear elastic (Owen and Hinton 1980). Therefore, the stiffness matrix has to be calculated as follows:

$$[D_m^{ep}] = [D_m] - [D_m^p] * \left(\frac{F_n - F}{F_n - F_o} \right) \qquad (4.36)$$

Where F_o is the last equivalent stress value still inside the yield surface, F_n is the first equivalent stress value lying outside the yield surface and F is the yield condition.

Substituting $d\sigma_m$ and $d\sigma_f$ from Eq(4.20) into Eq(4.23), the following relationship is obtained.

$$[D_m] de_m + ([\beta] - [D_m]) d\epsilon_m^p = [\alpha][D_f] d\epsilon_f \qquad (4.37)$$

By substituting for $d\epsilon_m{}^p$ from Eq(4.35)

$$([D_m] + ([\beta] - [D_m])[\delta]) de_m = [\alpha][D_f] d\epsilon_f$$

$$d\epsilon_f = ([\alpha][D_f])^{-1}([D_m] + ([\beta] - [D_m])[\delta]) de_m \qquad (4.38)$$

$$d\epsilon_f = [S_f][\alpha^{-1}]([D_m] + ([\beta] - [D_m])[\delta]) de_m$$

Then using Eq(4.19) followed by Eqs(4.27, 4.28 and 4.35)

$$de_c=(V_m[I]+V_f[S_f][\alpha^{-1}]\{([D_m]+([\beta]-[D_m])[\delta]\})de_m=[\zeta]de_m$$

or

$$[\zeta]=V_m([I]+[S_f]([D^{\epsilon}{}_c][S_f]-[I])^{-1}([I]-[D^{\epsilon}{}_c][S_m])\{[\beta]+([I]-[\beta][S_m])[D_m^{ep}]\})$$

therefore **(4.39)**

$$de_m^p=[\delta][\zeta]^{-1}de_c$$

$$d\sigma_c=[D^{\epsilon}{}_c][I-[\gamma][\delta][\zeta]^{-1}]de_c=$$

$$([D^{\epsilon}{}_c]-[D^{\epsilon}{}_c][\gamma]([I]-[S_m][D_m^{ep}])[\zeta]^{-1})de_c=[D^{ep}{}_c]de_c$$

This is the incremental form of the constitutive relationship of the average stress and the average strain in the composite.

It has to be noted that the elastic plastic matrix of the composite depends on the elastic plastic matrix of the resin. This in turn depends on the stress in the resin. Therefore, it is necessary to find an explicit relationship between the stress of the composite and the stress in the resin.

Solving Eq(4.23) for $d\sigma_f$

$$d\sigma_f=[\alpha]^{-1}\{d\sigma_m+[\beta]de_m^p\} \quad \textbf{(4.40)}$$

Substituting from Eqs(4.20, 4.27, 4.35 and 4.40) into Eq(4.19)

$$d\sigma_c=V_m\{[I]+([D^{\epsilon}{}_c][S_f]-[I])^{-1}([I]-[D^{\epsilon}{}_c][S_m])([I]-[\beta][S_m])\}d\sigma_m+$$
$$V_m([D^{\epsilon}{}_c][S_f]-[I])^{-1}([I]-[D^{\epsilon}{}_c][S_m])[\beta]de_m \quad \textbf{(4.41)}$$

but from Eq(4.21)

$$[\beta]de_m=[\beta]de_f=[\beta]de_c$$

therefore

$$d\sigma_c=V_m([\eta]d\sigma_m+[\theta][\beta]de_c)$$

where **(4.42)**

$$[\eta]=[I]+([D^{\epsilon}{}_c][S_f]-[I])^{-1}([I]-[D^{\epsilon}{}_c][S_m])([I]-[\beta][S_m])$$

$$[\theta]=([D^{\epsilon}{}_c][S_f]-[I])^{-1}([I]-[D^{\epsilon}{}_c][S_m])$$

It is important to note that the matrices eta and theta are constant and therefore, it is possible to sum the increments to obtain:

$$\sigma_c = V_m([\eta]\sigma_m + [\theta][\beta]\epsilon_c)$$

$$or \qquad (4.43)$$

$$\sigma_m = [\eta^{-1}](\frac{1}{V_m}\sigma_c - [\theta][\beta]\epsilon_c)$$

This means that by knowing the stress and the strain in the composite, it is possible to calculate the stress in the resin.

4.7.1.1. THE NON-LINEAR BEHAVIOUR OF POLYMERS

In order to complete the characterisation of the deformational behaviour of the composite, it is necessary to choose a suitable yield condition for the matrix. The published experimental results for the behaviour of the polymers are scarce and they do not cover all combinations of stress in three dimensions (Garg and Mai 1988). The data provided to advocate the use of a certain yield surface can usually be represented using other yield conditions with the same degree of accuracy. Therefore, and because of the approximate nature of the theory presented above, only yield surfaces which do not depend on the third stress invariant will be considered.

The yield surfaces which satisfy the above given condition can be characterised according to their shape in the principal stress space. The most basic surface is the cylindrical surface (Von Mises). A better approximation of the material behaviour can be achieved using a conical surface (Prager-Drucker) or a paraboloidal surface. The reason for this is that the cylindrical surface fails to represent the increase in the yield stress with increasing hydrostatic pressure.

The expressions of these yield surfaces when written using the stresses are very cumbersome. Therefore, it is customary to use the following stress invariants for this task (Zienkiewicz 1977):

$$J_1=\sigma_x+\sigma_y+\sigma_z=3\sigma_m$$
$$J_2=.5(s_x^2+s_y^2+s_z^2)+\tau_{xy}^2+\tau_{yz}^2+\tau_{zx}^2=t_d^2 \qquad (4.44)$$
$$where$$
$$s_x=\sigma_x-\sigma_m\ ,\quad s_y=\sigma_y-\sigma_m\ ,\quad s_z=\sigma_z-\sigma_m$$

where σ_m is the mean hydrostatic pressure and t_d is the deviatoric shear stress. Accordingly, the yield surfaces can be written as:

$$\begin{array}{ll} CYLINDER & \sqrt{J_2}=C \\ CONE & bJ_1+\sqrt{J_2}=C \\ PARABOLOID & bJ_1+J_2=C \end{array} \qquad (4.45)$$

Where 'b' and 'C' are constants to be determined using uniaxial testing. When the material is subjected to uniaxial tensile stress of magnitude 'σ', J_1 equals σ and J_2 is equal to $1/3\sigma^2$. In the case of uniaxial compressive stress '$-\sigma$', J_1 is equal to $-\sigma$ and J_2 is equal to $1/3\sigma^2$. Accordingly the yield surfaces can be written using the uniaxial yield stresses Y_t and Y_c for tension and compression as follows:

$$\begin{array}{ll} CYLINDER & \sqrt{J_2}=\sqrt{\frac{1}{3}}Y_t=\sqrt{\frac{1}{3}}Y_c \\ CONE & (Y_c-Y_t)J_1+\sqrt{3}(Y_c+Y_t)\sqrt{J_2}=2Y_cY_t \\ PARABOLOID & (Y_c-Y_t)J_1+3J_2=Y_cY_t \end{array} \qquad (4.46)$$

It has to be noted that the cylindrical surface is not capable of handling a difference between the tensile and the compressive yield stresses. For polymers, the ratio between the compressive and the tensile yield stresses was shown to be about 1.3 (Raghava, Caddell and Yeh 1973). Therefore, the cylindrical yield surface is not suitable for modelling polymers. Fig(4.80) compares the yield stresses for the cases of plane stress and plane strain. It can be seen that the conical and paraboloidal yield surfaces are very similar for a ratio of compressive

to tensile yield stresses equal to 1.3 when plane stress conditions prevail. Under plane strain conditions, however, the paraboloidal surface is more conservative compared to the conical surface. In addition, the variation of the deviatoric shear stress with the mean hydrostatic pressure for the parabolic criterion is smooth, while a discontinuity of the stress gradient exists for the conical criterion. Although Garg and Mai (1988) have proposed a more detailed yield surface, the paraboloidal yield surface will be considered because of the absence of sufficient experimental results.

In order to obtain the yield condition in the standard form given in Eq(4.29), Yc in the paraboloidal surface given in Eq(4.46) is replaced by S*Yt. When solving the resulting expression for Yt, the following result is obtained:

$$F(\sigma)=Y_t=\frac{(S-1)}{2S}J_1+\sqrt{\left(\frac{S-1}{2S}\right)^2 J_1^2+3\frac{J_2}{S}} \qquad (4.47)$$

Here it has to be noted that the negative solution of the root in Eq(4.47) was not considered because this would have resulted in a negative right hand side. The quantity on the right hand side of the equation can be considered as an effective stress. This quantity can now be differentiated with respect to J_1 and the $\sqrt{(J_2)}$ to give

$$\frac{\partial F}{\partial J_1}=\frac{S-1}{2S}+\frac{\left(\frac{S-1}{2S}\right)^2 J_1}{\sqrt{\left(\frac{S-1}{2S}\right)^2 J_1^2+\frac{3J_2}{S}}}$$

$$\frac{\partial F}{\partial \sqrt{J_2}}=\frac{\frac{3}{S}\sqrt{J_2}}{\sqrt{\left(\frac{S-1}{2S}\right)^2 J_1^2+\frac{3J_2}{S}}} \qquad (4.48)$$

By multiplying these partial derivatives of F by the partial derivatives of J_1 and $\sqrt{(J_2)}$, the vector 'a' required in Eq(4.31) is obtained (Zienkiewicz 1977).

4.7.1.2. THE CALCULATION OF THE STIFFNESS AND THE STRESS

Using the results of the previous sections, it is possible to define uniquely the stress strain behaviour of the material. The procedure for calculating the stiffness and the stresses of a composite under the action of known stress and strain and subjected to a further increment of strain using the above given equations will be discussed now.

Eq(4.43) can be used in conjunction with the stress and strain values at the beginning of the increment to calculated the stress prevailing in the matrix. The knowledge of that quantity allows the calculation of the plastic matrix of the resin. Based on these values, it is possible to use Eq(4.47) to calculate the equivalent stress of the old configuration. In addition, it is possible to calculate the plastic matrix of the resin using Eq(4.35). The new stress is then calculated based on the elastic matrix of the composite and again the stress in the matrix is calculated using Eq(4.43) and the corresponding new equivalent stress is obtained Eq(4.47). The elastic plastic matrix of the resin is then found using Eq(4.36). Using this stiffness, it is possible to calculate the stiffness matrix of the composite Eq(4.39) which in turn is used to calculate the total stress increment.

Fig(4.81) shows the variation of the yield stress in a plane parallel to the fibres with varying the glass fibre volume fraction. On the same graph, the yield surface of the resin when subjected to plane strain conditions is shown. It is seen that the increase of the fibre volume fraction of the composite results in the same tendency of increasing the size of the yield surface. A plane containing the fibres was also considered in the same figure. It is interesting to note that the uniaxially stressed material will not yield because it will fracture first. Fig(4.82) shows a plot of the π-plane for $J_1 = .2$ GPa where it can be seen that the yield surface increases with increasing the fibre volume fraction. The case of pure resin is not considered in this case because all the points lying on that plane lie below the yield paraboloid of the resin. The effect of varying the hydrostatic pressure on the yield stresses is shown in Fig(4.83). For increasing compressive hydrostatic stresses, the yield curves move in the direction of the -ve σ_1 direction and their size increases. This means that the yield surface is a paraboloidal surface which is inclined to the space diagonal and which is elongated in the plane containing the space diagonal and the σ_1 axis. A check of the model was performed using the experimental results reported by Frost (1990). The stress-strain curves for the different fibre directions compared to the experimental results are shown in Fig(4.84). The results of the comparison are encouraging and show that even using this simple linear hardening model, the accuracy is sufficient.

4.7.2. FAILURE OF UNIAXIAL FIBRE REINFORCED COMPOSITES

The second stage of modelling the material is concerned with failure. The failure of composite materials has been widely investigated and various failure hypotheses and criteria have been proposed. The failure criteria are the conditions at which failure of a material point is expected. The direct application of these conditions to the different points of a structure applies only to brittle materials. The behaviour of fibre reinforced composite materials varies between tough and brittle according to the reinforcement type, the reinforcement directions and the lay-up of the material (Harris 1986). Accordingly, the failure of a highly stressed point in a structure does not necessarily mean that the latter has failed. In order to relate the failure of the structure to the failure of the material, failure hypotheses are used.

Failure criteria range from maximum stress and strain criteria to criteria involving different stress combinations at the point under consideration. The latter class of failure criteria was found to satisfactorily represent the failure of the material under different loading conditions, however, they had no physical meaning. The application of the simpler former criteria, on the other hand, resulted in better insight into the failure mechanisms of the material but their quantitative predictions were poor.

The failure hypotheses, range from 'point stress', 'average stress' and 'damage zone criterion' hypotheses which are applied either at the laminate or lamina level to detailed progressive damage models. The former types of hypotheses are easy to apply but they suffer from their high degree of empiricism. This means that their field of application is narrow and they need a constant feed of experimental data. The latter are more general because they are based on more sound assumptions which approximate the physical behaviour of the material.

Although the strength of the constituents of composite materials are different from their strength within the composite, their failure form remains the same. Therefore, in order to understand the failure behaviour of fibre reinforced composite materials, it is important to study the basic failure mechanisms of the constituents. In addition, in order to arrive at reasonable estimates of the strength of the composite, it is necessary to consider the interaction of the phases of the composite.

Composites reinforced using unidirectional fibres may fail in two possible directions, namely:

a) normal to the fibres or
b) parallel to the fibres.

The first type of failure is associated with fibre breakage and therefore it is usually referred to as the fibre failure mode. The failure parallel to the fibres is usually associated with matrix or interface failure and therefore, it is customarily called the matrix failure mode (Hashin 1983).

Generally speaking, failure on a plane can result from either shearing or axial straining. Shear failure of the material normal to the fibres does not usually take place because any shear action on such a plane has a complementary shear of equal value acting parallel to the fibres. The shear strength within the planes parallel to the fibres are much lower than those of the planes perpendicular to the fibres and therefore, failure occurs parallel to them.

The failure in the axial direction may be due to fracture of the fibres or crushing of the composite associated with buckling of the fibres. In both cases, it is possible to predict the failure in that direction using the strain of the composite in that direction. To characterise this, two critical strains are needed; one for the fracture failure and the other is for the crushing failure.

Transverse failure can result due to any of the following causes:

a) the principal axial strain exceeds a threshold value,
b) the maximum in-plane shear stress exceeds a threshold value,
c) the resultant longitudinal shear strain exceeds its failure value.

It has to be noted that cases a) and b) represent the failure behaviour due to the in-plane actions in the planes normal to the fibres while case c) indicates failure due to out-of-plane shearing. Although the direction of the failure surface depends on the cause of failure and on the direction of the critical stress component, it is known that the failure due to these cases will be on a plane parallel to the fibres. Therefore, it is not possible to use the principal stress resulting from the transverse normal action and the longitudinal shear stress to predict failure.

The material properties and strength of composite materials depend on the fibre volume fraction. However, the limiting strains in this work will be assumed independent of the fibre volume fraction. This assumption is justified because the variation of the strength is similar to the variation in the elastic constants, resulting in approximately constant failure strains. In addition, the experimental findings of Sigley, Wronski and Parry (1990) showed that this approach is more accurate in considering the effect of hydrostatic pressure than considering the stresses. The case which will be estimated to occur first will control the strength. Finally, the use of strain based failure criteria will avoid the problems that might develop due to the simultaneous consideration of the elastic-plastic model and the failure model.

The failure due to the in-plane action was separated into two cases based on the known behaviour of polymeric materials. The failure of polymeric materials occurs in shear when it is subjected to compressive loading (Maccrum, Buckley and Bucknall 1988) and they fail by crazing under tensile loading. The same behaviour was reported by (Hull 1981) for fibre reinforced composite polymers. The prediction of crazing will be undertaken by monitoring the maximum positive principal strain. This strain will be compared to the failure strain of a transverse tension specimen. It is known that this strain decreases with increasing the fibre volume fraction. This was explained by the increase in the strain concentration due to the more tightly packed fibres. The principal strains can be calculated from the following relationship:

$$\epsilon_1=\left(\frac{\epsilon_x+\epsilon_y}{2}\right)^2+\sqrt{\left(\frac{\epsilon_x-\epsilon_y}{2}\right)^2+\left(\frac{\gamma_{xy}}{2}\right)^2}$$
$$\epsilon_2=\left(\frac{\epsilon_x+\epsilon_y}{2}\right)^2-\sqrt{\left(\frac{\epsilon_x-\epsilon_y}{2}\right)^2+\left(\frac{\gamma_{xy}}{2}\right)^2} \qquad (4.49)$$

In this case, the failure plane will be assumed in the principal direction that has a more 'positive' normal strain. These directions are given as

$$\phi=.5\tan^{-1}\left(\frac{\gamma_{yz}}{\epsilon_y-\epsilon_z}\right)$$
$$or \qquad (4.50)$$
$$\phi=.5\tan^{-1}\left(\frac{\gamma_{yz}}{\epsilon_y-\epsilon_z}\right)+\frac{\pi}{2}$$

Case b) will occur if Von Mises criterion for strain is satisfied. The use of this criterion in conjunction with strain assumes plane strain condition. This is justified because of the relatively small strains in the axial direction. The value of the equivalent strain will be compared to the transverse shear strength of the composite. This strain is reported to be independent of the fibre volume fraction for practical values (Hull 1981). The failure direction for the present case will be taken as the plane at an angle equal to 45° to the principal strain

direction found above. The direction chosen is again the one corresponding to the numerically larger normal strain. The condition for failure is given as (Cook, Malkus and Plesha 1989)

$$\gamma_{trans}=\sqrt{\frac{2}{3}(2*(\epsilon_y^2-\epsilon_y*\epsilon_z+\epsilon_z^2)+1.5*\gamma_{yz}^2)} \qquad (4.51)$$

Case c) is checked using the resultant of the longitudinal shear. That resultant is obtained directly as the square root of the sum of squares of the strains.

$$\gamma_{long}=\sqrt{\gamma_{xy}^2+\gamma_{zx}^2} \qquad (4.52)$$

This is correct because their complementary shears are acting on the same area and can be summed up to a single resultant force. The strain is now compared to the failure in-plane shear strain.

The plane of failure is taken as the plane of action of the resultant. The latter is given as

$$\phi=\tan^{-1}\left(\frac{\gamma_{zx}}{\gamma_{xy}}\right) \qquad (4.53)$$

In all cases, if the failure plane is acted upon by a tensile strain, then the stresses and the stiffness related to that plane are reduced to zero. If the failure plane has compression strain acting on it, only the stiffness is reduced to zero. The enforcement of the stiffness reduction due to failure in the elastic-plastic analysis was achieved simply by applying the reductions to the original material matrices describing the elastic behaviour. The reduction of the stiffness was undertaken by reducing the elastic material properties in the appropriate direction. These values were then used to construct the orthotropic stiffness matrix which was later rotated to the correct direction.

The above described model was implemented as a user defined subroutine in the finite element package ABAQUS. The listing of the subroutine is included in Appendix(3). Fig(4.85) shows a block diagram for the quantities which are needed as output from ABAQUS and the results which are fed back into the program. It can be seen that the subroutine is composed of four modules. The first module prepares the elastic properties of the composite. The equations

used in that part were derived in Chapter 3. The next module checks the failure of the node under consideration. This is followed by a module that performs the degradation of the material properties due to damage. Finally the non-linear stress-strain model is considered.

An example problem was analyzed using this material model. The problem under consideration is meshed according to Fig(4.66). Fig(4.86) compares the load-deformation behaviour predicted using the present material model with the experimentally obtained data. Here it has to be noted that different methods for investigating failure were considered.

First only the non-linearity of the stress-strain behaviour was considered. For this case (curve A), it can be seen from Fig(4.86) that the strength of the lug was overestimated while for low stress levels, the correspondence with the experimental data was fairly good. It has to be noted here that the consideration of the non-linearity of the stress-strain behaviour of the chopped strand mat did not have an effect on the load deformation curve. The small discrepancy between the experimental and theoretical curves under low loads was possibly due to the effect of the washer.

When the failure of the material was considered, the theoretical failure load dropped to a value which was much less than the experimental value (curve B). The load deflection behaviour, however, was identical to the case where only non-linearity was considered. The reason for this was the assumed sudden loss of strength of the points at which failure was predicted. This, however, was not an accurate representation of the actual behaviour of the material. The failure mechanisms in composite materials involve crack arrest by neighbouring laminates and friction between a fractured fibre and the surrounding matrix which result in slowing the rate of crack propagation. This means that the stress of a failed material does not instantaneously drop to zero.

Accordingly, the model was updated in order to account for this behaviour of the material. This was achieved by keeping the stress at a maximum constant value equal to that attained when failure was predicted. The result of this case (curve C) corresponded reasonably well with the experimental results.

The effect of considering the non-linearity of the material on the in-plane stresses around the hole are given in Fig(4.87). This figure shows that when the load increases, the radial stresses acting on the uniaxial layer becomes concentrated near the axis of symmetry of the plate. This is associated with a small increase in the tangential stresses acting on the minimum cross section. The relative magnitudes of the stresses in the randomly orientated layer show that the radial stresses increase while the tangential stresses change sign from tension to compression over a large part of the contact area.

In order to visualise the areas of non-linear behaviour, the strain in the radial and tangential direction was plotted in Fig(4.88). This figure shows that large tangential plastic strains developed at theta=0°. The consideration of friction is expected to prevent the development of these strains. The out-of-plane strain around the hole is given in Fig(4.89). These strains show that the contact area develops large through thickness strains which indicate the development of non-linear behaviour in that direction. This means that the failure type expected for this specimen is a bearing mode; this is the type of failure which was observed experimentally.

4.8. THE EFFECT OF VARYING THE COMPOSITION OF THE LAMINATE

The assessment of the performance of joints in different composite materials irrespective of the geometry of the joint can be achieved by considering an infinite anisotropic plate containing a loaded hole. This solution can demonstrate the effect of varying the material parameters of pultruded members on the stress distributions around the loaded hole. The solution of this problem using analytical methods is more efficient than the finite element method. Therefore, a closed form formula for the tangential stresses on the boundary of a radially loaded hole in an infinite orthotropic plate is developed. The solution is based on the general technique given by Green (1945) using the complex variable approach. The radial stresses are approximated using the formula given by Zhang and Ueng (1984).

The difficulty of the problem under consideration is due to the non-smoothness of the tractions acting on the surface of the hole. Therefore, all previous solutions used Fourier series to represent the tractions on the hole of the boundary. This meant that the accuracy of the solution at the point of transition from separation to contact between the plate and the pin was poor. This necessitated the use of excessive numbers of terms of the series. For example De Jong (1977) used 35 terms of the series to represent the sine stress distribution on half the hole perimeter.

4.8.1. GREEN'S COMPLEX VARIABLE SOLUTION

Green and Taylor (1939) used the equilibrium and compatibility conditions to derive the governing differential equation for an anisotropic plate lying in the x-y plane. The resulting equation for an orthotropic plate in terms of a stress function X is:

$$\left(\frac{\partial^2}{\partial x^2}+\alpha_1\frac{\partial^2}{\partial y^2}\right)\left(\frac{\partial^2}{\partial x^2}+\alpha_2\frac{\partial^2}{\partial y^2}\right)\chi=0 \tag{4.54}$$

Where α_1 and α_2 are parameters describing the material. They are related to the coefficients of the material flexibility matrix using the following two relations:

$$\alpha_1\alpha_2=\frac{s_{11}}{s_{22}},\qquad \alpha_1+\alpha_2=\frac{(s_{66}+2s_{12})}{s_{22}}$$
$$s_{11}=\frac{1}{E_x},\qquad s_{22}=\frac{1}{E_y},\qquad s_{66}=\frac{1}{G_{xy}},\qquad s_{12}=\frac{-\nu_{yx}}{E_y}=\frac{-\nu_{xy}}{E_x} \tag{4.55}$$

Where E and G are the axial and shear rigidities. Poisson's ratio ν_{ab} is taken as the ratio characterizing the contraction in the direction b when tension is applied in the direction a. They showed that the general solution of this equation can be taken as the real part of:

$$\chi = Re\left[f(z+\gamma_1\bar{z})+g(z+\gamma_2\bar{z})\right] \tag{4.56}$$

where

$$z=x+iy \qquad \bar{z}=x-iy$$
$$\gamma_1=\frac{\alpha_1^{\frac{1}{2}}-1}{\alpha_1^{\frac{1}{2}}+1} \qquad \gamma_2=\frac{\alpha_2^{\frac{1}{2}}-1}{\alpha_2^{\frac{1}{2}}+1} \tag{4.57}$$

and f and g are arbitrary analytic functions of the complex variable z.

The stresses with respect to cylindrical coordinates were obtained from this general stress function and are given in Eqs('4.9 to 4.11') in Green's paper (1945). When introducing the two functions $\alpha(z)$ and $\beta(z)$ the following simplified form is obtained.

$$\sigma_r(z)=Re\left(-\frac{(z-\gamma_1\bar{z})^2}{z\bar{z}}\alpha(z)-\frac{(z-\gamma_2\bar{z})^2}{z\bar{z}}\beta(z)\right) \tag{4.58}$$

$$\sigma_\theta(z)=Re\left(\frac{(z+\gamma_1\bar{z})^2}{z\bar{z}}\alpha(z)+\frac{(z+\gamma_2\bar{z})^2}{z\bar{z}}\beta(z)\right) \tag{4.59}$$

$$\tau_{r\theta}(z)=Re\left(-i\frac{(z^2-\gamma_1^2\bar{z}^2)}{z\bar{z}}\alpha(z)-i\frac{(z^2-\gamma_2^2\bar{z}^2)}{z\bar{z}}\beta(z)\right) \tag{4.60}$$

where $\alpha(z)$ and $\beta(z)$ are given as

$$\alpha(z)=\left[f''(z+\gamma_1\bar{z})+\frac{A*(1-\gamma_2)(s_{12}-\alpha_2 s_{22})+iB*(1+\gamma_2)(s_{12}-\alpha_1 s_{22})}{z+\gamma_1\bar{z}}\right]$$
$$\beta(z)=\left[g''(z+\gamma_2\bar{z})-\frac{A*(1-\gamma_1)(s_{12}-\alpha_1 s_{22})+iB*(1+\gamma_1)(s_{12}-\alpha_2 s_{22})}{z+\gamma_2\bar{z}}\right] \quad (4.61)$$

here, f'' and g'' indicate the second derivative with respect to z. The constants A and B are related to the resultant forces in the x and y directions as follows:

$$F_x=2\pi A*(1-\gamma_1)(1-\gamma_2)(\alpha_1-\alpha_2)s_{22}$$
$$F_y=2\pi B*(1+\gamma_1)(1+\gamma_2)(\alpha_1-\alpha_2)s_{22} \quad (4.62)$$

In order to satisfy the boundary conditions, two functions V and W are introduced. These functions, previously used by Bickley (1928) and Green (1945), are functions of the complex variable z which are finite at infinity. On the edge of the hole, V has a real part equal to $-\sigma_r$ while W has an imaginary part equal to $-\tau_{r\theta}$. Because the most general expression for the edge loading can be described using Fourier series, Bickley (1928) chose these functions such that they gave loadings in a Fourier series form on the boundary of the hole. The terms of these series, excluding the constant term, were summed by Bickley (1928) to give the following expressions:

$$V(z)=\frac{1}{2\pi}\int_0^{2\pi}\left[\frac{ze^{-i\gamma}+a}{ze^{-i\gamma}-a}\right]\sigma_r(\gamma)d\gamma \quad (4.63)$$

$$W(z)=\frac{-i}{2\pi}\int_0^{2\pi}\left[\frac{ze^{-i\gamma}+a}{ze^{-i\gamma}-a}\right]\tau_{r\theta}(\gamma)d\gamma \quad (4.64)$$

It has to be noted that when the stresses are constant, the above given integrals are not applicable; this case has to be considered separately. Green (1945) showed that this case can be considered if V is chosen equal to -W.

Based on Eq('4.15 and 4.16') in Green's paper, the functions $\alpha(z)$ and $\beta(z)$ introduced in the present work can be expressed in terms of the two functions V(z) and W(z) as follows:

$$(\gamma_1-\gamma_2)(z-\gamma_1\bar{z})\alpha(z)=$$
$$K_1*(1-\gamma_2)-iK_2*(1+\gamma_2)$$
$$-\frac{V(z+\gamma_1\bar{z})*(z+\gamma_2\bar{z})+W(z+\gamma_1\bar{z})*(z-\gamma_2\bar{z})}{2} \quad (4.65)$$

$$(\gamma_1-\gamma_2)(z-\gamma_2\bar{z})\beta(z)=$$
$$-K_1*(1-\gamma_1)-iK_2*(1+\gamma_1)$$
$$+\frac{V(z+\gamma_2\bar{z})*(z+\gamma_1\bar{z})+W(z+\gamma_2\bar{z})*(z-\gamma_1\bar{z})}{2} \quad (4.66)$$

where

$$K_1=A*[(1-\gamma_1)(s_{12}-\alpha_1 s_{22})-(1-\gamma_2)(s_{12}-\alpha_2 s_{22})]$$
$$K_2=B*[(1+\gamma_2)(s_{12}-\alpha_1 s_{22})+(1+\gamma_1)(s_{12}-\alpha_2 s_{22})] \quad (4.67)$$

substituting for gamma and alpha we get

$$K_1=\frac{F_x}{4\pi}\left[\frac{\frac{s_{12}}{s_{22}}+\alpha_1^{\frac{1}{2}}\alpha_2^{\frac{1}{2}}+\alpha_1^{\frac{1}{2}}+\alpha_2^{\frac{1}{2}}}{\alpha_1^{\frac{1}{2}}+\alpha_2^{\frac{1}{2}}}\right] \quad (4.68)$$

$$K_2=\frac{F_y}{4\pi}\left[\frac{\frac{s_{12}}{s_{22}}\left(2\alpha_1^{\frac{1}{2}}\alpha_2^{\frac{1}{2}}+\alpha_1^{\frac{1}{2}}+\alpha_2^{\frac{1}{2}}\right)-\alpha_1^{\frac{1}{2}}\alpha_2^{\frac{1}{2}}\left(\alpha_1^{\frac{1}{2}}+\alpha_2^{\frac{1}{2}}+\alpha_1+\alpha_2\right)}{\alpha_1^{\frac{1}{2}}\alpha_2^{\frac{1}{2}}(\alpha_1-\alpha_2)}\right] \quad (4.69)$$

Here it has to be noted that K_1 is purely real while K_2 is only conditionally real.

Now adding Eq(4.58) to Eq(4.59) and considering the hole boundary only, we get

$$\sigma_r(\theta)+\sigma_\theta(\theta)=4Re\ (\gamma_1\alpha(\theta)+\gamma_2\beta(\theta)) \quad (4.70)$$

This result is general and can be used in conjunction with any stress conditions on the hole boundary. It has to be stressed that the integrals in Eqs(4.63 & 4.64) only represent the variable part of the stress distribution. Therefore, it is necessary to split any general loading

in two parts, the first is equal to the average of the applied loads while the second is the difference between the total load and the average.

4.8.2. TANGENTIAL STRESS AROUND THE HOLE DUE TO RADIAL STRESS

The results of the general solution given in the previous section will now be used to find a manageable formula for the tangential stresses on the hole boundary due to the action of a radial stress distribution. The stress distributions which will be considered are restricted to those which do not have a resultant in the y direction i.e. $F_y=B=K_2=0$. This restriction means that the load has to be parallel to one of the material planes of symmetry. This is satisfied if the stress distribution is chosen as an even function.

Now assuming the radial load on the hole boundary is given using the function S_r(theta), the average stress S_{ra} and the resulting force F_x can be calculated using the following two equations:

$$S_{ra}=\frac{1}{2\pi}\int_0^{2\pi}S_r(\gamma)d\gamma$$
$$F_x=-a\int_0^{2\pi}S_r(\gamma)\cos(\gamma)d\gamma \qquad (4.71)$$

The solution for the case of a uniform radial stress was given in Green's paper (1945). Evaluating the real part of his formula we get the following contribution of the average stress:

$$\sigma_\theta(\theta)=S_{ra}\frac{(c^2s^2(\alpha_1+\alpha_2-\alpha_1\alpha_2-1)-(\alpha_1^{\frac{1}{2}}+\alpha_2^{\frac{1}{2}})(c^2+\alpha_1^{\frac{1}{2}}\alpha_2^{\frac{1}{2}}s^2)+\alpha_1^{\frac{1}{2}}\alpha_2^{\frac{1}{2}}}{c^4+(\alpha_1+\alpha_2)c^2s^2+\alpha_1\alpha_2} \qquad (4.72)$$

where c is cos(theta) and s is sin(theta).

The hoop stresses due to the variable part of the load can be described using Eqs(4.63 & 4.64). Because the shear on the boundary is assumed to be equal to zero, W will therefore vanish. V, on the boundary of the hole, can be expressed as:

$$V(\theta)=-S_r(\theta)+S_{ra}+iS_{rc}(\theta)$$
$$S_{rc}(\theta)=\frac{1}{2\pi}\int_0^{2\pi}S_r(\gamma)\frac{\sin(\theta-\gamma)}{1-\cos(\theta-\gamma)}d\gamma \qquad (4.73)$$

Therefore, after substituting for $\alpha(z)$ and $\beta(z)$ in Eq(4.70) we get:

$$\sigma_r(\theta)+\sigma_\theta(\theta)=\frac{2K_1}{a}\left[\frac{(\alpha_1^{\frac{1}{2}}+\alpha_2^{\frac{1}{2}})c+i(\alpha_1^{\frac{1}{2}}\alpha_2^{\frac{1}{2}}+1)s}{(c^2-\alpha_1^{\frac{1}{2}}\alpha_2^{\frac{1}{2}}s^2)+ics(\alpha_1^{\frac{1}{2}}+\alpha_2^{\frac{1}{2}})}\right]$$
$$+V(\theta)\left[\frac{(c^2-s^2)(\alpha_1^{\frac{1}{2}}\alpha_2^{\frac{1}{2}}+1)+i2cs(\alpha_1^{\frac{1}{2}}+\alpha_2^{\frac{1}{2}}}{(c^2-\alpha_1^{\frac{1}{2}}\alpha_2^{\frac{1}{2}}s^2)+ics(\alpha_1^{\frac{1}{2}}+\alpha_2^{\frac{1}{2}})}\right] \quad (4.74)$$

The real part of this expression is:

$$\sigma_r(\theta)+\sigma_\theta(\theta)=\frac{2K_1}{a}\left[\frac{c(\alpha_1^{\frac{1}{2}}+\alpha_2^{\frac{1}{2}})}{c^4+c^2s^2(\alpha_1+\alpha_2)+\alpha_1\alpha_2s^4}\right]$$
$$+(S_r(\theta)-S_{ra})\left[\frac{2(\alpha_1+\alpha_2)c^2s^2+\alpha_1^{\frac{1}{2}}\alpha_2^{\frac{1}{2}}+(c^2-s^2)(c^2-\alpha_1\alpha_2s^2)}{c^4+(\alpha_1+\alpha_2)c^2s^2+\alpha_1\alpha_2s^4}\right] \quad (4.75)$$
$$-S_{rc}(\theta)\left[\frac{cs(\alpha_1^{\frac{1}{2}}\alpha_2^{\frac{1}{2}}-1)(\alpha_1^{\frac{1}{2}}+\alpha_2^{\frac{1}{2}})}{c^4+c^2s^2(\alpha_1+\alpha_2)+\alpha_1\alpha_2s^4)}\right]$$

Now solving for hoop stress, adding the contribution from Eq(4.72) and noting that the radial stress is equal to S_r(theta), Eq(4.76) is derived:

$$\sigma_\theta(\theta)=C*F_1(\theta)+S_r(\theta)F_2(\theta)+S_{ra}F_3(\theta)+S_{rc}(\theta)F_4(\theta)$$

$$C=\frac{F_x}{2\pi a}\left[\frac{\frac{S_{12}}{S_{22}}+\alpha_1^{\frac{1}{2}}\alpha_2^{\frac{1}{2}}+\alpha_1^{\frac{1}{2}}+\alpha_2^{\frac{1}{2}}}{\alpha_1^{\frac{1}{2}}+\alpha_2^{\frac{1}{2}}}\right] \quad (4.76)$$

$$F_1(\theta)=\frac{(\alpha_1^{\frac{1}{2}}+\alpha_2^{\frac{1}{2}})c}{c^4+c^2s^2(\alpha_1+\alpha_2)+\alpha_1\alpha_2s^4}$$

$$F_2(\theta)=\frac{\alpha_1^{\frac{1}{2}}\alpha_2^{\frac{1}{2}}+c^2s^2(\alpha_1+\alpha_2-\alpha_1\alpha_2-1)}{c^4+c^2s^2(\alpha_1+\alpha_2)+\alpha_1\alpha_2s^4}$$

$$F_3(\theta) = -\frac{(\alpha_1^{\frac{1}{2}} + \alpha_2^{\frac{1}{2}})(c^2 + s^2\alpha_1^{\frac{1}{2}}\alpha_2^{\frac{1}{2}})}{c^4 + c^2s^2(\alpha_1 + \alpha_2) + \alpha_1\alpha_2 s^4}$$

$$F_4(\theta) = -\frac{cs(\alpha_1^{\frac{1}{2}} + \alpha_2^{\frac{1}{2}})(\alpha_1^{\frac{1}{2}}\alpha_2^{\frac{1}{2}} - 1)}{c^4 + c^2s^2(\alpha_1 + \alpha_2) + \alpha_1\alpha_2 s^4}$$

It should be noted that the quantities $\alpha_1+\alpha_2$ and $\alpha_1\alpha_2$ are real and they are given in Eq(4.55) in terms of the engineering constants of the material. The sum of the roots $\alpha_1^{1/4}+\alpha_2^{1/4}$ can be obtained using the expression:

$$\alpha_1^{1/4} + \alpha_2^{1/4} = \left[\alpha_1 + \alpha_2 + 2(\alpha_1\alpha_2)^{1/2}\right]^{1/4} \qquad \textbf{(4.77)}$$

The product and the sum of the square roots of α is equal to the parameters k and n respectively used in the solutions by Lekhnitskii (1968) if the directions 1 and 2 are chosen appropriately. If the directions are reversed, then the quantities become 1/k and n/k respectively.

The expression given in Eq(4.76) is greatly simplified for quasi-isotropic materials. In this case F_4(theta) becomes zero and therefore

$$\sigma(\theta) = \frac{Fx}{2\pi a}(3-\nu)\cos(\theta) + S_r(\theta) - 2S_{ra} \qquad \textbf{(4.78)}$$

It has to be noted that the resulting expression does not contain the function S_{rc}(theta).

4.8.3. DETERMINING THE FUNCTION S_{rc}:

To calculate the function S_{rc}(theta) which is the imaginary part of the function V on the boundary, it is necessary to evaluate the integral given in Eq(4.73). A closer examination of that integral reveals that it has a singularity when theta equals gamma. This complicates the evaluation of the integral. In order to be able to evaluate the integral using general numerical integration techniques, it is necessary to isolate the singularity. To achieve this, the integrand can be written as:

$$S_r(\gamma)\frac{\sin(\theta-\gamma)}{1-\cos(\theta-\gamma)} = (S_r(\gamma) - D)\frac{\sin(\theta-\gamma)}{1-\cos(\theta-\gamma)} + D\frac{\sin(\theta-\gamma)}{1-\cos(\theta-\gamma)} \qquad \textbf{(4.79)}$$

The constant D has to be chosen such that the first quantity is finite when gamma is equal to theta. L'hospital's rule was applied to that expression and it was found that it became finite only when D was taken equal to S_r(theta). The singular part of the integrand can be integrated in closed form while the first part can be integrated either numerically or analytically.

Exact formulae will now be given for S_{rc}(theta) corresponding to two useful stress distributions. The first is a constant pressure on a part of the boundary extending from -ß to +ß. For this case:

$$S_r(\theta) = -p \qquad if |\theta| < \beta$$

$$S_r(\theta) = 0 \qquad if |\theta| > \beta$$

$$S_{rc}(\theta) = \frac{p}{2\pi} \ln\left[\frac{1-\cos(\theta-\beta)}{1-\cos(\theta+\beta)}\right] \tag{4.80}$$

$$S_{ra} = -p\frac{\beta}{\pi}$$

$$Fx = 2ap\ \sin(\beta)$$

When the radial stress is given as a cosine distribution between -ß and +ß we get:

$$S_r(\theta) = -p\ \cos(\theta) \qquad if |\theta| < \beta$$

$$S_r(\theta) = 0 \qquad if |\theta| > \beta$$

$$S_{rc}(\theta) = \frac{p\ \cos(\theta)}{2\pi} \ln\left[\frac{1-\cos(\theta-\beta)}{1-\cos(\theta+\beta)}\right] - \frac{p\beta}{\pi}\sin(\theta) \tag{4.81}$$

$$S_{ra} = -\frac{p}{\pi}\sin(\beta)$$

$$F_x = pa\left(\beta + \frac{1}{2}\sin(2\beta)\right)$$

These two solutions can be combined together to get the approximate radial stress distribution proposed by Pradhan and Ray (1984). In order to have the possibility of using closed formulae for determining the tangential stresses of a relatively general radial stress, the case where the radial stress is distributed as a cosine function of double the angle is also evaluated.

$$S_r(\theta) = -p\cos(2*\theta) \qquad if|\theta| < \beta$$

$$S_r(\theta) = 0 \qquad if|\theta| > \beta$$

$$S_{r\theta}(\theta) = \frac{p\cos(2*\theta)}{2\pi}\ln\left[\frac{1-\cos(\theta-\beta)}{1-\cos(\theta+\beta)}\right]$$

$$-\frac{p\beta}{\pi}\sin(2*\theta) - \frac{p\sin(\beta)}{\pi}\sin(3*\theta) \qquad (4.82)$$

$$-\frac{p\sin(2*\beta)}{2\pi}\sin(4*\theta)$$

$$S_{r\theta} = -\frac{p}{2\pi}\sin(2*\beta)$$

$$F_x = pa\left[\frac{\sin(3*\beta)}{3} + \sin(\beta)\right]$$

4.8.4. CHECKING THE FORMULA:

To check the correctness of these expressions, the problem of a plate loaded by a cosine distribution on one half of the plate was considered. Solutions for this problem under radial cosine stress distribution for the isotropic case were given by Bickley (1928) and for CFRP laminates by De Jong (1977). The solutions generated using Eq(4.76) are given in Fig(4.90). They were found to be identical to the solutions of De Jong (1977).

For more general contact stresses, the evaluation of the integrals analytically becomes a tedious job. A straight forward alternative is the use of numerical integration. In this work, gaussian 3 point integration was used for each half of the integral. The solutions for the problem given above using numerical integration are compared in Fig(4.91) with the exact solutions. It can be seen that the results are identical except for the discontinuities at the integration points. These discontinuities are due to the indefiniteness of the expressions at these points. It has to be noted, however, that it is possible to evaluate the limit of these expressions using L'hospital's rule to obtain the missing points on the curve.

Zhang and Ueng (1984) presented an approximate solution for the contact stress between an orthotropic plate and a pin. This solution was found to give reasonably accurate results for the frictionless case. Their corresponding hoop stress estimations were unacceptably crude. Therefore, they are replaced with the present exact solution. The solution of Zhang and Ueng (1984) for the radial stresses was rewritten in the following simpler form:

$$\sigma_r = k_1\cos(\theta) + k_3\cos(3*\theta) + k_5\cos(5*\theta)$$

$$k_1 = -\frac{P}{\pi a}\frac{n^2(7k^2+22k+1)+2n(k-\nu_{xy})(13k+7)+10(k-\nu_{xy})^2}{3n^2k(k+4)+n(k-\nu_{xy})(13k+7)+5(k-\nu_{xy})^2}$$

$$k_3 = -\frac{P}{2\pi a}\frac{n^2(13k^2-6k-7)+20n(k-\nu_{xy})(k-1)}{3n^2k(k+4)+n(k-\nu_{xy})(13k+7)+5(k-\nu_{xy})^2} \qquad (4.83)$$

$$k_5 = -\frac{P}{2\pi a}\frac{5n^2(k-1)^2}{3n^2k(k+4)+n(k-\nu_{xy})(13k+7)+5(k-\nu_{xy})^2}$$

Using this approximation, the corresponding hoop stresses were calculated and they are given in Fig(4.92) for the material considered by De Jong (1977). When these results are compared with the results given by De Jong, it was found that the predictions are reasonably accurate Figs(4.93 and 4.94). In these graphs it is interesting to note that the small difference between the correct and the approximate contact stress affects the stress distribution only in the contact area. The general behaviour of both sets of results is similar, but the values obtained are different due to the difference in the contact angle.

The stress distributions obtained by Crews, Hong and Raju (1981) using the finite element method for infinite plates were also compared with the results of the present analysis in Fig(4.95) and Fig(4.96). The comparison revealed that the finite element results were consistently lower than the prediction of the present solution. At first it was thought that this was due to the approximation of the stress distribution, but Fig(4.96) shows that even when the correct radial stresses are used, the peak stresses remain low. This is thought to be due to the finite size of the plates considered in the finite element analysis.

4.8.5. THE EFFECT OF MATERIAL CHANGES

The formula derived above will be used in conjunction with the formula of Zhang and Ueng (1984) to calculate the stresses in infinite plates made from pultruded glass polyester material. The material properties used are those obtained in Chapter 3. This means that it will be composed of a central layer of unidirectional material surrounded by two chopped strand mat layers.

First, the effect of varying the fibre volume fraction in a unidirectional material is investigated. Fig(4.97) shows the radial contact and hoop stresses for fibre volume fractions varying from .5 to .75. for a unidirectional material with the fibres running parallel to the loading direction. It can be seen that the maximum stresses are sensitive to the variation in the

fibre volume fraction in spite of the seemingly constant values of the parameters n, k and v reported in the Chapter 3. The maximum hoop stresses for this case occurred at 90° to the loading direction. This was due to the half circle contact assumption made by Zhang and Ueng (1984). The maximum stresses for the different volume fractions is given in Table(4.10). It is interesting to note that both maximum stresses decrease with increasing the fibre volume fraction. This is in accordance with the fact that both factors k and n decrease with increasing the fibre volume fraction.

Vf	Bearing	Hoop
.5	-1.58543	1.328508
.55	-1.57928	1.308882
.6	-1.56960	1.282861
.65	-1.55625	1.250575
.7	-1.53892	1.211932
.75	-1.51709	1.166587

Table(4.10) Stress values for different volume fractions

This suggests that the increase of the fibre volume fraction will increase the strength of a sufficiently large plate even if the strength of the material of the plate was independent of the fibre volume fraction. Knowing that the longitudinal tensile strength of the material increases with the fibre volume fraction, it becomes clear that the benefits of increasing the fibre content are large.

It has also to be noted that because the increase in the fibre volume fraction decreases the anisotropy of the material, the effect of the edge distance will die out more rapidly than for the case of low fibre volume fraction. This means that the increase in the stress concentration due to shorter edge distances will be less. The correction for finite width, on the other hand, will be needed for larger widths, but the stress concentration of the correction solution will decrease and therefore, the net increase in the hoop stresses is expected to be less.

The stress distribution in a transversely reinforced plate was also investigated. The results for this case are given in Fig(4.98) where it can be seen that the effect of changing the fibre volume fraction on the radial stresses is of the same order as the axial case. The variation of the tangential stresses in the contact area, however, becomes large at an angle equal to 0°. Outside that area, the stresses seem to be unaffected by the variation of the fibre content. It is important to note that the stresses at an angle equal to 90° do not change substantially with the variation of the fibre volume fraction. A summary of the resulting stresses are given in Table(4.11), where the bearing stresses reported there are the maxima; the hoop stresses are

the ones developed at 0°. The positions for the maximum bearing stress are given in the column designated "THET".

Vf	Bearing	Hoop	THET
.5	-1.09738	1.099931	41
.55	-1.09549	1.066969	40
.6	-1.09283	1.024787	39
.65	-1.09007	0.974043	37
.7	-1.08822	0.915179	34
.75	-1.08916	0.848440	29

Table(4.11) Stress values for different volume fractions

It can be seen that the largest stress concentrations correspond to the lower fibre volume fractions. It has to be noted that, in this analysis, the effect of friction was ignored. This effect is expected to reduce the tangential stresses in the contact area. This reduction will be higher for larger fibre volume fractions due to the reduced stiffness of the layer. Noting the high 'transverse' strength of the plate, failure is expected to be on the minimum cross section. This means that the failure load is expected to increase by reducing the fibre volume fraction due to the increased transverse strength of the layer.

Contrary to the previous axial case, the increase in the fibre content is expected to increase the axial distance and decrease the transverse distance which is affected by the load applied through the pin. This means that the stress distributions are expected to be more sensitive to the variation of the edge distance than they are for the width of the plate. This sensitivity, however, will not affect the strength of real joints because the practical edge distances used are larger than the maximum edge distances that affect the stresses.

Finally, a layered plate made up of uniaxial and chopped strand layers is also considered. The parameters considered in this case were the proportion of the uniaxially reinforced layers in the plate, the fibre volume fraction of the uniaxial fibres and the fibre volume fraction of the chopped fibres. The stresses were evaluated for nine different combinations of fibre volume fractions for the layers. The fibre volume fractions considered for the uniaxial layer were .5, .6 and .7. For the chopped strand mat layer, the fibre volume fraction was considered as .1, .3 and .5. The proportion of the uniaxial layers in the plate was taken as 0, .25, .5, .75 and 1. The stresses for each of the layers was calculated using the laminated plate theory. These stresses were calculated even for the cases when the actual plate was made up of only one material. The resulting 'imaginary' stress in the other layer was calculated because it is the limiting value for the stresses that can develop in the layer.

The results of the parametric study are given in Fig(4.99 to 4.107). In these figures, the stresses are normalised using the same stress considered throughout this chapter. This was

considered to be the most suitable way of representation which allows meaningful comparisons to be undertaken.

The increase in the fibre volume fraction of the uniaxial layer results in increasing the stresses in the axial layers. The increase is larger for smaller percentage of uniaxial (Fig(4.99) layers in the plate because of the reduced stiffness of the plate; this is the result of increasing the amount of chopped strand layers in the plate. Therefore, the strains are larger than the strains that would develop if the plate were made entirely of the uniaxial material. The resulting stresses in that layer are therefore larger than those for a plate made of uniaxial material. The opposite is true for the stresses in the chopped strand mat layers, because adding the uniaxial layer results in a reduction of the strains developed in the plate, consequently the stresses are smaller.

The above given trend does not apply to the central contact area when the fibre volume fraction in the uniaxial layer is low while the fibre volume fraction in the chopped strand layer is high. In this case, the tangential stresses in the central part of the contact area in the uniaxial ply decrease and the corresponding stresses in the chopped strand mat layer increase Fig(4.105 to 4.108). This is due to the decrease of the transverse stiffness of the uniaxial layer to a value which is less than the equivalent stiffness in the chopped strand layer.

The use of the laminated plate theory has been a matter of concern for engineers. The main reason for this is the fact that in some cases, this theory results in non zero stresses that develop on the free surfaces of the plies. The results obtained above show that the radial stresses that develop over the separation area in the plies are negligibly small when compared with the corresponding stresses developed in the contact stresses. The shear stresses were also checked and they were found negligible. This shows that the use of the laminated plate theory for the material under consideration is justified.

The error in the radial stresses was found to increase with an increase in the fibre volume fraction of the chopped strand mat layers. This is the result of increasing the effect of the properties of these layers on the material parameters of the plate and therefore the difference between the constituent plies and the plate. The decrease of the fibre volume fraction of the uniaxial layer also increases the error due to the increased anisotropy of the uniaxial layer resulting in higher difference between the properties of the plies and the plate. The same effect is emphasised when the percentage of the uniaxial layers is increased.

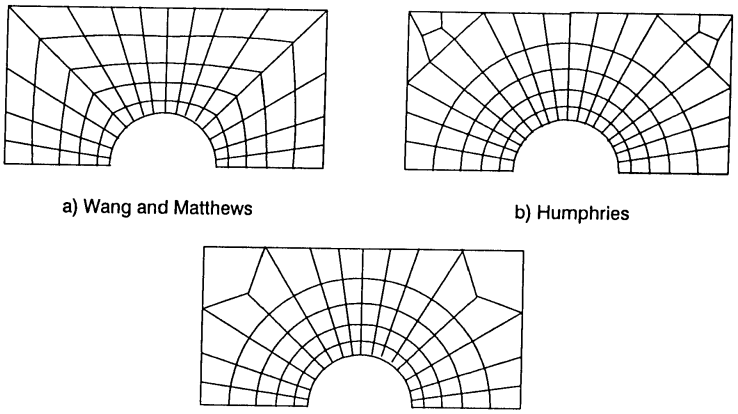

a) Wang and Matthews

b) Humphries

c) Mahajereen and Agrawal

Fig(4.1) Basic Meshing Approaches

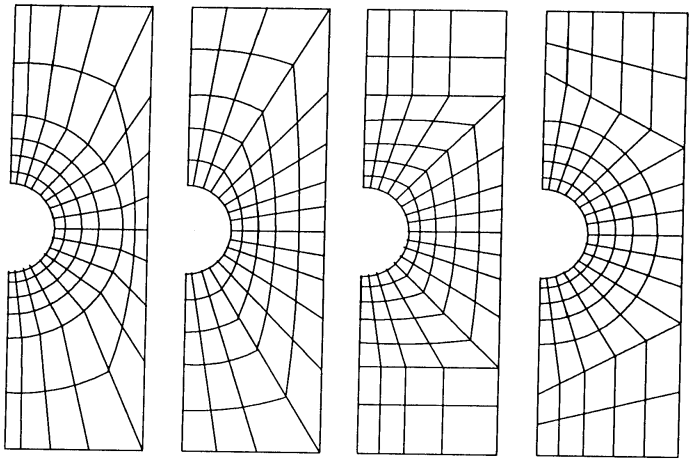

a) b) c) d)

Fig (4.2) Different Applications of the Meshing Strategy

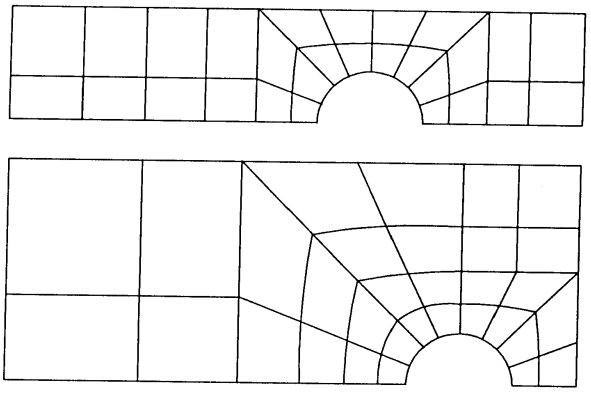

Fig (4.3) The Recommended Meshing Technique

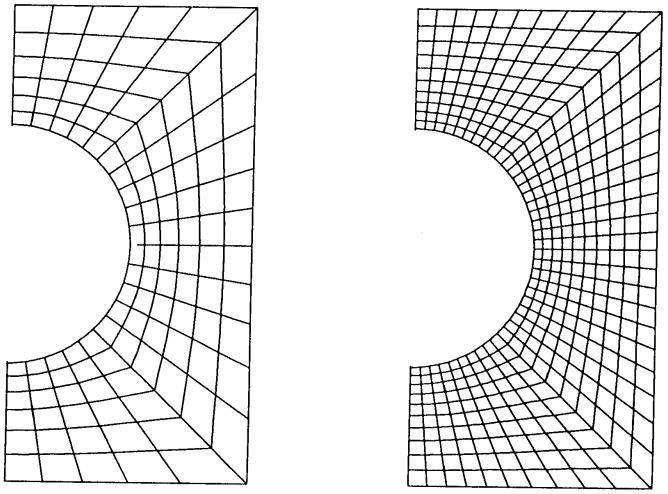

Fig(4.4) The Mesh Densities Considered

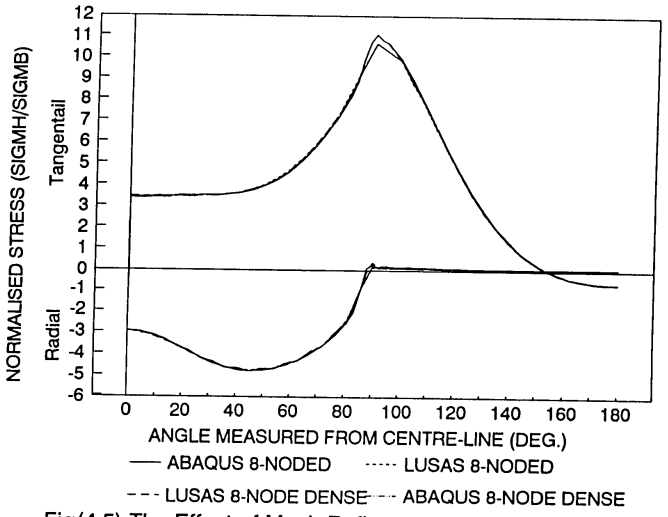

Fig(4.5) The Effect of Mesh Refinement on the Stresses

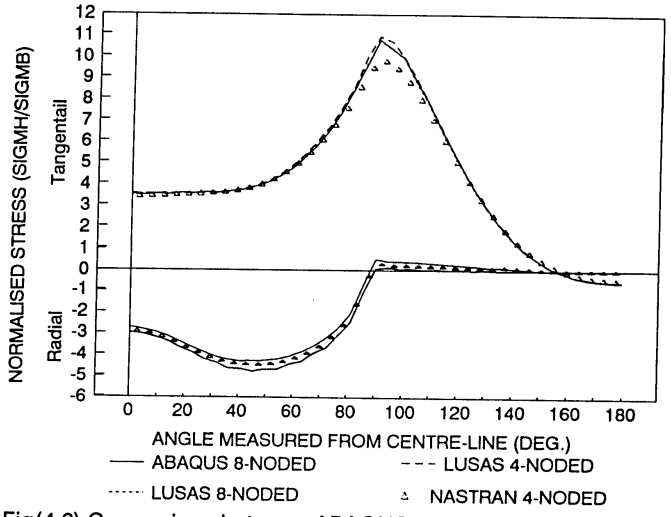

Fig(4.6) Comparison between ABAQUS, NASTRAN and LUSAS

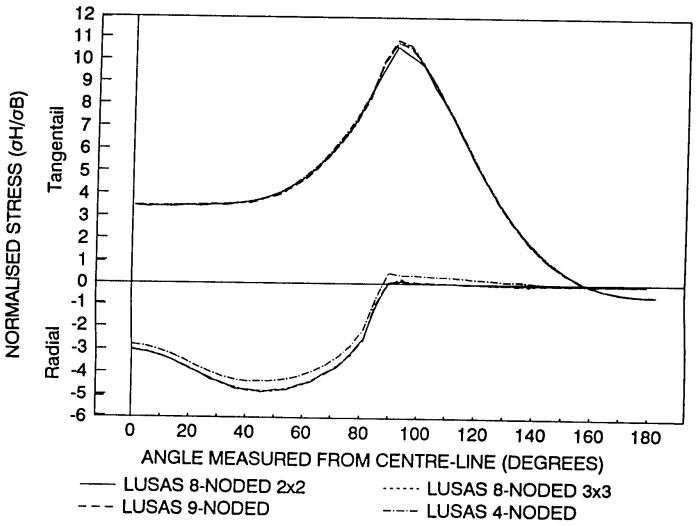

Fig(4.7) The Effect of the Type of Element on the Stresses

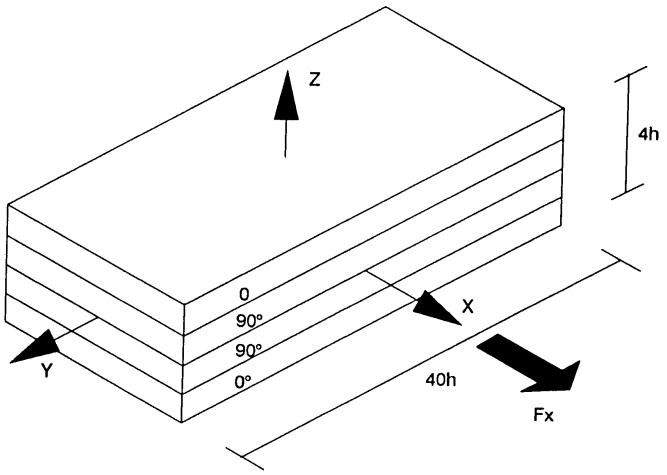

Fig(4.8) The Test Problem

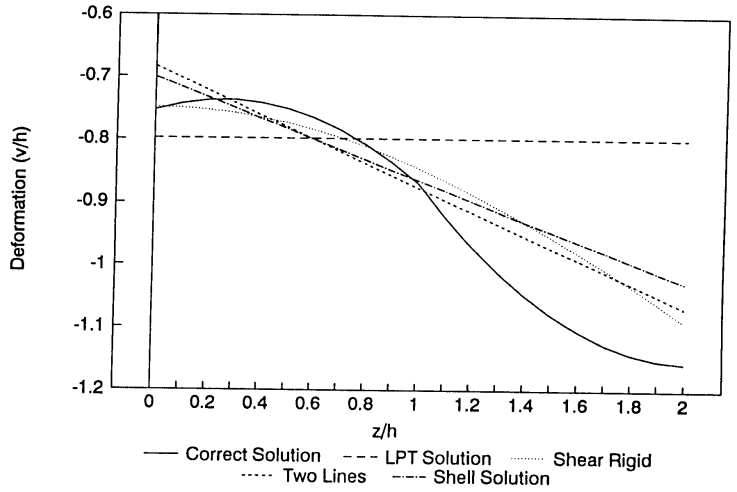

Fig(4.9) Deformations of the Edge

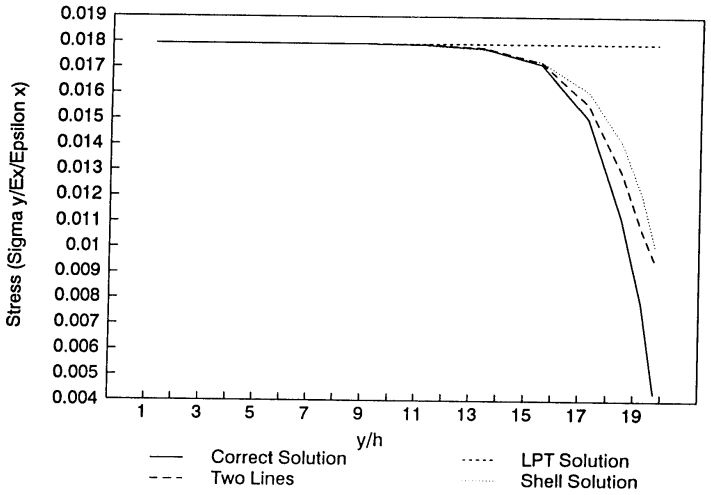

Fig(4.10) The Stress in the 'Y' Direction

Fig(4.11) The Geometries and Meshes Considered

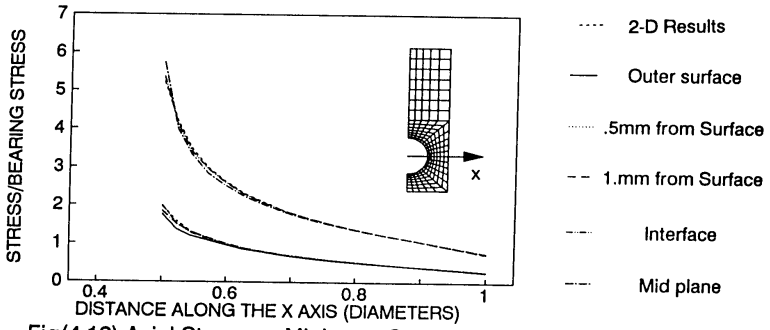

Fig(4.12) Axial Stress on Minimum Cross Section for Specimen TS

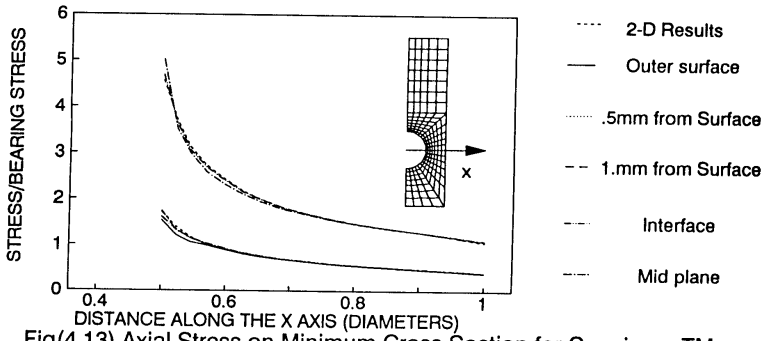

Fig(4.13) Axial Stress on Minimum Cross Section for Specimen TM

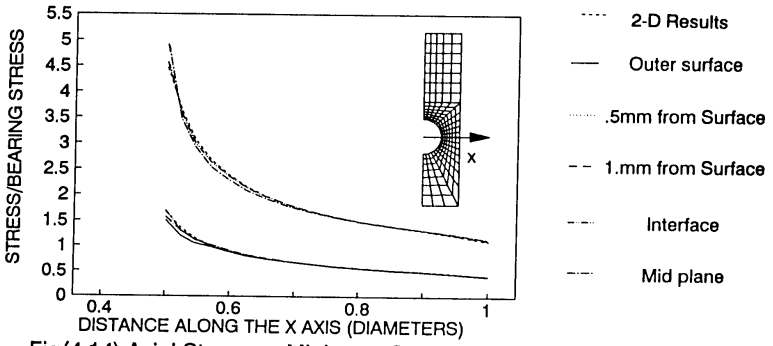

Fig(4.14) Axial Stress on Minimum Cross Section for Specimen TL

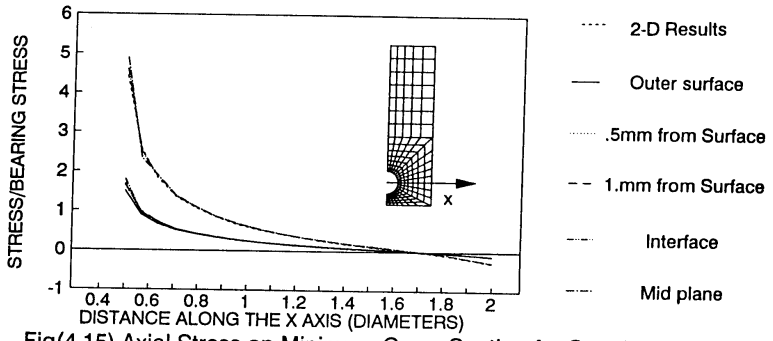

Fig(4.15) Axial Stress on Minimum Cross Section for Specimen MS

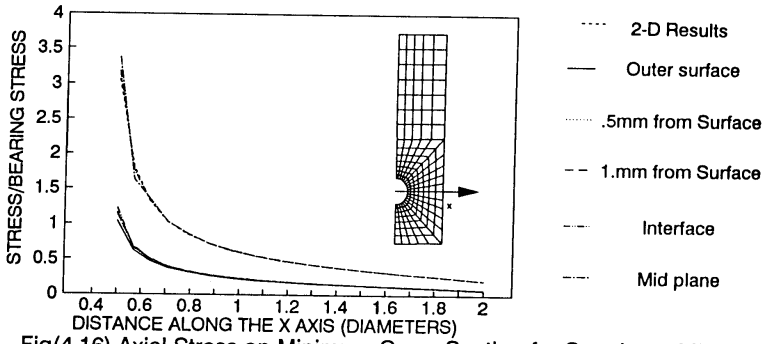

Fig(4.16) Axial Stress on Minimum Cross Section for Specimen MM

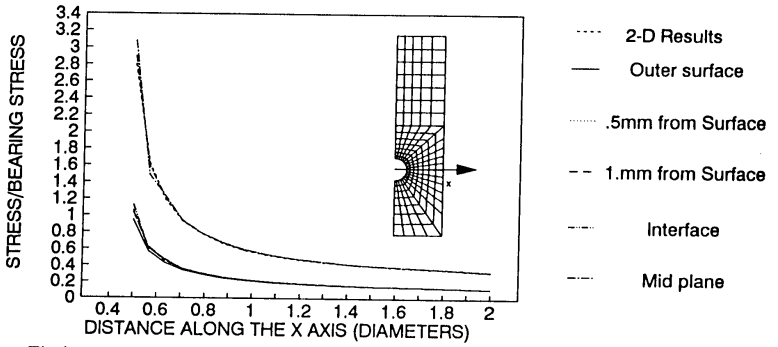

Fig(4.17) Axial Stress on Minimum Cross Section for Specimen ML

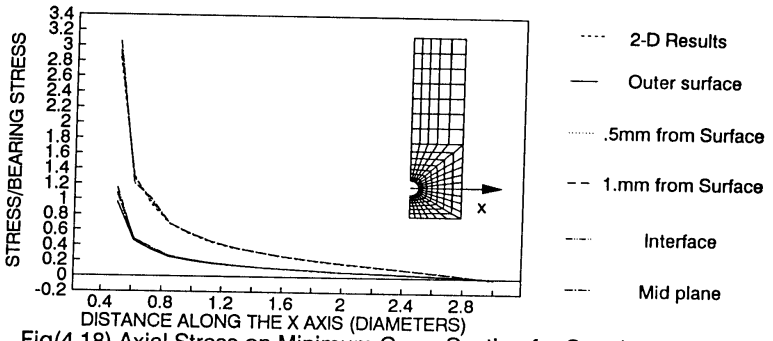

Fig(4.18) Axial Stress on Minimum Cross Section for Specimen WS

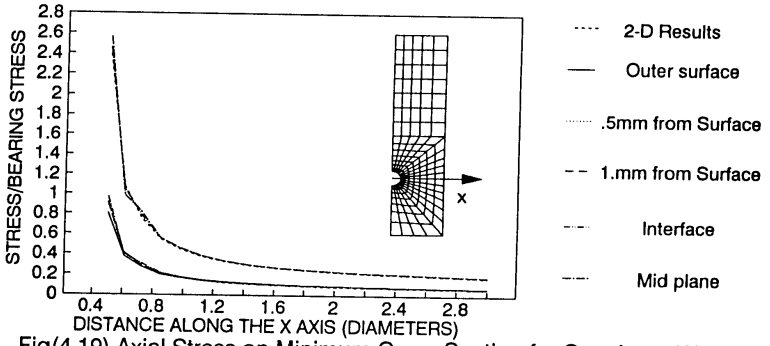

Fig(4.19) Axial Stress on Minimum Cross Section for Specimen WM

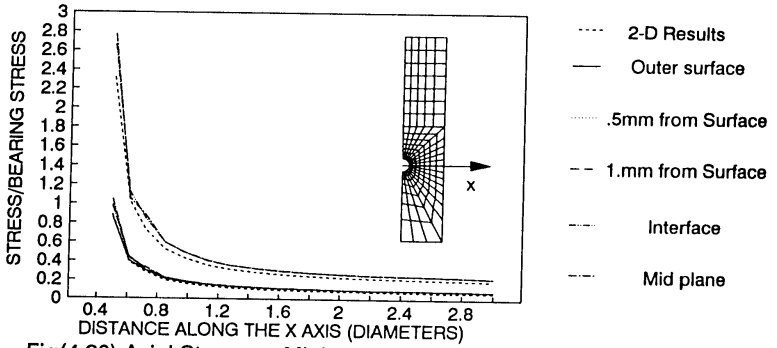

Fig(4.20) Axial Stress on Minimum Cross Section for Specimen WL

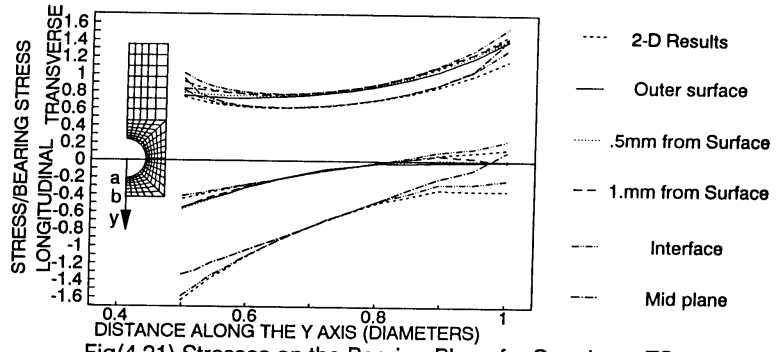

Fig(4.21) Stresses on the Bearing Plane for Specimen TS

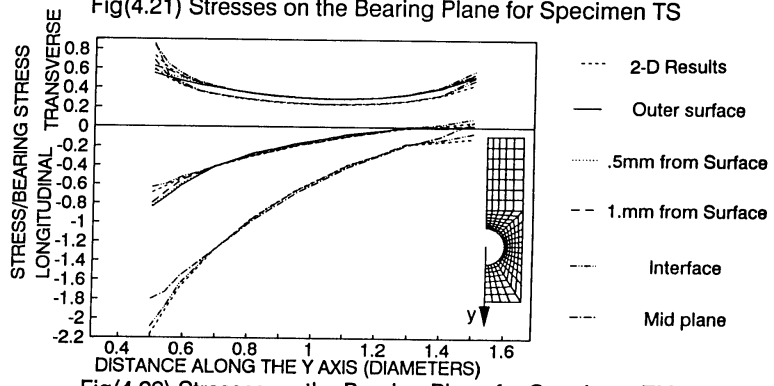

Fig(4.22) Stresses on the Bearing Plane for Specimen TM

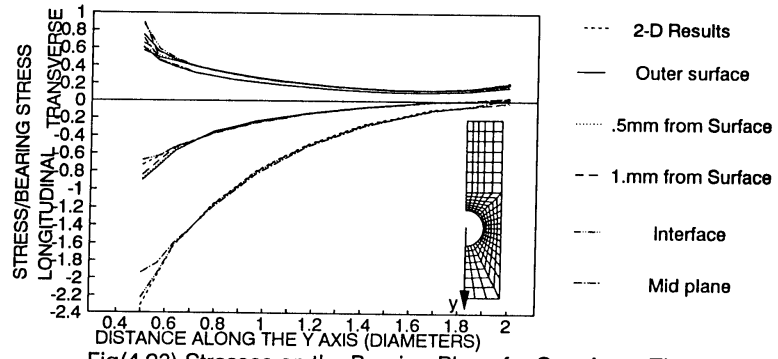

Fig(4.23) Stresses on the Bearing Plane for Specimen TL

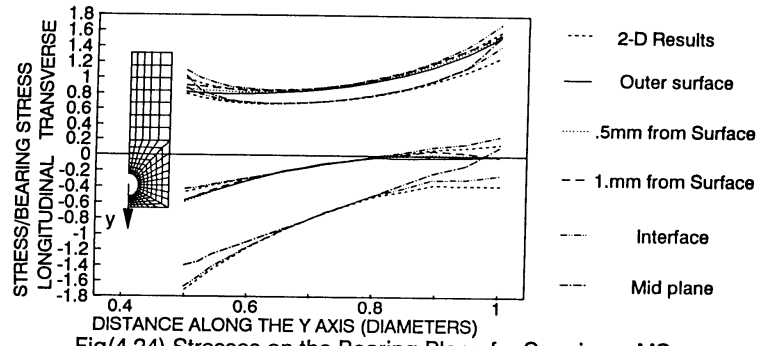

Fig(4.24) Stresses on the Bearing Plane for Specimen MS

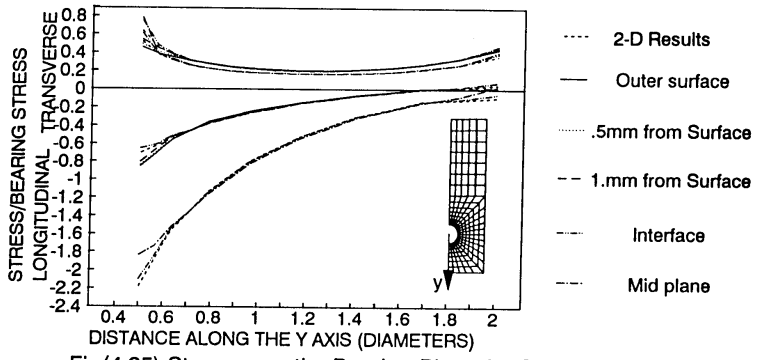

Fig(4.25) Stresses on the Bearing Plane for Specimen MM

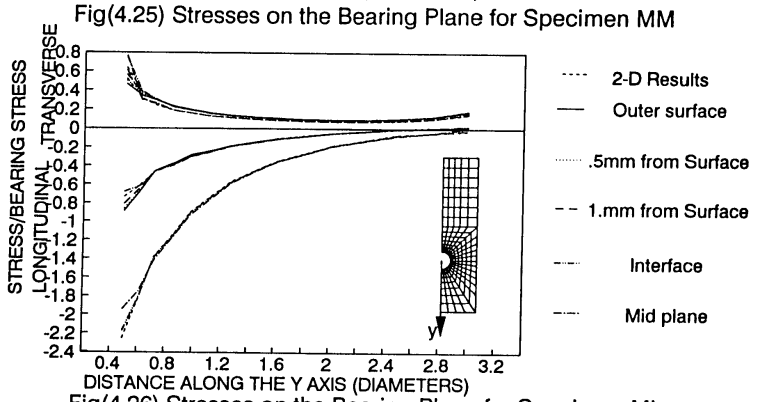

Fig(4.26) Stresses on the Bearing Plane for Specimen ML

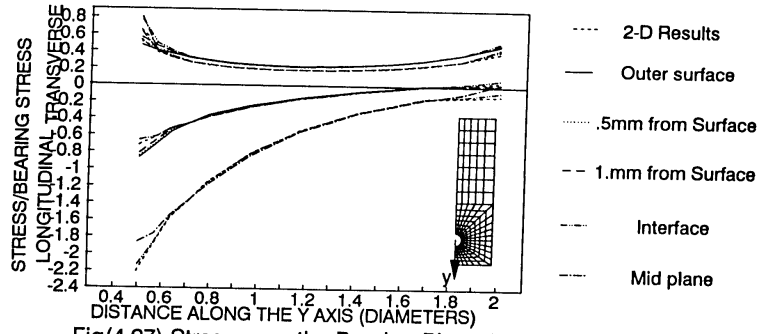

Fig(4.27) Stresses on the Bearing Plane for Specimen WS

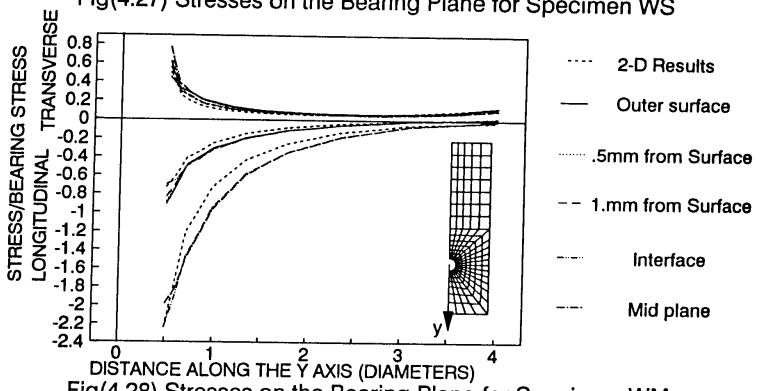

Fig(4.28) Stresses on the Bearing Plane for Specimen WM

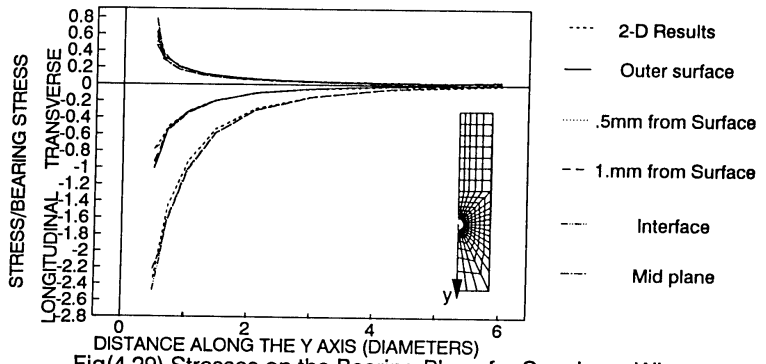

Fig(4.29) Stresses on the Bearing Plane for Specimen WL

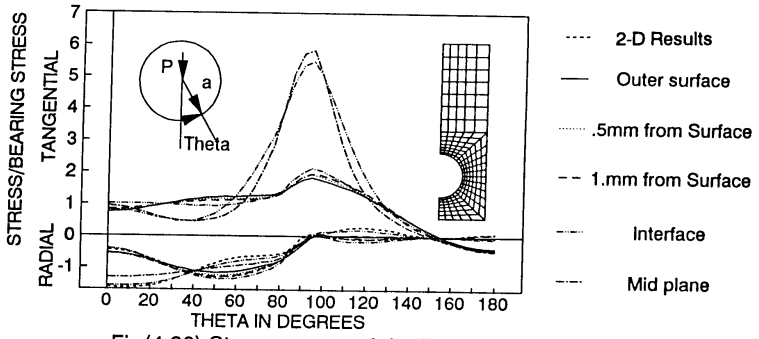

Fig(4.30) Stresses around the Hole for Specimen TS

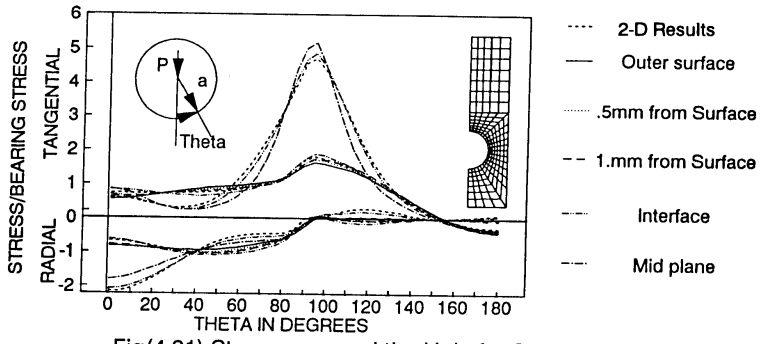

Fig(4.31) Stresses around the Hole for Specimen TM

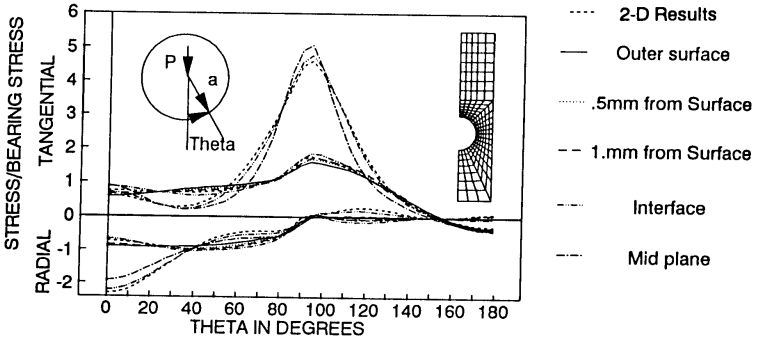

Fig(4.32) Stresses around the Hole for Specimen TL

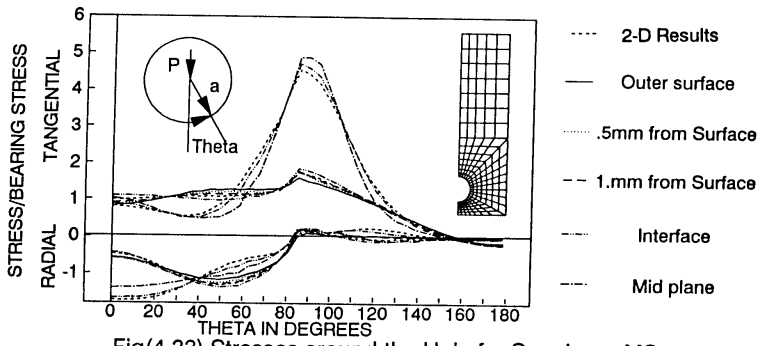

Fig(4.33) Stresses around the Hole for Specimen MS

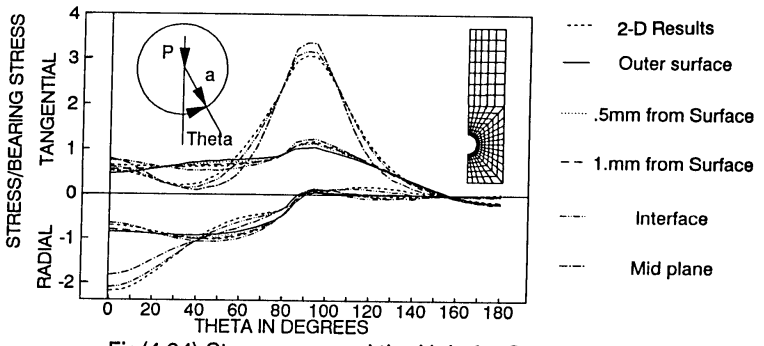

Fig(4.34) Stresses around the Hole for Specimen MM

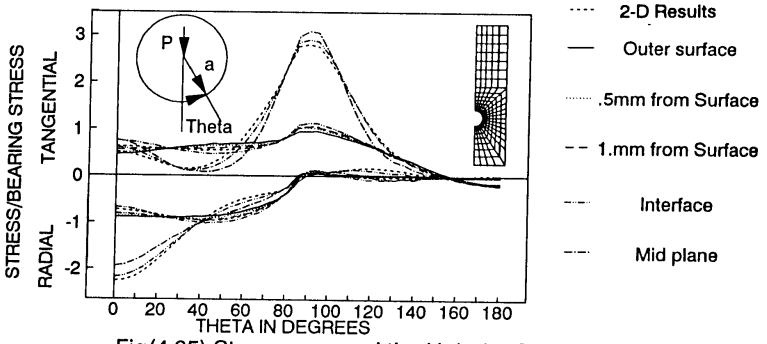

Fig(4.35) Stresses around the Hole for Specimen ML

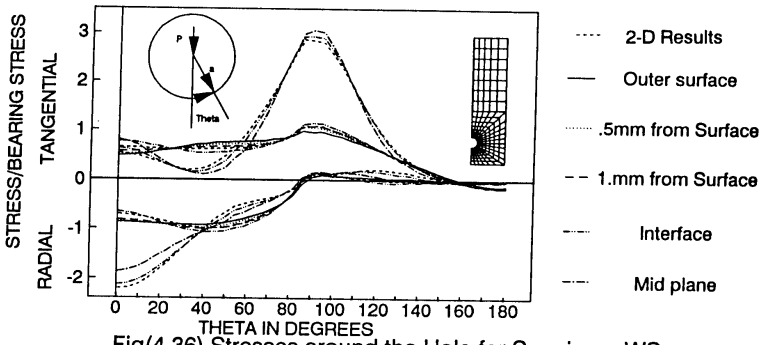

Fig(4.36) Stresses around the Hole for Specimen WS

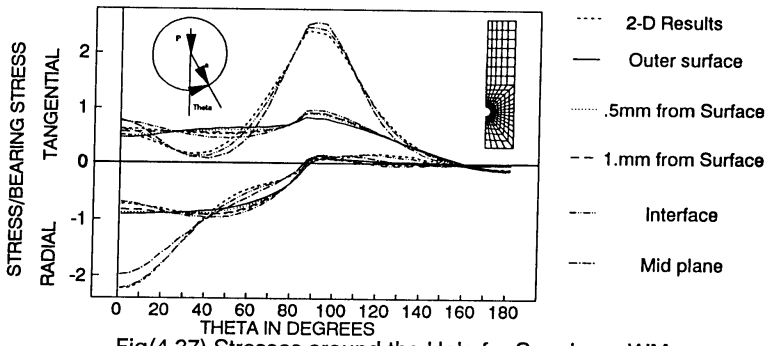

Fig(4.37) Stresses around the Hole for Specimen WM

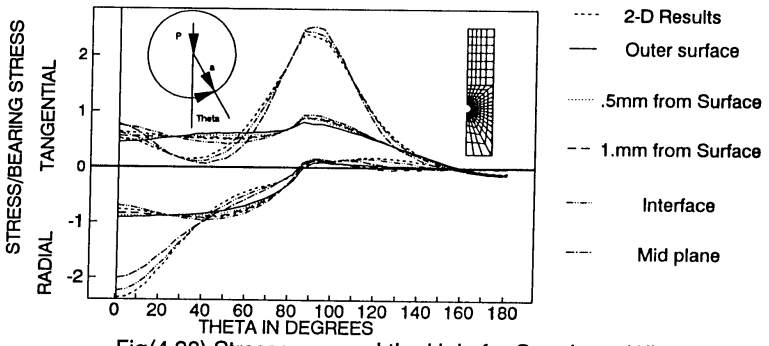

Fig(4.38) Stresses around the Hole for Specimen WL

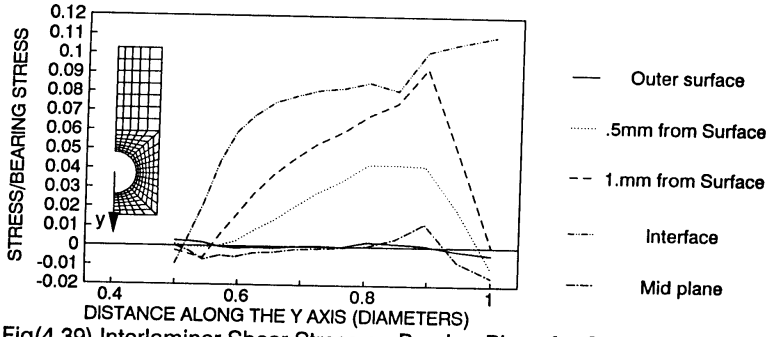

Fig(4.39) Interlaminar Shear Stress on Bearing Plane for Specimen TS

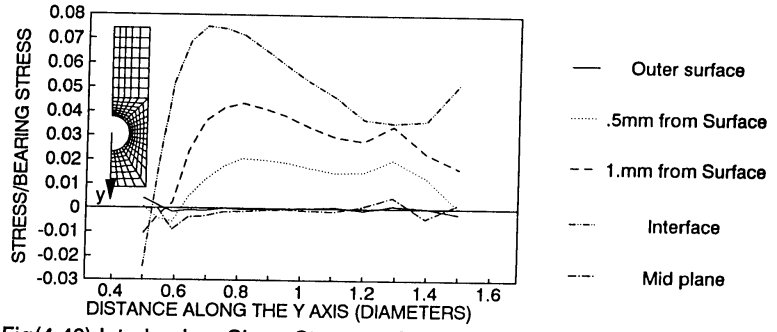

Fig(4.40) Interlaminar Shear Stress on Bearing Plane for Specimen TM

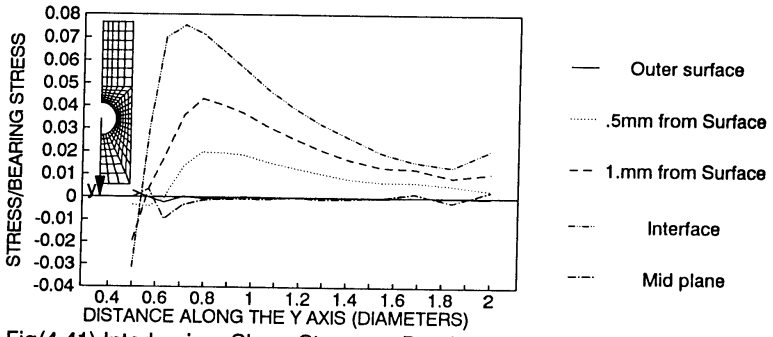

Fig(4.41) Interlaminar Shear Stress on Bearing Plane for Specimen TL

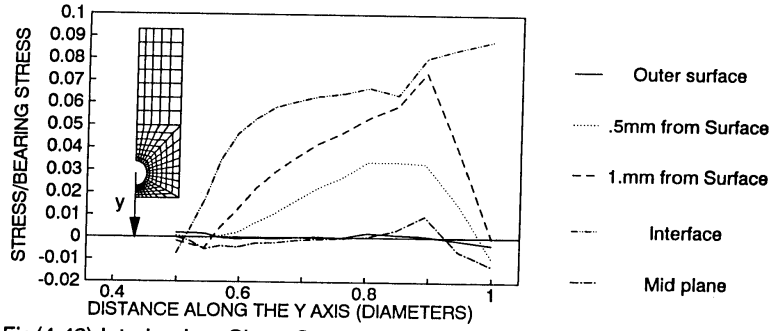

Fig(4.42) Interlaminar Shear Stress on Bearing Plane for Specimen MS

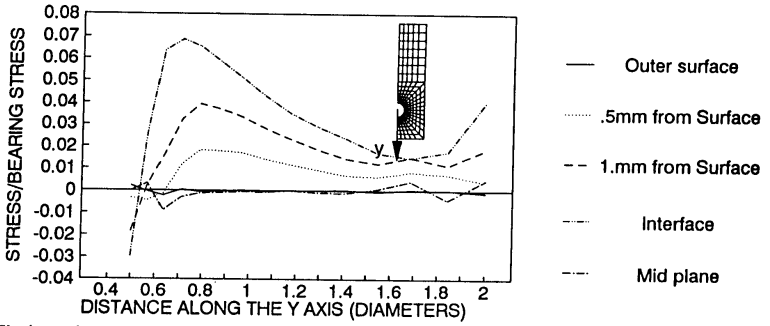

Fig(4.43) Interlaminar Shear Stress on Bearing Plane for Specimen MM

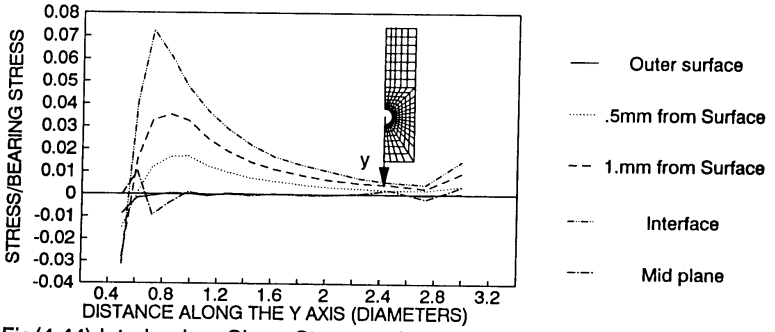

Fig(4.44) Interlaminar Shear Stress on Bearing Plane for Specimen ML

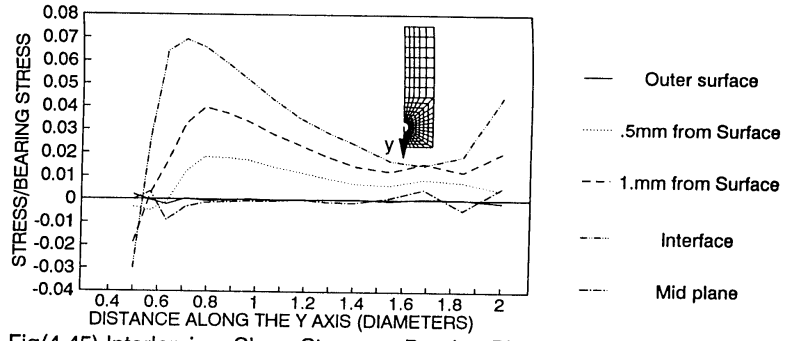

Fig(4.45) Interlaminar Shear Stress on Bearing Plane for Specimen WS

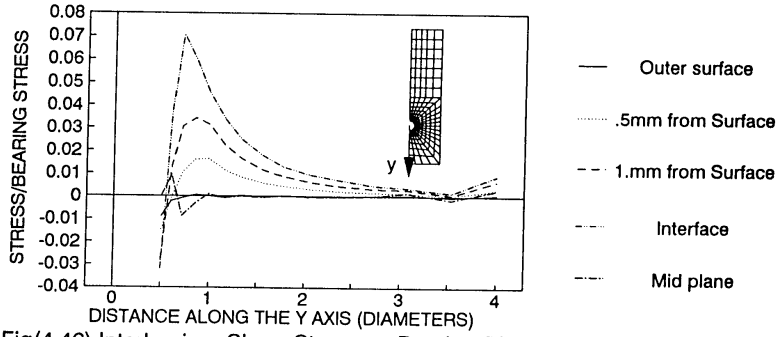

Fig(4.46) Interlaminar Shear Stress on Bearing Plane for Specimen WM

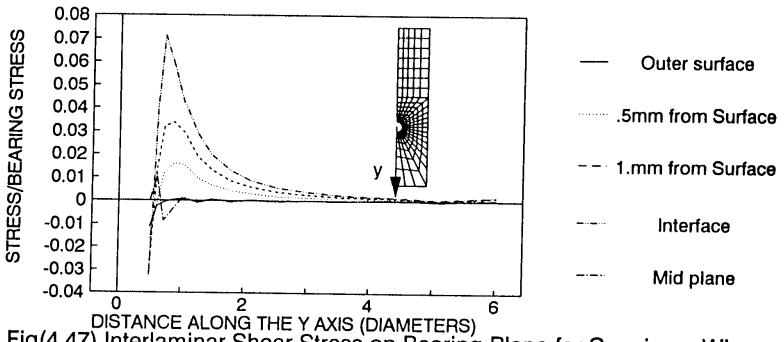

Fig(4.47) Interlaminar Shear Stress on Bearing Plane for Specimen WL

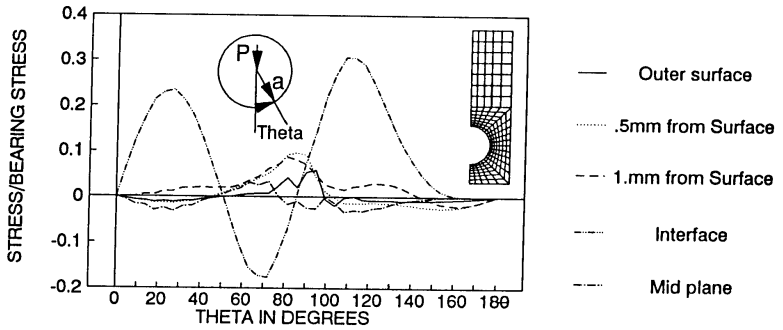

Fig(4.48) Tangential Interlaminar Shear Stress for Specimen TS

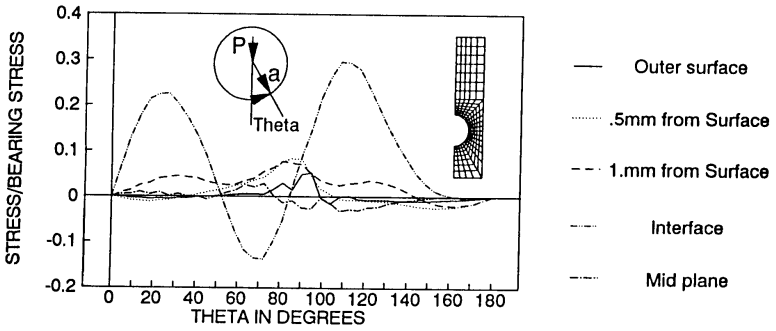

Fig(4.49) Tangential Interlaminar Shear Stress for Specimen TM

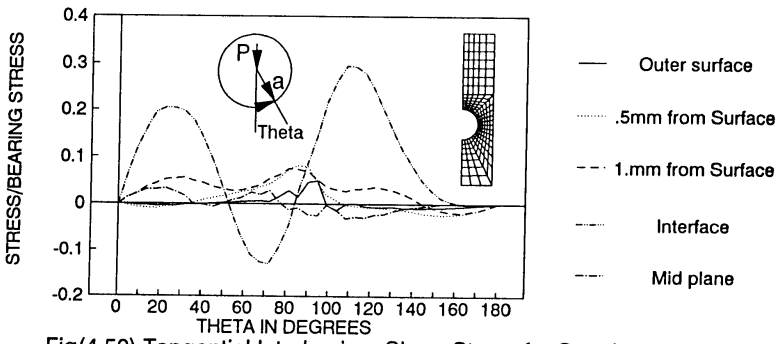

Fig(4.50) Tangential Interlaminar Shear Stress for Specimen TL

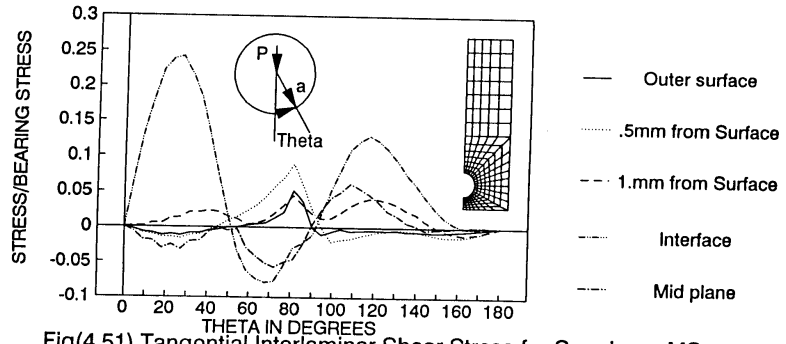

Fig(4.51) Tangential Interlaminar Shear Stress for Specimen MS

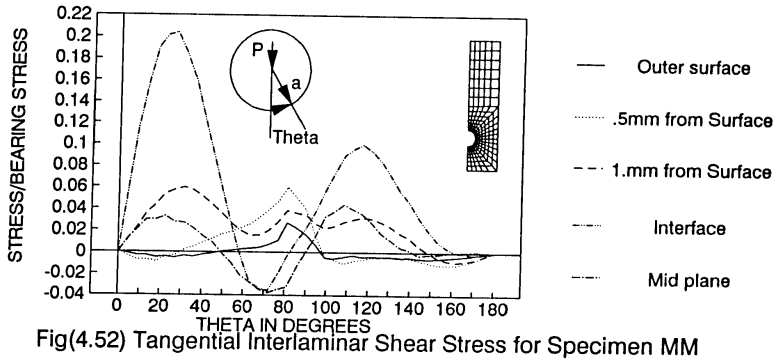

Fig(4.52) Tangential Interlaminar Shear Stress for Specimen MM

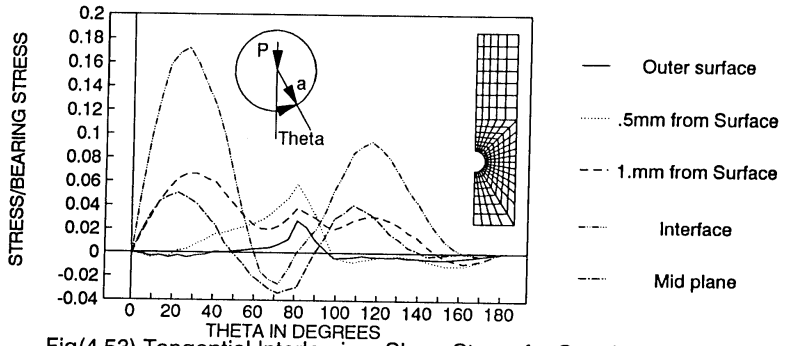

Fig(4.53) Tangential Interlaminar Shear Stress for Specimen ML

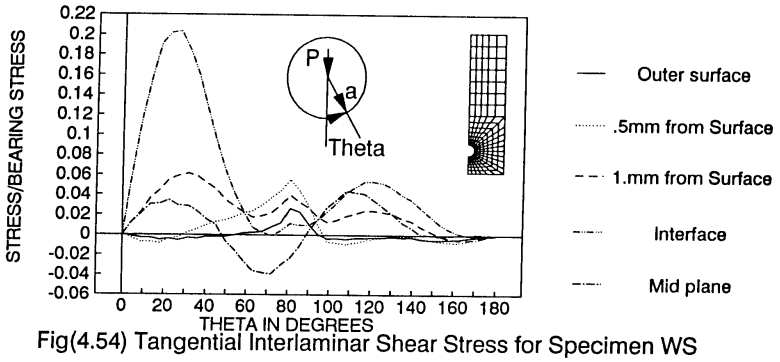

Fig(4.54) Tangential Interlaminar Shear Stress for Specimen WS

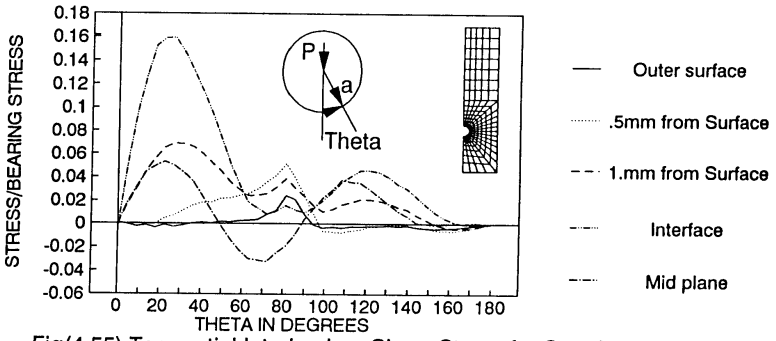

Fig(4.55) Tangential Interlaminar Shear Stress for Specimen WM

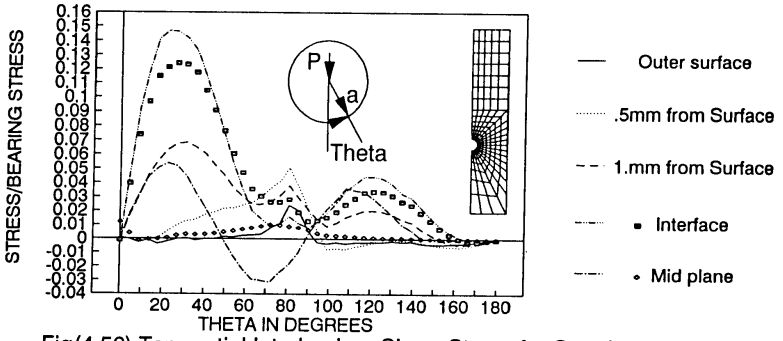

Fig(4.56) Tangential Interlaminar Shear Stress for Specimen WL

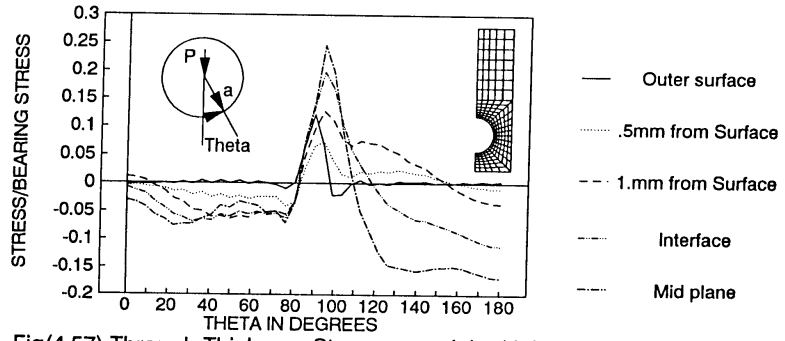

Fig(4.57) Through Thickness Stress around the Hole for Specimen TS

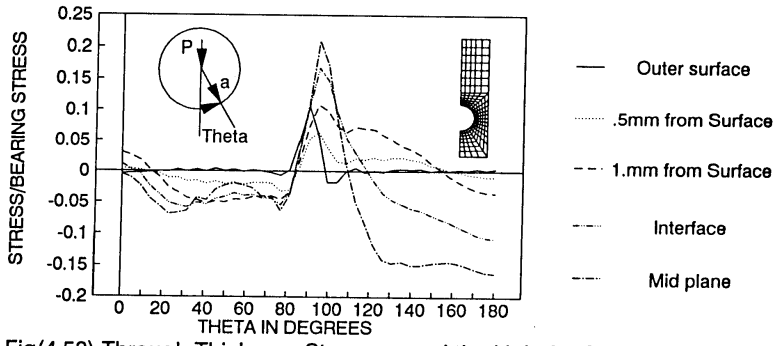

Fig(4.58) Through Thickness Stress around the Hole for Specimen TM

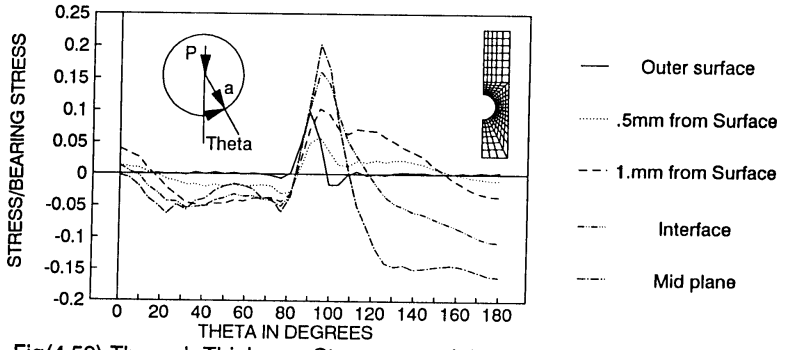

Fig(4.59) Through Thickness Stress around the Hole for Specimen TL

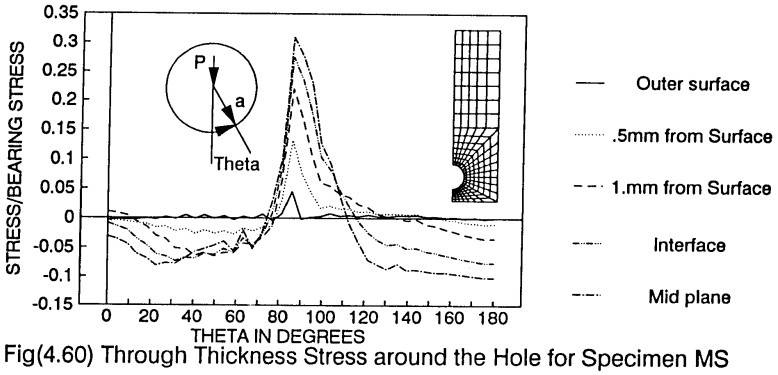

Fig(4.60) Through Thickness Stress around the Hole for Specimen MS

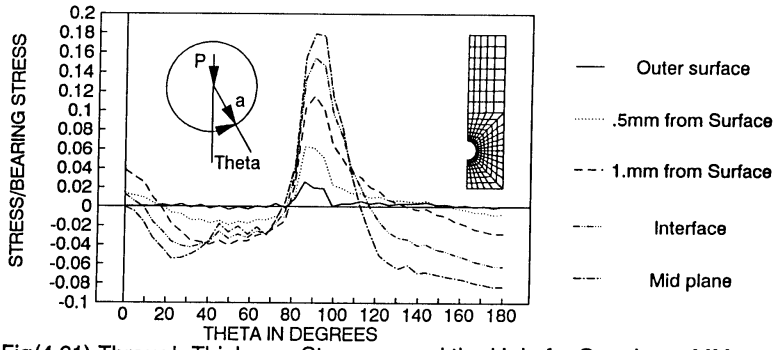

Fig(4.61) Through Thickness Stress around the Hole for Specimen MM

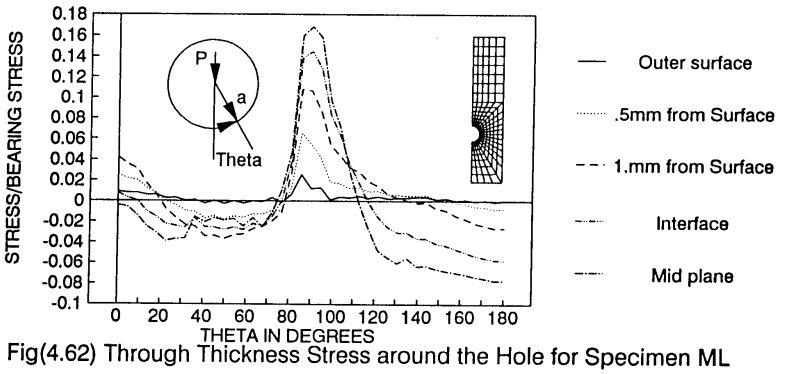

Fig(4.62) Through Thickness Stress around the Hole for Specimen ML

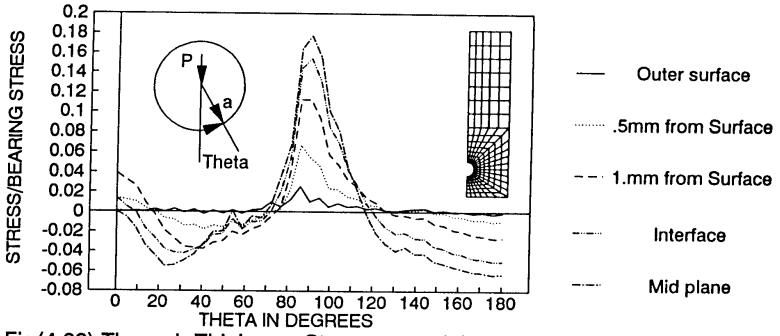

Fig(4.63) Through Thickness Stress around the Hole for Specimen WS

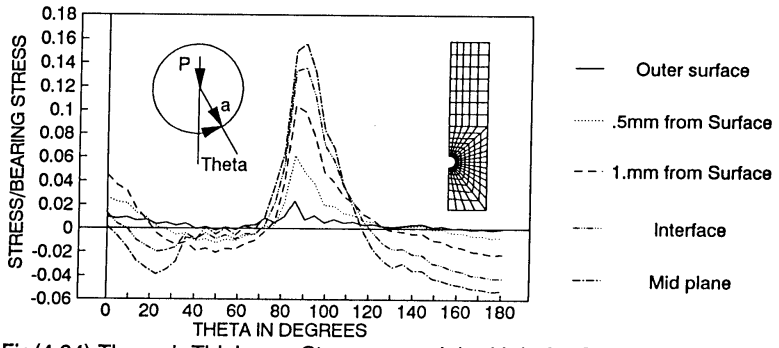

Fig(4.64) Through Thickness Stress around the Hole for Specimen WM

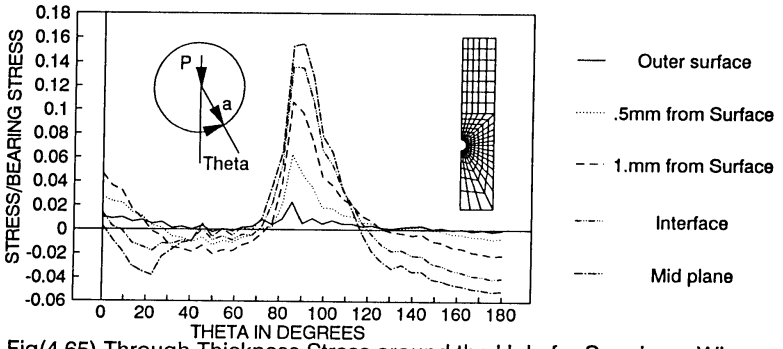

Fig(4.65) Through Thickness Stress around the Hole for Specimen WL

Fig(4.66) The Mesh used for the Non-linear Analysis

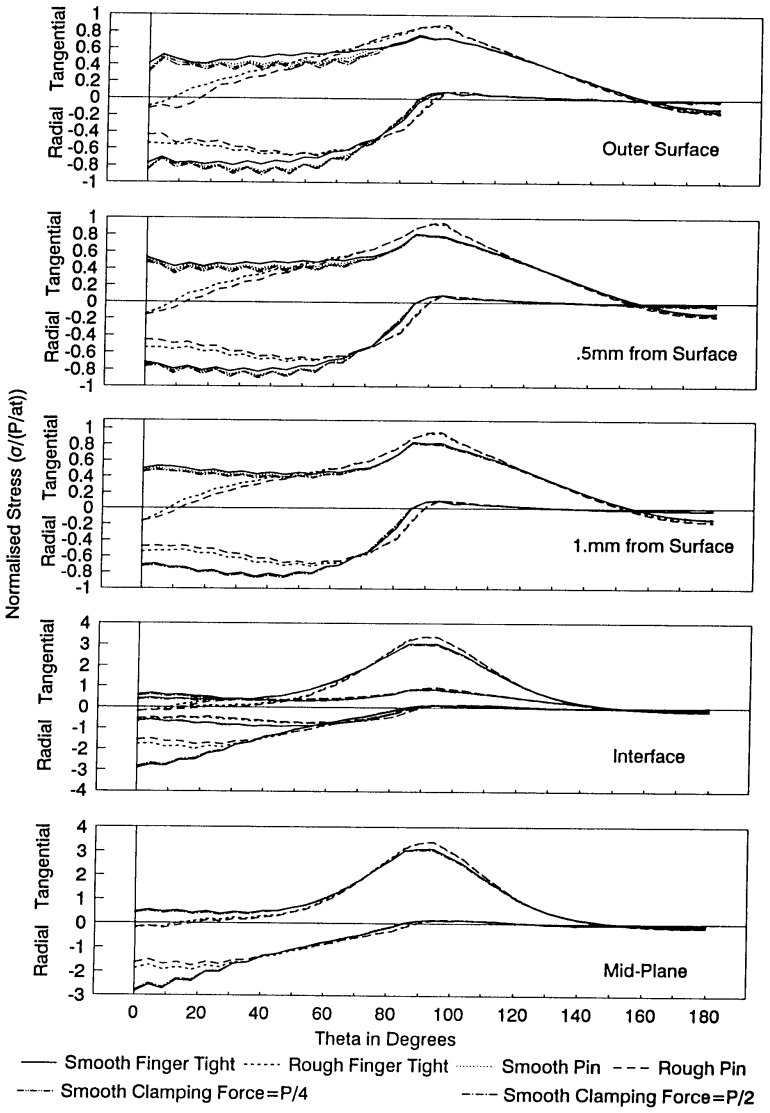

Fig(4.67) The Effect of the Washer on the In-plane Stresses

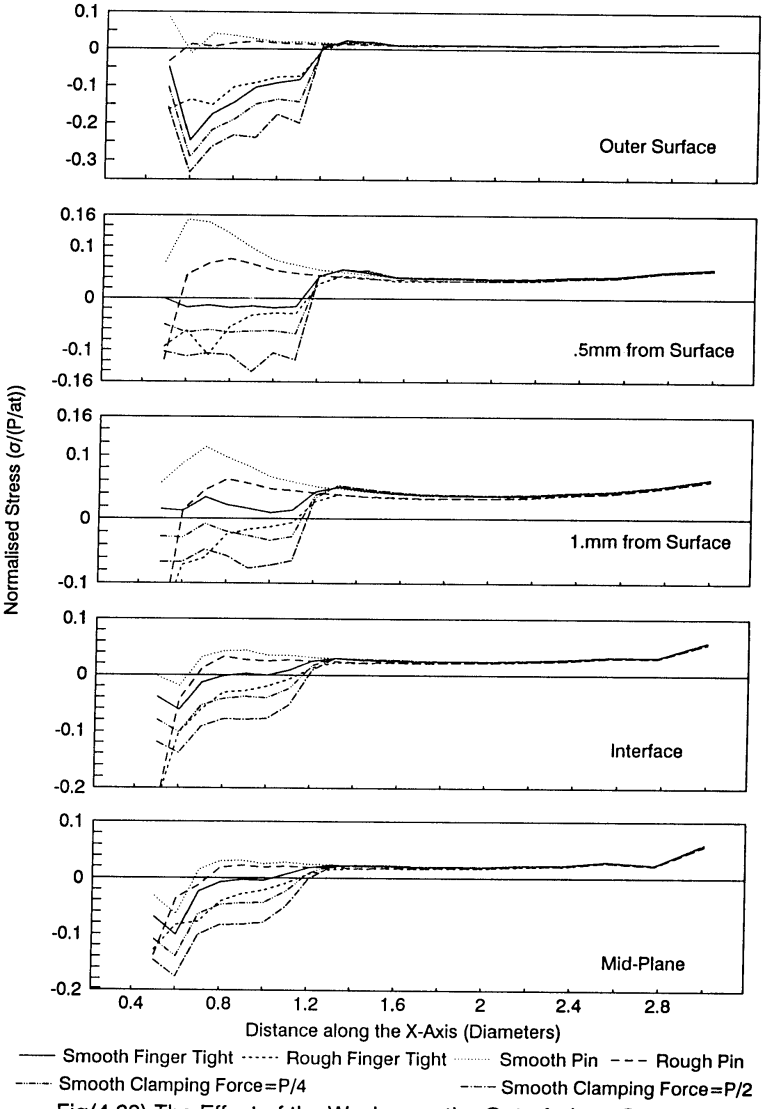

Fig(4.68) The Effect of the Washer on the Out-of-plane Stresses

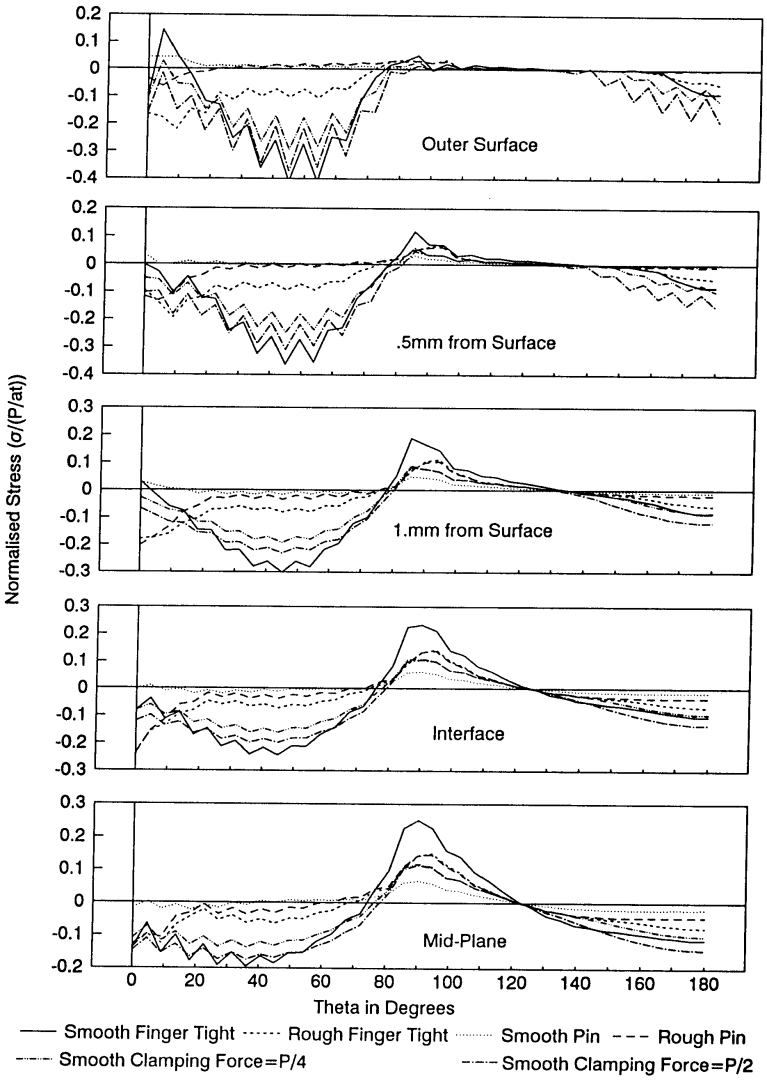

Fig(4.69) The Effect of the Washer on the Out-of-plane Stresses around the Hole

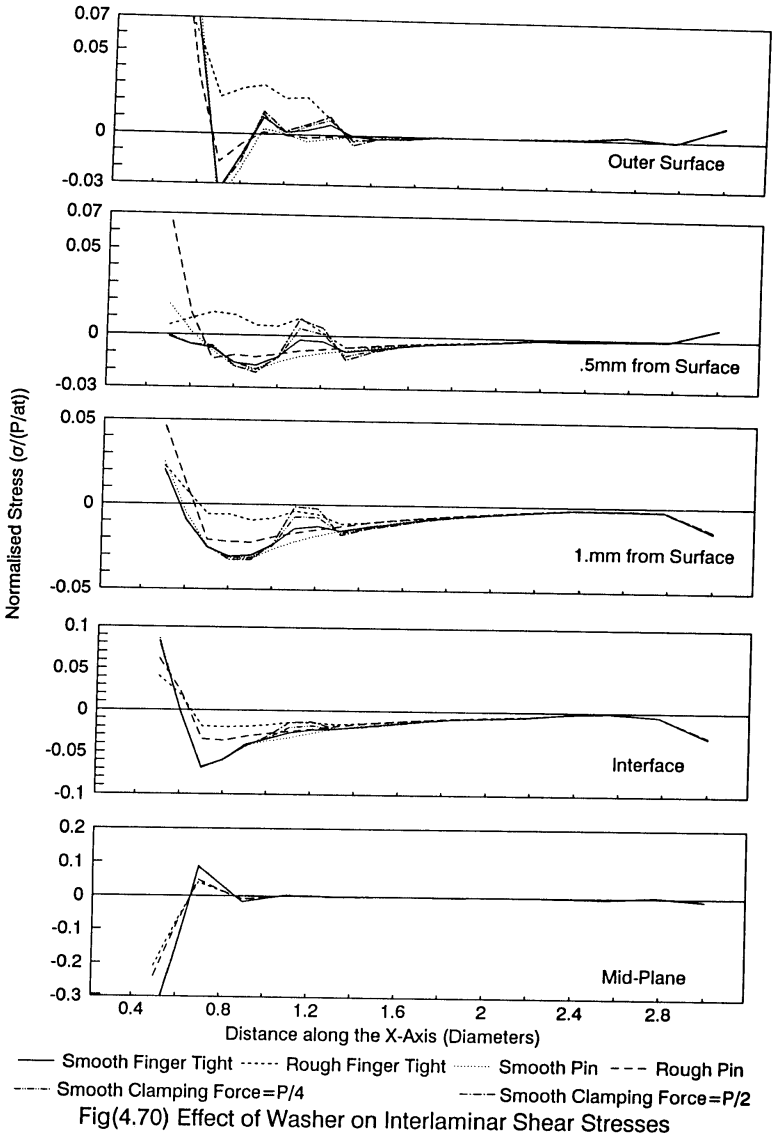

Fig(4.70) Effect of Washer on Interlaminar Shear Stresses

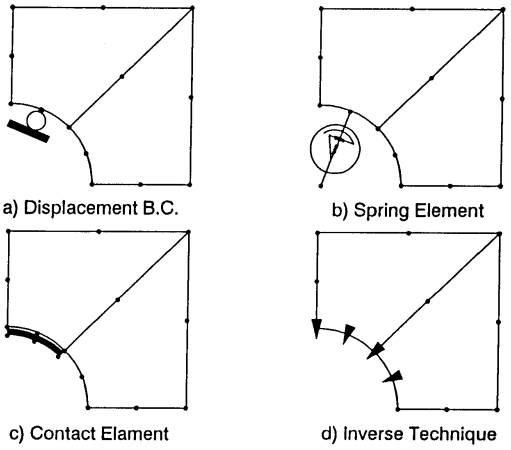

Fig(4.71) Methods of Modelling a Rigid Pin

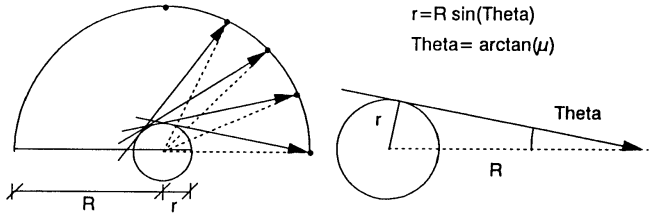

Fig(4.72) Simplified Method for considering Friction

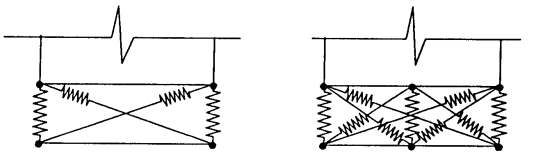

Fig(4.73) Spring Elements equivalent to the Contact Elements

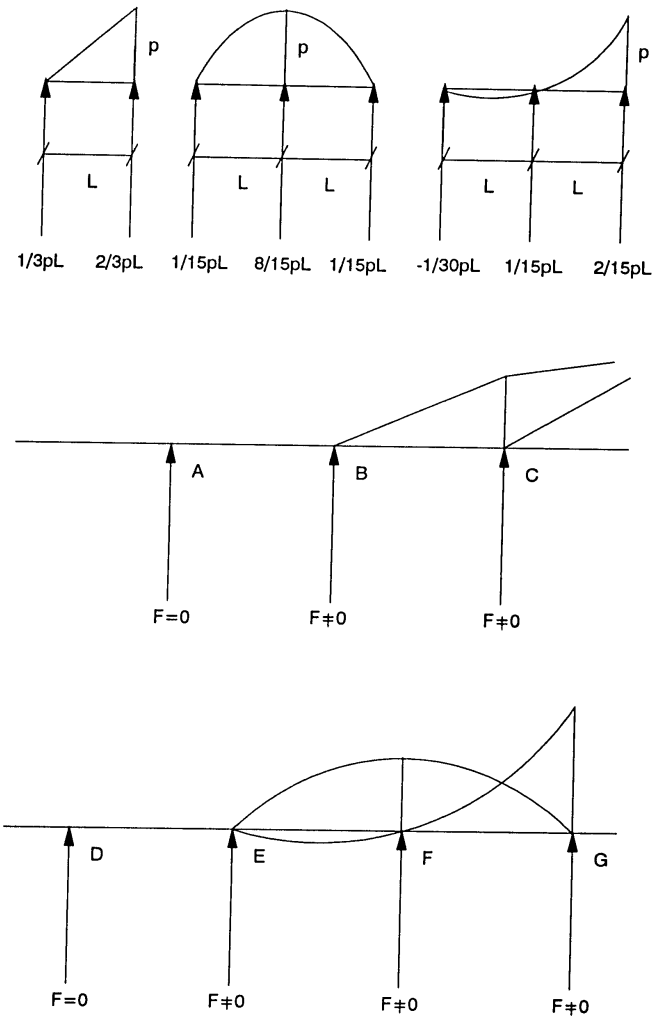

Fig(4.74) The Effect of Assuming Zero Radial Forces

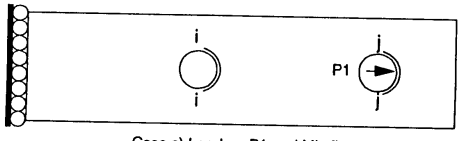

Case a) Load on P1 and Mis-fit

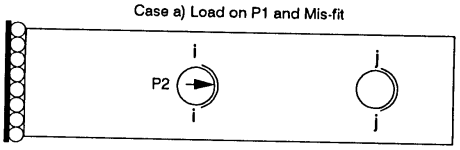

Case b) Load on P2 and Mis-fit

P1 and P2 result in zero radial stress at points I and j

Fig(4.75) The Use of the Inverse Technique for Two Pin Loading

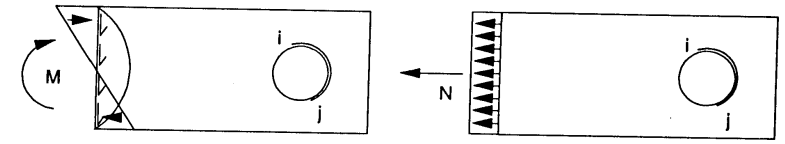

Case a) Bending and Radial Mis-fit Effect

Case b) Axial and Mis-fit Effect

(The shear considered is the internal shear of a continious plate)
M and N are chosen such that the radial stress at I and j is zero

Fig(4.76) The Invesre Technique for Combined Axial and Bending Load

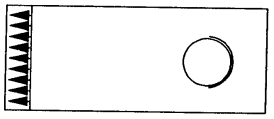

The magnitude of the different shear distributions is obtained using the Least Squares Technique

Case a) Axial and Misfit case

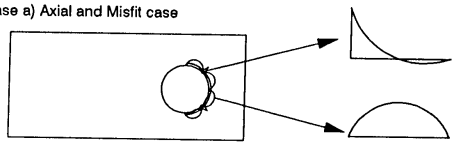

Other Cases: Prescribed shear stresses

Fig(4.77) The Invesre Technique Considering the Effect of Friction

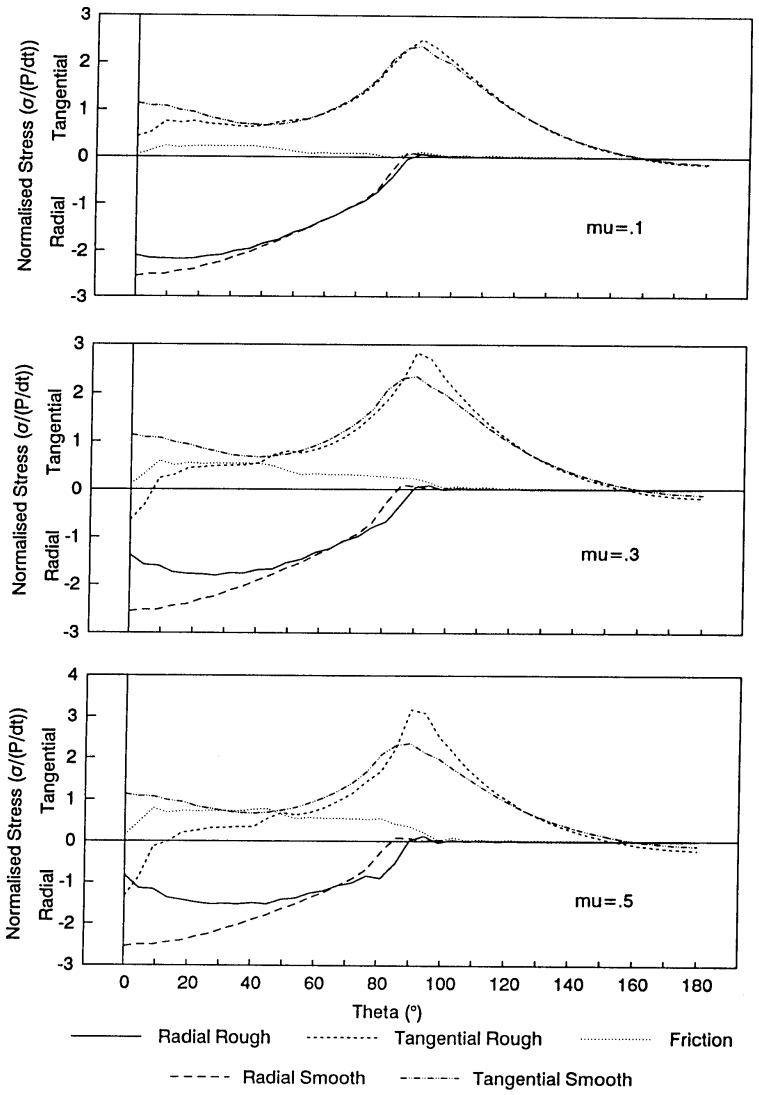

Fig(4.78) The Effect of Friction on In-plane Stresses

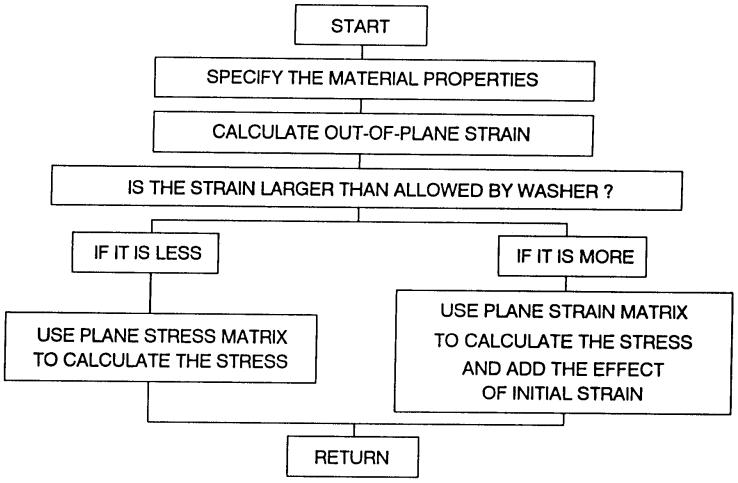

Fig(4.79) Flow Chart for Subroutine WASHER

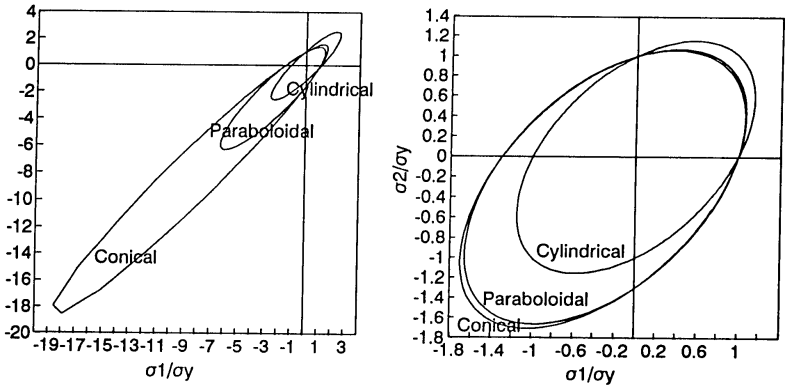

Plane Strain Condition
ν=.3

Plane Stress Condition

σc/σt=1.3

Fig(4.80) The Yield Surfaces Considered for the Polymer

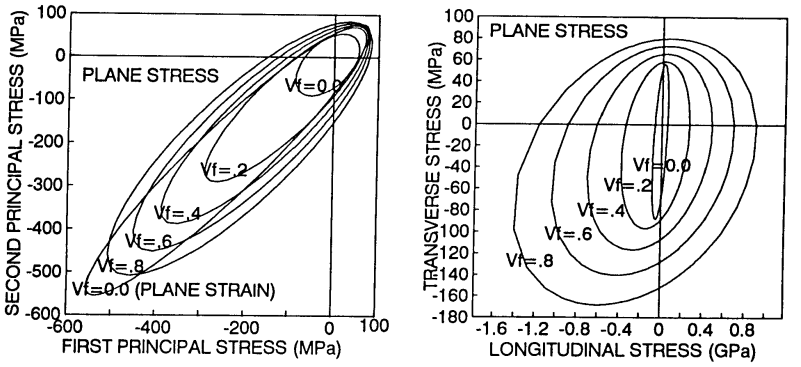

FOR A TRANSVERSE PLANE

FOR A LONGITUDINAL PLANE

$\sigma t = 53MPa$

$\sigma c/\sigma t = 1.3$

Fig(4.81) The Resulting Yield Surfaces for the Composite Material

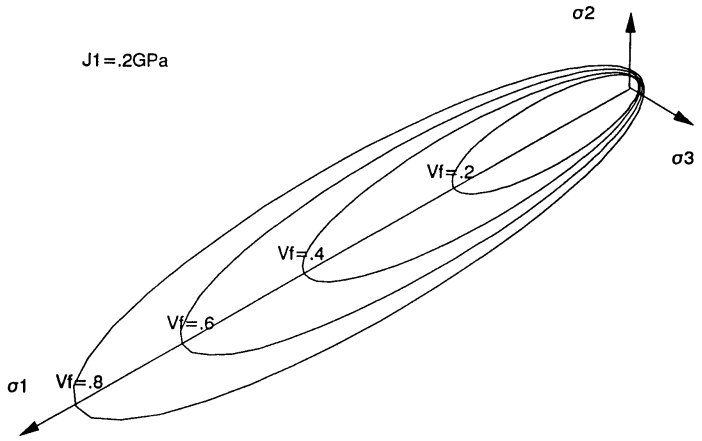

Fig(4.82) Plots of the Yield Surface for Different Fibre Volume Fractions

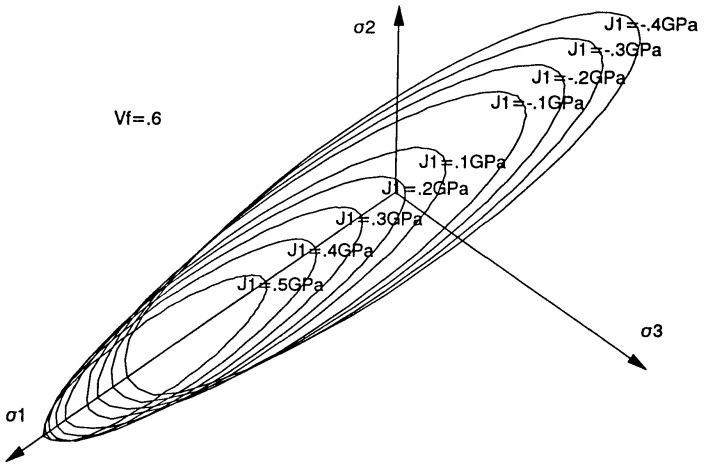

Fig(4.83) Plots of the Yield Surface For Different Hydrostatic Stresses

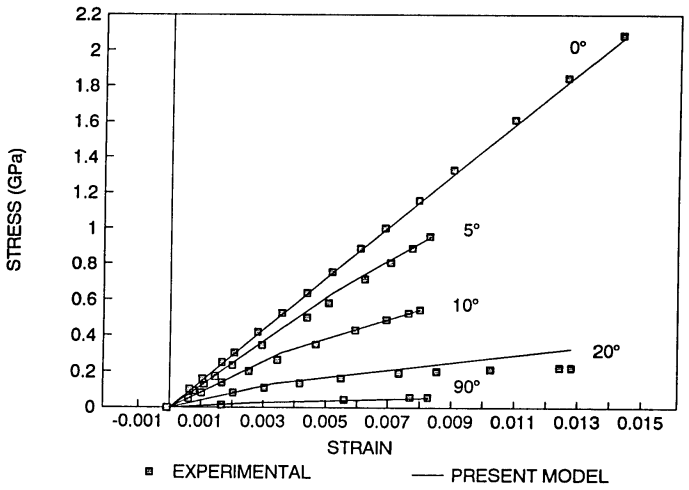

Fig(4.84) Stress-Strain Curves for Composite

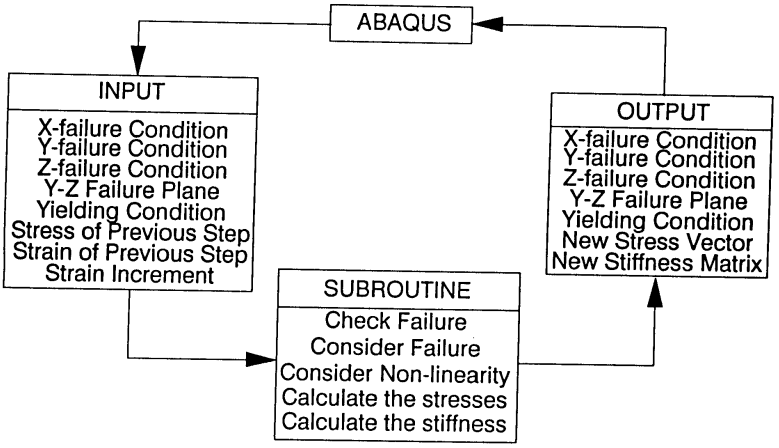

Fig(4.85) Block Diagram for Input and Output

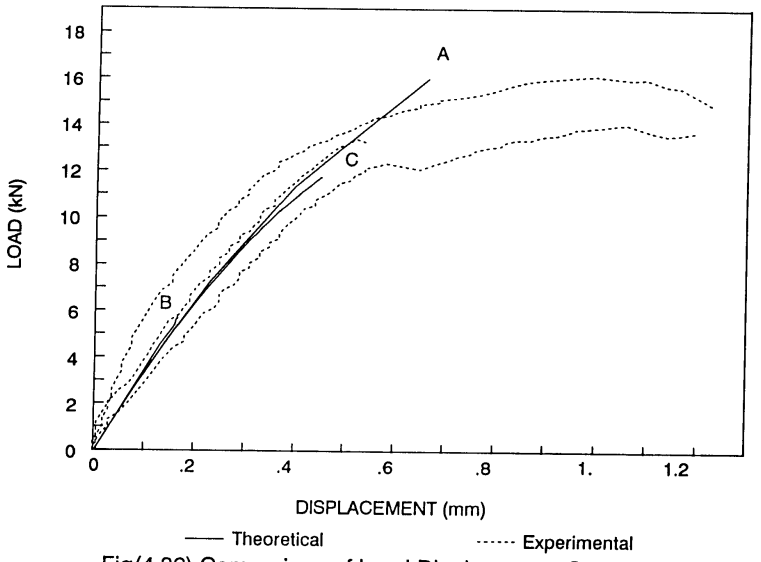

Fig(4.86) Comparison of Load Displacement Curves

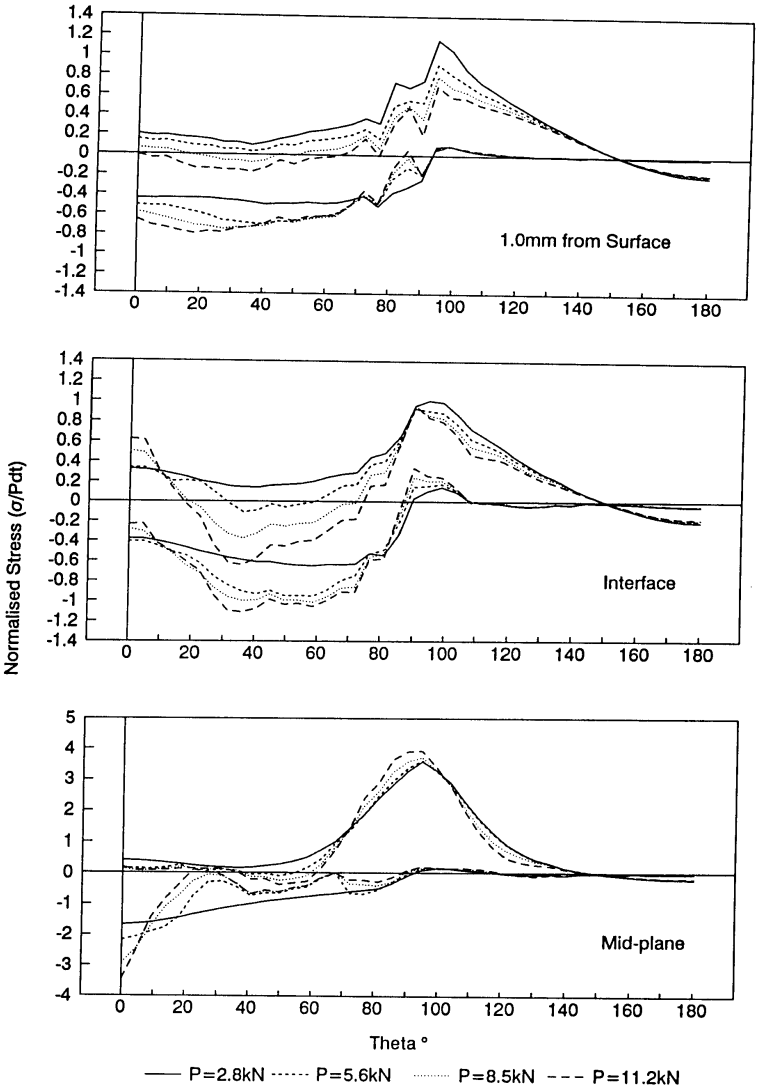

Fig(4.87) In-Plane Stresses Considering Non-Linearity and Fracture

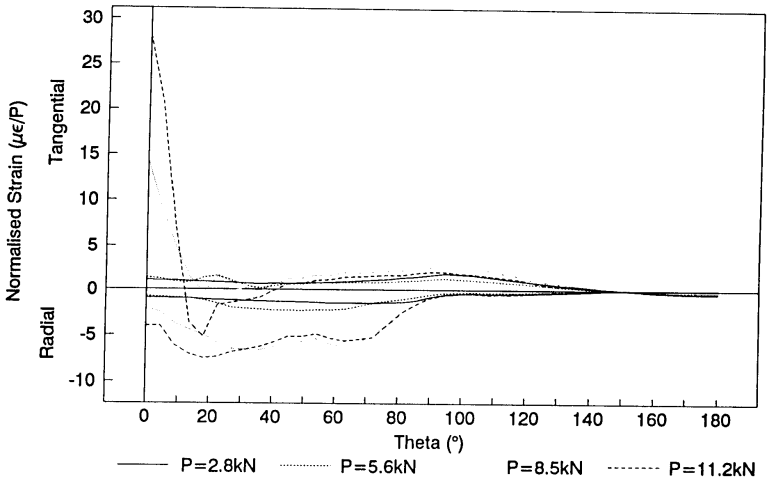

Fig(4.88) In-Plane Strain on Mid-Plane

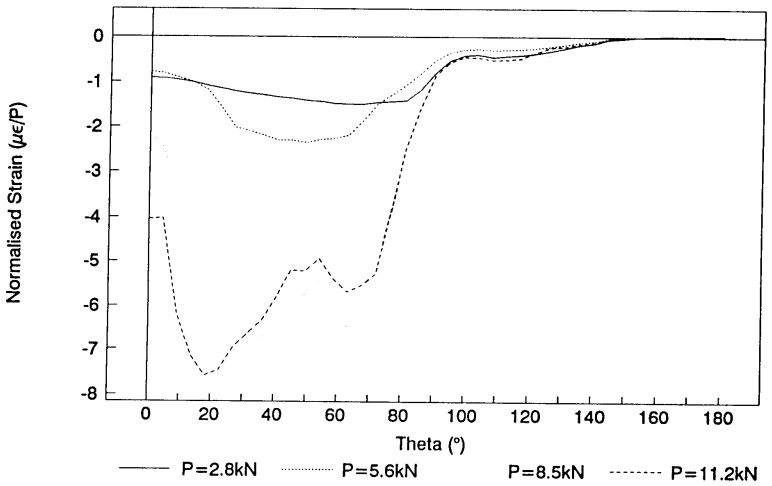

Fig(4.89) Out-Of-Plane Strain on Mid-Plane

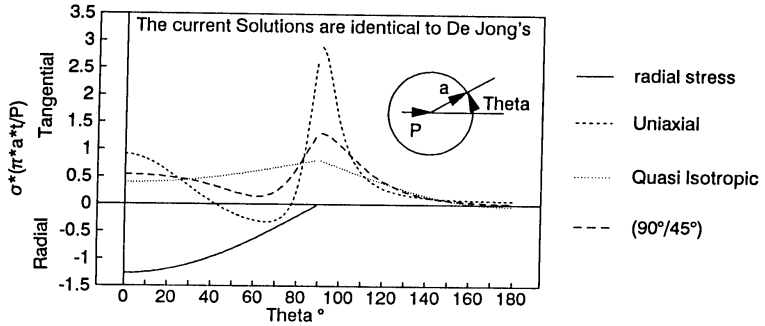

Fig(4.90) Solution using a Cosine Radial Distribution

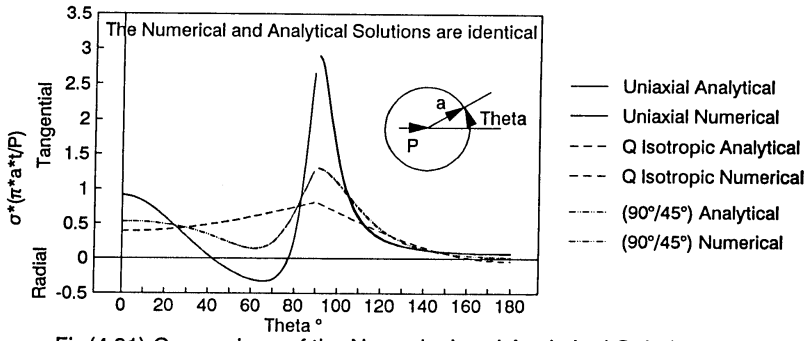

Fig(4.91) Comparison of the Numerical and Analytical Solutions

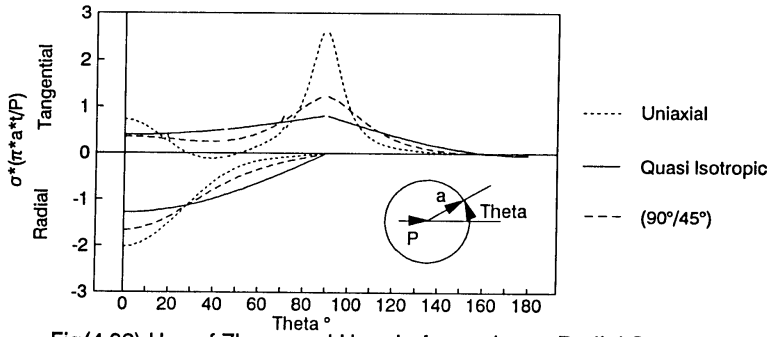

Fig(4.92) Use of Zhang and Ueng's Approximate Radial Stresses

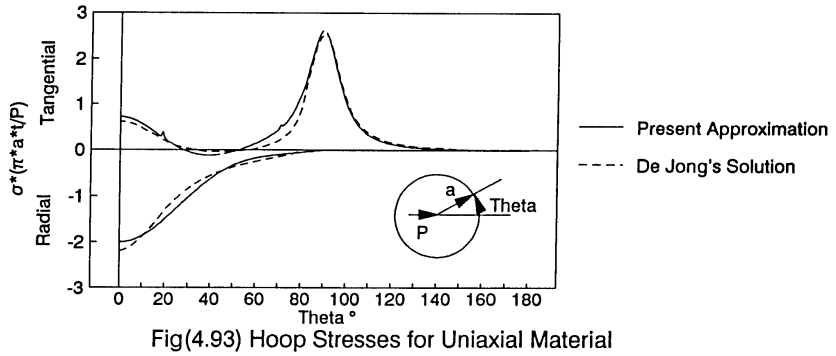

Fig(4.93) Hoop Stresses for Uniaxial Material

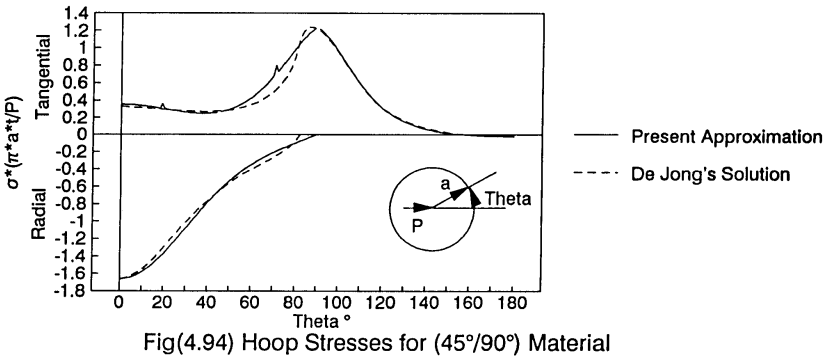

Fig(4.94) Hoop Stresses for (45°/90°) Material

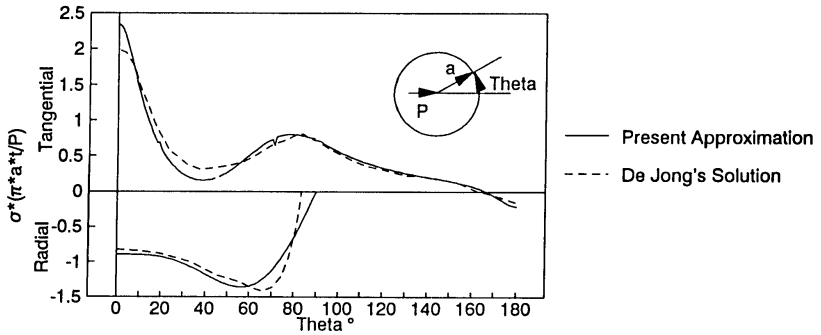

Fig(4.95) Hoop Stresses for 90° Material

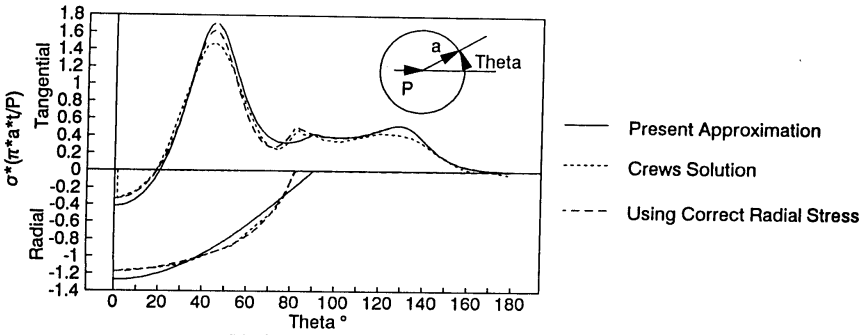

Fig(4.96) Hoop Stress for 45° Material

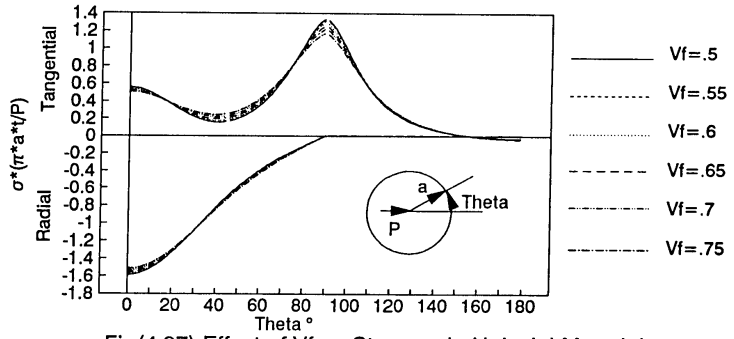

Fig(4.97) Effect of Vf on Stresses in Uniaxial Material

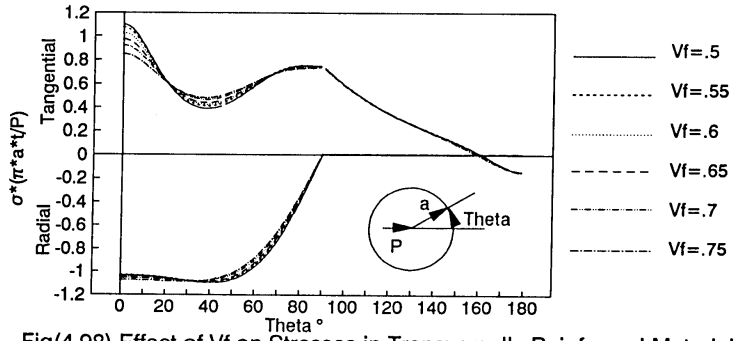

Fig(4.98) Effect of Vf on Stresses in Transversally Reinforced Material

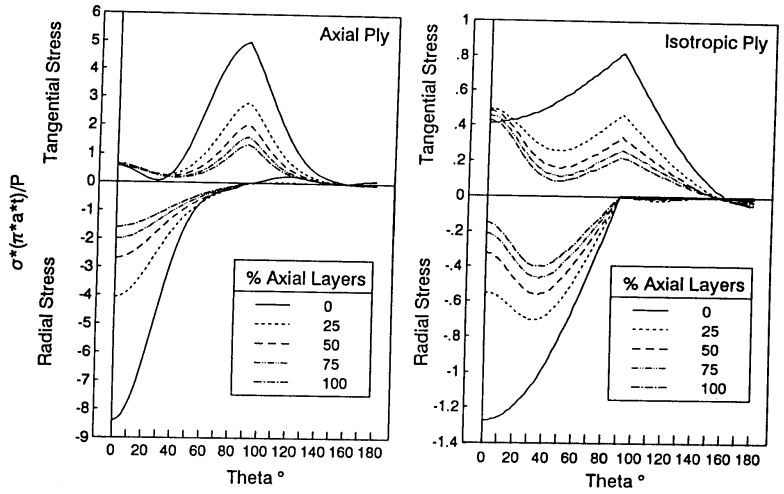

Fig(4.99) The Ply Stresses around the Hole

Vf-csm=.1, Vf-uni=.5

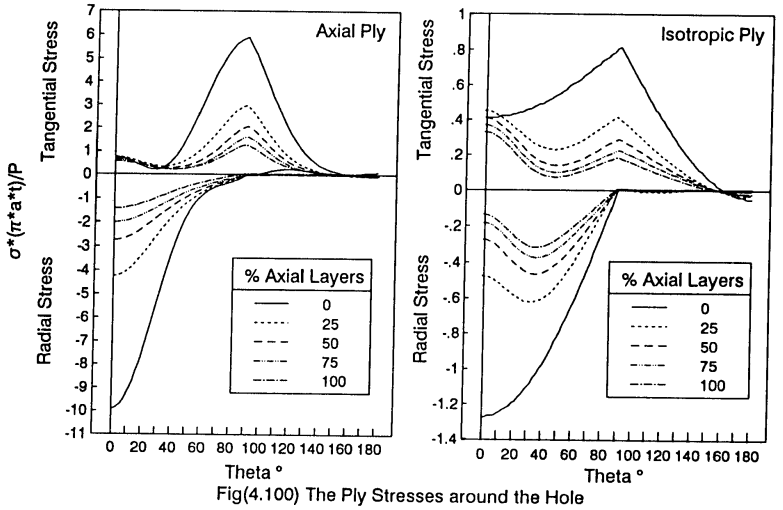

Fig(4.100) The Ply Stresses around the Hole

Vf-csm=.1, Vf-uni=.6

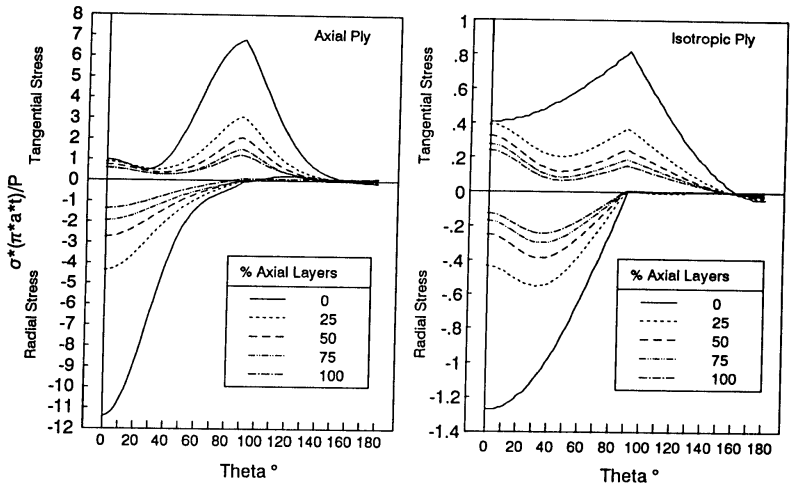

Fig(4.101) The Ply Stresses around the hole
Vf-csm=.1, Vf-uni=.7

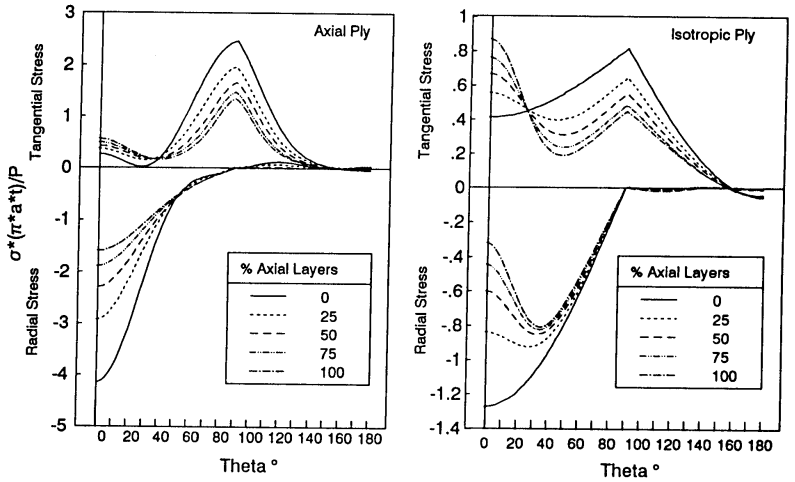

Fig(4.102) The Ply Stresses around the hole
Vf-csm=.3, Vf-uni=.5

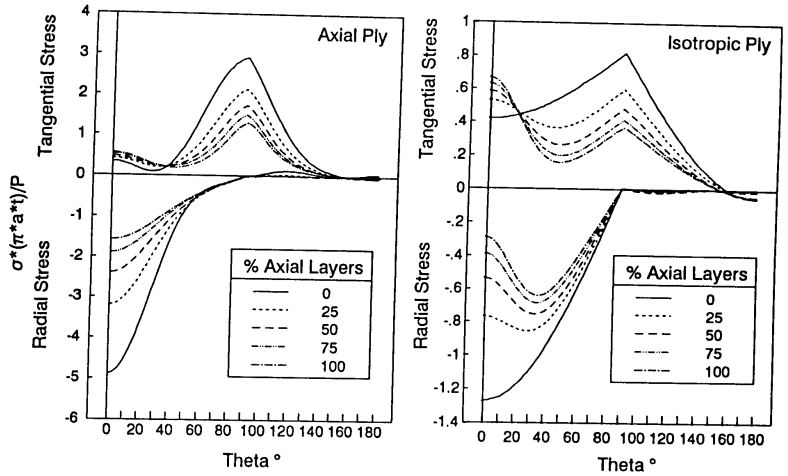

Fig(4.103) The Ply Stresses around the hole
Vf-csm=.3, Vf-uni=.6

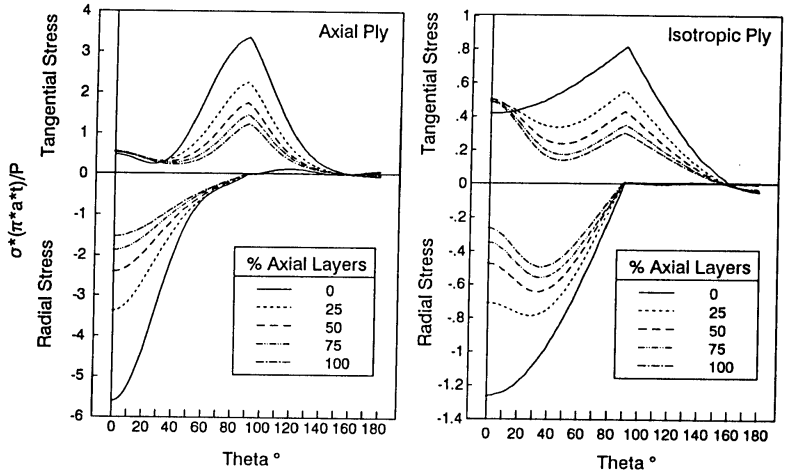

Fig(4.104) The Ply Stresses around the hole
Vf-csm=.3, Vf-uni=.7

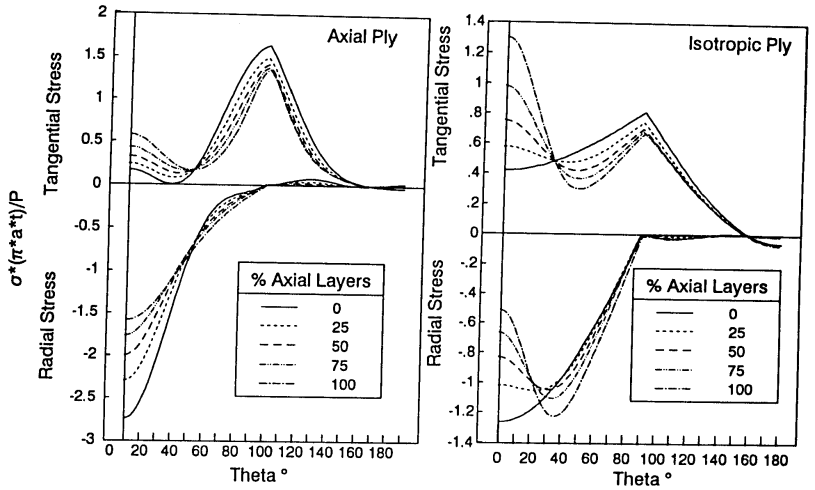

Fig (4.105) The Ply Stresses around the hole
Vf-csm=.5, Vf-uni=.5

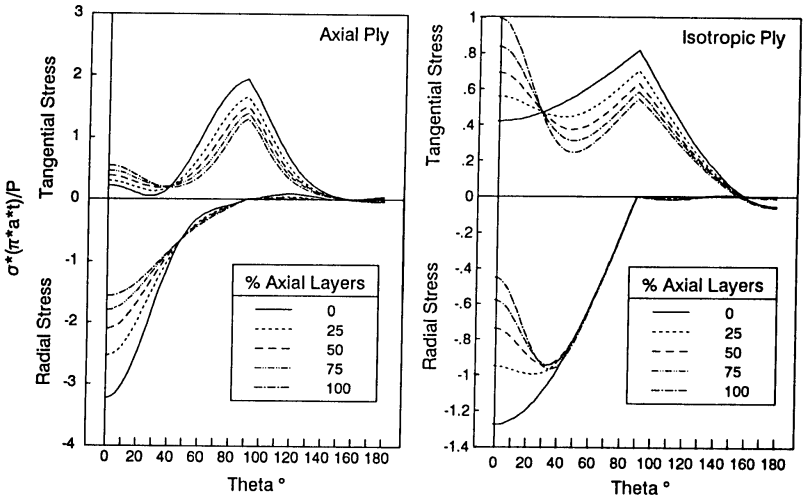

Fig(4.106) The Ply Stresses around the hole
Vf-csm=.5, Vf-uni=.6

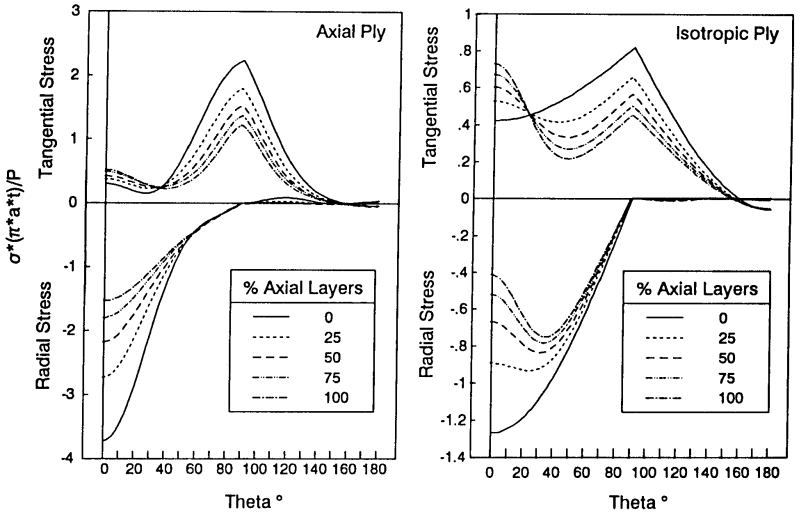

Fig(4.107) The Ply Stresses around the hole

Vf-csm=.5, Vf-uni=.7

CHAPTER FIVE

5. DESIGN CONSIDERATIONS

5.1. INTRODUCTION:

The design process aims at determining the dimensions that will satisfy the strength, safety and economy requirements. For composite materials, this process is complicated due to the large number of parameters involved. The variables which can be manipulated when the design of the joint is undertaken are:

a) the number of bolts,
b) the diameter of the bolts
c) the pattern in which the bolts are organized; this will involve:
   - the end distance,
   - the side distance,
   - the spacing between the bolts,
d) the washer size,
e) the degree to which the bolts are to be tightened

It has to be noted that the above given list assumes that the member shape, dimensions and lay-up are predetermined in previous stages of design.

For bolted joints, the cost of the joint is directly proportional to the number of bolts (Kedward 1990). This means that the number of bolts should be minimised and therefore, the design of mechanical joints in composite materials can be dealt with as an optimization problem which states:

> Find the minimum number of bolts that will transfer the load safely between members of given material properties and geometry.

The solution of the optimization problem given above requires the understanding of the behaviour of each bolt and the interaction between them. The previous chapters investigated these topics for pultruded materials. In this chapter the results of the experimental and theoretical investigations reported in this work will be discussed and used to establish the basis

for the design of structural joints for pultruded composite materials. For this purpose, simple formulae for predicting some aspects of the behaviour of the joints will be proposed.

5.2. THE PREDICTION OF THE STRENGTH OF THE JOINTS:

The review given in Chapter 2 showed that there are basically three methods which were applied to predict the strength of composite joints. These are the stress concentration methods, the point and average stress methods and the successive damage techniques. Although the second class of method is the most popular one, it has been shown by Tsiang and Mandrell (1985) that these methods of prediction are only curve fitting techniques with no physical meaning. The interpolation using these techniques is undertaken between the two limiting cases where the material is notch sensitive and the one where the material is considered notch insensitive. Therefore, the author believes that such involved methods are not justified specially because they complicate the qualitative understanding of the behaviour of the joints.

In the present work, it was found that the stress concentration method can be used to obtain reasonable predictions of the strength. The failure load of the specimens manufactured from the material 'Blue 1', which were tested in chapter 3, was predicted using the linear elastic stress results obtained in Chapter 4. It was shown in the latter chapter, that the use of the laminated plate theory was sufficiently accurate for the purpose of estimating the in-plane stresses.

The strength prediction was based on the hypothesis of Soni (1981) which assumed that the strength of the joint would be exhausted only when the strongest ply has failed. The justification of such an approach is that the contribution of the plies, which will fail first, to the total stiffness is negligible. Table(5.1) gives the stresses which are responsible for triggering the experimentally observed failure mode.

It can be seen from the table that the stresses corresponding to one and the same failure mode are nearly equal. This means that it is possible to predict the strength of the joint using the stresses calculated based on linear elastic behaviour. It has to be noted, however, that the material parameters to which these stresses are to be compared are not necessarily equal to the strength of the material.

In addition, the above adopted hypothesis is not necessarily applicable to other types of lay-up. This is due to the effect of the lay-up on the notch sensitivity and the damage tolerance of composite layered materials.

Group	Failure Mode	Calculated Stress MPa
TS	Cleavage a	259.1
TM	Tension	1144.96
TL	Tension	1269.41
MS	Cleavage a	192.89
MM	Cleavage b	200.43
ML	Combined	-
	Tension	1195.6
	Cleavage b	295.02
	Bearing	846.25
WS	Cleavage b	220.06
WM	Bearing	811.68
WL	Bearing	881.31

Table(5.1) Stresses at Failure

Where 'Cleavage a' indicates failure starting from the end of the specimen while 'Cleavage b' indicates failure initiating from the bolt.

The point which is demonstrated using the above given results is that it is possible to predict the strength of the joint based on stresses obtained using linear elastic stresses and modified material strength instead of using modified stresses with the material strength. This approach is supported by results obtained by Crews and Naik (1986) and the design methods adopted by Hart-Smith (1978) and Ruben (1983) which indicated that the empirical factors can be contained in the values of the material strength parameters.

5.3. EFFECT OF THE LAY-UP OF THE MEMBER:

The ultimate strength and the notch sensitivity of composite materials depend on their lay-up. The difference in the behaviour (after the initial failure) is due to the preservation of the integrity of some laminates while others delaminate.

When the laminate behaves as a unit up to final failure, the ultimate strength is expected to be near the load resulting in failing the strongest layer. This is due to the capability of the load to bridge the failed laminae through the adjacent plies. In this case, the material is expected to behave in a brittle manner.

When the material delaminates after the weakest layer is damaged, the composite action is gradually weakened and therefore the plate is expected to develop nonlinear behaviour resulting in redistribution of the stresses; which is a process similar to yielding of metals resulting in notch insensitive behaviour. From a different point of view, such materials are notch insensitive because they are able to dissipate large amounts of energy which results in

retarding the final failure. This means that the fracture toughness of composite layered materials increases when the failure is associated with delamination of the laminate (Harris 1986).

Delamination can take place using two mechanisms. The first mechanism is exhausting the interlaminar shear capacity, while the second mechanism is developing tensile interlaminar stresses. Equilibrium requires the development of interlaminar normal stresses when interlaminar shear stresses exist. Accordingly, both reasons for delamination depend on the interlaminar shear stresses.

It has been shown (Whitecomb and Raju 1983) that it is possible to calculate the interlaminar stresses in layered materials by applying the stresses, which would have developed on the free edges of the composite, if the laminated plate theory was used, to the surface of a three dimensional model. This means that the stresses developed on the free surfaces using the laminated plate theory are equivalent to the interlaminar stresses. This means that it is possible to estimate the relative values of the shear stresses on any interlaminar boundary by calculating the sum of the stresses developed by the laminated plate analysis on the surfaces which ought to be stress free and are lying above that boundary (Goonetilleke, Poursartip and Teghtsoonian 1985). This technique provides a qualitative method for assessing the shear stress that develops in the composite.

Such a qualitative estimate shows directly that interlaminar stresses can be substantially reduced by increasing the number of the layers and by adopting a cyclic lay-up procedure which will result in self balancing groups of plies.

The out-of-plane stresses can play an important role in the delamination process if they are tensile. Accordingly, it is necessary to chose the stacking sequence such that the normal stresses developed between the plies are compressive. This usually means that in the main loading direction, the layers which have a low elastic modulus should be placed near the outer layers.

5.4. THE EFFECT OF GEOMETRY ON STRENGTH:

For most composite materials, it is possible to design the joint such that it fails in bearing. However, it has been demonstrated in Chapter 3 that some materials can not develop such a type of failure due to their low shear strength. Figure(3.32) shows the dependence of the shear strength on the end distance and width for the materials 'Grey 2' and 'Yellow'. This figure shows clearly that there exists a critical end distance above which the increase in the end

distance does not increase the strength. Similar results were quoted by Hart-Smith (1987) for CFRP.

The experimental results showed that the shearing mode could yield a progressive failure provided a sufficiently long end distance was used. The progress of the shear failure under these conditions showed similarity with the bearing failure process in spite of the different nature of the developed damage. Both failure mechanisms started at the hole and they extended towards the free edge of the member under increasing or at least constant load. When damage reached a certain distance from the edge of the hole, the joint failed completely due to cleavage-splitting failure mode. The latter suggestion, for the condition resulting in final failure, is based on the load deflection curves for the samples of 'Grey 1', 'Grey 2' and 'Yellow'. The first set of specimens indicated the existence of a relationship between the method of damage spreading and the ductility. The other two groups showed that increasing the end distance was associated with an increase in the extensibility of the joint. Both phenomena can be explained by setting the condition of final failure as a function of the position of the damage front.

5.4.1. ESTIMATING THE CRITICAL DIMENSIONS

The maximum strength of the joint forms a plateau that is only reached if the end distance and width are to be chosen larger than certain critical values. The dimensions which ensure attaining the maximum strength were traditionally related to the diameter of the bolt irrespective of the width of the plate. This approach originated from codes of practice for the design of metal joints. This method was acceptable for these materials due to the relatively small end distances associated with isotropic materials. This meant that the difference between the critical end distance of a wide and of a narrow joint was not large. Accordingly, it was feasible to adopt the maximum critical end distance as a minimum design requirement. This critical end distance will be shown to be dependent on the diameter of the bolt only. Such an approach is not economically feasible due to the long end distances needed for composite materials. The experimental results for the 'Grey 2' and 'Yellow' materials show that the critical end distances obtained experimentally in chapter 3 changed with the width Fig(5.1).

In order to find a theoretical means for determining the critical dimensions of the joint, it is necessary to investigate the reason for their existence. The plateau under consideration indicates the independence of the strength from the geometry. Because the strength is a function of the stresses, the latter must also be independent of the geometry.

This condition is certainly achieved when the dimensions of the plate are increased indefinitely. In reality, however, there exist finite dimensions after which the change in the stresses becomes negligible. These critical dimensions can be regarded as the critical length associated with St Venant's principle. For isotropic materials, this principle "states that the local stress concentrations can be considered insignificant at a distance greater than the largest characteristic dimension of the domain over which the loads are acting" (Tranis, Bogetti, Gillespie and Pipes 1988). An approximation of the critical length for orthotropic materials was given by Choi and Horgan (1977). The resulting critical length depended on the required decay of the stresses, the width of the plate and the material properties.

MATERIAL	w(mm)	e/l crit
Grey 2	30	.777
	45	.777
	70	.666
Yellow	20	.644
	30	.572
	38	.677

Table (5.2) Correlation between St Venant's length and the critical end distance.

The choice of the decay ratio of the stress that has to be considered to determine the critical end distance can be determined based on the experimental results by normalising the experimentally obtained critical end distances using St Venant's critical length given by (Choi and Horgan 1977) as

$$l_{crit} \propto w * \sqrt{\left(\frac{E_L}{G_{LT}}\right)} \qquad (5.1)$$

The results are given in Table (5.2) and they show that a reasonable correlation between the two quantities exists.

The average of the results of Table(5.2) was used to obtain the following estimate of the critical end distance as a function of the material properties and plate width.

$$e_{crit} = .686 * w * \sqrt{\left(\frac{E_L}{G_{LT}}\right)} \qquad (5.2)$$

Fig(5.1) shows that reasonable correspondence exists between the experimental and the theoretical results. This means that it is possible to determine the end distance which will ensure the maximum strength for a given width of the joint using the elastic properties of the laminate. It has to be noted, however, that this result has to be used cautiously because the formula used to estimate St Venant's length assumes that the material is highly orthotropic. The factor used in that equation is similar to the factor used by Carlesson, Sindlar and Nilsson (1986) (.73) to estimate the length at which the stresses decrease to 1% of their original value. Accordingly, it can be concluded that the required stress decay ratio is about .01.

It is important to note that the above given result implies that if the plate is very wide, the end distance will also become very long. This contradicts reality because for a very large plate, the stress applied over the width of the plate becomes negligible compared to the stresses acting on the hole. Accordingly, the characteristic loading domain (given in the definition of St Venant's length) changes from being the width of the plate to become the hole diameter. Therefore, the critical end distance is expected to reach a limiting value which is independent of the width of the plate but depends on the diameter of the bolt.

In order to verify this behaviour, the fundamental definition of St Venant's critical distance was used in association with two-dimensional finite element models of infinite strips which were loaded using a bolt and fixed at one of their ends to calculate the critical length which was defined as the distance measured on the axis of the model from the centre of the bolt to the point where the axial compressive stresses were equal to 1% of the bearing stress. Here it has to be noted that in the area between the end of the hole and the end of the infinite plate, the loads on the infinite strips are self equilibrating and therefore, according to St Venants principle, the stresses will decay to zero.

Such an analysis was undertaken for different widths and for the two limiting material properties of chopped strand material and the unidirectional materials. The results are given in Fig(5.2) where it can be seen that the distance increases with increasing width. However, the rate of increase becomes less for wider specimens. This means that, as expected, the use of St Venant's length is not correct for large widths.

Therefore, it is necessary to limit the area over which the above given formula is applicable. In order to accommodate a washer, the minimum end distance has to be equal to its radius. An upper limit for the end distance can be obtained from the solution of an infinite plate loaded via a pin by finding the distance resulting in 1% decay of the compressive stress in front of the pin. When investigating areas which are far away from the bolt, this solution

will be similar to that of a concentrated load. For the latter case, the following formula was obtained based on the solution given by Lekhinitskii 1968:

$$\sigma_r = \frac{P}{2\pi\ t\ n\ \tau}(k + \nu_{xy} - n^2) \qquad (5.3)$$

where n and k are Lekhinitskii's parameters of orthotropy, t is the thickness of the plate and 'a' is the radius measured in the loading direction.

The stress obtained using equation(5.3) has to be compared with the bearing stress acting on the hole. An approximation of the radial stress at the centre line of the plate can be obtained using the formula of Zhang and Ueng (1984) which gives for theta=0° the following expression:

$$\sigma_r = \frac{-2P}{\pi a t} * \left[\frac{n^2 k(8k+7) + 2n(k-\nu_{xy})(9k+1) + 5(k-\nu_{xy})^2}{3n^2 k(k+4) + n(k-\nu_{xy})(13k+7) + 5(k-\nu_{xy})^2} \right] \qquad (5.4)$$

Accordingly, using equations (5.3) and (5.4) it is possible to determine the distance which will yield the required decay in the stress. It has to be noted that this latter distance depends only on the size of the pin.

It is important to note that the above given critical end distance is not the end distance which will ensure the development of bearing failure. It is the end distance which ensures the development of the maximum attainable strength of a joint of specified width.

5.5. THE BEARING STRENGTH:

The bearing strength is usually considered to be independent of the geometry (Eriksson 1990) and can therefore be considered as a material property. This approach is usually justified because this type of failure occurs only when the joint has both sufficiently long end distance and width to prevent tension through the hole and shear failures from developing. For such a geometry, the stresses acting near the loaded hole are independent of the geometry, which means that, as argued above, the strength is also independent of the geometry.

However, some results reported by Kretsis and Matthews (1985) show that the bearing strength increases with increasing the size of the joint. This is because the end distance at which the mode of failure changes to bearing is shorter than the critical end distance needed to ensure the independence of the stresses of the geometry.

The bearing strength obtained for the different materials used in this investigation are given in the following table:

MATERIAL	Vf	%uni	%±45	Vfcsm	F/t(N/mm)
Blue 1	.365	41.9	-	.279	3615.0
Grey 1	.375	11.3	54.5	-	4498.5
Blue 2	.411	52.2	-	.298	4031.9
Yellow	.534	63.6	-	.461	4511.0

Table(5.3) Effect of the Material Composition on the Bearing Strength

In that table, the strength is normalised with respect to the thickness of the plate only. The results show that the material 'Grey 1' which contained $\pm 45°$ layers possessed high bearing strength which was comparable with the bearing strength of the material 'Yellow' which had about 50% more fibre content. In addition, the end distance required to ensure the development of the bearing mode for the material 'Grey 1' was much smaller.

When comparing the results of the materials which contained unidirectional and randomly orientated plies only, it can be seen that the strength increased with the fibre volume content which was a function of the percentage of unidirectional plies in the laminate.

The mechanism of bearing failure is complicated and different assumptions were made concerning its development. Collings (1977), (1982) assumed that it was due to compressive failure near the pins. Accordingly, he related the bearing strength to the compressive strength of the plies while Eriksson (1990) considered bearing failure as an instability phenomenon of the plies.

A more fundamental approach is to consider a material model that represents its non-linear and failure characteristics in a three-dimensional analysis. The results of such an analysis which was performed in Chapter 4 showed that the approach was capable of predicting the failure load and the load deformation behaviour.

The model considered showed that a generalisation of the rule of mixtures which takes into consideration the non-linearity of the matrix behaviour was possible. The approach considered was general and can be considered as a frame work for modelling such class of materials rather than being a single model.

It was shown in chapter 4 that although the non-linear behaviour of the matrix material was considered to be sufficient for predicting the load deformation behaviour of a joint, it failed to predict failure. This deficiency was overcome by incorporating a model for describing the failure characteristics of the composite. The latter model was basic but it succeeded in predicting the strength of the joint. Here it is essential to note that the predicted strength

depended strongly on the assumed post fracture behaviour of the material. The consideration of this subject in association with the finite element method has received little attention in spite of its fundamental importance for correctly predicting failure of structures and assemblies made from fibre reinforced materials. This issue involves the problem of tuning the material model using the fracture toughness of the material and the mesh size in order to achieve 'mesh objectivity' (Schellekens and DeBorst 1991).

From a designers point of view, the bearing strength can be obtained from tests performed on sufficiently large specimens. Here it is necessary to remember that such tests must be performed in tension and under the same clamping conditions as the real joint. This is due to the higher bearing strength which will be obtained from compression and /or clamped tests. The difference between the two cases is due to the difference in the stress distribution (Hart-Smith 1987).

5.5.1. THE EFFECT OF CLAMPING THE BEARING AREA:

The clamping of the bearing area is known to increase the strength of the joint (Stockdale and Matthews 1976). The investigation of the effect of the size of the clamping area on the bearing behaviour (Chapter 3) has shown that increasing the clamping area resulted in increasing the ultimate strength of the joint but it resulted, at the same time, in spreading the damage zone over a larger area. This in turn resulted in the non-linear behaviour of the specimens which was associated with increased deformations at the peak load, while the ultimate ductility of the joint was reduced.

The increased displacements with increasing load are favourable specially when the bolting system is complex and indeterminate. This is the case when multiple bolts are used in a joint because this non-linearity allows load redistribution to take place between the bolts and therefore failure of all bolts is reached simultaneously.

The increase in strength associated with clamping the material can be explained by the reduction of the stress concentration resulting from the development of the damage. This is in addition to the increase which is due to the friction between the washer and the plate. This is in accordance with the results of Stockdale and Matthews (1976) for GFRP which showed that the increase in strength was not proportional to the increase due to friction.

This explanation is supported by the theoretical comparison undertaken in Chapter 4 between the behaviour of a plate loaded by a pin and that of a plate loaded by a bolt. This investigation showed that for the finger tight condition, no substantial differences in the in-plane

stresses between the two cases exist. However, the consideration of the nonlinear behaviour for the pinned case showed that excessive out-of-plane strains developed for the pinned case indicating failures in that direction. This is in accordance with the results of Serabian (1991) using Moire interferometry. Therefore, an increase in strength can be achieved by preventing the joint from failure due to this effect while allowing the damage to spread and thus reduce the in-plane stress concentration.

5.6. THE TENSILE STRENGTH:

The tensile strength of the joint is basically dependent on the ratio between the diameter of the bolt and the width of the member. Reducing the size of the bolt results in increasing the strength of the joint until the bearing or shear failure loads become more critical than the load for the tensile failure. After that, any further reduction of the diameter will reduce the bearing strength.

The stress analyses reported in Chapter 4 showed that the stress responsible for the development of the tensile mode of failure increased when the end distance was reduced. However, there was a critical end distance after which the stresses became practically constant. Accordingly, for a plate with sufficiently large geometry and which is supported at both its ends, the stress concentration becomes approximately equal to the stresses of an infinite plate. The closed form solution given in Chapter 4 for the infinite plate results in the following simple equation for the stress at the point lying on the hole at 90° to the loading direction which is considered responsible for initiating tensile failure.

$$\sigma_\theta(90) = -S_{ra}\left(\frac{\alpha_1^{\frac{1}{2}} + \alpha_2^{\frac{1}{2}}}{\alpha_1^{\frac{1}{2}}\alpha_2^{\frac{1}{2}}}\right) = -S_{ra}\sqrt{\frac{E_x}{G_{xy}} - 2\nu_{xy} + 2\sqrt{\frac{E_x}{E_y}}} = -S_{ra}n \qquad (5.5)$$

Where S_a is the average stress acting on the hole and n is one of Lekhinitskii's parameters (1968) for orthotropy. The average stress as a function of the applied load for the approximate stress distribution recommended by Pradhan and Ray (1984) was calculated for a variable contact area ß. The resulting relationship is as follows:

$$\sigma_r(\theta) \propto (\cos(\theta)-\cos(\beta)) \qquad for\ |\theta| \le \beta$$

$$then \qquad (5.6)$$

$$S_{ra} = \frac{-P}{\pi at}\left(\frac{\beta\cos(\beta)-\sin(\beta)}{\beta-.5\sin(2\beta)}\right)$$

where P is the applied force and beta is half the contact angle. The resulting average stress varies from .317P/dt to .405P/dt when beta changes from zero to 90°, which means that the average stress for the same load increases with increasing the contact angle. This is due to the inefficiency of the area near theta equal to 90° in supporting the load which results in increased radial stresses compared to the stresses which would have developed near theta equal to 0° to support the same load.

The dependence of the stresses on the parameter n was checked by collecting data about the stress concentration at the point under consideration from different sources of the literature and they were amended using two dimensional finite element analyses performed by the present author. Fig(5.3) shows a plot of these data point against their respective n value. The figure shows that the general trend is in accordance with the present average given as .361 nP/dt which is obtained as the average of the two limiting cases. It is clear that some variation around the present result exists. This variation is due to the effect of varying the contact area and the contact stress distribution. In order to take these effects into consideration, a regression line was obtained for the gathered data. The resulting relationship is also shown on Fig(5.3) and it is given as:

$$\sigma_\theta(90) \approx \frac{P}{dt}(.187+.298n) \qquad (5.7)$$

When the plate is supported at one end only, additional stresses develop according to Fig(5.4). For sufficiently wide joints, the solution by Lekhinitskii 1968 for an infinite plate in tension can be used to calculate the stress at theta equal to 90° as

$$\sigma_r(90) = \frac{P}{2wt}(1+n) \qquad (5.8)$$

By adding the two contributions, a reasonable approximation of the stresses can be obtained. It has to be noted that the stress concentration due to the presence of the bolt is higher than the stress concentration due to tension applied at the ends of the plate.

The above given formulae can be used for designing for notch sensitive materials while it is sufficient to consider the net area for notch insensitive materials.

5.7. EFFICIENCY OF COMPOSITE JOINTS:

The efficiency of a joint is defined as the ratio between the strength of the joint and the strength of the parent material. This method of assessing the efficiency can be used for optimizing the geometry, however, it should be noted that when the performance of different material lay-ups is investigated, this definition of the efficiency can be deceiving because, for the same joint strength, it will show higher efficiency when the strength of the parent material is reduced.

A different approach was applied by Dallas (1967) where he assessed the efficiency of a single bolt joint as the ratio between the net cross section and the gross cross section of the member. Although this method disregarded the stress concentration associated with some lay-ups, the approach can be considered as a method of establishing an upper limit on the tensile strength of the joint. His analysis also assumed that the maximum attainable strength of the joint will occur if tension and bearing failures occur simultaneously.

Based on the above mentioned assumptions, Dallas (1967) showed that the maximum attainable efficiency of the joint will increase if the ratio between the material bearing strength and the material tensile strength is increased. He also showed that by increasing the ratio indefinitely, the strength reaches a limiting value. An infinite ratio between the bearing and tensile strength means that the joint can only fail in tension, therefore, the maximum attainable strength of the joint is the tensile strength.

The reason for the above given limit on strength becomes clear when the results for the two bolt joint reported in Chapter 3 are considered. The first set of joints had a width which ensured development of bearing failure for a single-bolt joint, however, when the joints were tested using two bolts, they failed in tension. The reason was that the bearing strength was improved while the tensile strength of the joint remained constant.

5.8. IMPROVING THE STRENGTH OF THE JOINT:

In order to improve the tensile strength of a joint, it is necessary to ensure that the chosen end distance is long enough to prevent the adverse effect which was noted from the theoretical analyses of chapter 4 which showed that for the same width to diameter ratio, the tensile stress concentration increased with reduced end distance. Again, if the limiting end distance requirements considered above are satisfied, the tensile strength is expected to become independent of the end distance. This condition is the upper limit of the strength of the joint.

Here, it is stressed that although it is desirable to increase the strength of the joint so that it is approximately the tensile strength, it is not recommended to design the joint to fail in this mode because the failure is of catastrophic nature (Hart-Smith 1987).

The bearing strength of the joint can be improved either by increasing the strength of the individual bolts or by using multiple bolts. The first option can be achieved without upsetting the tensile strength by clamping the bearing area as discussed above. The improvement using this approach is limited and is dependent on the quality of labour.

A more reliable method is the use of multiple bolts. Here it is important to remember that these fasteners must have a sufficient back-spacing such that they do not adversely affect each other. This back spacing can be estimated using the critical end distance discussed above.

When considering more than one bolt in a line, a simple analysis by Feodoseyev (1977) showed that the load on the inner bolts will always be less than the two outer bolts. In the limit, when the local deformation developed in the bearing area becomes very large, the loads on the bolts become equal. But for the other limiting case, when no local deformations develop, the load on the inner bolts becomes equal to zero. Zahn (1991) used a similar analysis to show that when the number of bolts was increased indefinitely, the strength of the joint reached a limiting value. He also showed that the gain achieved by increasing the number of bolts, reduced as their number increased. This was basically due to the non uniform distribution of the load between the bolts which were arranged in series resulting in higher loads on the outer bolts. This result was in agreement with the results of Abd-El-Naby, Hollaway and Gunn (1991) and those of Yang and Ye (1989) which were obtained using the finite element method assuming linear elastic material properties.

However, the experimental investigation undertaken in Chapter 3 showed that this load distribution was only correct for low levels of loading. For higher loads, the non-linear behaviour of the bolts resulted in redistributing the loads between them and accordingly, the loads on the two bolts became equal at failure. This behaviour was noted for bearing and shearing failures. However, in order to ensure the development of that behaviour, it is recommended to choose the materials and the geometry of the jointing lap plates such that, even under low loading levels, the loads on the two bolts are equal.

The choice of the number of bolts has to be undertaken such that they satisfy the requirements of the optimization problem formulated at the beginning of this chapter. Noting the low efficiency of the middle bolt in a three bolt joint, it is proposed to improve the bearing strength of the joint by using two bolts only. The use of two bolt is preferred over the use of one bolt because the behaviour of this type of joint is more predictable. Matthews and Pyner

(1979) showed that, contrary to the single bolt case, this type of joint does not show sudden increase of deformations due to the load sharing between the two bolts.

5.8.1. THE STRENGTH OF A PLATE LOADED BY TWO BOLTS:

Consider the case of a plate loaded by two pins Fig(5.5). Let the total load applied on the joint be P and the load transmitted using the first and second pin be P_1 and P_2 respectively. In order to satisfy equilibrium, the following relationship between the P, P_1 and P_2 must be satisfied.

$$P=P_1+P_2 \quad or \quad 100=\%P_1+\%P_2 \tag{5.9}$$

If $\%P_1$ and $\%P_2$ are the percentages of the total load transmitted by pins 1 and 2 respectively, the total load on the joint can be expressed in terms of the load on each of the pins as follows.

$$P=\frac{100}{\%P_1}*P_1$$
$$P=\frac{100}{\%P_2}*P_2=\frac{100}{100-\%P_1}*P_2 \tag{5.10}$$

The joint under consideration can fail in one of the following failure modes:

a) the outer pin fails in bearing,
b) the outer pin fails in shear or cleavage,
c) the plate fails in tension at the outer pin,
d) the inner pin fails in bearing,
e) the plate fails in tension at the inner pin,
f) both pins shear out of the plate.

It has to be noted that all these failure modes except e) depend on the load distribution between the two bolts. The failure mode e) basically depends on the total load to be transmitted using the joint. However, experimental evidence (Tsiang and Mandrell 1985, Kretsis and Matthews 1985) suggests that the tensile strength of a plate with a loaded hole is less than for one open hole. Matthews and Kretsis (1985) reported a reduction of 12% while Oplinger 1978

reported that this dependence is not active when the by-pass load is less than 75% of the total load. Failure mode f) will be similar in behaviour to bearing failure of both pins provided the dimensions of the plate are large enough to ensure ductile failure.

Assuming that the dimensions of the joint result in the independence of the ultimate loads on the bolts from the geometry, the strength of the joint is controlled by the strength achievable at each of the bolts. These can be estimated using Eq(5.10) by substituting the local bolt strength for P_1 and P_2. Plotting these results against the percentage of load taken by the first pin, the graph in Fig(5.6) is obtained.

From that graph it can be seen that the maximum achievable theoretical strength of this type of joint is equal to double the strength of a joint with one pin. The minimum theoretical strength of the joint can also be seen to be equal to the strength of a joint with one bolt. The optimum strength of the joint requires that the load is shared equally between the two pins.

This result is general and can be applied to joints with any pattern of n bolts. In that case, the maximum strength of the joint will be n times the strength of a joint with a single pin while the minimum will be equal to the strength of a single bolt joint. It has to be noted that small variations from the optimum distribution of the load will result in large reductions in the strength of the joint. This reduction is more likely for more complicated joints.

It has to be remembered that the experimental results of the first group of specimens which used two bolts in series in chapter 3 did not develop double the strength of the single bolt joint due to their failure in tension. This failure type imposes an upper limit on the maximum strength attainable for a certain width of the of the joint. This failure type can be represented by the horizontal line in Fig(5.6).

The relative movement between the two bolts of the tested joints was shown to be dependent on the load distribution between them. When this variation is taken as linear, Fig(5.5) can be used to determine the expected load distribution in the joint connecting two plates. The experimental results of chapter 3 showed that increasing the total load on the plate changed the slope of these lines. This was the reason for the change in the load distribution during the tests. The construction in Fig(5.5) represents a set of two linear equations. In general, a set of (n-1) equations will result by enforcing the compatibility conditions between n holes and an additional equation will be available from equilibrium. This set of n equations in n unknowns is sufficient for determining the load transmitted using each of the bolts.

5.8.2. CHOOSING THE FASTENER PATTERN:

In order to make decisions about the fastener pattern, the effect of having multiple bolts in a row is discussed. The load distribution between parallel loaded holes was shown to be almost uniform (Wan and Yang 1991, Conti 1986 and Oplinger 1978). Although the presence of the bolts near to each other will result in increasing the stress concentration (Savin 1961), this effect is expected to be small for sufficiently large bolt spacings. In order not to reduce the tensile strength of these joints, the sum of the diameters of the bolts has to remain constant. Here it is important to remember that the minimum diameter of the bolt has to ensure that the ratio of the diameter to the thickness of a glass fibre plate has to be less than 3 in order to prevent local buckling and it has to be greater than 1 to avoid bending of the bolt. The decision about the number of bolts and their diameter depends also on the width of the plate.

Because the bearing stress is inversely proportional to the diameter of the bolt, the sum of the strength of the above mentioned bolts will remain constant. Therefore, the use of more than one bolt in a row for a material which can fail in bearing is not recommended because this will result in increasing the cost of the joint without achieving any gain in the strength. When the load carrying capacity of the joint is controlled by the shear strength, the use of multiple bolts in a row becomes feasible because the area which is resisting the failure is increased. Therefore, for such material, it is recommended to use such bolt patterns. It has to be noted that for both cases, the limit on the critical end distance will reduce because of the reduction of the diameter of the bolts.

5.9. MAXIMUM ATTAINABLE STRENGTH:

The maximum attainable strength of the joint was shown to be equal to the notched strength under tensile loading at the ends of the plate. The reason for considering this as the maximum strength is due to the fact that in multiple row joints, the cross section controlling the strength is subjected to a high bypass load compared to the bearing load of the bolt.

At this stage, it is necessary to discuss the ability of joints which use fasteners to transfer loads between members which are fully stressed. A problem arises for tensile members due to the fact that the holes of the fasteners will always result in reducing the cross sectional area. This establishes an upper limit on the maximum strength of the joint which will always be less than the maximum strength of the member. For a constant area and lay-up, this upper limit can be increased by reducing the thickness of the member. This serves two functions; the

first is to reduce the area (d*t) which is occupied by the bolt and at the same time it increases (w/d) and accordingly, the stress concentration is reduced. Therefore, when choosing the cross section of the member, the designer should choose the smallest allowable thickness of the member. For compressive members whose joints fail in bearing, minimising the thickness of the member has a beneficial effect on the overall slenderness of the members but the bearing strength per bolt is reduced. The resulting reduction in the bearing strength can be catered for by using more than one bolt. For other loading configurations which combine moment and axial force, the problem under consideration is not important because it is possible to choose the position of the joint in an area which is not highly stressed. It has to be noted that the complication associated with the tensile load is also present in the design of joints for metallic constructions. The general approach for correcting this deficiency inherent in bolted joints is to increase the cross sectional area of the members to ensure that the net area is sufficient for supporting the load.

5.10. REINFORCING THE JOINT:

The design procedure described above will exhaust the available strength of the material. However, when the strength of one of the failure modes is very low, the overall strength of a joint becomes very low under a general loading condition.

In a real structure, however, a member is expected to be subjected to bending in addition to the applied axial force. This loading condition would result in forces in the bolted connection which are not acting parallel to the member axis. A simple test which gives information about the behaviour of the joints under these conditions was performed using specimens whose fibres were inclined to the loading direction. The similarity of both cases is due to the load not being applied parallel to the fibres.

The failure of these specimens was in tension on a plane which ran parallel to the axial fibre direction, while the specimens which had a large proportion of fibres running in the axial direction always failed in shear-out mode irrespective of the end distance. This resulting drop in the strength of the joint highlights the inadequacy of the material from the point of view of jointing because it is expected to split parallel to the fibres. Accordingly, this material needs local reinforcement in the jointing area.

As shown in the literature, it is possible to reinforce the jointing area locally. This can be achieved either by gluing reinforced polymer plies or metal plates to the surface of the joint or by gluing an inclusion to reduce the stress concentration.

The addition of reinforcement plies to the plate should be undertaken in order to compensate for the reduction of strength due to the presence of the hole and at the same time to increase the transverse strength of the laminate. Therefore, the properties of the reinforcing layer has to satisfy the above given requirements, but at the same time it has to possess properties compatible with the material properties of the original plate in order to prevent the failure of the glue which can result in delamination of the reinforcement and the accordingly the failure of the joint.

The ends of the plate have to be sloping in order to prevent the development of high local stress concentrations which can result in weakening the member outside the jointing area. This also reduces the peeling problems at the end of the reinforcement patch. The problem of peeling can also be controlled by the correct stacking of the layers of the patch such that the straining results in convex deformations which will apply compressive stresses in the potential peeling area. The bolt should be situated at the centre of the reinforcing plate in order to make the maximum use of the outer areas of the reinforcement which are responsible for transmitting the load into the reinforcement.

The inspection of the results of the 'Grey 1' material, suggested that improved performance of the specimens was achieved by clamping them using composite plates. This was partially due to an interlocking mechanism between the expanding plate and the clamping one. Therefore, the use of an interlocking surface between the members which are to be jointed can improve the efficiency of the joints.

Reinforcing the plate using a glued insert was reinvestigated recently by Harrera-Franco and Cloud (1992). Their results show that this type of reinforcement can be used to control the stress distribution in the joint. The shape of the insert should be chosen such that it results in the minimum interface stresses. This is important because this will reduce the possibility of failure of the glue and at the same time it will reduce the stresses in the plate. The material of the insert should be chosen such that it can allow large bolt displacements prior to its failure in order to improve the uniformity of the load distribution between bolts which are in series. A similar idea was recommended by Eisenmann and Leonhart (1981) for CFRP where they proposed the use of softening strips to accommodate the holes of the bolts.

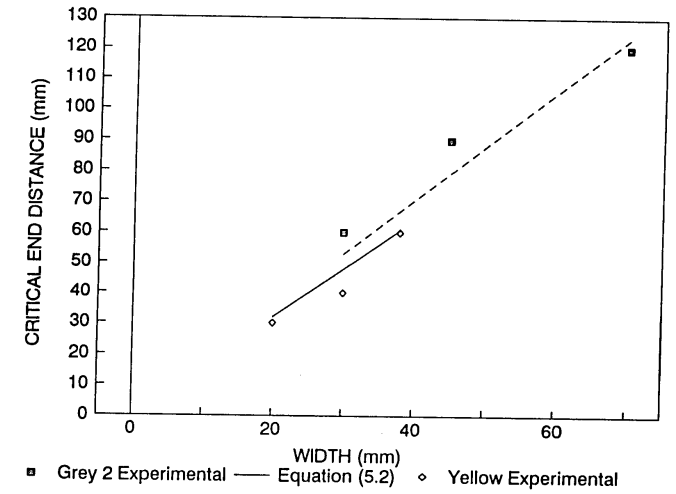

Fig(5.1) Variation of the Critical End Distance with the Width

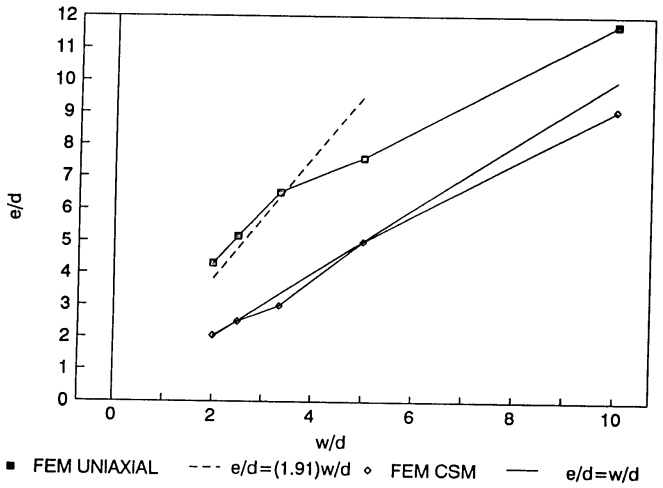

Fig(5.2) The Critical Distance Satisfying $\sigma y/\sigma b=.01$

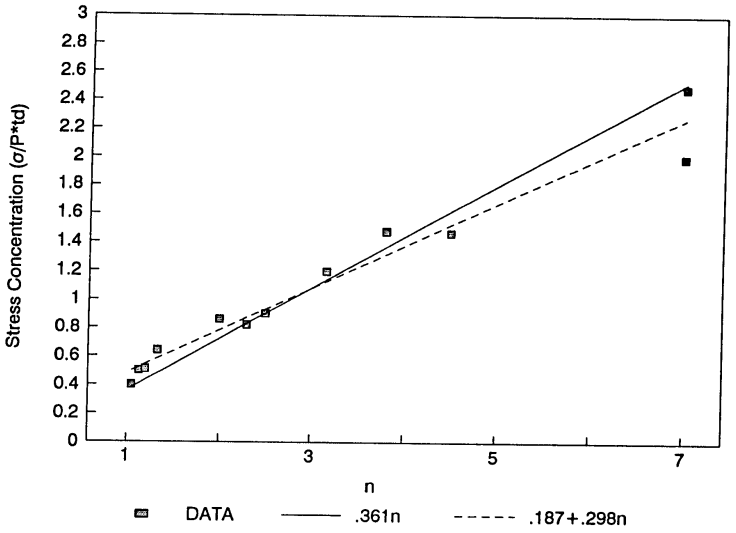

Fig(5.3) The Stress Concentration at Theta = 90°

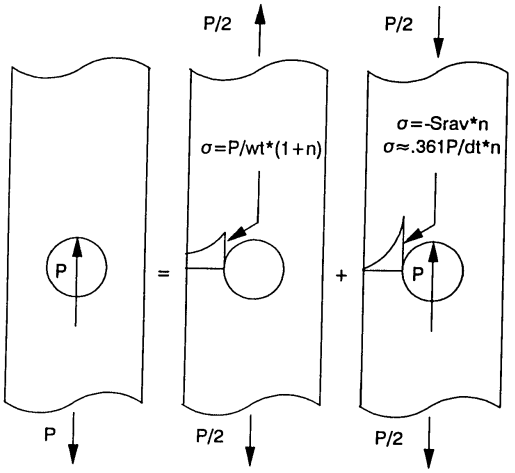

Fig(5.4) The Tensile Stress Concentration

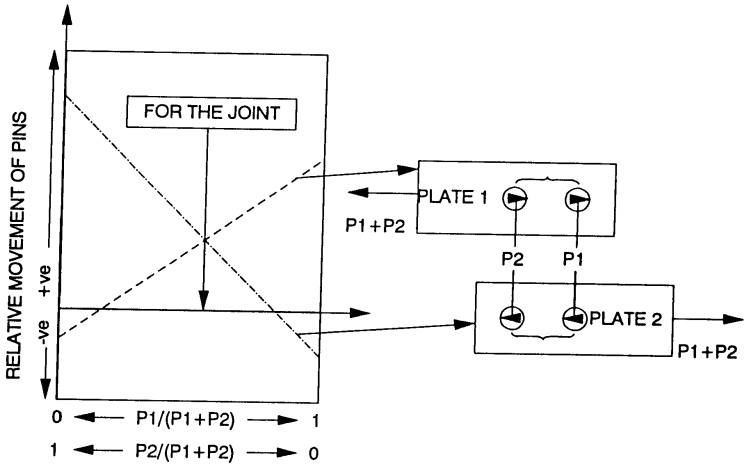

Fig(5.5) The Dependence of the load Distribution on the relative movement of the pins

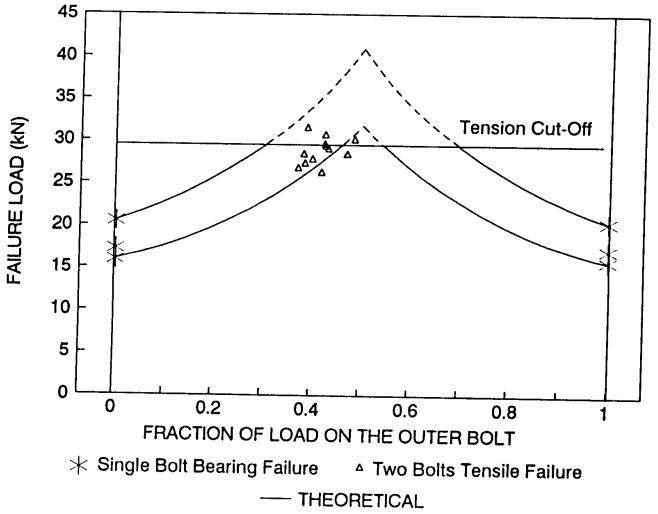

Fig(5.6) Strength of a Plate Loaded by Two Bolts

CHAPTER SIX

6.CONCLUSIONS AND RECOMMENDATIONS

6.1. GENERAL:

The present work investigated bolted joints in pultruded composite materials. The investigations undertaken can be divided into the following parts:

a) An experimental investigation of the behaviour of the joints which concentrated on the special nature of the material.
b) A theoretical investigation which investigated the performance of the numerical techniques used for the analysis of bolted joints.
c) A theoretical investigation which used analytical methods and simplified models of the behaviour of a joint to provide simple formulae which can be used as guidelines during the preliminary design stages.

The use of experimental techniques was necessary because the numerical methods could not replace them because of the following problems:

a) The computing resources needed to perform accurate analyses of the behaviour are very large.
b) No generally reliable theoretical procedure for calculating the strength of the joints exists.

The results of each of the above given investigations are presented in the following sections followed by the recommendations for future work.

6.2. EXPERIMENTAL RESULTS:

The materials used in this investigation were glass fibre polyester pultrusions with a variable content of axial fibres. The experimental testing of coupons loaded by one bolt showed that the failure modes of the joints for pultruded composite materials is similar to other composites. However, it was found that when the amount of fibres parallel to the loading

direction was excessive, failure occurred in shear mode irrespective of the end distance used. Increasing the end distance resulted in increasing the strength of the joint until a critical length of that distance was reached. Subsequently, any increase in the end distance did not result in a noticeable increase in the strength. However, increasing the end distance over its critical value was associated with the development of a plateau in the load displacement curve, where the load was constant while the displacement increased. This indicated that it was possible to achieve ductile failure for such joints, in spite of the absence of a bearing failure mode. Accordingly, it is proposed to redefine the minimum end distance for design to become 'the minimum end distance which will result in the maximum possible strength of the joint for a given width' rather than 'the minimum end distance that ensures the development of bearing failure'.

The effect of the size of the confinement area and the material which is used to clamp the bolt was investigated and it was found that clamping the whole of the potential swelling area resulted in an increase in the strength of the joint compared to clamping using washers. The displacement of the bolt which was associated with the peak strength of the bolt also increased due to the resulting non-linear behaviour of the joint. Although the strength of the joints, which were clamped using washers, decreased after reaching the ultimate load, this load remained subsequently constant while large displacements developed.

It was noted that for all specimens which failed in bearing or shear modes, the ultimate failure was due to cleavage or splitting when the damage reached a certain distance from the edge of the specimen. Accordingly, this explained the increased ductility associated with the longer end distances.

A limited number of specimens was used to investigate the effect of having the unidirectional fibres lying in directions which were not parallel to the loading axis. All these specimens failed in tension on planes parallel to the fibres.

The behaviour of joints loaded using two bolts which were in series was studied by monitoring the load distribution between the two bolts while the load was increasing. The load distribution tended to become equal near the failure load. This was due to the development of local deformations at the bolts which were originally supporting a higher proportion of the load. This local deformation allowed the load to be redistributed to achieve a more uniform loading. However, for the specimens tested, tension and shear failures developed before the redistribution was fully achieved. Therefore, the resulting strength of these latter joints was less than double the strength of single bolt joints.

6.3. THEORETICAL RESULTS:

The comparison of the stress calculated using the classical laminated plate theory and those calculated using the more general three dimensional analyses showed that the use of the laminated plate theory was justified for calculating the in-plane stresses. It was also found that improved results for the stresses could be achieved using a variant of the laminated shell theory. This was based on approximating the variation of the in-plane deformations through the thickness using two straight lines contrary to the classical laminated plate theory where only one straight line was used. During the investigation of the effect of applying this condition, an analogy between the quasi three dimensional problem of a strip subjected to tension and the plane problem subjected to initial stresses was noted. The latter was similar to the problem of calculating the stresses due to temperature variation.

The effect of the presence of a washer was also investigated numerically using three dimensional finite elements. The results of that investigation showed that the presence of a smooth washer or a rough tight fitting washer was not affecting the in-plane stresses to a large extent. Accordingly, a simplified technique for modelling the effect of the washer in a two dimensional analysis was developed. This model included the confinement and friction effects.

The modelling of friction between the shaft of the bolt and the hole was also considered because of its important effect on the contact stress. A novel approximate method was proposed for this problem where no iteration was needed. The accuracy of the method depended on the number of stress distributions considered for approximating the friction stresses developing between the shaft of the bolt and the hole. However, the exact solution can be achieved by increasing the number of these distributions to a certain finite number.

The use of the inverse technique for modelling the non-linear contact between the hole and the pin was briefly considered and it was shown that it was possible to extend the method in order to use it for problems in which combined axial and bending loads are applied and where more than one pin is loading the plate.

The absence of non-empirical reliable strength prediction procedures was identified as a result of the scarcity of objective material models of composite materials which can consider the non-linear behaviour of fibre reinforced polymers. This situation was related to the lack of a general micro-mechanics procedure that can consider the non-linear behaviour of the matrix and the stiffness degradation due to fracture. A material model was proposed in this work, where the non-linearity of the matrix was considered using a plasticity model. It has to be noted here that the use of a plasticity model for the matrix was decided because the mathematical

deformation theory of plasticity was considered as a well developed computational tool for considering non-linear behaviour irrespective of the physical reason for the non-linearity. The use of this model allowed the consideration of the non-linear behaviour of the material, but it did not succeed in predicting the failure of the joint.

Therefore, the model was updated such that it could consider the various macroscopic failure modes of the composite. When this was considered in the numerical application example, it was found that the assumed behaviour of the material after the initial failure played an important role in determining the ultimate strength of the joint.

6.4. DEVELOPMENT OF DESIGN FORMULAE:

An analytical formula was developed in order to calculate the hoop stresses around a radially loaded hole in an infinite orthotropic plate. For the quasi isotropic case, the resulting formula had a very simple form. This formula was used to derive a simple approximate equation for calculating the stress concentration due to a bolt loading the plate. The latter formula can be used in conjunction with the well known stress concentration for an open hole in order to consider the cases of by-pass loads.

The critical end distance for a joint (as defined above) was identified as a variant of St Venant's length and accordingly, it was possible to develop a formula for determining that distance based on the elastic properties of the orthotropic materials. This approached showed that the practice of relating the minimum design end distance to the diameter of the bolt only was not accurate.

6.5. RECOMMENDATIONS:

Based on the results and the experience gathered during the present research program, the following recommendations for future work are suggested.

When performing tests similar to the tests undertaken in this work using two bolts, it is of importance to assure that the plates which are holding the bolts are of sufficient thickness to prevent permanent local deformations. In addition, the holes which are provided for the bolts must be tight fitting.

There is a need for investigating the merits of local reinforcement of bolted joints. This local reinforcement can take the form of an insert or additional plies which are bonded to the

surface. The points which have to be clarified in such an analysis are the shape and materials for such reinforcements. The use of interlocking surfaces between the plates to be jointed seems to be a possibility for improving the efficiency of the joint.

The long term behaviour and that under general loading conditions needs to be investigated. The long term behaviour of the material can be incorporated into the detailed material model proposed in the present work. A limited experimental investigation to relate the results obtained from coupon tests to the behaviour of full-scale joints of pultrusions having general practical shapes is needed.

In order to gain deeper insight into the bearing failure mechanism, three dimensional numerical investigations which consider the non-linear behaviour of the material are needed. The material model developed in this work is a suitable starting point for such a study, but it does require improvement in that experimental investigations are needed for characterising the behaviour of the polymer under general three dimensional loading conditions. In addition an experimental testing program is needed for calibrating the material failure criteria. These investigations should be designed such that they can give information about the post failure behaviour. Knowing the latter experimental behaviour, an effort in needed to relate these results with the mesh size of the finite elements used to achieve mesh objectivity.

The formula proposed for calculating the end distance needs a large experimental data base before it can be used with confidence. This means that any experimental data to be published in the open literature should include sufficient data about the sizes of the coupon specimens used. Unfortunately this information was not always available for the published experimental results.

There use of the empirical strength prediction procedures should be considered as a temporary means for solving the problem of the strength of bolted joints rather than being a goal. This means that while experimental data can be used to calibrate these methods, the main researchers effort should be concentrated on developing more fundamental techniques.

When performing three dimensional finite element analyses, it is necessary to ensure that the element sizes near the free edges is reduced in order to allow the modelling of the high inter laminar stress gradients near these areas. The size of the problem in these cases can be reduced by combined use of two dimensional finite elements in the inner regions (where the laminated plate theory gives the correct results) while modelling the outer ones using three dimensional elements. For design purpose, the use of the two dimensional washer model proposed in this work can result in large reductions in the modelling and solution time.

The development of closed form solutions for practical problems simplifies the design process and allows deeper understanding of the behaviour. In the past, the development of such solutions was very tedious because they relied on human beings for performing large number of routine algebraic manipulations. However, these conditions have changed now and algebraic symbolic manipulation software is becoming more and more powerful. Therefore, the feasibility of developing analytical solutions in addition to the numerical ones should be reinvestigated.

The analytical solution for the loaded hole in an infinite orthotropic plate can be used to investigate the radial contact stresses between the infinite plate and a rigid pin. In addition, the effect of having a finite size for the plates on the stresses around the pin needs to be investigated.

APPENDIX ONE

DATA LOGGING PROGRAM

The following is a list of the program written for data logging from an INTERCOLE SPECTRA data-logger and an INSTRON 1185 testing machine. The program was run using an HP200 computer and was written in HPBASIC-5.

LISTING

```
10   CLEAR SCREEN
20   Spacer(5)
30!  DIMENSION THE VARIABLES AND ARRAYS
40   COM /Data/ Dta(32766,7),Answer$[11],Group$(2)[31],Buffer$[32766]
BUFFER,Temp(7),Temp$[120]
50   ON ERROR GOSUB 1060                          ! TRACE THE ERROR
60   Rs232=9                                      ! THE RS232 IS DEVICE NO 9
70   CONTROL Rs232,0;1                            ! RESET INTERFACE
80   CONTROL Rs232,4;7                            ! CHOOSE INTERFACE
PARAMETERS
90   CONTROL Rs232,3;2400                         ! CHOOSE BAUD RATE
100  ASSIGN @Path1 TO Rs232                       ! OPEN THE Rs232
110  ASSIGN @Path2 TO BUFFER Buffer$              ! OPEN THE BUFFER
120  OUTPUT @Path1;";X"                           ! RESET THE INTERCOLE
130  WAIT 1                                       ! WAIT
140  OUTPUT @Path1;";E0,0,10,0"                   ! SET INTERLINE AND
INTERDATA DELAY min=10
150  Elrad(Answer$,@Path1,@Path2,"ECHO")          ! GET THE ANSWER AND
PRINT THE ERROR
160  OUTPUT @Path1;";S1,0,2,0"                    ! SPECIFY LOAD AND
TRANSDUCERS AS GROUP 1
170  Elrad(Answer$,@Path1,@Path2,"Group1")        ! GET THE ANSWER AND
PRINT THE ERROR
180  OUTPUT @Path1;";S2,16,19,15"                 ! SPECIFY STRAIN GAUGES
AS GROUP 2
190  Elrad(Answer$,@Path1,@Path2,"Group2")        ! GET THE ANSWER AND
PRINT THE ERROR
200  OUTPUT @Path1;";P15,1,120,2.09"              ! SET THE STRAIN GAUGE
VALUES
210  PRINT "          STRAIN GAUGE PARAMETERS: NUMBER OF ARMS=1,
RESISTANCE=120 Ohm, FACTOR=2.09 Microstrain/ Ohm"
220  Elrad(Answer$,@Path1,@Path2,"Parameters")    ! GET THE ANSWER AND
PRINT THE ERROR
230  OUTPUT @Path1;";L3"                          ! INQUIRE WHICH SCAN
GROUPS ARE CURRENTLY SPECIFIED
240  FOR I=1 TO 2                                 ! LOOP OVER TWO GROUPS
```

```
250  TRANSFER @Path1 TO @Path2;DELIM CHR$(13)          ! PUT GROUP
INFORMATION INTO BUFFER
260  ENTER @Path2;Group$(I)                         ! PUT GROUP INFORMATION
INTO Group$(I)
270  NEXT I                                     ! END LOOP
280  Elrad(Answer$,@Path1,@Path2,"Summary")          ! GET THE FINAL
RESPONSE AND PRINT THE ERROR
290  Spacer(5)
300  PRINT "
____________________________________________________________________________
___________________________"
310  PRINT "        |GROUP NUMBER|LOW  CHANNEL|HIGH
CHANNEL|OUTPUT  TYPE|FULL READING|ENERG. LEVEL|INTG.
PERIOD|RLY.ST. TIME|"
320  PRINT "
|___________|___________|___________|___________|___________|_________
__|___________|___________|"
330  Temp$="         |         |         |         |         |        mV|
mA|       sSec|       sSec|"
340  FOR I=1 TO 2                                ! LOOP OVER GROUPS
350  Translate(Group$(I),Temp$,I)                 ! TRANSLATE THE CODE
GIVEN BY THE INTERCOLE TO A STRING
360  PRINT Temp$                                 ! PRINT THE INFORMATION FOR
GROUP I
370  PRINT "
|___________|___________|___________|___________|___________|_________
__|___________|___________|"
380  NEXT I                                     ! END LOOP
390  K=0                                        ! SET THE SCAN NUMBER TO 0
400  Spacer(5)
410  PRINT "                              TO END DATA LOGGING PRESS
FUNCTION KEY 5"
420  Spacer(9)
430  PRINT "                        IN CASE OF EMERGENCY TYPE (CONT
830) TO SAVE THE DATA"
440  Spacer(8)
450  PRINT "                    (kg)   (1>10mm)  (3>8mm)    mic.S.    mic.S.
mic.S.    mic.S."
460  PRINT "                 SCAN   LOAD   TRANSD.1  TRANSD.2  STR.GA.1
STR.GA.2  STR.GA.3  STR.GA.4"
470  K=K+1                                      ! INFINITE LOOP FOR GETTING
THE DATA
480  Dta(K,0)=K                                 ! WRITE THE SCAN NUMBER
490  CONTROL @Path2,4;0                            ! RESET THE BUFFER
500  ON KEY 5 LABEL "f5= STOP" GOTO 800                 ! TO INTERRUPT THE
LOOP
510  OUTPUT @Path1;";G1"                           ! SCAN GROUP1
520  Elrad(Answer$,@Path1,@Path2,"Group1")              ! GET THE RESPONSE
AND PRINT THE ERROR
530  TRANSFER @Path1 TO @Path2;DELIM CHR$(13)           ! GROUP NUMBER
540  ENTER @Path2;Answer$
```

```
550  FOR J=1 TO 3                                  ! LOOP OVER MEMBERS OF
GROUP1
560  TRANSFER @Path1 TO @Path2;DELIM CHR$(13)       ! GET DATA
570  ENTER @Path2;Dta(K,J)                          ! PUT DATA IN ARRAY DTA
580  NEXT J                                         ! END LOOP
590  TRANSFER @Path1 TO @Path2;DELIM CHR$(13)       ! GROUP END
MESSAGE
600  ENTER @Path2;Answer$
610  OUTPUT @Path1;";G2"                            ! SCAN GROUP2
620  Elrad(Answer$,@Path1,@Path2,"Group2")          ! GET AND CHECK
RESPONSE
630  TRANSFER @Path1 TO @Path2;DELIM CHR$(13)       ! GROUP NUMBER
640  ENTER @Path2;Answer$
650  FOR J=4 TO 7                                   ! LOOP OVER MEMBERS OF
GROUP2
660  TRANSFER @Path1 TO @Path2;DELIM CHR$(13)       ! GET STRAIN
DATA
670  ENTER @Path2;Dta(K,J)                          ! PUT THEM IN DTA
680  NEXT J                                         ! END LOOP
690  TRANSFER @Path1 TO @Path2;DELIM CHR$(13)       ! GROUP END
MESSAGE
700  ENTER @Path2;Answer$
710  Dta(K,1)=Dta(K,1)*517.2971                     ! CALIBRATE THE LOAD
720  Dta(K,2)=Dta(K,2)*.658793+6.680783             ! CALIBRATE LVDT1
730  Dta(K,3)=Dta(K,3)*.404251+5.957019             ! CALIBRATE LVDT2
740  FOR J=1 TO 7
750  Dta(K,J)=DROUND(Dta(K,J),8)
760  NEXT J
770  MAT Temp= Dta(K,*)                             ! STORE CURRENT SCAN IN
ARRAY TEMP
780  DISP USING "28X,K,X,K,X,K,X,K,X,K,X,K,X,K,X,K";Temp(*)      !
DISPLAY CURRENT SCAN
790  GOTO 470                                       ! END OF INFINITE LOOP
800  CLEAR SCREEN                                   ! PROCEDURES FOR DISK
STORAGE
810  ASSIGN @Path1 TO *                             ! CLOSE THE RS232
820  ASSIGN @Path2 TO *                             ! CLOSE THE BUFFER
830  CLEAR SCREEN
840  MASS STORAGE IS ":,1400"                       ! SPECIFY THE DRIVE
850! IN CASE OF TROUBLE:
860! CREATE ASCII "Trouble",70/128*K
870! OR
880! CREATE ASCII "Trouble",SIZE
890! ASSIGN @Path3 TO "Trouble"
900! OUTPUT @Path3; Dta(*)
910! ASSIGN @Path3 TO *
920  CAT                                            ! LIST EXISTING FILES ON DISK
930  INPUT "                                        INPUT THE FILE NAME",File$
940  CREATE ASCII File$,70/128*K                    ! GIVE A SUFFICIENLY
HIGH VALUE FOR K
950  ASSIGN @Path3 TO File$                         ! OPEN THE FILE
```

```
960  FOR I=1 TO K                                  ! LOOP FOR WRITING THE
DATA
970  MAT Temp= Dta(I,*)                            ! STORE CURRENT SCAN IN
ARRAY TEMP
980  OUTPUT Temp$ USING "K,X,K,X,K,X,K,X,K,X,K,X,K,X,K";Temp(*)    !
WRITE CURRENT SCAN
990  OUTPUT @Path3;Temp$
1000 NEXT I                                        ! END LOOP
1010 CLEAR SCREEN
1020 Spacer(20)
1030 PRINT "                                     PROGRAM FINISHED"
1040 ASSIGN @Path3 TO *                            ! CLOSE THE FILE
1050 STOP
1060 IF ERRN< >54 THEN GOTO 1120                   ! CHECK FOR
REPEATED FILE NAME
1070 CLEAR SCREEN
1080 PRINT "                          ";ERRM$      ! PRINT ERROR MESSAGE
1090 Spacer(10)
1100 PRINT "                          FILE ALREADY EXISTS: CHOOSE ANOTHER
NAME"
1110 GOTO 840                                      ! RETURN TO FILE NAME
SPECIFICATION
1120 Leih                                          ! CHECK THE TROUBLE WITH
ERROR 167
1130 STOP
1140 END                                           ! END OF MAIN PROGRAM
1150 !
1160 !!
1170 !
1180 !
1190 SUB Resp(S$,Me$)                              ! SUBROUTINE FOR
TRANSLATING INTERCOLE ERRORS
1200 Number=VAL(S$[5,10])                          ! GET THE CODE OF THE
RESPONSE
1210 IF NUM(S$[2])=82 THEN GOTO 1820               ! IF THE RESPONSE IS
"READY" THEN EXIT THIS SUBROUTINE
1220 IF NUM(S$[3])=82 THEN GOTO 1820               ! IF THE RESPONSE IS
"READY" THEN EXIT THIS SUBROUTINE
1230 PRINT Me$,S$                                  ! PRINT THE MESSAGE AND
THE RESPONSE
1240! FOR I=1 TO LEN(S$)
1250! IF S$[I,I]="R" THEN PRINT "POSITION IN STRING = ";I
1260! NEXT I
1270 IF Number< >1 THEN GOTO 1300                  ! PRINT THE MEANING
OF INTERCOLE ╚ ERROR CODE
1280 PRINT "INTERCOLE ERROR: INVALID COMMAND IDENTIFIER"
1290 GOTO 1820
1300 IF Number< >2 THEN GOTO 1330
1310 PRINT "INTERCOLE ERROR: INSUFFICIENT ARGUMENTS"
1320 GOTO 1820
1330 IF Number< >3 THEN GOTO 1360
```

```
1340  PRINT "INTERCOLE ERROR: INVALID VALUE OF ARGUMENT"
1350  GOTO 1820
1360  IF Number< >4 THEN GOTO 1390
1370  PRINT "INTERCOLE ERROR: INVALID CHANNEL NUMBER"
1380  GOTO 1820
1390  IF Number< >5 THEN GOTO 1420
1400  PRINT "INTERCOLE ERROR: GROUP CURRENTLY ACTIVE"
1410  GOTO 1820
1420  IF Number< >6 THEN GOTO 1450
1430  PRINT "INTERCOLE ERROR: GROUP NOT DEFINED"
1440  GOTO 1820
1450  IF Number< >7 THEN GOTO 1480
1460  PRINT "INTERCOLE ERROR: GROUP ALREADY DEFINED"
1470  GOTO 1820
1480  IF Number< >8 THEN GOTO 1510
1490  PRINT "INTERCOLE ERROR: INVALID ENERGIZING"
1500  GOTO 1820
1510  IF Number< >9 THEN GOTO 1540
1520  PRINT "INTERCOLE ERROR: NO PRT AVAILABLE FOR COLD JUNCTION
COMPENSATION"
1530  GOTO 1820
1540  IF Number< >10 THEN GOTO 1570
1550  PRINT "INTERCOLE ERROR: NO FREE USER MEMORY"
1560  GOTO 1820
1570  IF Number< >11 THEN GOTO 1600
1580  PRINT "INTERCOLE ERROR: NOT SUPPORTED ON CURRENT HARDWARE"
1590  GOTO 1820
1600  IF Number< >12 THEN GOTO 1630
1610  PRINT "INTERCOLE ERROR: CONFLICTING DIGITAL DEVICE MODES"
1620  GOTO 1820
1630  IF Number< >13 THEN GOTO 1660
1640  PRINT "INTERCOLE ERROR: COMMAND INCONSITANT WITH DIGITAL
GROUP MODE"
1650  GOTO 1820
1660  IF Number< >14 THEN GOTO 1690
1670  PRINT "INTERCOLE ERROR: DATA STRING NOT DEFINED FOR DIGITAL
OUTPUT DEVICE"
1680  GOTO 1820
1690  IF Number< >15 THEN GOTO 1720
1700  PRINT "INTERCOLE ERROR: DATA STRING NUMBER ALREADY USED"
1710  GOTO 1820
1720  IF Number< >16 THEN GOTO 1750
1730  PRINT "INTERCOLE ERROR: DATA STRING ACTIVE - DELETION
DISALLOWED"
1740  GOTO 1820
1750  IF Number< >101 THEN GOTO 1780
1760  PRINT "INTERCOLE ERROR: INVALID INTEGER NUMBER"
1770  GOTO 1820
1780  IF Number< >102 THEN GOTO 1810
1790  PRINT "INTERCOLE ERROR: INVALID REAL NUMBER"
1800  GOTO 1820
```

```
1810  PRINT "INTERCOLE ERROR: NOT IDENTIFIED"
1820  SUBEND
1830  !
1840  !
1850  SUB Elrad(S$,@Path1,@Path2,Message$)              ! SUBROUTINE TO READ
RS232 INTO BUFFER THEN TO S$ AND PRINTING POSSIBLE ERRORS
1860  TRANSFER @Path1 TO @Path2;DELIM CHR$(13)          ! TRANSFER TO
THE BUFFER UNTILL A "CR" IS MET
1870  ENTER @Path2;S$                                   ! MOVE THE RESULT TO S$
1880  Resp(S$,Message$)                                 ! CHECK THE RESULT AND
PRINT ERROR MESSAGES
1890  SUBEND
1900  !
1910  !
1920  SUB Translate(G$,Temp$,I)                        ! SUBROUTINE TO
TRANSLATE THE CODES TO GROUP DESCRICTION
1930  ! Temp$ IS THE STRING THAT WILL BE PRINTED ON THE SCREEN
1940  Temp$[17,20]=VAL$(I)                              ! WRITE THE GROUP
NUMBER
1950  Temp$[31,33]=G$[5,7]                              ! WRITE THE LOW CHANNEL
1960  Temp$[43,46]=G$[9,11]                             ! WRITE THE HIGH CHANNEL
1970  Type=VAL(G$[13,14])                               ! TRANSLATE THE TYPE
CODE
1980  SELECT Type
1990  CASE 0
2000! PRINT "123456789012"
2010  Kalam$="  DVM bits  "
2020  CASE 1
2030  Kalam$="    VOLTS   "
2040  CASE 2
2050  Kalam$="Th.Cpl.T    "
2060  CASE 3
2070  Kalam$="Th.Cpl.K    "
2080  CASE 4
2090  Kalam$="Th.Cpl.R    "
2100  CASE 5
2110  Kalam$="Th.Cpl.S    "
2120  CASE 6
2130  Kalam$="Th.Cpl.J    "
2140  CASE 7
2150  Kalam$="Th.Cpl.E    "
2160  CASE 8
2170  Kalam$="Th.Cpl.T NO "
2180  CASE 9
2190  Kalam$="Th.Cpl.K NO "
2200  CASE 10
2210  Kalam$="Th.Cpl.R NO "
2220  CASE 11
2230  Kalam$="Th.Cpl.S NO "
2240  CASE 12
2250  Kalam$="Th.Cpl.J NO "
```

```
2260  CASE 13
2270  Kalam$="Th.Cpl.E NO "
2280  CASE 14
2290  Kalam$="Pl.Rs.Therm."
2300  CASE 15
2310  Kalam$=" S.G. Par.  "
2320  CASE >15
2330  Kalam$="User Conver."
2340  END SELECT
2350  Temp$[52,63]=Kalam$                    ! WRITE THE SENSOR TYPE
2360  Scale=VAL(G$[16,17])                   ! FULL SCALE VOLTAGE
2370  SELECT Scale
2380  CASE 0
2390! PRINT "123456789012"
2400  Kalam$="  10.24 V   "
2410  CASE 1
2420  Kalam$="   5.12 V   "
2430  CASE 2
2440  Kalam$="   2.56 V   "
2450  CASE 3
2460  Kalam$="   1.28 V   "
2470  CASE 4
2480  Kalam$="   640 mV   "
2490  CASE 5
2500  Kalam$="   320 mV   "
2510  CASE 6
2520  Kalam$="   160 mV   "
2530  CASE 7
2540  Kalam$="    80 mV   "
2550  CASE 8
2560  Kalam$="    40 mV   "
2570  CASE 9
2580  Kalam$="    20 mV   "
2590  END SELECT
2600  Temp$[65,76]=Kalam$                    ! WRITE THE VOLTAGE
2610  Energ=VAL(G$[19,20])                   ! ENERGISING CURRENT
2620  SELECT Energ
2630  CASE 0
2640! PRINT "123456789012"
2650  Kalam$="    O  mA   "
2660  CASE 1
2670  Kalam$="   1.0 mA   "
2680  CASE 2
2690  Kalam$="   2.5 mA   "
2700  CASE 3
2710  Kalam$="   5.0 mA   "
2720  END SELECT
2730  Temp$[78,89]=Kalam$                    ! WRITE THE CURRENT
2740  Period=VAL(G$[22,27])                  ! INTEGRATION TIME
2750  Period=Period*2000/30                  ! OTHERWISE USE THE CODED
PERIODS
```

```
2760  Kalam$="              "
2770  IF Period>1000000 THEN GOTO 2850                    ! CHOOSE THE UNITS
2780  IF Period>1000 THEN GOTO 2820
2790  Kalam$[2,5]=VAL$(Period)
2800  Kalam$[7,10]="sSec"
2810  GOTO 2870
2820  Kalam$[2,5]=VAL$(Period/1000)
2830  Kalam$[7,10]="mSec"
2840  GOTO 2870
2850  Kalam$[1,7]=VAL$(Period/1000000)
2860  Kalam$[8,10]="Sec"
2870  Temp$[91,102]=Kalam$                          ! WRITE THE PERIOD
2880  Settle=VAL(G$[29,31])                        ! SETTLING TIME
2890  Settle=Settle*660
2900  Temp$[104,111]=VAL$(Settle)                    ! WRITE THE SETTLING
TIME
2910  SUBEND
2920  !
2930  !
2940  SUB Leih                                    ! SUBROUTINE TO EXPLAIN
ERROR 167
2950  PRINT "                              ";ERRM$
2960  IF ERRN<>167 THEN GOTO 3030
2970  STATUS Rs232,10;Which
2980  IF BIT(Which,1) THEN PRINT "RS232 ERROR:RECEIVE BUFFER OVERRUN
ERROR"
2990  IF BIT(Which,2) THEN PRINT "RS232 ERROR:PARITY ERROR DETECTED"
3000  IF BIT(Which,3) THEN PRINT "RS232 ERROR:FRAMING ERROR DETECTED"
3010  IF BIT(Which,4) THEN PRINT "RS232 ERROR:BREACK RECEIVED"
3020  IF BIT(Which,0) THEN PRINT "RS232 ERROR:RECEIVER BUFFER FULL"
3030  SUBEND
3040  !
3050  !
3060  SUB Spacer(N)                                 ! SUBROUTINE TO POSITION
THE OUTPUT
3070  FOR I=1 TO N
3080  PRINT ""
3090  NEXT I
3100  SUBEND
```

APPENDIX TWO

SUBROUTINE FOR THE PLANE MODEL OF WASHER

The following is a listing of the UMAT subroutine written inorder to be included in the finite element software package ABAQUS for modelling the effect of the washer on the in-plane stresses using a two dimensional representation.

Listing:

```
*USER SUBROUTINES
c234567
      SUBROUTINE UMAT(STRESS,STATEV,DDSDDE,SSE,SPD,SCD,
     1 RPL,DDsDDT,DRPLDE,DRPLDT,STRAN,DSTRAN,TIME,DTIME,
     2 TEMP,DTEMP,PREDEF,DPRED,CMNAME,NDI,NSHR,NTENS,NSATV,
     3 PROPS,NPROPS,COORDS,DROT)
      IMPLICIT DOUBLE PRECISION(A-H,O-Z)
      CHARACTER*8 CMNAME
      DIMENSION STRESS(NTENS),STATEV(NSATV),DDSDDE(NTENS,NTENS),
     1 DDSDDT(NTENS),DRPLDE(NTENS),STRAN(NTENS),DSTRAN(NTENS),
     2 PREDEF(1),DPRED(1),PROPS(NPROPS),COORDS(3),DROT(3,3)
C
C ******* DIMENSION THE LOCAL MATRICES
C
      DIMENSION DSTRS(3,3),DSTRN(3,3),STRAIN(3)
C
C ******* SPECIFY THE MATERIAL PROPERTIES
C
      El=45900.
      Et=14300.
      vlt=.23
      vtl=vlt*Et/El
      vtt=.45
      Glt=5000.
C
C ******* CALCULATE THE NEW TOTAL STRAIN
C
      Do 1 i=1,NTENS
1     STRAIN(i)=STRAN(i)+DSTRAN(i)
C
C ******* CALCULATE THE OUT-OF-PLNE STRESS BASED ON PLANE STRAIN
C                        CONDITION
      ez=-vlt*(1+vtt)/(1-vlt*vtl)*STRAIN(1)-(vtt+vlt*vtl)
     //(1-vlt*vtl)*STRAIN(2)
      V=1./(1+vtt)/(1-vtt-2.*vlt*vtl)
```

```
      stresz=(vtt+vlt*vtl)*V*Et*STRAIN(2)
     + +vtl*(1+vtt)*V*El*STRAIN(1)
C
C ******* CHECK THE CONDITION
C
      ezo=-1.6e-3
      dstr=ez-ezo
      IF(dstr.GT.0.) GOTO 555
C
C ******* CALCULATE THE PLANE STRESS MATERIAL MATRIX
C
      DDSDDE(1,1)=El/(1.-vlt*vlt*Et/El)
      DDSDDE(2,2)=DDSDDE(1,1)/El*Et
      DDSDDE(1,2)=DDSDDE(2,2)*vlt
      DDSDDE(2,1)=DDSDDE(1,2)
      DDSDDE(3,3)=Glt
      DDSDDE(1,3)=0.
      DDSDDE(2,3)=0.
      DDSDDE(3,1)=0.
      DDSDDE(3,2)=0.
C
C ******* CALCULATE THE STRESES BASED ON THE PLANE STRESS
CONDITION
C
      Do 6 i=1,NTENS
      STRESS(i)=0.
      Do 6 j=1,NTENS
6     STRESS(i)=STRESS(i)+DDSDDE(i,j)*STRAIN(j)
      RETURN
C
C ******* FOR THE PLANE STRAIN CASE
C
555   CONTINUE
C
C ******* CALCULATE THE PLANE STRAIN MATERIAL MATRIX
C
      V=1./(1.+vtt)/(1.-vtt-2.*Et/El*vlt*vlt)
      DDSDDE(1,1)=El*V*(1.-vtt*vtt)
      DDSDDE(2,2)=Et*V*(1.-vlt*vlt*Et/El)
      DDSDDE(1,2)=vlt*(1.+vtt)*V*Et
      DDSDDE(2,1)=DDSDDE(1,2)
      DDSDDE(3,3)=Glt
      DDSDDE(1,3)=0.
      DDSDDE(2,3)=0.
      DDSDDE(3,1)=0.
      DDSDDE(3,2)=0.
C
C ***** CALCULATE THE ADDITIONAL STRAIN
C
      Do 7 i=1,NTENS
      STRESS(i)=0.
```

```
      Do 7 j=1,NTENS
7     STRESS(i)=STRESS(i)+DDSDDE(i,j)*STRAIN(j)
      STRESS(1)=STRESS(1)+V*vlt*(1+vtt)*Et*ezo
      STRESS(2)=STRESS(2)+V*(vtt-vlt*vtl)*Et*ezo
      RETURN
      END
```

APPENDIX THREE

SUBROUTINE FOR MODELLING COMPOSITE MATERIALS

The following is a listing of the UMAT subroutine written in order to be included in the finite element software package ABAQUS for modelling uniaxial composite materials.

Listing:

```
*MATERIAL,NAME=A1
*DEPVAR
5
*USER MATERIAL
*USER SUBROUTINES
CCCCCCCCCCCCCCCCCCCCCCCCCCCCCCCCCCCCCCCCCCCCCCCCCCCCCCC
CCCCCCCCCCCCCCCCC
C     SUBROUTINE UMAT FOR THE ELASTIC PLASTIC MODELLING OF
COMPOSITE   C
C                   MATERIALS 1-1-1992                          C
CCCCCCCCCCCCCCCCCCCCCCCCCCCCCCCCCCCCCCCCCCCCCCCCCCCCCCC
CCCCCCCCCCCCCCCCC
C NOTE THAT THE ORDER OF THE MATERIAL MATRIX IS
C S11,S22,S33,S12,S13,S23
      SUBROUTINE UMAT(STRESS,STATEV,DDSDDE,SSE,SPD,SCD,
     1 RPL,DDsDDT,DRPLDE,DRPLDT,STRAN,DSTRAN,TIME,DTIME,
     2 TEMP,DTEMP,PREDEF,DPRED,CMNAME,NDI,NSHR,NTENS,NSATV,
     3 PROPS,NPROPS,COORDS,DROT)
      IMPLICIT DOUBLE PRECISION(A-H,O-Z)
      CHARACTER*8 CMNAME
      DIMENSION STRESS(NTENS),STATEV(NSATV),DDSDDE(NTENS,NTENS),
     1 DDSDDT(NTENS),DRPLDE(NTENS),STRAN(NTENS),DSTRAN(NTENS),
     2 PREDEF(1),DPRED(1),PROPS(NPROPS),COORDS(3),DROT(3,3)
C
C ******* DIMENSION THE LOCAL MATRICES
C
      DIMENSION Dm(6,6),DmP(6,6),DA(6),AD(6),DAAD(6,6),A(6),STR(6)
     1,Smm(6,6),Sf(6,6),D(6,6),DmEP(6,6),ZETA(6,6),ETA(6,8)
     2,DGAM(6,6),AA(6,12),BB(6,6),CC(6,6),THET(6,6),STRo(6)
C
C ******* GET THE INFORMATION ABOUT PREVIOUS CONDITIONS
C
      COND1=STATEV(1)
      COND2=STATEV(2)
      COND3=STATEV(3)
      COND4=STATEV(4)
      THETA=STATEV(5)
```

```
CCCCCCCCCCCCCCCCCCCCCCCCCCCCCCCCCCCCCCCCCCCCCCCCCCCCCCC
CCCCCCCCCCCCCCCCC
C                MODULE FOR THE MATERIAL PROPERTIES                  C
CCCCCCCCCCCCCCCCCCCCCCCCCCCCCCCCCCCCCCCCCCCCCCCCCCCCCCC
CCCCCCCCCCCCCCCCC
C
C ******* SPECIFY THE FIBRE PROPERTIES
C
      Ef=71000.
      vnuf=.25
C
C ******* SPECIFY THE MATRIX PROPERTIES
C
      Em=3700.
      vnum=.35
C
C ******* SPECIFY THE YIELD PROPERTIES OF MATRIX
C
      YIELD=53.
      YIELDC=68.9
      SI=YIELDC/YIELD
      TANG=0.001
      HARD=TANG/(1.-TANG/Em)
C
C ******* CALCULATE THE PROPERTIES OF THE GLASS EPOXY COMPOSITE
C
      Vf=.66
      Vm=1.-Vf
      Ecl=(3.7+67.3*Vf)*1000.
      Ect=(3.7+2.02*Vf)/(1.-.9195*Vf)*1000.
      vlt=.35-.1*Vf
      vtl=vlt*Ect/Ecl
      Glt=(1.37+2.152*Vf)/(1.-.885*Vf)*1000.
      vt=(.022+.536*Vf-.292*Vf*Vf)/(.0628+Vf)
      Gt=Ect/2./(1.+vt)
C
C ******* SPECIFY THE FAILURE STRAINS
C
C THESE VALUES ARE FROM THE TESTS AND SUPPLEMENTED FROM HULL
1981
C                    p147+p163
      efmax=.015
      efmin=-.01
      emmax=.002
      gamax=.01
C
C ******* INITIALIZE THE VARIABLES
C
      Do 1 i=1,6
      A(i)=1.0
      STR(i)=0.0
```

```
      Do 1 j=1,6
      Smm(i,j)=0.0
      Sf(i,j)=0.0
      Dm(i,j)=0.0
1     D(i,j)=0.0
CCCCCCCCCCCCCCCCCCCCCCCCCCCCCCCCCCCCCCCCCCCCCCCCCCCCCCCC
CCCCCCCCCCCCCCCCC
C                   MODULE FOR DAMAGE CHECKING                    C
CCCCCCCCCCCCCCCCCCCCCCCCCCCCCCCCCCCCCCCCCCCCCCCCCCCCCCCC
CCCCCCCCCCCCCCCCC
C
C ******* CHECK OLD FIBRE DAMAGE
C
C ******* ARE THE FIBRES FRACTURED?
C
      IF(COND1.EQ.1.) GOTO 8001
C
C ******* ARE THE FIBRES CRUSHED?
C
      IF(COND1.EQ.2.) GOTO 8001
C
C ******* CHECK NEW FIBRE DAMAGE
C
C ******* ARE THE FIBRES FRACTURED?
C
      IF(STRAN(1).GT.efmax) COND1=1.
C
C ******* ARE THE FIBRES CRUSHED?
C
      IF(STRAN(1).LT.efmin) COND1=2.
8001  CONTINUE
C
C ******* CHECK OLD MATRIX DAMAGE
C
C ******* IS THE MATRIX FRACTURED
C
      IF(COND2.EQ.1.) GOTO 8009
C
C ******* IS THE MATRIX CRUSHED
C
      IF(COND2.EQ.2.) GOTO 8008
C
C ******* CALCULATE THE NORMAL MATRIX FAILURE FACTOR
C
C
C ******* FAILURE FACTOR FOR PRINCIPAL TENSION
C
      Rn=(STRAN(2)+STRAN(3)+sqrt((STRAN(2)-STRAN(3))**2
     + +STRAN(6)**2))/2./emmax
      KEY=1
      IF(Rn.GT.1.) GOTO 8080
```

```
C
C ******* FAILURE FACTOR FOR PRINCIPAL SHEAR
C
      Rn=sqrt((STRAN(2)**2-STRAN(2)*STRAN(3)+STRAN(3)**2
     ++1.5*STRAN(6)**2)/(1.5*gamax**2))
      KEY=2
8080  continue
C
C ******* CALCULATE THE LONGITUDINAL SHEAR MATRIX FAILURE FACTOR
C
      Rs=sqrt(STRAN(4)**2+STRAN(5)**2)/gamax
C
C ******* CHECK WHICH CONDITION IS CRITICAL
C
      IF(Rn.GE.Rs) Goto 8004
C
C ******* THE MATRIX WILL FAIL IN LONGITUDINAL SHEAR
C
C ******* DID THE MATERIAL FAIL ?
C
      IF(Rs.LT.1.) GOTO 8005
C
C ******* CALCULATE THE FAILURE ANGLE
C
      THETA=1.570796326
      IF(STRAN(4).NE.0.) THETA=atan(STRAN(5)/STRAN(4))
      c=cos(THETA)
      s=sin(THETA)
      c2=c*c
      s2=s*s
      cs=c*s
C
C ******* CALCULATE THE STRAINS IN THIS DIRECTION
C
      ST=STRAN(2)*c2+STRAN(3)*s2+cs*STRAN(6)
      GOTO 8007
8004  Continue
C
C ******* THE MATRIX WILL FAIL IN THE TRANSVRSE PLANE
C
C ******* DID THE MATERIAL FAIL ?
C
      IF(Rn.LT.1.) GOTO 8005
C
C ******* WILL THE MATRIX FAIL DUE TO SHEAR?
C
      IF(KEY.EQ.2) GOTO 8081
C
C ******* IT WILL FAIL DUE TO NORMAL STRAIN
C ******* DETERMINE A MAX STRAIN PLANE
C
```

```
      THETA=1.570796326/2.
      IF(STRAN(2).NE.STRAN(3)) THETA=(ATAN(STRAN(6)/
     /(STRAN(2)-STRAN(3))))/2.
      THETAa=THETA
      THETAb=THETA+1.570796326
      ca=cos(THETAa)
      sa=sin(THETAa)
      ca2=ca*ca
      sa2=sa*sa
      csa=ca*sa
C
C ******* CALCULATE THE STRAINS IN THIS DIRECTION
C
      STa=STRAN(2)*ca2+STRAN(3)*sa2+csa*STRAN(6)
      STb=STRAN(2)*sa2+STRAN(3)*ca2-csa*STRAN(6)
C
C ******* DETERMINE WHICH DIRECTION IS MORE CRITICAL
C
C ******* FAILURE WILL OCCUR IN THE MORE POSITIVE DIRECTION
C
      IF(STa.GT.STb) GOTO 8006
C
C ******* PRINCIPAL DIRECTION b IS MORE CRITICAL
C
      GOTO 8017
C
C ******* DETERMINE A MAX SHEAR PLANE
C
8081  THETA=1.570796326/2.
      IF(STRAN(2).NE.STRAN(3)) THETA=(ATAN(STRAN(6)/
     /(STRAN(2)-STRAN(3))))/2.
      THETA=THETA-1.570796326/2.
C
C ****** CALCULATE THE FAILURE DIRECTION ANGLES IRRESPECTIVE OF
THE CASE
C
      THETAa=THETA
      THETAb=THETA+1.570796326
      ca=cos(THETAa)
      sa=sin(THETAa)
      ca2=ca*ca
      sa2=sa*sa
      csa=ca*sa
C
C ******* CALCULATE THE STRAINS IN THIS DIRECTION
C
      STa=STRAN(2)*ca2+STRAN(3)*sa2+csa*STRAN(6)
      STb=STRAN(2)*sa2+STRAN(3)*ca2-csa*STRAN(6)
C
C ******* DETERMINE WHICH DIRECTION IS MORE CRITICAL
C
```

```
C ******* FAILURE WILL OCCUR IN THE MORE POSITIVE DIRECTION
C
      IF(ABS(STa).GT.ABS(STb)) GOTO 8006
C
C ******* PRINCIPAL DIRECTION b IS MORE CRITICAL
C
8017  THETA=THETAb
      ST=STb
      GOTO 8007
C
C ******* PRINCIPAL DIRECTION a IS MORE CRITICAL
C
8006  THETA=THETAa
      ST=STa
C
C ******* FIND THE TYPE OF FAILURE
C
8007  IF(ST.LT.0.) GOTO 8008
C
C ******* TENSILE FAILURE
C
8009  COND2=1.
      IF((COND4.EQ.1.).OR.(COND4.EQ.2.)) GOTO 7777
      ca=cos(THETA)
      sa=sin(THETA)
      ca2=ca*ca
      sa2=sa*sa
      csa=ca*sa
      STb=STRAN(2)*sa2+STRAN(3)*ca2-csa*STRAN(6)
      IF(STb.GT.emmax) COND4=1.
      IF(STb.LT.-gamax*sqrt(1.5)) COND4=2.
7777  GOTO 8005
C
C ******* COMPRESSION FAILURE
C
8008  COND2=2.
      IF((COND4.EQ.1.).OR.(COND4.EQ.2.)) GOTO 8005
      ca=cos(THETA)
      sa=sin(THETA)
      ca2=ca*ca
      sa2=sa*sa
      csa=ca*sa
      STb=STRAN(2)*sa2+STRAN(3)*ca2-csa*STRAN(6)
      IF(STb.GT.emmax) COND4=1.
      IF(STb.LT.-gamax*sqrt(1.5)) COND4=2.
8005  CONTINUE
      STATEV(1)=COND1
      STATEV(2)=COND2
c *** STATEV(3) will contain the yield condition !
      STATEV(4)=COND4
      STATEV(5)=THETA
```

```
CCCCCCCCCCCCCCCCCCCCCCCCCCCCCCCCCCCCCCCCCCCCCCCCCCCCC
CCCCCCCCCCCCCCCC
C                CALCULATE THE ELASTIC MATRICES                C
CCCCCCCCCCCCCCCCCCCCCCCCCCCCCCCCCCCCCCCCCCCCCCCCCCCCCC
CCCCCCCCCCCCCCCC
C ******* CALCULATE THE ELASTIC MATRIX STIFFNESS
C
      A1=1.
      A2=1.
      A3=1.
      A4=1.
      A5=1.
      A6=1.
      IF((COND1.EQ.1.).OR.(COND1.EQ.2.)) A1=0.01
      IF((COND2.EQ.1.).OR.(COND2.EQ.2.)) A2=0.01
      IF((COND4.EQ.1.).OR.(COND4.EQ.2.)) A3=0.01
      IF((A1.NE.1.).OR.(A2.NE.1.)) A4=0.01
      IF((A1.NE.1.).OR.(A3.NE.1.)) A5=0.01
      IF((A2.NE.1.).OR.(A3.NE.1.)) A6=0.01
      E1=Em*A1
      E2=Em*A2
      E3=Em*A3
      v21=vnum*A4
      v12=v21/E1*E2
      v31=vnum*A5
      v13=v31/E1*E3
      v23=vnum*A6
      v32=v23/E3*E2
      GG=Em/2./(1+vnum)
      G4=GG*A4
      G5=GG*A5
      G6=GG*A6
      VVV=1./(1.-v12*v21-v32*v23-v13*v31-2.*v21*v13*v32)
      Dm(1,1)=(1.-v23*v32)*E1*VVV
      Dm(2,2)=(1.-v31*v13)*E2*VVV
      Dm(3,3)=(1.-v21*v12)*E3*VVV
      Dm(1,2)=(v12+v13*v32)*E1*VVV
      Dm(1,3)=(v13+v12*v23)*E1*VVV
      Dm(2,3)=(v23+v21*v13)*E2*VVV
      Dm(3,1)=Dm(1,3)
      Dm(2,1)=Dm(1,2)
      Dm(3,2)=Dm(2,3)
      Dm(4,4)=G4
      Dm(5,5)=G5
      Dm(6,6)=G6
C
C ******* CALCULATE THE ELASTIC MATRIX COMPLIANCE
C
      Smm(1,1)=1/E1
      Smm(2,2)=1/E2
      Smm(3,3)=1/E3
```

```
      Smm(1,2)=-v12/E2
      Smm(1,3)=-v13/E3
      Smm(2,3)=-v23/E3
      Smm(2,1)=Smm(1,2)
      Smm(3,1)=Smm(1,3)
      Smm(3,2)=Smm(2,3)
      Smm(4,4)=1/G4
      Smm(5,5)=1/G5
      Smm(6,6)=1/G6
C
C ******* CALCULATE THE ELASTIC FIBRE COMPLIANCE
C
      E1=Ef*A1
      E2=Ef*A2
      E3=Ef*A3
      v21=vnuf*A4
      v12=v21/E1*E2
      v31=vnuf*A5
      v13=v31/E1*E3
      v23=vnuf*A6
      v32=v23/E3*E2
      GG=Ef/2./(1+vnuf)
      G4=GG*A4
      G5=GG*A5
      G6=GG*A6
      Sf(1,1)=1/E1
      Sf(2,2)=1/E2
      Sf(3,3)=1/E3
      Sf(1,2)=-v12/E2
      Sf(1,3)=-v13/E3
      Sf(2,3)=-v23/E3
      Sf(2,1)=Sf(1,2)
      Sf(3,1)=Sf(1,3)
      Sf(3,2)=Sf(2,3)
      Sf(4,4)=1/G4
      Sf(5,5)=1/G5
      Sf(6,6)=1/G6
C
C ******* CALCULATE THE ELASTIC COMPOSITE STIFFNESS
C
      E1=Ecl*A1
      E2=Ect*A2
      E3=Ect*A3
      v21=vlt*A4
      v12=v21/E1*E2
      v31=vlt*A5
      v13=v31/E1*E3
      v23=vt*A6
      v32=v23/E3*E2
      GG=Ect/2./(1+vt)
      G4=Glt*A4
```

```
      G5=Glt*A5
      G6=GG*A6
      VVV=1./(1.-v12*v21-v32*v23-v13*v31-2.*v21*v13*v32)
      D(1,1)=(1.-v23*v32)*E1*VVV
      D(2,2)=(1.-v31*v13)*E2*VVV
      D(3,3)=(1.-v21*v12)*E3*VVV
      D(1,2)=(v12+v13*v32)*E1*VVV
      D(1,3)=(v13+v12*v23)*E1*VVV
      D(2,3)=(v23+v21*v13)*E2*VVV
      D(3,1)=D(1,3)
      D(2,1)=D(1,2)
      D(3,2)=D(2,3)
      D(4,4)=G4
      D(5,5)=G5
      D(6,6)=G6
CCCCCCCCCCCCCCCCCCCCCCCCCCCCCCCCCCCCCCCCCCCCCCCCCCCCCC
CCCCCCCCCCCCCCCCC
C                   MODULE FOR DAMAGE CONSIDERATION                 C
CCCCCCCCCCCCCCCCCCCCCCCCCCCCCCCCCCCCCCCCCCCCCCCCCCCCCC
CCCCCCCCCCCCCCCCC
C
C ******** PREPARE THE FAILURE VECTOR FOR STRESS
C
      A1=1.
      A2=1.
      A3=1.
      A4=1.
      A5=1.
      A6=1.
      IF(COND1.EQ.1.) A1=0.01
      IF(COND2.EQ.1.) A2=0.01
      IF(COND4.EQ.1.) A3=0.01
      IF((A1.NE.1.).OR.(A2.NE.1.)) A4=0.01
      IF((A1.NE.1.).OR.(A3.NE.1.)) A5=0.01
      IF((A2.NE.1.).OR.(A3.NE.1.)) A6=0.01
      A(1)=A1
      A(2)=A2
      A(3)=A3
      A(4)=A4
      A(5)=A5
      A(6)=A6
C
C ******* CALCULATE THE TRIGONOMETRIC FUNCTIONS
C
      c=cos(THETA)
      s=sin(THETA)
      c2=c*c
      c4=c2*c2
      s2=s*s
      s4=s2*s2
      cs=c*s
```

```
      cs2=cs*cs
C
C ******* ROTATE THE TOTAL STRESSES
C
      STR(1)=STRESS(1)
      STR(2)=STRESS(2)*c2+STRESS(3)*s2+2.*STRESS(6)*cs
      STR(3)=STRESS(3)*c2+STRESS(2)*s2-2.*STRESS(6)*cs
      STR(6)=(STRESS(3)-STRESS(2))*cs+STRESS(6)*(c2-s2)
      STR(5)=STRESS(5)*c-STRESS(4)*s
      STR(4)=STRESS(4)*c+STRESS(5)*s
C
C ******* CONSIDER THE EFFECT OF FAILURE
C
      Do 8010 i=1,6
8010  STR(i)=STR(i)*A(i)
C
C ******* ROTATE THE STRESSES BACK
C
      STRESS(1)=STR(1)
      STRESS(2)=STR(2)*c2+STR(3)*s2-2.*STR(6)*cs
      STRESS(3)=STR(3)*c2+STR(2)*s2+2.*STR(6)*cs
      STRESS(6)=(STR(2)-STR(3))*cs+STR(6)*(c2-s2)
      STRESS(5)=STR(5)*c+STR(4)*s
      STRESS(4)=STR(4)*c-STR(5)*s
C
C ****** CONSIDER THE EFFECT OF FAILURE ON THE MATRICES
C
C ****** BECAUSE THE ORIGINAL MATRICES ARE ISOTROPIC
C ******        OR TRASVERSELY ISOTROPIC
C ******        NO ROTATION IS NECESSARY
C
C ***** ROTATE THE STIFFNESS MATRICES TO THE GLOBAL DIRECTIONS
C
C ***** ROTATE THE TOTAL STIFFNESS
C ***** THIS IS NEGATIVE ROTATION
C
      Do 8090 i=1,6
      Do 8090 j=i,6
8090  BB(i,j)=0.
      BB(1,1)=D(1,1)
      BB(1,2)=D(1,2)*c2+D(1,3)*s2
      BB(1,3)=D(1,3)*c2+D(1,2)*s2
      BB(1,6)=(D(1,2)-D(1,3))*cs
      BB(2,2)=D(2,2)*c4+D(3,3)*s4+2*(D(2,3)+2.*D(6,6))*cs2
      BB(2,3)=D(2,3)*(c4+s4)+(D(2,2)+D(3,3)-4.*D(6,6))*cs2
      BB(2,6)=(D(2,2)*c2-D(3,3)*s2-(D(2,3)+2.*D(6,6))*(c2-s2))*cs
      BB(3,3)=D(2,2)*s4+D(3,3)*c4+2.*(D(2,3)+2.*D(6,6))*cs2
      BB(3,6)=(D(2,2)*s2-D(3,3)*c2+(D(2,3)+2.*D(6,6))*(c2-s2))*cs
      BB(6,6)=D(6,6)*(c2-s2)**2+(D(2,2)+D(3,3)-2.*D(2,3))*cs2
      BB(5,5)=D(5,5)*c2+D(4,4)*s2
      BB(4,5)=(D(4,4)-D(5,5))*cs
```

```
      BB(4,4)=D(4,4)*c2+D(5,5)*s2
      Do 8013 i=1,6
      Do 8013 j=i,6
      D(i,j)=BB(i,j)
      D(j,i)=BB(i,j)
 8013  BB(i,j)=0.
C
C ***** ROTATE THE RESIN's STIFFNESS
C ***** THIS IS NEGATIVE ROTATION
C
      BB(1,1)=Dm(1,1)
      BB(1,2)=Dm(1,2)*c2+Dm(1,3)*s2
      BB(1,3)=Dm(1,3)*c2+Dm(1,2)*s2
      BB(1,6)=(Dm(1,2)-Dm(1,3))*cs
      BB(2,2)=Dm(2,2)*c4+Dm(3,3)*s4+2*(Dm(2,3)+2.*Dm(6,6))*cs2
      BB(2,3)=Dm(2,3)*(c4+s4)+(Dm(2,2)+Dm(3,3)-4.*Dm(6,6))*cs2
      BB(2,6)=(Dm(2,2)*c2-Dm(3,3)*s2-(Dm(2,3)+2.*Dm(6,6))*(c2-s2))*cs
      BB(3,3)=Dm(2,2)*s4+Dm(3,3)*c4+2.*(Dm(2,3)+2.*Dm(6,6))*cs2
      BB(3,6)=(Dm(2,2)*s2-Dm(3,3)*c2+(Dm(2,3)+2.*Dm(6,6))*(c2-s2))*cs
      BB(6,6)=Dm(6,6)*(c2-s2)**2+(Dm(2,2)+Dm(3,3)-2.*Dm(2,3))*cs2
      BB(5,5)=Dm(5,5)*c2+Dm(4,4)*s2
      BB(4,5)=(Dm(4,4)-Dm(5,5))*cs
      BB(4,4)=Dm(4,4)*c2+Dm(5,5)*s2
      Do 8014 i=1,6
      Do 8014 j=i,6
      Dm(i,j)=BB(i,j)
      Dm(j,i)=BB(i,j)
 8014  BB(i,j)=0.
C
C ***** ROTATE THE RESIN's FLEXIBILITY
C ***** THIS IS NEGATIVE ROTATION
C
      BB(1,1)=Smm(1,1)
      BB(1,2)=Smm(1,2)*c2+Smm(1,3)*s2
      BB(1,3)=Smm(1,3)*c2+Smm(1,2)*s2
      BB(1,6)=-2.*(Smm(1,3)-Smm(1,2))*cs
      BB(2,2)=Smm(2,2)*c4+Smm(3,3)*s4+(2.*Smm(2,3)+Smm(6,6))*cs2
      BB(2,3)=Smm(2,3)*(c4+s4)+(Smm(2,2)+Smm(3,3)-Smm(6,6))*cs2
      BB(2,6)=(2.*(Smm(2,2)*c2-Smm(3,3)*s2)
     --(2.*Smm(2,3)+Smm(6,6))*(c2-s2))*cs
      BB(3,3)=Smm(2,2)*s4+Smm(3,3)*c4+(2.*Smm(2,3)+Smm(6,6))*cs2
      BB(3,6)=(2.*(Smm(2,2)*s2-Smm(3,3)*c2)
     + +(2.*Smm(2,3)+Smm(6,6))*(c2-s2))*cs
      BB(6,6)=Smm(6,6)*(c2-s2)**2+
     +4.*(Smm(2,2)+Smm(3,3)-2.*Smm(2,3))*cs2
      BB(5,5)=Smm(5,5)*c2+Smm(4,4)*s2
      BB(4,5)=-(Smm(5,5)-Smm(4,4))*cs
      BB(4,4)=Smm(4,4)*c2+Smm(5,5)*s2
      Do 8015 i=1,6
      Do 8015 j=i,6
      Smm(i,j)=BB(i,j)
```

```
      Smm(j,i)=BB(i,j)
8015  BB(i,j)=0.
C
C ***** ROTATE THE FIBRE's FLEXIBILITY
C ***** THIS IS NEGATIVE ROTATION
C
      Do 8093 i=1,6
      Do 8093 j=1,6
8093  BB(i,j)=0.
      BB(1,1)=Sf(1,1)
      BB(1,2)=Sf(1,2)*c2+Sf(1,3)*s2
      BB(1,3)=Sf(1,3)*c2+Sf(1,2)*s2
      BB(1,6)=-2.*(Sf(1,3)-Sf(1,2))*cs
      BB(2,2)=Sf(2,2)*c4+Sf(3,3)*s4+(2.*Sf(2,3)+Sf(6,6))*cs2
      BB(2,3)=Sf(2,3)*(c4+s4)+(Sf(2,2)+Sf(3,3)-Sf(6,6))*cs2
      BB(2,6)=(2.*(Sf(2,2)*c2-Sf(3,3)*s2)
     --(2.*Sf(2,3)+Sf(6,6))*(c2-s2))*cs
      BB(3,3)=Sf(2,2)*s4+Sf(3,3)*c4+(2.*Sf(2,3)+Sf(6,6))*cs2
      BB(3,6)=(2.*(Sf(2,2)*s2-Sf(3,3)*c2)
     ++(2.*Sf(2,3)+Sf(6,6))*(c2-s2))*cs
      BB(6,6)=Sf(6,6)*(c2-s2)**2+
     +4.*(Sf(2,2)+Sf(3,3)-2.*Sf(2,3))*cs2
      BB(5,5)=Sf(5,5)*c2+Sf(4,4)*s2
      BB(4,5)=-(Sf(5,5)-Sf(4,4))*cs
      BB(4,4)=Sf(4,4)*c2+Sf(5,5)*s2
      Do 8016 i=1,6
      Do 8016 j=i,6
      Sf(i,j)=BB(i,j)
      Sf(j,i)=BB(i,j)
8016  BB(i,j)=0.
CCCCCCCCCCCCCCCCCCCCCCCCCCCCCCCCCCCCCCCCCCCCCCCCCCCCCCCC
CCCCCCCCCCCCCCCCCC
C              MODULE FOR ELASTIC PLASTIC BEHAVIOUR                    C
CCCCCCCCCCCCCCCCCCCCCCCCCCCCCCCCCCCCCCCCCCCCCCCCCCCCCCCC
CCCCCCCCCCCCCCCCCC
C
C ******* INITIALIZE THE VARIABLES
C
      ADA=0.0
      Do 8021 i=1,6
      A(i)=0.0
      AD(i)=0.0
      DA(i)=0.0
      STR(i)=0.0
      Do 8021 j=1,6
      AA(i,j)=0.0
      AA(i,j+6)=0.0
      BB(i,j)=0.0
      CC(i,j)=0.0
      DAAD(i,j)=0.0
      DmEP(i,j)=0.0
```

```
      ZETA(i,j)=0.0
      THET(i,j)=0.0
      ETA(i,j)=0.0
      DGAM(i,j)=0.0
 8021  DmP(i,j)=0.0
C ***********************************************************************
C
C ****** MULTIPLY D*Smm
C
      EmVm=Em*Vm
C
C ****** CALCULATE THE MATRIX THET AND DGAM
C
      DO 7 I=1,6
      DO 7 J=1,6
      x1=0.
      x2=0.
      Do 8 k=1,6
C ****** MULTIPLY AA=D*Sf
      x1=x1+D(i,k)*Sf(k,j)
C ****** MULTIPLY BB=-D*Smm
8     x2=x2-D(i,k)*Smm(k,j)
      AA(i,j)=x1
C ****** PUT BB in THE SECOND part of AA
      AA(i,j+6)=x2
7     BB(i,j)=x2
C
C ****** ADD [I] TO GET AA=D*Sf-I AND BB=I-D*Smm
C
      Do 4 i=1,6
      AA(i,i)=AA(i,i)-1.
      BB(i,i)=BB(i,i)+1.
C ****** PUT BB in THE SECOND part of AA
      AA(i,i+6)=BB(i,i)
4     DGAM(i,1)=BB(i,1)*EmVm
      Do 6 i=1,6
      Do 6 j=1,6
6     DGAM(i,j)=DGAM(i,j)+Vm*D(i,j)
C
C ****** CALCULATE THE INVERSE OF AAmultiplied by BB
C ****** THIS IS OBTAINED BY SOLVING THE SET OF EQUATIONS AA
C
      Do 10 k=1,6
      T=1./AA(k,k)
      Do 11 j=k,12
11    AA(k,j)=AA(k,j)*T
      Do 12 i=1,6
      IF(k.EQ.i) GOTO 12
      T=AA(i,k)
      Do 13 j=k,12
13    AA(i,j)= AA(i,j)-T*AA(k,j)
```

```
12    CONTINUE
10    CONTINUE
C
C ****** CALCULATE THET=AA*BB
C
      DO 33 i=1,6
      DO 33 j=1,6
33    THET(i,j)=AA(i,j+6)
C
C ****** Calculate CC=I-BETA*Smm
C
      CC(1,1)=1.-Em*Smm(1,1)
      Do 16 i=2,6
      CC(1,i)=-Em*Smm(1,i)
16    CC(i,i)=1.
C
C ****** CALCULATE ETA
C
      DO 17 i=1,6
      DO 17 j=1,6
      x=0.
      Do 18 k=1,6
18    x=x+THET(i,k)*CC(k,j)
17    ETA(i,j)=x
      DO 19 i=1,6
19    ETA(i,i)=ETA(i,i)+1.
C
C ****** CALCULATE THE OLD AND NEW COMPOSITE STRESSES devided by Vm
C     BASED ON ELASTIC PROPERTIES
C
      Do 8061 i=1,6
      ETA(i,7)=STRESS(i)/Vm
      x=0.
      Do 8091 j=1,6
8091  x=x+D(i,j)*DSTRAN(j)
8061  ETA(i,8)=ETA(i,7)+x/Vm
C
C ****** CALCULATE THE RESIN STRESSES
C
      Facto=Em*STRAN(1)
      Factn=Em*(STRAN(1)+DSTRAN(1))
      Do 8062 i=1,6
      ETA(i,7)=ETA(i,7)-Facto*THET(i,1)
8062  ETA(i,8)=ETA(i,8)-Factn*THET(i,1)
C
C ****** SOLVE TO GET THE RESIN's STRESSES
C
      Do 8073 k=1,6
      T=1./ETA(k,k)
      Do 8074 j=k,8
8074  ETA(k,j)=ETA(k,j)*T
```

```
      Do 8075 i=1,6
      IF(k.EQ.i) GOTO 8075
      T=ETA(i,k)
      Do 8076 j=k,8
 8076 ETA(i,j)=ETA(i,j)-T*ETA(k,j)
 8075 CONTINUE
 8073 CONTINUE
C
C ****** DETERMINE RESIN'S STRESSES FOR PREVIOUS STEP
C
      sigmx=ETA(1,7)
      sigmy=ETA(2,7)
      sigmz=ETA(3,7)
      tauxy=ETA(4,7)
      tauzx=ETA(5,7)
      tauyz=ETA(6,7)
C
C ******* DETERMINE THE STRESS INVARIANTS
C
      sm=(sigmx+sigmy+sigmz)/3.
      sx=sigmx-sm
      sy=sigmy-sm
      sz=sigmz-sm
      td=sqrt(.5*(sx*sx+sy*sy+sz*sz)
     + +tauyz**2+tauzx**2+tauxy**2)
      Root3=1.732050807
      IF(td.NE.0.0) GOTO 303
      Fold=.0
      GOTO 501
  303 CONTINUE
C
C ******* CALCULATE THE OLD F VALUE
C
C     Fold=td*Root3
      C1=(SI-1.)/2./SI
      C2=C1*3.*sm
      SQ=SQRT(C2*C2+3.*td*td/SI)
      Fold=C2+SQ
C
C ******* CALCULATE THE VECTOR A
C
C     Fact2=Root3/2./td
C     A(1)=Fact2*sx
C     A(2)=Fact2*sy
C     A(3)=Fact2*sz
C     A(6)=Fact2*2.*tauyz
C     A(5)=Fact2*2.*tauzx
C     A(4)=Fact2*2.*tauxy
      Fact2=3./SI/SQ/2.
      Fact3=C1+C1*C1*3.*sm/SQ
      A(1)=Fact2*sx+Fact3
```

```
      A(2)=Fact2*sy+Fact3
      A(3)=Fact2*sz+Fact3
      A(4)=Fact2*2.*tauxy
      A(5)=Fact2*2.*tauzx
      A(6)=Fact2*2.*tauyz
C
C ******* CALCULATE THE PLASTIC MATRIX
C         MAKE SURE THAT THE MATRICES ARE ZEROED
C
      DO 20 I=1,6
      DO 20 J=1,6
      DA(I)=DA(I)+Dm(I,J)*A(J)
20    AD(J)=AD(J)+Dm(I,J)*A(I)
      DO 30 I=1,6
      ADA=ADA+A(I)*DA(I)
      DO 30 J=1,6
30    DAAD(I,J)=DAAD(I,J)+DA(I)*AD(J)
      DO 40 I=1,6
      DO 40 J=1,6
40    DmP(I,J)=DAAD(I,J)/(HARD+ADA)
C
C ****** CALCULATE DmEP BASED ON THE CURRENT VALUE OF DSTRNm
C
C ******* DETERMINE THE NEW RESIN'S STRESSES
C
501   sigmx=ETA(1,8)
      sigmy=ETA(2,8)
      sigmz=ETA(3,8)
      tauxy=ETA(4,8)
      tauzx=ETA(5,8)
      tauyz=ETA(6,8)
C
C ******* DETERMINE THE STRESS INVARIANTS
C
      sm=(sigmx+sigmy+sigmz)/3.
      sx=sigmx-sm
      sy=sigmy-sm
      sz=sigmz-sm
      td=sqrt(.5*(sx*sx+sy*sy+sz*sz)
     ++tauyz**2+tauzx**2+tauxy**2)
C
C ******* CALCULATE THE NEW F VALUE
C
C     Fnew=td*Root3
      C1=(SI-1.)/2./SI
      C2=C1*3.*sm
      SQ=SQRT(C2*C2+3.*td*td/SI)
      Fnew=C2+SQ
C
C ******* CHECK THE PAST
C
```

```
      IF(COND3.NE.1.) GOTO 777
C     IF(Fold.LT.YIELD) GOTO 777
C
C ******* THE POINT HAS YIELDED PREVIOUSLY
C
C ******* CHECK FOR UNLOADING
C
      STATEV(3)=1.
c     IF(Fnew.LT.YIELD) GOTO 999
C
C ******* THE POINT IS STILL PLASTIC
C
      FACTOR=1.
      GOTO 808
C
C ******* THE POINT WAS ELASTIC
C
777   CONTINUE
C
C ******* CHECK THE YIELD CONDITIONS
C
      IF(Fnew.LE.YIELD) GOTO 999
C
C ******* THE POINT HAS JUST YIELDED
C
      STATEV(3)=1.
C
C ******* FIRST TIME TO YIELD
C
      FACTOR=(Fnew-YIELD)/(Fnew-Fold)
      GOTO 808
C ***********************************************************************
C
C ******* THE POINT IS STILL ELASTIC
C
999   CONTINUE
      FACTOR=0.
808   CONTINUE
C
C ******* CALCULATE THE ELASTIC PLASTIC MATRIX
C
      Do 70 i=1,6
      Do 70 j=1,6
70    DmEP(i,j)=Dm(i,j)-DmP(i,j)*FACTOR
C
C ****** CALCULATE ZETA
C
C ****** MULTIPLY THET BY Sf
C
      Do 14 i=1,6
      Do 14 j=1,6
```

```
      x=0.
      Do 15 k=1,6
 15    x=x+Sf(i,k)*THET(k,j)
 14    AA(i,j)=x
 C
 C ****** MULTIPLY ZETA=CC*DmEP
 C
      Do 100 i=1,6
      Do 100 j=1,6
      x=0.
      Do 110 k=1,6
 110   x=x+CC(i,k)*DmEP(k,j)
 100   ZETA(i,j)=x
 C
 C ****** Add beta
 C
      ZETA(1,1)=ZETA(1,1)+Em
 C
 C ****** GET BB=AA*ZETA
 C
      Do 120 i=1,6
      Do 120 j=1,6
      y=0.
      Do 130 k=1,6
 130   y=y+AA(i,k)*ZETA(k,j)
 120   BB(i,j)=y
 C
 C ****** Add [I]
 C
      Do 140 i=1,6
      Do 140 j=1,6
 140   ZETA(i,j)=BB(i,j)*Vm
      Do 141 i=1,6
 141   ZETA(i,i)=ZETA(i,i)+Vm
 C
 C ****** INVERT ZETA TO GET ZETA!
 C
      Do 150 k=1,6
      Con=ZETA(k,k)
      ZETA(k,k)=1.
      Do 160 j=1,6
 160   ZETA(k,j)=ZETA(k,j)/Con
      Do 150 i=1,6
      If(i.EQ.k) GOTO 150
      Con=ZETA(i,k)
      ZETA(i,k)=0.
      Do 170 j=1,6
 170   ZETA(i,j)=ZETA(i,j)-ZETA(k,j)*Con
 150    CONTINUE
 C
 C ****** MULTIPLY CC=Smm*DmEP
```

```
C
      Do 230 i=1,6
      Do 230 j=1,6
      x=0.
      Do 240 k=1,6
240   x=x-Smm(i,k)*DmEP(k,j)
230   CC(i,j)=x
C
C ****** ADD [I]
C
      Do 250 i=1,6
250   CC(i,i)=CC(i,i)+1.
C
C ****** GET CC=DGAM*CC*ZETA
C
      Do 260 i=1,6
      Do 260 j=1,6
      x=0.
      Do 270 k=1,6
270   x=x+DGAM(i,k)*CC(k,j)
260   BB(i,j)=x
      Do 280 i=1,6
      Do 280 j=1,6
      x=0.
      Do 285 k=1,6
285   x=x+BB(i,k)*ZETA(k,j)
280   CC(i,j)=x
C
C ****** CALCULATE THE ELASTIC PLASTIC MATRIX
C
      Do 290 i=1,6
      Do 290 j=1,6
290   DDSDDE(i,j)=D(i,j)-CC(i,j)
C
C ****** CALCULATE THE STRESS
C
      Do 301 i=1,6
      x=0.0
      Do 300 j=1,6
300   x=x+DDSDDE(i,j)*DSTRAN(j)
301   STRESS(i)=STRESS(i)+x
      RETURN
      END
```

REFERENCES

Abd-El-Naby,S.F.M, Hollaway,L. and Gunn,M.
"Load Distribution in Two-Pinned Polymer Composite Joints"
in Composite Structures 6, Ed.by Marshall,I.H., p.553, 1991

Aboudi,J.
"Effective Behaviour of inelastic Fibre Reinforced Composites"
Int. J. Eng. Sci., Vol.22, p.439, 1984

Aboudi,J.
"Micromechanical Characterisation of Non-linear Viscoelastic Behaviour of Resin Matrix Composites"
Composite Science and Technology, Vol.38, p.371, 1990

Adams,D.F., King,T.R. and Blackketter,D.M.
"Evaluation of the Transverse Flexure Test Method For Composite Materials"
Composite Science and Technology, Vol.39, p.341, 1990

Agrawal,B.L.
"Static Strength Prediction of Bolted Joint in Composite Material"
AIAA J.,Vol.18, p.1371, 1980

Akasaka, T.
"A practical method of evaluating the isotropic elastic constants of glass mat reinforced plastics"
Comp. Mater. Struct. (Japan), Vol. 3, p.21, 1974

Arnold,W.S.
"The Behaviour of Mechanically Fastened Joints in Composite Structures"
Ph.D. Thesis, Dept. of Mechanical Eng., Paisley College of Technology, 1989

Arnold,W.S., Marshall,I.H. and Wood,J.
"Optimum Design Considerations for Mechanically Fastened Composite Joints"
Composite Structures, Vol.16, p.85, 1990

Barboni,R., Gaudenzi,P. and Carlini,S.
"A Three-Dimensional Analysis of Edge Effects in Composite Laminates with Circular Holes"
Composite Structures, Vol.15, p.115, 1990

Baumann,E.
"Finite Element Analysis of Advanced Composite Structures Containing Mechanically Fastened Joints"
Nuclear Engineering and Design, Vol.70, p.67, 1982

Blosser,M.L.
"Thermal-Stress-Free Fasteners for Jointing Orthotropic Materials"
AIAA J., Vol.27, p.472, 1989

Bickley,W.G.
"The Distribution of Stress Round a Circular Hole in a Plate"
Phil. Trans. Royal Society of London, Vol.227A, p.383, 1928

Bohlmann,R.E., Renieri,G.D. and Liebeskind,M.
"Bolted Field Repair of Graphite/Epoxy Wing Skin Laminates"
in Joining of Composite Materials, Ed.by Kedward,K.T., STP 749, ASTM, p.97, 1981

Bohlmann,R.E., Renieri,G.D. and Riley,B.L.
"Bolted Composite Repairs Subjected to Biaxial or Shear Loads"
in Composite Materials: Testing and Design, 7th Conf., Ed.by Whitney,J.M., STP 893, ASTM, p.34, 1986

Carlesson,L., Sindlar,P. and Nilsson,S.
"Decay of end effects in Graphite/Epoxy Bolted Joints"
Composite Science and Technology, Vol.26, p.307, 1986
Carter III,A.B.
"Preserving the Structural Integrity of Advanced Composite Materials Through the Use of Surface Mounted Fasteners"
34th Int. SAMPE Symposium, p.2011, 1989
Chamis,C.C.
"Simplified Procedures for Designing Composite Bolted Joints"
J. Reinforced Plastics and Composites, Vol.9, p.614, 1990
Chandra,R. and Kumar,M.
"Joint Allowables of Some Composite-Composite Joints"
Symposium on Jointing in Fibre Reinforced Plastics, Imperial College, London, p.142, 1978
Chang,F.
"The Effect of Pin Load Distribution on the Strength of Pin Loaded Holes in Laminated Composites"
J. Composite Materials, Vol.20, p.401, 1986
Chang,F. and Chang,K.
"Post-Failure Analysis of Bolted Composite Joints in Tension or Shear-out Mode Failure"
J. Composite Materials, Vol.21, p.809, 1987
Chang,F., Scott,R.A. and Springer,G.S.
"Strength of Mechanically Fastened Composite Joints"
J. Composite Materials, Vol.16, p.470, 1982
Chang,F., Scott,R.A. and Springer,G.S. (a)
"Failure of Composite Laminates Containing Pin Loaded Holes -Method of Solution"
J. Composite Materials, Vol.18, p.255, 1984
Chang,F., Scott,R.A. and Springer,G.S. (b)
"Design of Composite Laminates Containing Pin Loaded Holes"
J. Composite Materials, VOL.18, p.279, 1984
Chang,F., Scott,R.A. and Springer,G.S. (c)
"Failure Strength of Nonlinear Elastic Composite Laminates Containing a Pin Loaded Hole"
J. Composite Materials, Vol.18, p.464, 1984
Choi,I. and Horgan,C.O.
"Saint-Venant's Principle and End Effects in Anisotropic Elasticity"
J Applied Mechanics, Trans. ASME, P.424, 1977
Cole,R.T., Bathe,E.J. and Potter,J.
"Fasteners for Composite Structures"
Composites, Vol.13, p.233, 1982
Collings, T.A.
"The strength of bolted joints in multi-directional CFRP laminates"
Composites, Vol.8, p.43, 1977
Collings,T.A.
"On the bearing strength of CFRP laminates"
Composites, Vol.13, p.241, 1982

Collings,T.A.
Experimentally Determined Strength of Mechanically Fastened Joints in Joining Fibre-Reinforced Plastics, Ed. Matthews,F.L., Elsevier Applied Science Publishers, 1987

Conti, P.
"Influence of Geometric Parameters on the Stress Distribution Around a Pin-Loaded Hole in Composite Laminates"
Composites Science and Technology, Vol.25, p.83, 1986

Cook,R.D., Malkus,D.S. and Plesha,M.E.
Concepts and Applications of Finite Element Analysis
Third Edition, John Wiley and Sons, New York, USA, 1989

CRAG
CRAG Test Methods For The Measurement of Engineering Properties of Fibre Reinforced Plastics
R.A.E. Farnborough, Technical Report 88012, Ed. Curtis,P.T., Feb. 1988

Crews,J.H.Jr., Hong,C.S. and Raju,I.S.
"Stress Concentration Factors for Finite Orthotropic Laminates With a Pin-Loaded Hole"
NASA Tech. Paper 1862, 1981

Crews,J.H. and Naik,R.A.
"Combined Bearing and Bypass Loading on a Graphite/Epoxy Laminate"
J. Composite Structures, Vol. 6, p.21, 1986

Curtis,P.T. and Moore,B.B.
"A Comparison of Plain and Double Waisted Coupons for Static and Fatigue Testing of Unidirectional GRP and CFRP"
Composite Structures 2, Ed. I.H. Marshall, p.383, 1983

Dallas,R.N.
"Mechanical Joints in Structural Composites"
SAMPE 12, Advances in Structural Composites, 12th National Symposium and Exhibition, p.D-4, 1967

Dastin,S.
"Jointing and Machining Techniques"
in Handbook of Fibreglass and Advanced Plastics Composites, Ed.by Lubin,G., Van Nostrand Reinhold, 1969

De Jong,T.
"Stresses Around Pin-Loaded Holes in Elastically Orthotropic or Isotropic Plates"
J. Composite Materials, Vol.11, p.313, 1977

De Jong,T.
"Stresses Around Pin-Loaded Holes in Composite Materials"
in Mechanics of Composite Materials, Recent Advances, Pergamon Press, p.339, 1982

Dvorak,G.J. and Bahei-El-Din,Y.A.
"Plasticity Analysis of Fibrous Composites"
J. Applied Mechanics, Trans. ASME, Vol.49, p.327, 1982

Eisenmann.J.R.
"Bolted Joint Static Strength Model For Composite Materials"
NASA TM-X-3377, p.563, April 1976Eisenmann,J.R. and Leonhart,J.L.
"Improving Composite Bolted Joint Efficiency By Laminate Tailoring"
Jointing of Composite Materials, Ed. Kedward,K.T., STP749, ASTM, p.117, 1981

Eriksson,L.I.
"Contact Stresses in Bolted Joints of Composite Laminates"
Composite Structures, Vol.6, p.57, 1986
Eriksson,I.
"On the Bearing Strength of Bolted Graphite/Epoxy Laminates"
J Composite Materials, Vol.24, p.1246, 1990
Feodosyev,V.I.
"Selected Problems and Questions in Strength of Materials"
Mir Publishers, Moscow, 1977
FIBREFORCE
Design Manual, Engineered Composite Profiles
FIBREFORCE Composites 1988
Found,M.S.
"The Performance of a Bonded Composite Fastener under Static and Fatigue Loading Conditions"
Composite Structures, Vol.6, p.95, 1986
Frost,S.R.
"An Approximate Theory for Predicting the Moduli of Uni-Directional Laminates with Non-linear Stress/Strain Behaviour"
J. Composite Materials, Vol.24, p.269, 1990
Fuchs,H. and Greenwood,J.H.
"The Use of Glass Fibre/Epoxy Laminates in Large Turbo Generators"
Composites, VOL.8, p.75, 1977
Gangalez,R.
"Development of Thermoplastic Bolts for Structural Applications"
7th. National SAMPE Tech. Conf., Vol.7, p.260, 1975
Garbo,S.P. and Ogonowski,J.M.
"Effect of Variances and Manufacturing Tolerances on the Design Strength and Life of Mechanically Fastened Composite Joints"
AFWAL-TR-81-3041, Air Force Wright Aeronautical Laboratory, Dayton, OH, April 1981
Garg,A.C. and Mai,Y.
"Failure Prediction in Toughened Epoxy Resins"
Composites Science and Technology, Vol.31, p.225, 1988
Gere,J.M. and Timoshenko,S.P.
Mechanics of Materials
Second SI Edition, Van Nostrand Reinhold, 1987
Godwin,E.W. and Matthews,F.L.
"A Review of Strength of Joints in Fibre-Reinforced Plastics - Part 1 Mechanically Fastened Joints"
Composites, Vol.11, p.155, 1980
Godwin,E.W., Matthews,F.L. and Kilty,P.F.
"Strength of Multi-Bolt Joints in GRP"
Composites, Vol.13, p.268, 1982
Goonetilleke,H.D., Poursartip,A. and Teghtsoonian,E.
"Estimating Interlaminar Stress Distributions Around Holes"
Proc. ICCM-V, 5th Int. Conf. on Composite Materials, San Deigo, USA, p.1233, 1985
Green,A.E. and Taylor,G.I.
"Stress systems in aelotropic plates. I"
Proc. Royl. Soc., Series A, Vol.173, p.162, 1939

Green,A.E.
"Stress systems in aelotropic plates. IV"
Proc. Royl. Soc., Series A, Vol.184, p.173, 1945
Ha,S.K., Wang,Q. and Chang,F.K.
"Modelling the Viscoplastic Behaviour of Fibre-Reinforced Thermoplastic Matrix Composites at Elevated Temperatures"
J. Composite Materials, Vol.25, p.334, 1991
Halpin,J.C. & Tsai,S.W.
"Environmental factors in composite materials design"
Air force materials laboratory technical report AFML-TR-67-423, 1967
Hamada,H., Maekawa,Z., Kaji,A. and Nagamori,M.
"Study of failure Mode and Strength of Mechanically Fastened Composite Joint"
in Composites 86, Recent Advances in Japan and US, p.371, 1986
Hamada,H., Maekawa,Z., Harino,T. Kaji,A. and Shina,Y.
"Study on Static and Long-Term Strength of Mechanically Fastened GFRP and CFRP"
in Composite Structures 4, Ed.by Marshall,I.H., p.74, 1987
Hart-Smith,L.J.
"Mechanically-Fastened Joints for Advanced Composites -Phenomenological Considerations and Simple Analysis"
in Fibrous Composites in Structural Design Ed.by Lenoe,E.M., Oplinger,D.W. and Burke,J.J. (Proc. of the 4th. Con. on Fibrous Composites in Structural Design, San Diego, California, p.543, 1978
Hart-Smith,L.J.
"Bonded-Bolted Composite Joints"
J. Aircraft, Vol.22, 1985, p.993
Hart-Smith,L.J.
Design and Empirical Analysis of Bolted or Riveted Joints
in Joining Fibre-Reinforced Plastics, Ed. Matthews,F.L., Elsevier Applied Science Publishers, 1987
Harries,B.
Engineering Composite Materials
The Institute of Metals, London, U.K., 1986
Harrington,P.D. and Sabbaghian,M.
"Factors affecting the friction coefficient between metallic washers and composite surfaces"
Composites, Vol.22, p.418, 1991
Hashin,Z.
"Analysis of Composite Materials -a Survey"
J. Applied Mechanics, Trans. Act. of ASME, Vol.50, p.481, 1983
Herrera-Franco,P.J. and Cloud,G.L.
"Strain-Relief Inserts for Composite Fasteners - An Experimental Study"
J. Composite Materials, Vol.26, p.751, 1992
Hoa,S.V., Lulham,I. and Sankar,T.S.
"Aluminium Inserts for Fastening Sheet Moulding Compounds"
in Composite Structures 3, Ed.by Marshall,I.H., p.575, 1985
Hoa,S.V., Di Maria,A. and Feldman,D.
"Inserts for Fastening Sheet Moulding Compounds"
in Composite Structures 4, Ed.by Marshall,I.H., p.89, 1987

Hollaway,L.
Glass Reinforced Plastics in Construction: Engineering Aspects
Surrey University Press, 1978

Hollaway,L.
Pultrusion
RAPRA Review Reports, Vol.2, No 3, Pergamon Press, 1989

Hull,D.
An Introduction to Composite Materials
Cambridge University Press, Cambridge, U.K., 1981

Humphris,N.P.
"Migration of the Point of Maximum Stress in a Laminated Composite Lug Structure - A Stepwise Approach"
Symposium on Jointing in Fibre Reinforced Plastics, Imperial College, London, p.79, 1978

Hyer,M.W. and Klang,E.C.
"Contact Stresses in Pin-Loaded Orthotropic Plates"
Int. J. Solids and Structures, Vol.21, p.957, 1985

Hyer,M.W., Klang,E.C. and Cooper,D.E.
"The Effect of Pin Elasticity,Clearance and Friction on the Stresses in a Pin-Loaded Orthotropic Plate"
J. Composite Materials, Vol.21, p.190, 1987

Hyer,M.W. and Liu,D.
"Photoelastic Determination of Stresses in multiple-pin connectors"
Experimental Mechanics, Vol.23, p.249, 1983

Hyer,M.W. and Liu,D.
"Stresses in a Quasi Isotropic Pin-Loaded Connectors Using Photoelasticity"
Experimental Mechanics, Vol.24, p.48, 1984

Hyer,M.W. and Liu,D.
"Stresses in Pin-Loaded Orthotropic Plates:Photoelastic Results"
J. Composite Materials, Vol.19, p.138, 1985

Imgrund,M. and Tetambe,R.
"Enhancements in Element Shape Checking for 2-D Solid and 3-D Shell Elements"
ANSYS news, No3, p.5, 1990

Johnson,G.R.
"An Investigation of Methods of Attaching Steel Components to Carbon/Glass Hybrid Laminates in the Construction of Body Support Systems"
Symposium on Jointing in Fibre Reinforced Plastics, Imperial College, London, p.133, 1978

Johnson,M. and Matthews,F.L.
"Determination of Safety Factors for Use when Designing Bolted Joints in GRP"
Composites, Vol.10, p.73, 1979

Kedward,K.T.
Joining and Repair
in Composite Materials Technology, Dept. Mat. Sci. and Eng., Univ. of Surrey, Lecture 13, July 1990

Klang,E.D. and De Jong,T.H.
"Elastic Response and Damage Accumulation of Composite Materials Used in Pinned Connections"
in Mechanical Characterisation of Load Bearing Fibre Composite Laminates, Ed.by Cardon,A.H. and Verchery,G., p.132, 1984

Knight,M.
"The Effect of Unbonded Inclusion on the Failure of Advanced Coupons with Circular Holes"
34th Int. SAMPE Symposium, p.569, 1989
Koshide,S.
"Investigation of the Pin Joints in Composites by the Moire Method"
Experimental Mechanics, Vol.26, p.113, 1986
Kretsis,G. and Matthews,F.L.
"The Strength of Bolted Joints in Glass Fibre/Epoxy Laminates"
Composites, Vol.16, p.92, 1985
Kutscha,D. and Hofer,K.E.Jr
"Feasibility of Joining Advanced Composite Flight Vehicle Structures"
Technical Report AFML-TR-68-391, US Air Force, Jan 1969
Lehman,G.M. and Hawley,A.V. et al.
"Investigation of Joints in Advanced Fibrous Composites for Aircraft Structures"
Mc Donnel-Douglas Corporation, Contract F33615-67-C-1582 June 1969
Lekhnitskii,S.G.
Anisotropic Plates
Translated by Tsai,S.W. and Cheron,T., Gordon and Breach Science Publishers 1968
Liu,F.L. and Li,Q.
"On the Prediction of Mechanical Joining Strength of Laminated Composite Plates"
in Composite Structures 6, Ed.by Marshall,I.H., p.541, 1991
Little,R.E. and Mallick,P.K.
"Fatigue of Bolted Joints in SMC-R18 Sheet Moulding Compound Composites"
J. Composite Technology and Research, Vol.12, p.155, 1990
Maccrum,N.G., Buckley,C.P. and Bucknall,C.B.
Principles of Polymer Engineering
Oxford University Press, Oxford, U.K., 1988
Maekawa,Z., Kaji,A., Hamada,H. and Nagamori,M.
"Failure Mode and Strength Predictions of Mechanically Fastened Composite Joint"
Proc. I.C.C.M.-5, p.99, 1985
Mahajerin,E. and Sikarskie,D.L.
"Boundary Element Study of Loaded Hole in an Orthotropic Plate"
J. Composite Materials, Vol.20, p.375, 1986
Mallick,P.K.
"Effects of Hole Stress Concentration and its Mitigation on the Tensile Strength on R-50 Sheet Moulding Compound Composites"
Composites, Vol.19, p.283, 1988
Malkan,S.R. and Ko,F.K.
"Effect of Fibre Reinforcement Geometry on Single-Shear and Fracture Behaviour of Three Dimensionally Braided Glass/Epoxy Composite Pins"
J. Composite Materials, Vol.23, p.798, 1989
Mangalgiri,P.D.
"Pin-Loaded Holes in Large Orthotropic Plates"
AIAA J., Vol.22, p.1478, 1984
Mangalgiri,P.D. and Dattaguru,B.
"A Large Orthotropic Plate With Misfit Pin Under Arbitrary Oriented Biaxial Loading"
Composite Structures, Vol.6, p.271, 1986

Mangalgiri,P.D., Dattaguru,B. and Rao,A.K.
"Finite Element Analysis of Moving Contact in Mechanically Fastened Joints"
Nuclear Engineering and Design, Vol.78, p.303, 1984
Marshall,I.H., Arnold,W.S., Wood,J. and Mousley
"Observations on Bolted Connections in Composite Structures"
Composite Structures, Vol.13, p.133, 1989
Matthews,F.L. (Ed.)
Joining Fibre-Reinforced Plastics
Elsivier Applied Science Publishers Ltd, 1987
Matthews,F.L., Godwin,E.W. and Kilty,P.F.
The Design of Bolted Joints in GRP
Tech Note TN82-105, Aeronautics Dept., Imperial College, 1982
Matthews,F.L. and Hirst,I.R.
"The Variation of Bearing Strength with Load Direction"
in Symposium on Jointing in Fibre Reinforced Plastics, Imperial College, London, p.126, 1978
Matthews,F.L., Nixon,A. and Want,G.R.
"Bolting and Riveting in Fibre Reinforced Plastics"
Reinforced Plastics Congress, Brighton, p.151, 1976
Matthews,F.L., Roshan,A.A. and Phillips,L.N.
"The Bolt Bearing Strength of Glass/Carbon Hybrid Composites"
Composites, Vol.13, p.225, 1982
Matthews,F.L., Wong,C.M. and Chyrassafitis,L.
"Stress Distribution Around a Single Bolt in Fibre-Reinforced Plastic"
Composites, Vol.13, p.316, 1982
Murphy,M.M. and Lenoe,E.M.
"Stress Analysis of Structural Joints and Interfaces"
Technical Report AMMRC-MS-74-10, US Army, Sept 1974
Murthy,A.V., Dattaguru,B., Narayana,H.V.L. and Rao,A.K.
"An Improved Iterative Finite Element Solution for Pin-Joints"
Computers and Structures, Vol.36, p.1121, 1990
Murthy,A.V.,Dattaguru,B.,Narayana,H.V.L. and Rao,A.K.
"Stress and Strength of Pin Joints in Laminated Anisotropic Plates"
Composite Structures, Vol.19, p.299, 1991Naidu,A.C.B., Dattauru,B., Mangalgiri,P.D. and Ramamurthy,T.S.
"Analysis of a Finite Composite Plate With Smooth Rigid Pin"
Composite Structures, Vol.4, p.197, 1985
Naik,R.A. and Crews,J.H.
"Stress Analysis Method For Clearance-Fit Bolt Under Bearing Loads"
AIAA J., Vol.24, p.1348, 1986
Naik,R.A. and Crews,J.H.
"Stress Analysis Method for Clearance-Fit Joints with Bearing-Bypass Loads"
AIAA J., Vol. 29, p.89, 1991
Nelson,W.D., Buinin,B.L. and Hart-Smith,L,J.
"Critical Joints in Large Composite Aircraft Structure"
Douglas Aircraft Company Paper DP7266 Jan 1983
Nilsson,S.
"Increasing Strength of Graphite/Epoxy Bolted Joints by Introducing an Adhesively Bonded Metallic Insert"
J. Composite Materials, Vol.23, p.642, 1989

Obraztsov,I.F.
Some Problems of Composite Mechanics
In Mechanics of Composites, Ed. Obraztov,I.F., Mir Publishers, 1982

Oken,S. and Deppa,P.W.
"Development of an Advanced Composite Hydrofoil Control Flap"
in Fibrous Composites in Structural Design Ed.by Lenoe,E.M.,Oplinger, D.W. and Burke,J.J., (Proc. of the 4th. Con. on Fibrous Composites in Structural Design, San Diego, California, p.659, 1978

Oplinger,D.W.
"On the Structural Behaviour of Mechanically Fastened Joints in Composite Structures"
in Fibrous Composites in Structural Design Ed.by Lenoe,E.M.,Oplinger, D.W. and Burke,J.J., (Proc. of the 4th. Con. on Fibrous Composites in Structural Design, San Diego, California, p.575, 1978

Oplinger ,D.W. and Gandhi,K.R.
"Stresses in Mechanically Fastened Orthotropic Laminates" in Proc. of the 2nd Conf on Fibrous Composites in Flight Vehicle Design, Dayton, Ohio, May 1974, AFFDL-TR-74-103, P.811, Sept 1974

Oplinger,D.W. and Gandhi,K.R.
"Analytical Studies of Structural Performance in Mechanically Fastened Fibre-Reinforced Plates"
in The Role of Mechanics in Design - Structural Joints, Ed.by Burke,J.J., Gorum,A.E. and Tarpinian,A., Proc. of the Army Symposium on Solid Mechanics 1974, Army Materials and Mechanics Research Center, AMMRC MS-74-8, Sept1974, Brook Hill Mass. USA, p.211, 1975

Owen,D.R.J. and Hinton,E.
Finite Elements in Plasticity
Pineridge Press Limited, Swansea, U.K., 1980

Pagano,N.J. and Pipes,R.B.
"Some observations on the interlaminar strength of composite laminates"
Intl. J.Mechanical Sciences, Vol.15, p.679, 1973

Poon,C.J.
"Literature Review on the Design of Mechanically Fastened Composite Joints"
Structures and Materials Laboratory, National Aeronautical Establishment, National Research Council Canada,NRCC/NAE Aeronautical Note NAE-AN-37 (NRC NO 254442) FEB 1986

Porter,R.M.
"Bolted Joints in Fibre Reinforced Plastics"
Msc Project Report, Aeronautics Dept., Imperial College, 1976

Prabhakaran,R.
"Photoelastic Investigation of Bolted Joints in Composites"
Composites, Vol.13, p.253, 1982

Pradhakaran,R. and Naik,R.A.
"Investigation of Non-Linear Contact for a Clearance-Fit Bolt in a Graphite/Epoxy Laminate"
Composite Structures, Vol.6, p.77, 1986

Pradhan,B. and Ray,K.
"Stresses Around Partial Contact Pin-Loaded Holes in F.R.P. Composite Plates"
J. Reinforced Plastics and Composites, Vol.3, p.69, 1984

Pyner,G.R. and Matthews,F.L.
"Comparison of Single and Multi-Hole Bolted Joints in Glass-Fibre Reinforced Plastic"
J. Composite Materials, Vol.13, p.232, 1979
Quinn,W.J. and Matthews,F.L.
"The Effect of Stacking Sequence on the Pin-Bearing Strength in Glass Fibre Reinforced Plastic"
J. Composite Materials, Vol.11, p.139, 1977
Raghava,R., Caddell,R.M. and Yeh,G.S.Y.
"The Macroscopic Yield Behaviour of Polymers"
J. Material Science, Vol.8, p.225, 1973
Rahman,M.U., Rowlands,R.E.,Cook,R.D. and Wilkinson,T.L.
"An Iterative Procedure for Finite Element Analysis of Frictional Contact Problems"
Computers and Structures, Vol.18, p.947, 1984
Ramamurthy,T.S. (a)
"Recent Studies on the Behaviour of Interference-Fit Pins in Composite Plates"
Composite Structures, Vol.13, p.81, 1989
Ramamurthy,T.S. (b)
"New Studies on the Effect of Bearing Loads in Lugs with Clearance Fit Pins"
Composite Structures, Vol.11, p.135, 1989
Ramkumar,R.L.
"Bolted Joint Design"
in Test Methods and Design Allowables For Fibrous Composites, STP 734, ASTM Philadelphia, p.376, 1981
Rao,A.K.
"Elastic Analysis of Pin Joints"
Computers and Structures, Vol.9, p.125, 1978
Rowlands,R.E. ,Rahman,M.U., Wilkinson,T.L. and Chiang,Y.I.
"Single and Multiple Bolted Joints in Orthotropic Materials"
Composites, Vol.13, p.273, 1982
Ruben,A.
"On the Calculation of Bolted Joints for GRP Plastics"
Composite Structures, Vol.1, p.175, 1983
Ruben,A.
"Fracture Behaviour of Non-Prestressed Bolted Joints of GRP Plastics"
in Advances in Fracture Research, Vol.4, (Valluri,S.R. et al. Ed), 6th International Conf. on Fracture, New Delhi, p.2997, 1984
Ruben,A
"On the Design of Prestressed and Non-Prestressed Bolted Joints in Glass Fibre Reinforced Laminates"
in Composite Structures 4, Ed.by Marshall,I.H., p.1.59, 1987
Rufolo,A.
"Design Manual for Joining Reinforced Plastics"
US Naval Material Laboratory Report NAVSHIP 250-634-1 Aug 1961
Salama,M.
"Lightweight Materials for Deep Water Offshore Structures"
Proc. 18th. Offshore Technology Conference, Houston, Texas, May 1986
Savin,G.N.
Stress Concentration around Holes
Pergamon Press, Oxford, 1961

Schellekens,J.C.J. and DeBrost,R.
"Numerical Simulation of Free Edge Delamination in Graphite-Epoxy Laminates under Uniaxial Tension"
in Composite Structures Ed.by Marshall,I.H., p.647, 1991

Serabian,S.M.
"The Effect of Non-linear Intralaminar Shear Behaviour on the Modelling Accuracy of $[(0/90)_3,0]_s$ and $[(+45/-45)]_{3s}$ Pin-Loaded Laminates"
J. Composite Technology and Research, Vol.13, p.236, 1991

Serabian,S.M. and Anastasi,R.F.
"Out-of-Plane Deflections of Metallic and Composite Pin-Loaded Coupons"
Experimental Mechanics, Vol.31, p.25, 1991

Serabian,S.M. and Oplinger,D.W.
"An Experimental and Finite Element Investigation Into The Mechanical Response of 0/90 Pin-Loaded Laminates"
J. Composite Materials, Vol.21, p.631, 1987

Shah,C.G. and Krishna Murty,A.V.
"Analysis of edge delaminations in laminates through combined use of quasi-three-dimensional, eight-noded, two-noded and transition elements"
Computers and Structures, Vol.39, p.231, 1991

Sigley,R.H., Wronski,A.S. and Parry,T.V.
"Transverse Tensile Strength of Glass/Polyester Unidirectionally Aligned Composites Determined in Diametral Compression"
Composites Science and Technology, Vol.39, p.233, 1990

Smith,P.A., Ashby,M.F. and Pascoe,K.J.
"Modelling Clamp-up Effects in Composite Bolted Joints"
J. of Composite Materials, Vol.21, p.878, 1987

Snyder,B.D., Burns, J.G. and Venkayya,V.B.
"Composite Bolted Joints Analysis Programs"
J. Composites Technology and Research, Vol.12, p.41, 1990

Soni,S.R. (a)
"Stress and Strength Analysis of Bolted Joints in Composite Laminates"
in Composite Structures 1, Ed.by Marshall,I.H., p.50, 1981

Soni,S.R. (b)
"In-plane stress analysis of multidirectional composite laminates with a fastener hole using stress distribution in the constituent angle ply laminates"
Intl. Symp. on The Mechanical Behaviour of Structural Media, Carleton University, Ottawa, 1981

Starr,T.F.
"FRP Geodesic Domes: One Example"
Composite Structures 3, Ed. I.H. Marshall, 1985

Stockdale,J.H. and Matthews,F.L.
"The Effect of Clamping Pressure on Bolt Bearing Loads in Glass Fibre-Reinforced Plastics"
Composites, Vol.7, p.34, 1976

Strauss,E.L.
"Mechanical Joints in Reinforced Plastics Structures"
Machine Design, Vol.32, p.197, 1960

Sturgeon,J.B.
"Joints in Carbon-Fibre-Reinforced Plastics"
Composites, Vol.2, p.104, 1971

Sun,C.T. and Chen,J.L.
"A Micromechanical Model for Plastic Behaviour of Fibrous Composites"
Comp. Sci and Tech., Vol.40, p.115, 1991
Sung,N.H. and Suh,N.P.
"Effect of Fibre Orientation on Friction and Wear of Fibre Reinforced Polymeric Composites"
Wear, Vol.53, p.129, 1979
Tang,S.
"Failure of Composite Joints Under Combined Tension and Bolt Loads"
J. Composite Materials, Vol.15, p.329, 1981
Tanis,C. and Poullos,M.
"Composite Fasteners - a Compatible Jointing Technique for Fibrous Composites in Structural Design"
in Fibrous Composites in Structural Design Ed.by Lenoe,E.M.,Oplinger, D.W. and Burke,J.J., (Proc. of the 4th. Con. on Fibrous Composites in Structural Design, San Diego, California, p.645, 1978
Theocaris,P.S. and Philippidis,T.P.
"True Bounds on Poisson's Ratios for Transversely Isotropic Solids"
J. of Strain Analysis, Vol. 27, 1992, p.43
Tranis,A., Bogetti,J.W.,Gillespie,Jr. and Pipes,R.B.
"Evaluation of the Compression test method for stiffness and strength determination"
Composite Science and Technology, Vol.32, p.57, 1988
Tsai,S.W.
Composites Design
Think Composites, 1987
Tsai,C.L. and Daniel,I.M.
"Determination of In-plane and out-of-plane shear moduli of composite materials"
Experimental Mechanics, Vol.30, p.295, 1990
Tsai,M.Y. and Morton,J.
"Stress and Failure Analysis of a Pin-Loaded Composite Plate: an Experimental Study"
J. Composite Materials, Vol.24, p.1101, 1990
Tsiang,T.
"Survey of Bolted-Joint Technology in Composite Laminates"
J. Composites Technology Review, Vol.6, p.74, 1984
Tsiang,T. and Mandrell,J.F.
"Damage Development in Bolted Bearing on Composite Laminates"
AIAA J., Vol.23, p.1570, 1985
Tsujimoto,Y. and Wilson,D.
"Elasto-Plastic Failure Analysis of Composite Bolted Joints"
J. Composite Materials, Vol.20, p.236, 1986
Tsukizoe,T. & Ohmae,N.
"Friction and Wear Performance of Unidirectionally Oriented Glass, Carbon, Aramid and Stainless Steel Fibre-reinforced Plastics"
in Friction and Wear of Polymer Composites, Ed. Friedrich, K.
Ueng,C.E.S. and Zhang,K.
"Strength Prediction of a Mechanically Fastened Joint in Laminated Composites"
AIAA J., Vol.23, p.1832, 1985

Vable,M. and Sikarskie,D.L.
"Stress Analysis in Plane Orthotropic Material by the Boundary Element Method"
Int. J. Solids and Structures, Vol.24, p.1, 1988
Van Siclen,R.C.
"Evaluation of Bolted Joints in Graphite/Epoxy"
AMMRC-MS-74-8, Army Materials and Mechanics Research Centre Watertown MA p.120, Sept 1974
Vinson,J.R. and Sierakowski,R.L.
The Behaviour of Structures Composed of Composite Materials
Martinus Nijhoff Publishers, 1987
Wan,X. and Yang,L.
"Effect of Joint Parameters, Patterns and Interference on Bolt Loading in Composite Multi-Bolt Joints"
6th. Int Conf. on Composite Structures, Paisley, p.519, 1991
Wang,S. and Han,Y.
"Finite Element Analysis for Loaded Distribution of Multi-Fastener Joints"
J. Composite Materials, Vol.22, p.124, 1988
Waszczak,J.P. and Cruse,T.A.
"Failure Mode and Strength Predictions of Anisotropic Bolt Bearing Specimens"
J. Composite Materials, Vol.5, p.421, 1971
Waszczak,J.P. and Cruse,T.A.
"A Synthesis Procedure for Mechanically Fastened Joints in Advanced Composite Materials"
Report SM-73-11 Carnege-Mellon University, Pittsburgh, or AFML-TR-73-145, April 1973
Webb,A.L.
"Riveting and Bolting in Carbon Fibre Composite"
Symposium:"Jointing in Fibre Reinforced Plastics" Imperial College of Sience and Technology, p.28, 1978
Whitecomb,J.D. and Raju,I.S.
"Superposition method for analysis of free edge stresses"
J. Composite Materials, Vol.17, p.492, 1983
Whitney,J.M., Daniel,I.M. and Pipes,R.B.
Experimental Mechanics of Fibre Reinforced Composite Materials
Society for Experimental Mechanics, Prentice-Hall Publishers, 1984
Wilkinson,T.L., Rowlands,R.E. and Cook,R.D.
"An Incremental Finite Element Determination of Stresses Around Loaded Holes in Wood Plates"
Computers and Structures, Vol.14, p.123, 1981
Wilson,D.W. and Pipes,R.B.
"Analysis of Shearout Failure Mode in Composite Bolted Joints"
in Composite Structures 1, Ed.by Marshall,I.H., p.34, 1981
Wilson,D.W. and Tsujimoto,Y.
"On Phenomenological Failure Criteria for Composite Bolted Joint Analysis"
J. Composites Science and Technology, Vol.26, p.283, 1986
Wong,C.M.S. and Matthews,F.L.
"A Finite Element Analysis of Single and Two-Hole Bolted Joints in Fibre Reinforced Plastics"
J. Composite Materials, Vol.15, p.481, 1981

Wu,J.F., Shephard,M.S., Dvorak,G.J. and Bahei-El-Din,Y.A.
"A Material Model for the Finite Element Analysis of Metal Matrix Composites"
Composites Science and Technology, Vol.35, p.347, 1989
Yang,L. and Ye,Y.
"Study of the Behaviour of a Composite Multi-Bolt Joint"
Computers and Structures, Vol.34, P.497, 1990
Yogeswaren,E.K. and Reddy,J.N.
"A Study of Contact Stresses in Pin-Loaded Orthotropic Plates"
Computers and Structures, Vol.30, p.1067, 1988
York,J.L.,Wilson,D.W. and Pipes, R.B.
"Analysis of the Net Tension Failure Mode in Composite Bolted Joints"
J. Reinforced Plastics and Composites, Vol.1, p.141, 1982
Zahn,J.J.
"Design Equation for Multiple-Fastener Wood Connections"
ASCE, ST 117, p.3477, 1991
Zhang,K. and Ueng,C.E.S.
"Stresses Around a Pin-Loaded Hole in Orthotropic Plates"
J. Composite Materials, Vol.18, p.432, 1984
Zhang,K.D. and Ueng,C.E.S.
"Stresses Around a Pin-Loaded Hole in Orthotropic Plates with Arbitrary Loading Direction"
J. Composite Structures, Vol.3, p.119, 1985
Zienkiewicz,O.C.
The Finite Element Method
Third Edition, Tata McGraw-Hill, New Delhi, India, 1977
Zimmerman,K.B.
"Mechanical Fastening of FGRP Composites"
AIAA J., VOL.29, p.1009, 1991